



AGC-2 Specimen Post-Irradiation Data Package Report

November 2023

William E. Windes, W. David Swank, David T. Rohrbaugh, and
David L. Cottle

Idaho National Laboratory



*INL is a U.S. Department of Energy National Laboratory
operated by Battelle Energy Alliance, LLC*

DISCLAIMER

This information was prepared as an account of work sponsored by an agency of the U.S. Government. Neither the U.S. Government nor any agency thereof, nor any of their employees, makes any warranty, expressed or implied, or assumes any legal liability or responsibility for the accuracy, completeness, or usefulness, of any information, apparatus, product, or process disclosed, or represents that its use would not infringe privately owned rights. References herein to any specific commercial product, process, or service by trade name, trade mark, manufacturer, or otherwise, does not necessarily constitute or imply its endorsement, recommendation, or favoring by the U.S. Government or any agency thereof. The views and opinions of authors expressed herein do not necessarily state or reflect those of the U.S. Government or any agency thereof.

AGC-2 Specimen Post-Irradiation Data Package Report

William E. Windes, W. David Swank, David T. Rohrbaugh, and David L. Cottle
Idaho National Laboratory

November 2023

**Idaho National Laboratory
Advanced Reactor Technologies
Idaho Falls, Idaho 83415**

<http://www.art.inl.gov>

**Prepared for the
U.S. Department of Energy
Office of Nuclear Energy
Under DOE Idaho Operations Office
Contract DE-AC07-05ID14517**

Page intentionally left blank


INL ART Program

AGC-2 Specimen Post-Irradiation Data Package Report

INL/EXT-15-36244
Revision 1

November 2023

Technical Reviewer: (Confirmation of mathematical accuracy, and correctness of data and appropriateness of assumptions.)

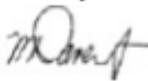


Austin Matthews
INL ART Graphite Engineer

10/13/2023

Date

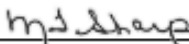
Approved by:



Michael E. Davenport
ART Project Manager

10/14/2023

Date



Michelle T. Sharp
INL Quality Assurance

11/1/2023

Date

Page intentionally left blank

SUMMARY

This report documents results of the post-irradiation examination material property testing of the creep, control, and piggyback specimens from the irradiation creep capsule Advanced Graphite Creep (AGC)-2 are reported. This is the second of a series of six irradiation test trains planned as part of the AGC experiment to fully characterize the neutron irradiation effects and radiation creep behavior of current nuclear graphite grades. The AGC-2 capsule was irradiated in the Idaho National Laboratory Advanced Test Reactor at a nominal temperature of 600°C and to a peak dose of 5 dpa (displacements per atom). One half of the creep specimens were subjected to mechanical stresses (an applied stress of either 13.8, 17.2, or 20.7 MPa) to induce irradiation creep. All post-irradiation testing and measurement results are reported with the exception of the irradiation mechanical strength testing, which is the last destructive testing stage of the irradiation testing program. Material property tests were conducted on specimens from 15 nuclear graphite grades using a similar loading configuration as the first AGC capsule (AGC-1) to provide easy comparison between the two capsules. However, AGC-2 contained an increased number of specimens (i.e., 487 total specimens irradiated) and replaced specimens of the minor grade 2020 with the newer grade 2114. The data reported include specimen dimensions for both stressed and unstressed specimens to establish the irradiation creep rates, mass and volume data necessary to derive density, elastic constants (Young's modulus, shear modulus, and Poisson's ratio) from ultrasonic time of flight velocity measurements, Young's modulus from the fundamental frequency of vibration, electrical resistivity, and thermal diffusivity and thermal expansion data from 100–500°C. No data outliers were determined after all measurements were completed.

A brief statistical analysis was performed on the irradiated data and a limited comparison between pre- and post-irradiation properties is presented. A more complete evaluation of trends in the material property changes, as well as irradiation-induced creep due to irradiation, temperature, and applied load on specimens will be discussed in later AGC-2 post-irradiation examination analysis reports.

Page intentionally left blank

CONTENTS

1.	INTRODUCTION.....	1
2.	ADVANCED GRAPHITE CREEP EXPERIMENT	2
2.1	Design Parameters of AGC Experiment	2
2.2	AGC Graphite Grades and Specimen Dimensions	4
2.3	General AGC Test Train Design.....	5
2.4	Establishing Specimen Dose and Applied Load	6
2.5	Physical Positions of Creep Specimens in the Stacks	8
3.	AGC-2 TEST TRAIN CAPSULE.....	9
3.1	Design Parameters of AGC-2 Test Train	10
3.2	AGC-2 Graphite Grades and Changes to Dimensions	10
3.3	AGC-2 Specimen Stack Positions.....	12
4.	TESTING	20
4.1	Dimensions, Mass and Density	21
4.2	Elastic Modulus.....	23
4.3	Resistivity.....	26
4.4	Thermal Diffusivity.....	27
4.5	Coefficient of Thermal Expansion	29
5.	REFERENCES.....	31
	Appendix A AGC-2 Post-Irradiation Data.....	33
	Appendix B Summary of Statistical Parameters	131

FIGURES

Figure 1. Irradiation dose and temperature parameters for the AGC experiment.....	3
Figure 2. The AGC-2 creep capsule.....	6
Figure 3. Elevation sketch of the AGC capsule.....	7
Figure 4. A typical dose profile for creep graphite specimens utilizing similar applied stress levels in matched stacks.....	9
Figure 5. Volume decrease due to irradiation creep for six major grades of graphite.....	22
Figure 6. Density increase due to volume shrinkage for six major grades of graphite and four stress conditions.....	23
Figure 7. Young's modulus derived from the measurement of fundamental frequency for six grades of graphite and four different stress conditions.....	25
Figure 8. Young's modulus derived from the measurement of ultrasonic velocity for six grades of graphite and four different stress conditions.....	25
Figure 9. Electrical resistivity for six grades of graphite and four different stress conditions.....	26
Figure 10. Ratio of irradiated diffusivity to unirradiated diffusivity for specimens of IG-110 at 500°C as a function of irradiation dose.....	28
Figure 11. Ratio of irradiated diffusivity to unirradiated diffusivity for specimens of IG-110 at 500°C as a function of irradiation temperature.....	28
Figure 12. Ratio of irradiated diffusivity to unirradiated diffusivity as a function of specimen temperature for seven grades of graphite.....	29
Figure 13. Percent increase in CTE at 500°C for graphite grade IG-110 as a function of irradiation dose for four different stress levels.....	30
Figure 14. Percent increase in CTE at 500°C for graphite grade IG-110 as a function of irradiation temperature for four different stress levels.....	30
Figure 15. Percent increase in CTE for six different grades of graphite as a function of temperature for stressed and unstressed conditions.....	31

TABLES

Table 1. Major, minor, alternate, and experimental graphite grades within the AGC-2 capsule.....	11
Table 2. Total number of irradiated-creep specimens in the AGC-2 test series capsule.....	12
Table 3. AGC-2 loading order for Stacks 1 and 2.....	13
Table 4. AGC-2 loading order for Stacks 3 and 4.....	14
Table 5. AGC-2 loading order for Stacks 5 and 6.....	15
Table 6. AGC-2 center channel loading order.....	16

ACRONYMS

AG	against grain
AGC	Advanced Graphite Creep
ATR	Advanced Test Reactor
CCL	Carbon Characterization Laboratory
COV	coefficient of variance
CTE	coefficient of thermal expansion
HOPG	Highly Ordered Pyrolytic Graphite
HTR	high temperature reactor
INL	Idaho National Laboratory
IQR	interquartile range
NGNP	Next Generation Nuclear Plant
PIE	post-irradiation examination
WG	with grain

Page intentionally left blank

AGC-2 Specimen Post-Irradiation Data Package Report

1. INTRODUCTION

The Advanced Reactor Technologies Graphite research and development program is conducting an extensive graphite irradiation program to provide data for licensing of a high temperature reactor (HTR) design. In past applications, graphite has been used effectively as a structural and moderator material in both research and commercial high temperature gas-cooled reactor designs.^[1,2] Nuclear graphite H-451, used previously in the United States for nuclear reactor graphite components, is no longer available. New nuclear graphite grades have been developed and are considered suitable candidates for new HTR reactor designs. To support the design and licensing of HTR core components within a commercial reactor, a complete properties database must be developed for these current grades of graphite. Quantitative data on in-service material performance are required for the physical, mechanical, and thermal properties of each graphite grade with a specific emphasis on data accounting for the life-limiting effects of irradiation creep on key physical properties of the HTR candidate graphite grades. Further details on the research and development activities and associated rationale required to qualify nuclear-grade graphite for use within the HTR are documented in the graphite technology research and development plan.^[3]

Based on experience with previous graphite core components, the phenomenon of irradiation-induced creep within the graphite has been shown to be critical to the total useful lifetime of graphite components. Irradiation-induced creep occurs under the simultaneous application of high temperatures, neutron irradiation, and applied stresses within the graphite components. Significant internal stresses within the graphite components can result from a second phenomenon—irradiation-induced dimensional change—where the graphite physically changes (i.e., first shrinking and then expanding with increasing neutron dose). This disparity in material volume change can induce significant internal stresses within graphite components. Irradiation-induced creep relaxes these large internal stresses, thus reducing the risk of crack formation and component failure. Obviously, higher irradiation creep levels tend to relieve more internal stress, thus allowing the components longer useful lifetimes within the core. Determining the irradiation creep rates of nuclear graphite grades is critical for determining the useful lifetime of graphite components and is a major component of the Advanced Graphite Creep (AGC) experiment.

The AGC experiment is currently underway to determine the in-service behavior of these new graphite grades for HTR. This test series will examine the properties and behaviors of nuclear-grade graphite over a large spectrum of temperatures, irradiation fluence, and applied stress levels that are expected to induce irradiation creep strains within an HTR graphite component. Irradiation data are provided through the AGC test series, which comprises six planned capsules irradiated in the Advanced Test Reactor (ATR) in a large flux trap at Idaho National Laboratory (INL). The AGC irradiation conditions are similar to the anticipated environment within a high temperature core design. Each irradiation capsule is comprised of over 400 graphite specimens that are characterized before and after irradiation to determine the irradiation-induced material properties changes and life-limiting irradiation creep rate for each graphite grade.

The data and information produced in this document and the referenced documents within were generated under the approved Quality Assurance programs for the respective organizations including INL and ORNL in compliance with the appropriate NQA-1 requirements. It is anticipated that all data will be robust enough to stand up to a review by the Nuclear Regulatory Commission as support for a graphite reactor design selection.

Revision 1 of this report modified Appendix A Figures 86-88, 90-92, 94-96, 98-100, 102-104, 106-108, 134-136, 138-140, 142-144, 146-148, 150-152, 154-156, 158-160, 162-164, 166-168, 170-172, 174-176, 178-180, 182-184, 186-188, 190-192 only. The rest of the report remains as written in 2015, Rev 0.

2. ADVANCED GRAPHITE CREEP EXPERIMENT

The AGC test series is designed to establish the data necessary to determine the safe operating envelope of graphite core components for an HTR by measuring the irradiated material property changes and the behavior of several new nuclear graphite grades over a large range of temperatures, neutron fluence, and mechanical compressive loads. The experiment consists of three interrelated stages: pre-irradiation characterization of the graphite specimens, the irradiation test series (designated as six separate irradiation test train capsules), and post-irradiation examination (PIE) and analysis of the graphite specimens after irradiation. Separate reports for each distinct stage are prepared after each individual activity is completed.

The pre-irradiation examination report details the total number of graphite grades and individual specimens, the specimen loading configuration designed to expose all specimens to the entire range of irradiation conditions, and the pre-irradiation material property testing data and results. The as-run irradiation report details the irradiation history of each capsule while in reactor, noting any changes from the technical and functional specifications for each specific test series capsule and identifying the possible improvements to the next test series capsule design. The disassembly report details specimen recovery from the irradiation capsule, noting any damage to the specimens and providing an inventory of recovered specimens for PIE testing. The PIE data report details the changes in specimen dimensional measurements as well as irradiated material properties upon exposure to neutron irradiation. Finally, the PIE analysis report analyzes the irradiation results reported within the data package reports, utilizing the irradiation conditions recorded within the as-run irradiation report. The PIE analysis report(s) determine the irradiation-induced creep rates for the major grades of graphite and assess any changes to the material properties in all graphite grades. The PIE analysis report(s) interpret the irradiation behavior of graphite to assist in determining a credible, safe operating envelope for graphite core components in an HTR design and licensing application. This report is an AGC PIE data report and provides the results and data from post-irradiation testing for AGC-2 specimens. A brief statistical analysis is performed here along with a limited comparison to the pre- and post-irradiation data. In this way, the consistency and soundness of the data is initially tested. A more detailed analysis and trends in the data will be reported within the subsequent AGC analysis report(s).

2.1 Design Parameters of AGC Experiment

The AGC test series is designed to measure changes in key thermal, physical, and mechanical material properties over the anticipated range of HTR operating conditions. By comparing the material properties of each specimen before and after irradiation, the experiment generates quantitative material property change data and irradiation creep data that will be used to predict the in-service behavior and operating performance of the current nuclear graphite grades for HTR designs. Specific emphasis is placed on data that account for the life-limiting effects of irradiation creep on graphite components and the effects creep may have on key irradiated material properties of several candidate graphite grades for use in an HTR design.

The critical component of the experiment is the irradiation test series, which irradiates the graphite specimens after pre-irradiation examination characterization has been completed. The AGC test series is comprised of six planned irradiation test trains that are irradiated in ATR in a large flux trap, as described in “Graphite Technology Development Plan.”^[3] The test series exposes test specimens of select nuclear graphite grades to temperatures and the initial range of irradiation dose that are expected within an HTR design. Specifically, graphite specimens will be exposed to a fast neutron dose ranging from 1 to 7 dpa and temperatures of 600, 800, and 1100°C, as shown in Figure 1. The first and second AGC capsules, AGC-1, and AGC-2, were designed to be irradiated within the ATR’s South Flux Trap.^[4] All other AGC capsules will be irradiated within ATR’s East Flux Trap. Generally, irradiations within the South Flux Trap require approximately 175 effective full-power days to provide a nominal fast neutron dose range (in graphite) of approximately 0.5–3.5 dpa. For those capsules requiring a large dose range of approximately 3.5–7.0 dpa, the irradiation capsule (containing the graphite specimens) is irradiated for twice as long inside the ATR, approximately 350 effective full-power days.

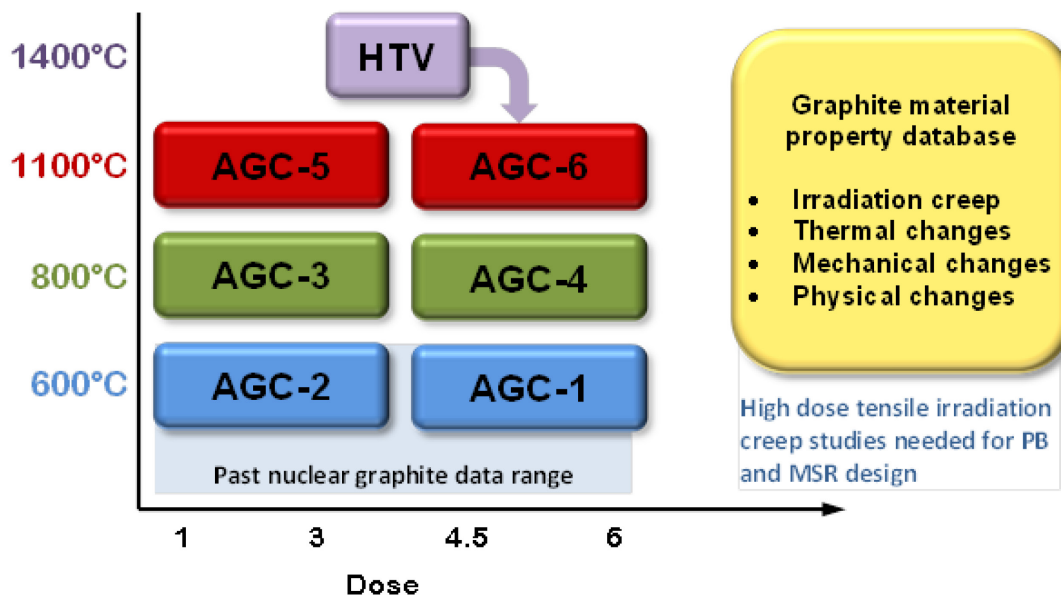


Figure 1. Irradiation dose and temperature parameters for the AGC experiment.

In addition to determining the irradiation-induced changes to the material properties of selected nuclear graphite grades, the AGC experiment dedicates a significant amount of scope to determining rates of irradiation-induced creep for different nuclear graphite grades. The traditional method for measuring irradiation-induced creep is to apply a significant mechanical load (inducing a mechanical stress within the graphite) to half the specimens during irradiation while leaving the remaining half of the specimens unloaded (unstressed). The resulting difference in dimensional change between the loaded and unloaded specimens (assuming that temperature and dose levels are the same) provides the amount of irradiation-induced strain for each “matched pair” of graphite specimens. From this strain level, a creep rate for each graphite grade can be calculated as a function of dose if both specimens were irradiated at the same constant temperature and dose level. Thus, each capsule is designed to be irradiated at a constant temperature, allowing only the dose and applied mechanical load to vary within the test train of each test-series capsule. With all graphite specimens at a constant temperature, only the applied stress level and dose will affect the calculated creep rate of each graphite grade within a test series capsule.

The AGC experiment is designed to measure the constant creep strain rate (secondary creep) of the various grades. The experiment assumes that the induced creep strain for all specimens is within the secondary creep regime and therefore behaves linearly with respect to received neutron dose.^[3] This assumption is valid provided the specimens do not go beyond their turn-around dose where creep strain can no longer be expected to be linear with irradiation dose (the onset of tertiary creep). Once the specimens begin to reach turnaround, the creep strain response becomes non-linear with received dose. To ensure specimens remain within the constant linear creep strain regime within AGC-5 and AGC-6 (the highest temperature and dose) test trains, a High Temperature Irradiation Vessel will be used to measure the dimensional changes of the graphite grades at a high temperature (1400°C) and moderate dose (4.5 dpa). Results from this high temperature dimensional change study will be utilized in the AGC-5 and AGC-6 designs, which constitute the upper bounds of the AGC experiment, Figure 1. In addition, if any graphite grade achieves turnaround within the High Temperature Irradiation Vessel, it will be considered to be outside the upper bounds of the AGC experiment and will be eliminated from the AGC-6 test train.

While the effects from applied mechanical stresses and neutron dose can be determined within each irradiation capsule, the temperature dependency of any irradiation-induced material property changes within the graphite grades is achieved by comparing the measured values of the specimens between irradiation capsules. Since each test train is irradiated at a constant temperature (either 600°C, 800°C, or 1100°C), the temperature induced/enhanced material property changes must be determined by comparing specimens in different capsules exposed to similar dose and applied mechanical load levels. All AGC capsules are designed to have the same specimen stacking patterns. Thus, if specimens of identical graphite grades are located in similar positions within each capsule, a similar dose and load level will be imposed on a consistent grade of graphite. Maintaining consistent specimen positions for each grade within the six different capsules will allow the determination of temperature-induced changes for irradiation creep and material properties across the AGC experiment.

2.2 AGC Graphite Grades and Specimen Dimensions

The AGC experiment is designed to ascertain the irradiation behavior of currently available nuclear graphite grades within the anticipated operating parameters of an HTR design. By exposing a variety of nuclear graphite grades representing the range of fabrication parameters (grain size, fabrication processes, and raw source material) to the expected operating conditions for an HTR design (600°C–1100°C and 0.5–7 dpa dose) a comprehensive understanding of the irradiation response and behavior of graphite components in general can be achieved. This will limit the need for additional research in the future if the current graphite grades are altered (i.e., new raw material sources are used) or new grades are utilized in future reactors.

The AGC experiment utilizes a variety of current graphite grades to envelope the major fabrication parameters believed to be responsible for the irradiation behavior of nuclear graphite.^[1] This range of fabrication parameters are represented by AGC major grades, which were deemed to be production-ready grades that could be used in current or future HTR designs. Major graphite grades are one type of sample within the AGC irradiation capsule. In addition, four other sample types are designated within the AGC experiment. The five AGC sample types are categorized as follows^[5]:

1. Major Grades (Irradiation Creep and Control Specimens)

These graphite grades are current reactor candidates for the core structures of an HTR design as well as historical (reference) grades. Due to their fabrication maturity and consistency, HTR core components are most likely to be formed from these major grades and are thus expected to receive reasonably large neutron doses in their lifetime. Only major grade specimens were used to determine the critical irradiation-induced creep strain rate.

2. Minor Grades (Piggyback Specimens)

These grades are HTR-relevant grades that are not yet production ready or are most likely to be used in low neutron dose regions of the core (e.g., the permanent structure of the prismatic block HTR design).

3. Alternate Grades (Piggyback Specimens)

Grades that current HTR vendors have identified as being of interest as alternate graphite grades for certain components within the reactor.

4. Experimental Grades (Piggyback Specimens)

Experimental graphite grades are included in AGC to assess the viability of new graphite grades whose manufacturing processes and raw materials are such that they may offer superior irradiation stability. Additionally, other carbonaceous materials such as fuel compact matrix materials, carbon-carbon composites, silicon-carbide composites, or other experimental materials that could offer superior performance within the extreme environment of an HTR core are included.

5. Single Crystal Graphite (Piggyback Specimens)

Samples of Highly Ordered Pyrolytic Graphite (HOPG) are included in AGC to assess the fundamental irradiation response of single crystal graphite. These specimens offer specific dimensional change behavior of graphite, which is particularly significant to the behavior of polycrystalline (polygranular) graphite grades.

To provide all necessary material property tests in the AGC experiments, each test series capsule contains two primary specimens: (1) “creep” specimens, providing irradiation creep-rate value as well as mechanical properties and (2) “piggyback” specimens, providing thermal material property changes to the graphite. Creep specimens are fabricated only from major grade graphite types.^[2, 6] Piggyback specimens are fabricated from major, minor, and experimental grade graphite. The piggyback specimens are not mechanically loaded and are subjected only to neutron irradiation at high operating temperatures to assess the effects of a reactor environment on the specific graphite grade.

All specimens are 12.7 mm in diameter, with the larger creep specimens being 25.4 mm long and the button-sized piggyback specimens being 6 mm long. Small graphite containers that are 12.7 mm in diameter by 6 mm long contain the thin wafer HOPG specimens. The large creep specimens provide accurate dimensional change, elastic modulus, thermal expansion, electrical resistivity, and mechanical strength measurements. However, the longer creep specimens make them unsuitable for thermal diffusivity measurements. The small piggyback specimens permitted only dimensional measurements, density, and thermal diffusivity testing to be performed. Together, both types of specimens provide the changes in material properties for stressed and unstressed graphite grades.^[7]

2.3 General AGC Test Train Design

All AGC test trains and irradiation capsules have the same general physical configuration to provide consistent dose and applied mechanical stresses on specimens of similar graphite grades. While there are key machining and structural differences between capsules to change the irradiation temperature for the different capsules, the majority of the AGC design is identical for all capsules. A schematic of the AGC-2 test train is shown in Figure 2.^[8]

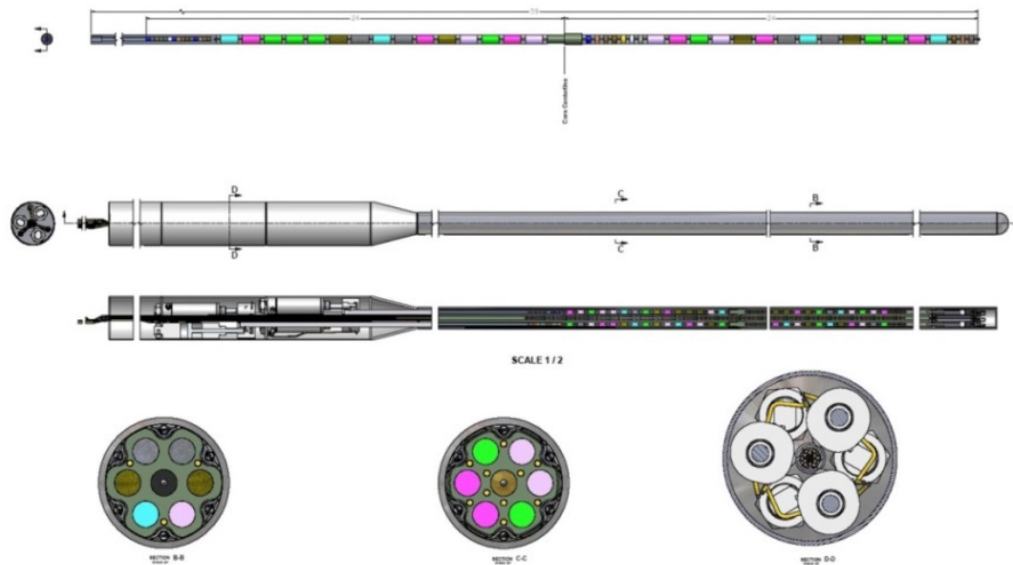


Figure 2. The AGC-2 creep capsule.

All irradiation capsules have six channels located on the outer perimeter of the graphite specimen holder body and a center channel. All channels are 12.9mm (0.51 inch) in diameter and are designed to hold all types of AGC specimens. The upper (top) half the outer channels has had mechanical loads applied to the specimens. However, the lower (bottom) half for these channels has had no mechanical load applied to the specimens in these locations. Due to the neutron flux profile in ATR, matched pairs with similar neutron fluence and temperatures are achieved by pre-ordering the specimen axial locations. Specimens in the upper half of the channels were stressed by the applied mechanical load while their matched pair received a similar dose in an unstressed state. Three stress levels—13.8MPa, 17.2MPa, and 20.7 MPa (2.0 ksi, 2.5 ksi and 3.0 ksi) nominal—are applied in all AGC capsules to provide a known stress upon the graphite specimens during irradiation. These induced stress levels are high enough to produce irradiation-induced creep strain with the graphite specimens.

Temperature values within all AGC capsules are calculated based upon thermocouple readings at select positions within the capsule. Specimen temperature is calculated with a Finite Element Model that has been calibrated to predict the known thermocouple readings in the capsule. Dose levels are calculated using Monte Carlo N-Particle Transport Code models and operating conditions in the ATR core and are corroborated from flux wire data.

2.4 Establishing Specimen Dose and Applied Load

To achieve the desired irradiation dose levels and applied mechanical loads to the specific specimens, an exact specimen loading order is critical. Because irradiation creep is usually determined by the difference in dimensional change occurring within specimens that have an applied load and those that do not, these “matched pair” specimens are assumed to have the same irradiation dose and irradiation temperature values. The AGC test train designs utilize the symmetric flux profile generated within the ATR to achieve these similar irradiation conditions for “matched pairs.”

Specimens within the upper half of the capsule have a mechanical load applied to them via a pneumatic ram system. Specimens within the lower half remain unloaded and thus have no applied stress. The ATR specimens in the upper half of the capsule are located in positions that receive a dose level similar to their “matched pair” specimens in the lower half of the capsule. A careful specimen loading order within the irradiation capsule is required to assure similar dose levels for each “matched pair.”^[9,10] Other considerations included the size of each creep specimen, the need for periodically placed spacers containing flux wires, and the space requirements in the top of the stacks for the pneumatic push rods. The core flux mid-plane, in relation to the capsule arrangement, was established so that the reactor neutron flux field could be correlated to the physical elevations and positions in the capsule to yield accurate “match pair” irradiation dose levels, Figure 3.^[11]

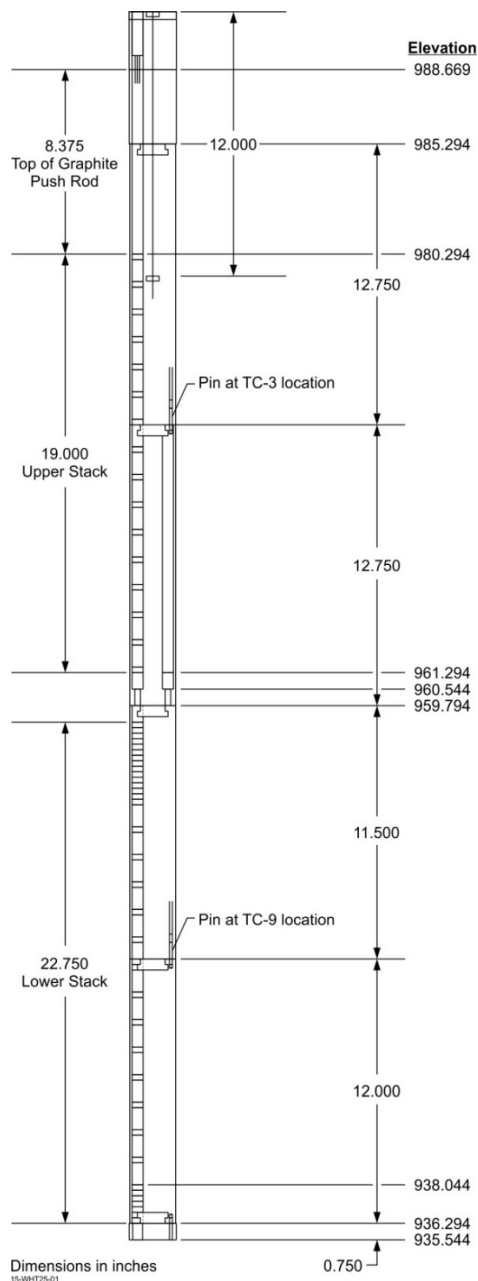


Figure 3. Elevation sketch of the AGC capsule.

Irradiation dose values, as a function of distance from the reactor core centerline, are calculated from the total calculated fluence using standard conversion factors for carbon in a fast neutron irradiation field ($E > 0.1$ MeV).^[12] There is a neutron flux gradient across the capsule thickness requiring the capsule to be rotated 180 degrees at the irradiation mid-point. This rotation results in a uniform neutron-fluence profile for all stacks, regardless of their position within the capsule.

As described in previous reports^[5] the ATR neutron flux profile is not completely symmetrical along the vertical axis. Thus, to produce matched-pair specimens that have similar dose profiles both above and below the core mid-plane, an offset position from the mid-plane is required. An offset distance of 1.25 in. from the core mid-plane for the bottom creep specimens produces the closest dose matches between specimens. While it was impossible to exactly match the dose levels for both the upper and lower specimens, the dose levels for each specimen pair were fairly close, ranging from 0–2%.^[13]

2.5 Physical Positions of Creep Specimens in the Stacks

Once the specimen-position offset is established for the bottom half of the specimens, the number of total creep specimens for each grade of graphite is determined. It should be noted that the specimen stacking order for subsequent AGC irradiation capsules was changed from that initially established for the AGC-1 test train. In the initial AGC capsule design, AGC-1 utilized 0.25-in.-long NBG-25 graphite spacers between all creep specimens to separate them from each other. It was determined that this was not necessary, and most of the 0.25-in.-long NBG-25 graphite spacers were eliminated. This decision to eliminate the spacers increased the total number of creep specimens in the AGC capsules to 216 total specimens (or 36 matched pairs in each outer perimeter channel). This allowed more specimens per graphite grade to be irradiated within the AGC-2 capsule.

As discussed, the six outer stacks in the capsule allow the specimens in two of the channel stacks to be loaded at 13.8 MPa, while the other two pairs of channels are loaded at 17.2 and 20.7 MPa, respectively. Because two stacks are at similar applied stress levels, the specimen loading order can be shifted between the two stacks, allowing the same grade of graphite to be mechanically loaded over a broader neutron dose range, as illustrated in Figure 4. Assuming both stacks will have the same applied stress level, receive similar dose levels per position, and have a constant temperature allows this shifting of the specimens and, consequently, a more uniform, smoother dose profile for each graphite grade.

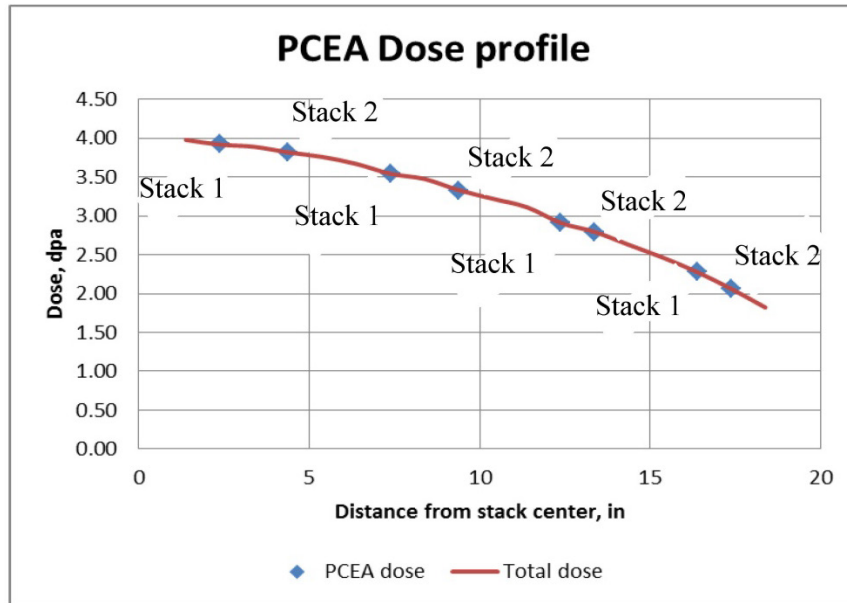


Figure 4. A typical dose profile for creep graphite specimens utilizing similar applied stress levels in matched stacks.

A final consideration when establishing the specimen loading positions is the grain orientation of the specimens. All AGC capsules attempt to account for the grain orientation to irradiation behavior. For extruded graphite grades, the against-grain (AG) and with-grain (WG) directions are obviously perpendicular and parallel to the extrusion direction, respectively. Isomolded grades have little to no grain direction and there is no consideration for their orientation. However, in the case of the vibration-molded graphites (i.e., NBG-17 and -18), there are actually two WG directions and one AG direction as a consequence of the fabrication process. The total number of WG and AG specimens is dependent upon the particular AGC capsule pair (i.e., AGC-1 and AGC-2 have the same number of specimens with similar orientation).

Once these considerations are accounted for, the dose-level profiles are determined for each graphite grade within each channel stack. It should be noted that due to the elimination of the majority of the NBG-25 spacers from the AGC-1 design, the dose-level profiles for each graphite grade have been altered for the succeeding AGC capsules.^[14,15,16] However, the changes are modest, allowing nearly direct comparison between AGC-1 and the subsequent AGC capsules.

3. AGC-2 TEST TRAIN CAPSULE

The AGC-2 capsule was irradiated in the ATR beginning with Cycle 149A on April 12, 2011, and ending with ATR Cycle 151B on May 5, 2012.^[17] The average estimated irradiation temperature for all samples was 600°C with a standard deviation of 65°C and a range of 705°C to 399°C. The average radiation dose of all specimens was 3 dpa with a standard deviation of 1 dpa and a range of 5 dpa to 1 dpa. While the temperature range was much better than the prototype AGC-1 irradiation capsule, the irradiation temperature range exceeded the design (600 ± 40°C).^[18] Estimates of AGC-2 dose, average temperature, and stress conditions are summarized in this report. Specific individual dose levels, temperature ranges, and stress conditions for all specimens contained within the irradiation capsule will be reported in the following AGC-2 analysis report. AGC-2 design documents and drawings pertinent to the AGC-2 graphite specimens have been reported in the previous AGC-2 graphite pre-irradiation data package, INL/EXT-10-19588.^[19]

The AGC-2 irradiation capsule is the companion capsule for AGC-1. The original AGC-2 capsule design was intended to be a mirror of AGC-1 but would be irradiated within ATR for twice as long to achieve the higher dose levels. However, due to the large and unintended temperature variation across the AGC-1 capsule, it was decided that AGC-1 would be exposed to the higher neutron dose (i.e., 3.5–7 dpa) to provide additional high dose data. Subsequently, the AGC-2 design was modified to provide irradiation data across the range of 1.5–5 dpa.^[17] The ATR irradiation cycles were chosen to achieve this new dose range.

While some significant modifications were made to the AGC-2 irradiation samples and layout (e.g., the elimination of the majority of NBG-25 spacers to provide more space for creep specimens), the overall design of AGC-2 was kept as close to AGC-1 as possible. All minor and experimental graphite grades were retained while only one alternate graphite grade was replaced with a new nuclear grade. This allows results from both capsules to be compared and combined into a larger data population.

3.1 Design Parameters of AGC-2 Test Train

It was decided that AGC-2 and subsequent capsules did not require the addition of SiC temperature monitors to provide independent temperature verification during capsule irradiation.^[20] Consequently, the central hole in each of the central piggyback specimens was not machined to accommodate the SiC temperature monitors. By eliminating the SiC monitors, the independent temperature monitoring capability for the AGC-2 capsule was excluded, but it was determined that being able to measure the changes to the thermal diffusivity at high temperatures was of more importance. Central holes in all subsequent AGC piggyback specimens for the remaining AGC irradiation capsules were eliminated.^[7]

As discussed previously, a majority of the 0.25-in.-long NBG-25 graphite spacers between all AGC-1 creep specimens was eliminated. Four spacers were left in each channel (two in the upper section of the channel and two in the lower section) to allow flux wires to be placed within them. Eliminating most of the spacers allowed 12 additional creep specimens to be tested within the AGC-2 capsule. The total number of creep specimens in the AGC-2 capsule was increased to 216 total specimens (or 36 matched pairs in each outer perimeter channel).^[18] This stacking configuration with minimal spacers will be utilized with subsequent AGC irradiation capsules (i.e., AGC-3, AGC-4, etc.).

3.2 AGC-2 Graphite Grades and Changes to Dimensions

One of the graphite grades in AGC-2 was changed by request of the graphite vendor (Mersen, USA). Piggyback specimens of graphite grade 2114 were directly substituted for graphite grade 2020 and irradiated within the AGC-2 central stack (axial spine of capsule). All other graphite grades irradiated within AGC-2 were similar to the graphite grades in AGC-1. However, the sample numbers for two major grades, H-451 and IG-430, were reduced to allow for more creep test specimens in the remaining major grade graphite.

Graphite grades used in AGC-2 were categorized as follows:

The major grades of the nuclear graphite to be tested in AGC-2 are similar to AGC-1 major grades and include NBG-17, NBG-18, PCEA, IG-110, H-451, and IG-430. Minor, alternate, and experimental grades of graphite are presented below.

1. Major graphite grades: NBG-17, NBG-18, PCEA, IG-110, H-451, and IG-430.
2. Minor graphite grades: NBG-25, NBG-10, HLM, PGX.
3. Alternate grades: PPEA, PCIB, and 2114 (replaced grade 2020).
4. Experimental grades: BAN and A3-3/A3-27 fuel compact matrix material.
5. Single crystal graphite: HOPG.

A more complete description of all of the graphite samples included in capsule AGC-2 is given in Table 1.^[18]

Table 1. Major, minor, alternate, and experimental graphite grades within the AGC-2 capsule.

Graphite Grade	Forming Method	Intended Purpose	AGC Code Letter
NBG-17	Vibrational molded	AREVA Next Generation Nuclear Plant design	A
NBG-18	Vibrational molded	Pebble Bed Modular Reactor (not currently being pursued)	B
H-451	Extruded	Historical grade (Reference grade)	C
PCEA	Extruded	AREVA Next Generation Nuclear Plant design	D
IG-110	Isostatically pressed	High Temperature Reactor – Pebble-Bed Module (China)	E
IG-430	Isostatically pressed	Candidate graphite	F
HOPG	Vapor deposited	Fundamental studies	G
A3 matrix	Hot pressed	Fuel matrix material	H
HLM	Molded	Low dose core component	I
PGX	Extruded	Low dose core component	J
PPEA	Extruded	Alternate candidate	L
NBG-25	Isostatically pressed	Low dose core component	M
PCIB	Isostatically pressed	Alternate candidate	P
BAN	Isostatically pressed and extruded	Experimental graphite	R
NBG-10	Isostatically pressed	Low dose core component	S
2114	Isostatically pressed	Candidate graphite	T

For grades NBG-17, NBG-18, and PCEA (codes A, B, and D) both WG and AG specimen orientations are included in the capsule.

3.3 AGC-2 Specimen Stack Positions

The final loading configuration for the outer channel/stacks was determined for each graphite grade to optimize the number of specimens for each grade, create a smooth irradiation profile for the creep and piggyback specimens, and to assure the proper position of creep specimens to create the matched-pairs.

A further decision was made to increase the creep specimen number population for the newer graphite grades because little-to-no irradiation data are available on these grades. Specifically, more specimens of graphite grades NBG-18 and PCEA were chosen to be irradiated instead of the IG-110, IG-430, and NBG-17 graphite grades.^[19] NBG-18 and PCEA were determined to have 16 specimens per applied stress level for a total of 48 specimens within AGC-2. Graphite grades IG-110 and IG-430 were represented by only 12 specimens per applied stress level, for a total of 36 specimens within AGC-2. Table 2 lists the total number of specimens irradiated per major graphite grade.

Table 2. Total number of irradiated-creep specimens in the AGC-2 test series capsule.

Graphite Grade	Number of Creep Specimens
PCEA	48
NBG-18	48
IG-110	36
IG-430	36
NBG-17	24
H-451	24
Total Creep	216

A final consideration before establishing the final loading configuration is the grain orientation of the specimens. A decision was made to have approximately 75% of the specimens be orientated in the WG direction and 25% of the specimens be AG. However, in the case of the vibration-molded graphite grades (i.e., NBG-17 and -18), there are actually two WG directions and one AG direction as a consequence of the fabrication process.^[2] As such, it was logical to split the WG and AG specimens evenly (i.e., 50/50 ratio) rather than following the 75/25 ratio established for the other specimens.

The orientation of the specimen is designated by the second digit in the sample identification number. Specimen identification numbers possessing a “W” in the second digit are specimens in the WG orientation (e.g., CW101). Specimen identification numbers possessing an “A” in the second digit are specimens machined from an AG orientation (e.g., DA402). As discussed previously, vibrationally molded grades are designated with an “L” or “P” for the two WG orientations (e.g., BP402 for an NBG-17 grade specimen).

The final loading configuration for AGC-2, including creep specimen matched-pair positions (above and below the capsule mid-plane), piggyback order, lower stack offset, and flux wire spacers, was mapped for each graphite specimen as it was loaded into the AGC-2 irradiation capsule during assembly (Table 3 through Table 6).^[18,21]

Table 3. AGC-2 loading order for Stacks 1 and 2.

S-1, Compressed				S-2, Compressed			
Work Order 137268 Loading Order	Work Order 137268 ID Number	Graphite Type	Initial Specimen COM Elevation (in)	Work Order 137268 Loading Order	Work Order 137268 ID Number	Graphite Type	Initial Specimen COM Elevation (in)
23	CW101	H451	19.500	23	EW0301	IG-110	19.500
22	1A	Flux Monitor	18.875	22	AW1707	NBG-17	18.875
21	DW101	PCEA	18.250	21	FW0301	IG-430	18.250
20	BW101	NBG-18	17.250	20	DA402	PCEA	17.250
19	EW0102	IG-110	16.250	19	BP402	NBG-18	16.250
18	FW0101	IG-430	15.250	18	AW103	NBG-17	15.250
17	DW102	PCEA	14.250	17	EW0302	IG-110	14.250
16	AY	Flux Monitor	13.625	16	2B	Flux Monitor	13.625
15	BW102	NBG-18	13.000	15	DW1103	PCEA	13.000
14	FW0102	IG-430	12.000	14	BW1103	NBG-18	12.000
13	EW0104	IG-110	11.000	13	CW1003	H451	11.000
12	DW1001	PCEA	10.000	12	AW1001	NBG-17	10.000
11	BW103	NBG-18	9.000	11	EW0303	IG-110	9.000
10	FW0103	IG-430	8.000	10	DA403	PCEA	8.000
9	1H	Flux Monitor	7.375	9	AW1708	NBG-17	7.375
8	CW102	H451	6.750	8	BP403	NBG-18	6.750
7	EW0201	IG-110	5.750	7	FW0302	IG430	5.750
6	DW1002	PCEA	4.750	6	AP402	NBG-17	4.750
5	BW1001	NBG-18	3.750	5	CW1101	H451	3.750
4	FW0104	IG-430	2.750	4	DW1104	PCEA	2.750
3	8H	Flux Monitor	2.125	3	37	Flux Monitor	2.125
2	AW101	NBG-17	1.500	2	BW1201	NBG-18	1.500
S-1, Uncompressed				S-2, Uncompressed			
Work Order 137268 Loading Order	Work Order 137268 ID Number	Graphite Type	Initial Specimen COM Elevation (in)	Work Order 137268 Loading Order	Work Order 137268 ID Number	Graphite Type	Initial Specimen COM Elevation (in)
36	AW102	NBG-17	-1.750	36	BW1202	NBG-18	-1.750
35	AO	Flux Monitor	-2.375	35	AW1709	NBG-17	-2.375
34	FW0201	IG-430	-3.000	34	DW1201	PCEA	-3.000
33	BW1002	NBG-18	-4.000	33	CW1102	H451	-4.000
32	DW1003	PCEA	-5.000	32	AP403	NBG-17	-5.000
31	EW0202	IG-110	-6.000	31	FW0303	IG-430	-6.000
30	CW103	H451	-7.000	30	BP501	NBG-18	-7.000
29	AL1402	NBG-17	-7.625	29	EW1509	IG-110	-7.625
28	FW0202	IG-430	-8.250	28	DA501	PCEA	-8.250
27	BW1003	NBG-18	-9.250	27	EW0304	IG-110	-9.250
26	DW1004	PCEA	-10.250	26	AW1002	NBG-17	-10.250
25	EW0203	IG-110	-11.250	25	CW1103	H451	-11.250
24	FW0203	IG-430	-12.250	24	BW1203	NBG-18	-12.250
23	BW1101	NBG-18	-13.250	23	DW1202	PCEA	-13.250
22	8U	Flux Monitor	-13.875	22	7D	Flux Monitor	-13.875
21	DW1101	PCEA	-14.500	21	EW0401	IG-110	-14.500
20	FW0204	IG-430	-15.500	20	AW1003	NBG-17	-15.500
19	EW0204	IG-110	-16.500	19	BP502	NBG-18	-16.500
18	BW1102	NBG-18	-17.500	18	DA502	PCEA	-17.500
17	DW1102	PCEA	-18.500	17	FW0304	IG-430	-18.500
16	AE	Flux Monitor	-19.125	16	EW1510	IG-110	-19.125
15	CW1002	H451	-19.750	15	EW0402	IG-110	-19.750
14	BP7 06	NBG-18	-20.375	14	J2 07	HLM	-20.375
13	L2 08	PPEA	-20.625	13	RW2 10	BAN	-20.625
12	K2 09	PGX	-20.875	12	H571	Compact Matrix	-20.875
11	P2-08	PCIB	-21.125	11	TP19	2114	-21.125
10	DW18 03	PCEA	-21.375	10	BP7 07	NBG-18	-21.375
9	M2 07	NBG-25	-21.625	9	L2 09	PPEA	-21.625
8	S2 07	NBG-10	-21.875	8	K2 10	PGX	-21.875
7	FW15 01	IG-430	-22.125	7	P2-09	PCIB	-22.125
6	EW14 01	IG-110	-22.375	6	DW18 04	PCEA	-22.375
5	J2 06	HLM	-22.625	5	M2-08	NBG-25	-22.625
4	RW2 09	BAN	-22.875	4	S2 08	NBG-10	-22.875
3	H562	Compact Matrix	-23.125	3	FW15 02	IG-430	-23.125
2	TP 18	2114	-23.375	2	EW14 02	IG-110	-23.375

Table 4. AGC-2 loading order for Stacks 3 and 4.

S-3, Compressed				S-4, Compressed			
Work Order 137268 Loading Order	Work Order 137268 ID Number	Graphite Type	Initial Specimen COM Elevation (in)	Work Order 137268 Loading Order	Work Order 137268 ID Number	Graphite Type	Initial Specimen COM Elevation (in)
23	CW1202	H451	19.500	23	EW0601	IG-110	19.500
22	TP 27	2114	18.875	22	AX	Flux Monitor	18.875
21	DW1203	PCEA	18.250	21	FW0602	IG-430	18.250
20	BW1301	NBG-18	17.250	20	DA503	PCEA	17.250
19	EW0403	IG-110	16.250	19	BP503	NBG-18	16.250
18	FW0401	IG-430	15.250	18	AW1103	NBG-17	15.250
17	DW1204	PCEA	14.250	17	EW0602	IG-110	14.250
16	2U	Flux Monitor	13.625	16	18	Flux Monitor	13.625
15	BW1302	NBG-18	13.000	15	DW1403	PCEA	13.000
14	FW0402	IG-430	12.000	14	BW1503	NBG-18	12.000
13	EW0404	IG-110	11.000	13	CW1303	H451	11.000
12	DW1301	PCEA	10.000	12	AW1201	NBG-17	10.000
11	BW1303	NBG-18	9.000	11	EW0603	IG-110	9.000
10	FW0404	IG-430	8.000	10	DA601	PCEA	8.000
9	TP 12	2114	7.375	9	AR	Flux Monitor	7.375
8	CW1203	H451	6.750	8	BP601	NBG-18	6.750
7	EW0501	IG-110	5.750	7	FW0603	IG-430	5.750
6	DW1302	PCEA	4.750	6	AP501	NBG-17	4.750
5	BW1401	NBG-18	3.750	5	CW201	H451	3.750
4	FW0501	IG-430	2.750	4	DW1404	PCEA	2.750
3	8Y	Flux Monitor	2.125	3	3F	Flux Monitor	2.125
2	AW1101	NBG-17	1.500	2	BW1601	NBG-18	1.500
S-3, Uncompressed				S-4, Uncompressed			
Work Order 137268 Loading Order	Work Order 137268 ID Number	Graphite Type	Initial Specimen COM Elevation (in)	Work Order 137268 Loading Order	Work Order 137268 ID Number	Graphite Type	Initial Specimen COM Elevation (in)
36	AW1102	NBG-17	-1.750	36	BW1602	NBG-18	-1.750
35	TP24	2114	-2.375	35	5B	Flux Monitor	-2.375
34	FW0502	IG-430	-3.000	34	DW1502	PCEA	-3.000
33	BW1402	NBG-18	-4.000	33	CW202	H451	-4.000
32	DW1303	PCEA	-5.000	32	AP502	NBG-17	-5.000
31	EW0502	IG-110	-6.000	31	FW0604	IG-430	-6.000
30	CW1301	H451	-7.000	30	BP602	NBG-18	-7.000
29	TP25	2114	-7.625	29	AL1403	NBG-17	-7.625
28	FW0503	IG-430	-8.250	28	DA602	PCEA	-8.250
27	BW1403	NBG-18	-9.250	27	EW0604	IG-110	-9.250
26	DW1304	PCEA	-10.250	26	AW1202	NBG-17	-10.250
25	EW0503	IG-110	-11.250	25	CW203	H451	-11.250
24	FW0504	IG-430	-12.250	24	BW1603	NBG-18	-12.250
23	BW1501	NBG-18	-13.250	23	DW1503	PCEA	-13.250
22	1Y	Flux Monitor	-13.875	22	2Y	Flux Monitor	-13.875
21	DW1401	PCEA	-14.500	21	EW0701	IG-110	-14.500
20	FW0601	IG-430	-15.500	20	AW1203	NBG-17	-15.500
19	EW0504	IG-110	-16.500	19	BP603	NBG-18	-16.500
18	BW1502	NBG-18	-17.500	18	DA701	PCEA	-17.500
17	DW1402	PCEA	-18.500	17	FW0701	IG-430	-18.500
16	TP26	2114	-19.125	16	8Z	Flux Monitor	-19.125
15	CW1302	H451	-19.750	15	EW0702	IG-110	-19.750
14	DW18 05	PCEA	-20.375	14	L3 05	PPEA	-20.375
13	M2-09	NBG-25	-20.625	13	L3 01	PPEA	-20.625
12	S2 09	NBG-10	-20.875	12	K3 02	PGX	-20.875
11	FW1503	IG-430	-21.125	11	P3-01	PCIB	-21.125
10	EW1403	IG-110	-21.375	10	DW18 06	PCEA	-21.375
9	J2 08	HLM	-21.625	9	M2-10	NBG-25	-21.625
8	RW4 01	BAN	-21.875	8	S2 10	NBG-10	-21.875
7	H572	Compact Matrix	-22.125	7	P3-06	PCIB	-22.125
6	TP 20	2114	-22.375	6	K3 05	PGX	-22.375
5	L3 04	PPEA	-22.625	5	J2 09	HLM	-22.625
4	L2 10	PPEA	-22.875	4	RW4 02	BAN	-22.875
3	K3 01	PGX	-23.125	3	H581	Compact Matrix	-23.125
2	P2-10	PCIB	-23.375	2	TP21	2114	-23.375

Table 5. AGC-2 loading order for Stacks 5 and 6.

S-5, Compressed				S-6, Compressed			
Work Order 137268 Loading Order	Work Order 137268 ID Number	Graphite Type	Initial Specimen COM Elevation (in)	Work Order 137268 Loading Order	Work Order 137268 ID Number	Graphite Type	Initial Specimen COM Elevation (in)
23	CW301	H451	19.500	23	EW0901	IG-110	19.500
22	EW1511	IG-110	18.875	22	TP16	2114	18.875
21	DW1504	PCEA	18.250	21	FW0903	IG-430	18.250
20	BW201	NBG-18	17.250	20	DA303	PCEA	17.250
19	EW0703	IG-110	16.250	19	BP401	NBG-18	16.250
18	FW0703	IG-430	15.250	18	AW1303	NBG-17	15.250
17	DW1601	PCEA	14.250	17	EW0902	IG-110	14.250
16	57	Flux Monitor	13.625	16	5F	Flux Monitor	13.625
15	BW202	NBG-18	13.000	15	DW201	PCEA	13.000
14	FW0704	IG-430	12.000	14	BW403	NBG-18	12.000
13	EW0704	IG-110	11.000	13	CW402	H451	11.000
12	DW1602	PCEA	10.000	12	AW1401	NBG-17	10.000
11	BW203	NBG-18	9.000	11	EA902	IG-110	9.000
10	FW0801	IG-430	8.000	10	DA302	PCEA	8.000
9	AW1710	NBG-17	7.375	9	TP17	2114	7.375
8	CW302	H451	6.750	8	BP303	NBG-18	6.750
7	EW0801	IG-110	5.750	7	FW0904	IG-430	5.750
6	DW1603	PCEA	4.750	6	AP503	NBG-17	4.750
5	BW301	NBG-18	3.750	5	CW403	H451	3.750
4	FW0802	IG-430	2.750	4	DW202	PCEA	2.750
3	AL	Flux Monitor	2.125	3	5H	Flux Monitor	2.125
2	AW1301	NBG-17	1.500	2	BW501	NBG-18	1.500
S-5, Uncompressed				S-6, Uncompressed			
Work Order 137268 Loading Order	Work Order 137268 ID Number	Graphite Type	Initial Specimen COM Elevation (in)	Work Order 137268 Loading Order	Work Order 137268 ID Number	Graphite Type	Initial Specimen COM Elevation (in)
36	AW1302	NBG-17	-1.750	36	BW502	NBG-18	-1.750
35	EW1508	IG-110	-2.375	35	TP13	2114	-2.375
34	FW0803	IG-430	-3.000	34	DW203	PCEA	-3.000
33	BW302	NBG-18	-4.000	33	CW501	H451	-4.000
32	DW1604	PCEA	-5.000	32	AP601	NBG-17	-5.000
31	EW0802	IG-110	-6.000	31	FW1001	IG-430	-6.000
30	CW303	H451	-7.000	30	BP302	NBG-18	-7.000
29	EW1507	IG-110	-7.625	29	TP14	2114	-7.625
28	FW0804	IG-430	-8.250	28	DA203	PCEA	-8.250
27	BW303	NBG-18	-9.250	27	EW0904	IG-110	-9.250
26	DW1701	PCEA	-10.250	26	AW1402	NBG-17	-10.250
25	EW0803	IG-110	-11.250	25	CW503	H451	-11.250
24	FW0901	IG-430	-12.250	24	BW503	NBG-18	-12.250
23	BW401	NBG-18	-13.250	23	DW204	PCEA	-13.250
22	7Z	Flux Monitor	-13.875	22	7Y	Flux Monitor	-13.875
21	DW1702	PCEA	-14.500	21	EW1001	IG-110	-14.500
20	FW0902	IG-430	-15.500	20	AW1403	NBG-17	-15.500
19	EW0804	IG-110	-16.500	19	BP301	NBG-18	-16.500
18	BW402	NBG-18	-17.500	18	DA202	PCEA	-17.500
17	DW1704	PCEA	-18.500	17	FW1002	IG-430	-18.500
16	EW1506	IG-110	-19.125	16	TP15	2114	-19.125
15	CW401	H451	-19.750	15	EW1002	IG-110	-19.750
14	J2 10	HLM	-20.375	14	CW14 06	H451	-20.375
13	RW4 03	BAN	-20.625	13	M2-12	NBG-25	-20.625
12	H582	Compact Matrix	-20.875	12	S2 12	NBG-10	-20.875
11	TP 22	2114	-21.125	11	K306	PGX	-21.125
10	L3 06	PPEA	-21.375	10	EW14 06	IG-110	-21.375
9	L3 02	PPEA	-21.625	9	J2 11	HLM	-21.625
8	K3 03	PGX	-21.875	8	RW4 04	BAN	-21.875
7	P3-02	PCIB	-22.125	7	H591	Compact Matrix	-22.125
6	DW18 07	PCEA	-22.375	6	TP23	2114	-22.375
5	M2-11	NBG-25	-22.625	5	P3-04	PCIB	-22.625
4	S2 11	NBG-10	-22.875	4	L3 03	PPEA	-22.875
3	P3-05	PCIB	-23.125	3	K3 04	PGX	-23.125
2	EW14 05	IG-110	-23.375	2	P3-03	PCIB	-23.375

Table 6. AGC-2 center channel loading order.

S-7, Uncompressed			
Work Order 137268 Loading Order	Work Order 137268 ID No.	Graphite Type	Initial Specimen COM Elevation (in)
170	A3P43Z12	A3 matrix	18.375
169	J1 11	HLM	18.125
168	K2 02	PGX	17.875
167	L2 01	PPEA	17.625
166	M1-12	NBG-25	17.375
165	TP 11	2114	17.125
164	P2-01	PCIB	16.875
163	RW2 02	BAN	16.625
162	S1 11	NBG-10	16.375
161	CPB101	H451	16.125
160	BP7 08	NBG-18	15.875
159	DW18 08	PCEA	15.625
158	BP7 09	NBG-18	15.375
157	FW15 04	IG-430	15.125
156	EW14 04	IG-110	14.875
155	CW14 05	H451	14.625
154	A3H08Z19	A3 matrix	14.375
153	J1 10	HLM	14.125
152	K2 01	PGX	13.875
151	L1 10	PPEA	13.625
150	M1-11	NBG-25	13.375
149	TP-10	2114	13.125
148	P1-10	PCIB	12.875
147	RW2 01	BAN	12.625
146	S1 10	NBG-10	12.375
145	CPB91	H451	12.125
144	BP7 10	NBG-18	11.875
143	DA8 05	PCEA	11.625
142	AP7 08	NBG-17	11.375
141	FW15 05	IG-430	11.125
140	EW15 03	IG-110	10.875
139	CW14 04	H451	10.625
138	H521	Compact matrix	10.375
137	J1 09	HLM	10.125
136	K1 10	PGX	9.875
135	L1 09	PPEA	9.625
134	M1-10	NBG-25	9.375
133	TP 09	2114	9.125

S-7, Uncompressed			
Work Order 137268 Loading Order	Work Order 137268 ID No.	Graphite Type	Initial Specimen COM Elevation (in)
132	P1-09	PCIB	8.875
131	RW1 10	BAN	8.625
130	S1 09	NBG-10	8.375
129	CPB81	H451	8.125
128	BW17 01	NBG-18	7.875
127	DA8 04	PCEA	7.625
126	AP7 09	NBG-17	7.375
125	FW15 06	IG-430	7.125
124	EW15 02	IG-110	6.875
123	CW14 03	H451	6.625
122	H512	Compact matrix	6.375
121	J1 08	HLM	6.125
120	K1 09	PGX	5.875
119	L1 08	PPEA	5.625
118	M1-09	NBG-25	5.375
117	TP 08	2114	5.125
116	P1-08	PCIB	4.875
115	RW1 09	BAN	4.625
114	S1 08	NBG-10	4.375
113	CPB71	H451	4.125
112	BW17 09	NBG-18	3.875
111	DA8 03	PCEA	3.625
110	AP7 10	NBG-17	3.375
109	FW16 01	IG-430	3.125
108	EW15 01	IG-110	2.875
107	CPB151	H451	2.625
106	A3P33Z09	A3 matrix	2.375
105	J1 07	HLM	2.125
104	K1 08	PGX	1.875
103	L1 07	PPEA	1.625
102	M1-08	NBG-25	1.375
101	TP 07	2114	1.125
100	P1-07	PCIB	0.875
99	RW1 08	BAN	0.625
98	S1 07	NBG-10	0.375
97	CPB61	H451	0.125
96	BW17 08	NBG-18	-0.125
95	DA8 02	PCEA	-0.375
94	AW17 01	NBG-17	-0.625

S-7, Uncompressed			
Work Order 137268 Loading Order	Work Order 137268 ID No.	Graphite Type	Initial Specimen COM Elevation (in)
93	FW15 12	IG-430	-0.875
92	EW14 12	IG-110	-1.125
91	CPB141	H451	-1.375
90	A3H08Z07	A3 matrix	-1.625
89	J1 06	HLM	-1.875
88	K1 07	PGX	-2.125
87	L1 06	PPEA	-2.375
86	M1-07	NBG-25	-2.625
85	TP 06	2114	-2.875
84	P1-06	PCIB	-3.125
83	RW1 07	BAN	-3.375
82	S1 06	NBG-10	-3.625
81	CPB51	H451	-3.875
80	BW17 07	NBG-18	-4.125
79	DA8 01	PCEA	-4.375
78	AW17 02	NBG-17	-4.625
77	FW15 11	IG-430	-4.875
76	EW14 11	IG-110	-5.125
75	CPB131	H451	-5.375
74	A3P43Z03	A3 matrix	-5.625
73	J1 05	HLM	-5.875
72	K1 06	PGX	-6.125
71	L1 05	PPEA	-6.375
70	M1-06	NBG-25	-6.625
69	TP 05	2114	-6.875
68	P1-05	PCIB	-7.125
67	RW1 06	BAN	-7.375
66	S1 05	NBG-10	-7.625
65	CPB41	H451	-7.875
64	BW17 05	NBG-18	-8.125
63	DW18 12	PCEA	-8.375
62	AW17 03	NBG-17	-8.625
61	FW15 10	IG-430	-8.875
60	EW14 10	IG-110	-9.125
59	CPB121	H451	-9.375
58	H491	Compact matrix	-9.625
57	J1 04	HLM	-9.875
56	K1 05	PGX	-10.125
55	L1 04	PPEA	-10.375

S-7, Uncompressed			
Work Order 137268 Loading Order	Work Order 137268 ID No.	Graphite Type	Initial Specimen COM Elevation (in)
54	M1-05	NBG-25	-10.625
53	TP 04	2114	-10.875
52	P1-04	PCIB	-11.125
51	RW1 05	BAN	-11.375
50	S1 04	NBG-10	-11.625
49	CPB31	H451	-11.875
48	BW17 04	NBG-18	-12.125
47	DW18 11	PCEA	-12.375
46	AW17 06	NBG-17	-12.625
45	FW15 09	IG-430	-12.875
44	EW14 09	IG-110	-13.125
43	CPB111	H451	-13.375
42	H482	Compact matrix	-13.625
41	J1 03	HLM	-13.875
40	K1 04	PGX	-14.125
39	L1 03	PPEA	-14.375
38	M1-04	NBG-25	-14.625
37	TP-03	2114	-14.875
36	P1-03	PCIB	-15.125
35	RW1 04	BAN	-15.375
34	S1 03	NBG-10	-15.625
33	CPB21	H451	-15.875
32	BW17 03	NBG-18	-16.125
31	DW18 10	PCEA	-16.375
30	AW17 05	NBG-17	-16.625
29	FW15 08	IG-430	-16.875
28	EW14 08	IB-110	-17.125
27	CA11 02	H451	-17.375
26	A3P33Z20	A3 matrix	-17.625
25	J1 02	HLM	-17.875
24	K1 03	PGX	-18.125
23	L1 02	PPEA	-18.375
22	M1-02	NBG-25	-18.625
21	TP 02	2114	-18.875
20	P1-02	PCIB	-19.125
19	RW1 03	BAN	-19.375
18	S1 02	NBG-10	-19.625
17	CPB11	H451	-19.875
16	BW17 02	NBG-18	-20.125

S-7, Uncompressed			
Work Order 137268 Loading Order	Work Order 137268 ID No.	Graphite Type	Initial Specimen COM Elevation (in)
15	DW18 09	PCEA	-20.375
14	AW17 04	NBG-17	-20.625
13	FW15 07	IG-430	-20.875
12	EW14 07	IG-110	-21.125
11	CA11 01	H451	-21.375
10	H472	Compact matrix	-21.625
9	J1 01	HLM	-21.875
8	K1 01	PGX	-22.125
7	L1 01	PPEA	-22.375
6	M1-01	NBG-25	-22.625
5	TP 01	2114	-22.875
4	P1-01	PCIB	-23.125
3	RW1 02	BAN	-23.375
2	CPB1	H451	-23.625
1	S101	NBG-10	-23.875
* Note: Specimen S101 (grade NBG-10) was lost during the disassembly of the AGC-2 irradiation capsule.			

Following irradiation in the ATR at INL, the AGC-2 capsule was disassembled.^[22,23] All specimens recovered from disassembly were visually inspected and physically measured within the INL Carbon Characterization Laboratory (CCL) before storage within the irradiated graphite storage vault. It should be noted that NBG-25 specimen S101 was lost during AGC-2 disassembly activities. After accounting for all recovered specimens from the AGC-2 capsule, PIE and testing were performed for each specimen at the INL Carbon Characterization Laboratory.

4. TESTING

A significant level of preparation was needed to meet Nuclear Quality Assurance Level 2 quality requirements prior to actual material property testing. An approved characterization plan was developed that was dependent upon the two graphite specimen geometries and on the material properties to be measured.^[23] In general, all testing was performed through American Society for Testing and Materials approved standards; however, due to the small size of the graphite specimens, some methods required modification and/or variation of the testing standards. Details of these testing standard variations, along with equipment calibration, personnel training on testing methodology, and data acquisition, are specified in a specimen characterization plan.

Thermal diffusivity, coefficient of thermal expansion (CTE), electrical resistivity, elastic modulus, and mass and dimensions measurements were performed on the AGC-2 irradiated specimens. These measurements were performed per “AGC-2 Graphite Specimen Postirradiation Characterization Plan,” PLN-4657. This plan describes in detail the measurement techniques, equipment, and standards used to gather the data presented here.

Data gathered for the characterization of AGC-2 specimens are contained in the appendices of this report. Appendix A contains plots of the individual data points for each specimen. Shown by the dashed lines in each plot are the upper and lower limits of the interquartile range (IQR). These limits are established by either the least or greatest value in the data or by multiplying the IQR by 1.5 and adding or subtracting this value from the third and first quartile. Any datum value outside of these established limits is considered a suspected outlier of the established pattern. However, it is important to note that these outlying values are not only subject to measurement variability but also material and dose variability and, therefore, cannot necessarily be discarded.

These outlying values are examined in the context of the entire data set, including pre-irradiation data. Other statistical parameters are calculated and presented in the tables of Appendix B. The mean, standard deviation, and coefficient of variance (COV) are all calculated for the various measurement data sets and graphite types. Upper and lower limits called out in the tables of Appendix B are the IQR limits described above. Raw, tabulated data can be found in the Nuclear Data Management and Analysis System database, including parameters specified by the applicable American Society for Testing and Materials standard (e.g., dates, performer identifier, and room conditions).

There are many ways to combine and compare the data presented here. In doing so, the validity of the data is exercised and scrutinized. First, the data sets are evaluated independently, utilizing the statistical analysis described above. Additionally, a limited comparison of pre- and post-irradiation values is made for each graphite grade to illustrate the effects of irradiation and applied stress (where applicable). Note that pre-irradiation properties were measured using the same techniques, equipment, and standards per PLN-3267, "AGC-2 Characterization Plan." Pre-irradiation data for the AGC-2 specimens can be found in INL/EXT-10-19588, "AGC-2 Graphite Preirradiation Data Package." These initial comparisons provide an initial examination of the data for trends and correlations that are intuitive and logical. In this way, the physical and thermal post-irradiation property measurements are vetted.

The data presented here include all AGC-2 specimens that were irradiated. Variables of irradiation temperature and dose are not considered for any property measurement in Figure 5Figure 9. The data are presented simply to illustrate the initial trends and correlations in irradiation induced material property changes. Data presented in Figure 10Figure 11Figure 13,Figure 14 demonstrate the induced changes as a function of either received irradiation dose or irradiation temperature. A more detailed analysis and trends in the data will be reported within the subsequent AGC-2 analysis report. From initial estimates of the as-run AGC-2 irradiation and temperature analysis, the average irradiation temperature is 600°C with a standard deviation of 65°C and a range of 705°C to 399°C. The average radiation dose of all specimens is 3 dpa with a standard deviation of 1 dpa and a range of 5 dpa to 1 dpa.

4.1 Dimensions, Mass, and Density

Specimens are weighed and dimensionally measured at room temperature^[23]. Plots of the measured mass, dimensions, and density for all AGC-2 irradiated specimens are shown in Figures A-1 through A-84 (see Appendix A). Prior to irradiation, the freshly machined surfaces produced consistent dimensional measurements with a COV of less than 0.05% for all specimens. Following irradiation, the surfaces are more irregular and inconsistent, resulting in a COV between 0.25% and 0.96%. (Table B-1 and B-2). Similar distributions in the pre- and post-irradiation mass data were observed with no difference in mass observed between pre- and post-irradiation measurements outside of the measurement uncertainty.

Figure 5 illustrates the overall volume decrease for the irradiated specimens as a function of graphite type and stress. Detailed volume dependency on irradiation dose and irradiation temperature will be addressed within the subsequent AGC-2 analysis report. As expected, all graphite types experienced an overall shrinkage due to neutron irradiation. Shrinkage for all graphite types increased as the specimen stress increased. This is consistent with trends observed in the literature.^[24,25]

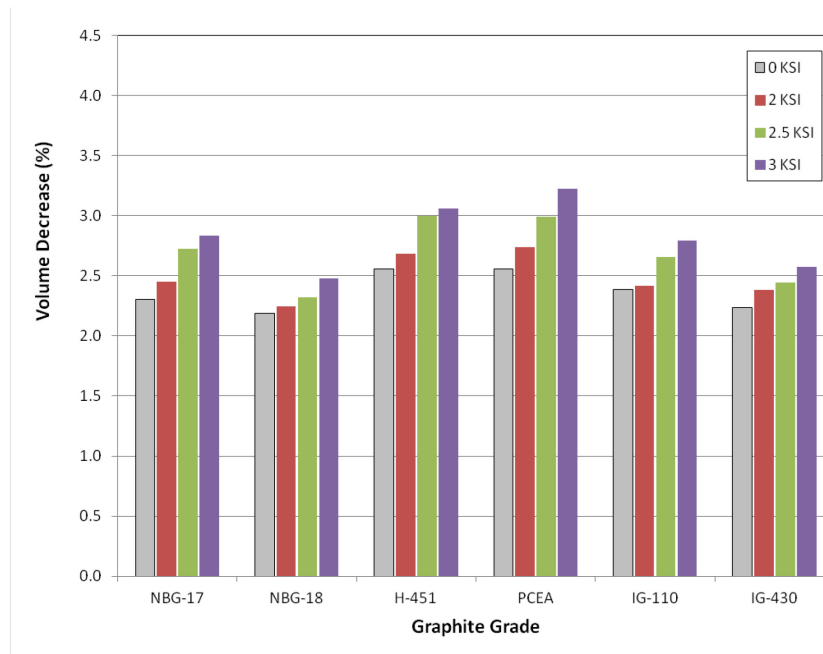


Figure 5. Volume decrease due to irradiation creep for six major grades of graphite. The dimensional change dependency on irradiation dose and irradiation temperature is not presented.

Naturally, a reduction in volume with no change in mass will result in an increase in density, Figure 6. As expected, density changes in a linear fashion with the decrease in volume and therefore demonstrates a general increase between 2.2% and 3.2%. The COV for density values of irradiated specimens of the individual graphite types was below 0.85%, Table B-4. Detailed density analysis and trends will be addressed within the subsequent AGC-2 analysis report.

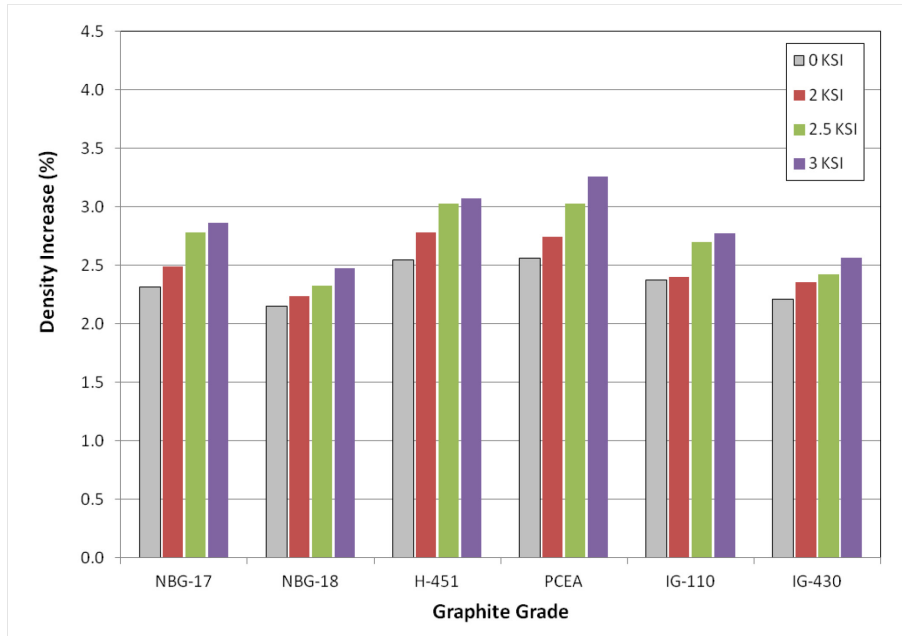


Figure 6. Density increase due to volume shrinkage for six major grades of graphite and four stress conditions. The density change dependency on irradiation dose and irradiation temperature is not presented.

4.2 Elastic Modulus

Elastic properties were measured with two dynamic nondestructive testing techniques at room temperature.^[23] In the fundamental frequency testing technique, Young's modulus is derived from the natural frequency of the creep specimens oscillating in the flexural mode. Due to the geometry of the specimens, the shear modulus can not be determined using this technique. However, both Young's modulus and shear modulus can be determined using the sonic velocity technique. In this case, an ultrasonic longitudinal or shear wave is sent through the specimen. The time it takes for this wave to pass through the specimen and the length of the specimen are used to determine the sonic velocity. Young's modulus and shear modulus can then be calculated from this time-of-flight measurement.

Young's modulus, determined by measurement of fundamental frequency, is plotted in Figures A-109 through A-114, and the statistical data are contained in Table B-8. Statistically, these data are well-behaved, with the IQR analysis showing no significant outliers. Figures A-121 through A-132 contain plots of Young's and shear moduli determined from the measurement of sonic velocity. Statistical parameters are shown in Tables B-10 and B-11 for Young's and shear moduli, respectively, and again the IQR analysis does not reveal any inconsistency or significant outliers. The spread in all modulus data is reasonable with the COV ~5%. The relatively high 10.8% COV value achieved in the PCEA graphite grade is due to the increased flaw and crack distribution within the microstructure of the graphite material.

It should be noted that for AGC-2 specimens the dynamic Young's modulus values determined by sonic velocity testing techniques are generally 2–3 GPa higher than the measurements obtained by the fundamental frequency testing technique (Appendix A). This difference between modulus measurements between the two standards has been noted for a number of years and was finally addressed in the latest version of the sonic velocity standard (ASTM-769-09).^[26] In this latest ASTM standard version the Young's modulus value is calculated from the time-of-flight measurement utilizing a correction factor designated as the Poisson's Factor (C_v) which is normally valued at 0.9. Calculating the modulus using the Poisson's Factor effectively lowers the value by 10%, bringing the measured sonic velocity values to values arrived at by the fundamental frequency test method.

However, AGC-2 pre-irradiation testing was performed under the previous ASTM sonic velocity standard, ASTM-769-98 (reapproved 2005),^[27] which does not use the Poisson Factor to calculate the modulus values. The AGC-2 Characterization Plan (PLN-4657) specifies that the testing standards used to measure the material properties for the graphite specimens must be the same version before and after irradiation. Using the same ASTM test method version assures the unirradiated and irradiated measurements will be consistent and comparable without testing method bias.

Since only the measured data is being corrected by the Poisson's Factor, and not the actual testing technique itself, the pre- and post-irradiation AGC-2 sonic velocity data can be re-calculated. Recalculating the data will be considered within the subsequent AGC-2 analysis report to provide a more accurate modulus value from the sonic velocity testing method.

While the absolute Young's modulus values between sonic velocity and fundamental frequency may be different for the AGC-2 measurement, when making relative comparisons between pre- and post-irradiation measurements, the difference is consistent between the two techniques. Dynamic Young's modulus generally increases when pre- and post-irradiation Young's modulus values (as a percentage) are compared. This increase is shown to be similar for the fundamental frequency and sonic velocity testing techniques, Figure 7 and Figure 8. Also notable is the modulus increase correlation with specimens tested in compressive stress. In general, the overall irradiated modulus increase is less for higher compressive stressed specimens. Detailed Young's modulus dependency on irradiation dose and irradiation temperature will be addressed within the subsequent AGC-2 analysis report.

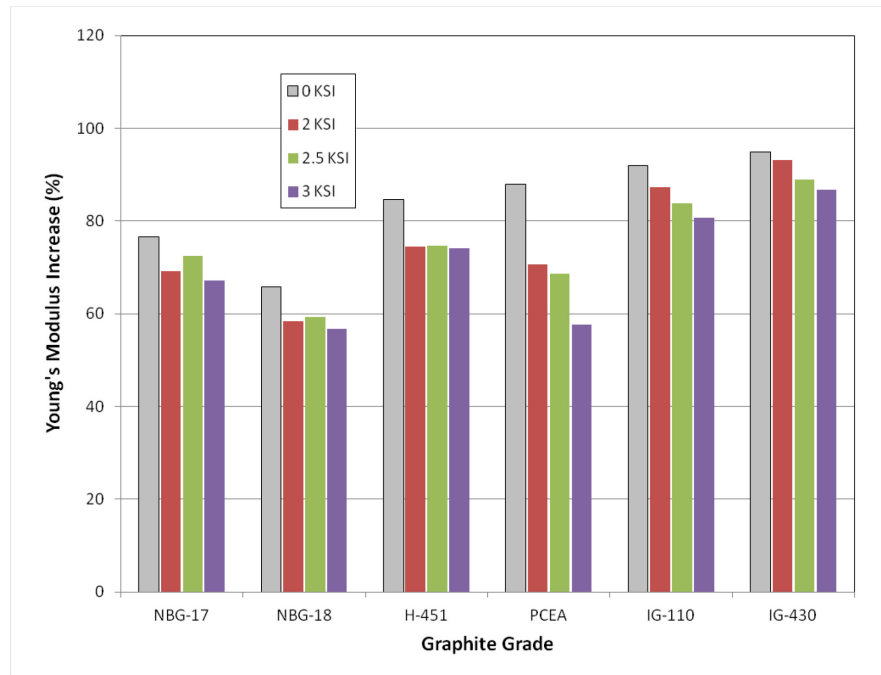


Figure 7. Young's modulus derived from the measurement of fundamental frequency for six grades of graphite and four different stress conditions. The Young's modulus dependency on irradiation dose and irradiation temperature is not presented.

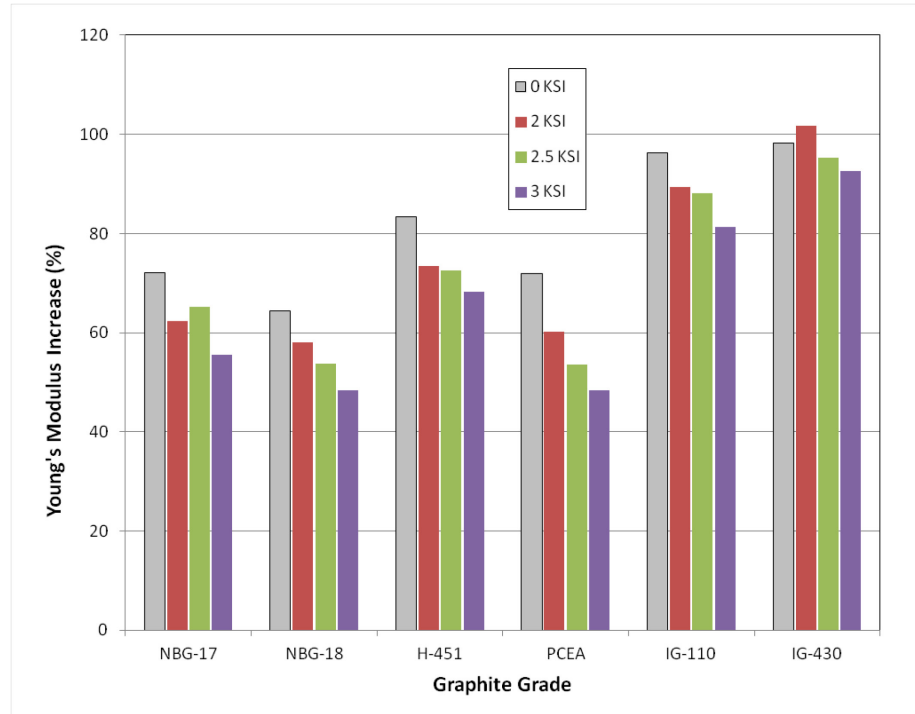


Figure 8. Young's modulus derived from the measurement of ultrasonic velocity for six grades of graphite and four different stress conditions. The Young's modulus dependency on irradiation dose and irradiation temperature is not presented.

4.3 Resistivity

Plots of electrical resistivity are shown in Figures A-115 through A-120 for graphite grades of PCEA, NBG-18, H-451, IG-110, IG-430, and NBG-17. All resistivity measurements were performed only on creep specimens.^[23] Statistical parameters can be found in Table B-9. The resistivity data are well behaved with no outliers and a COV ranging from 2.7% to 4.8%.

Specimen resistivity is measured at room temperature using a four point testing method. A constant current is passed through the long axis of the specimen, and voltage is measured at a fixed distance along the specimen axis. Resistivity is calculated from these values and the specimen geometry. Figure 9 indicates an overall general increase in resistivity after neutron irradiation. This increase is believed to occur primarily from atomic level defects that disrupt the flow of electrons. It is interesting to note that stress may initially have an effect on electrical resistivity but the effects appear to saturate with only limited changes with increasing the stress. Detailed electrical resistivity analysis including irradiation dose and irradiation temperature effects will be addressed within the subsequent AGC-2 analysis report.

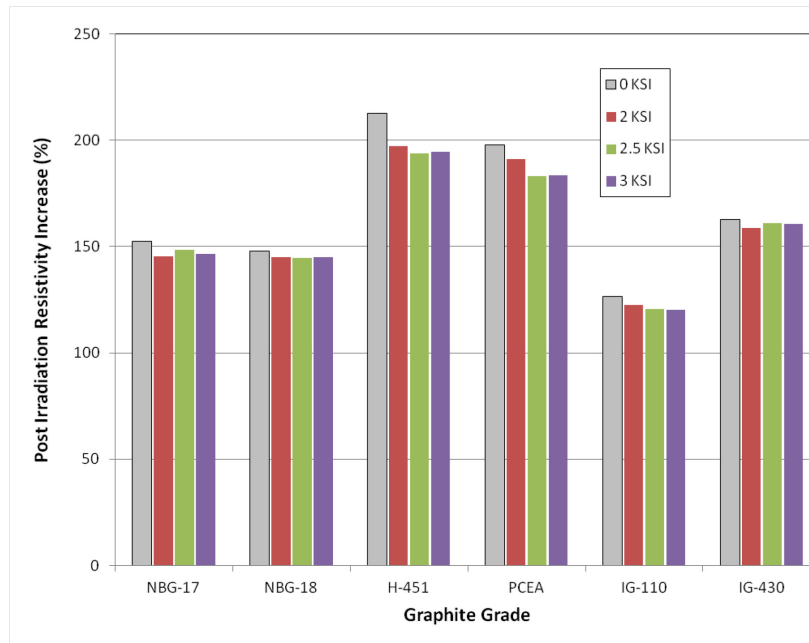


Figure 9. Electrical resistivity for six grades of graphite and four different stress conditions. The electrical resistivity dependency on irradiation dose and irradiation temperature is not presented.

4.4 Thermal Diffusivity

Thermal diffusivity was measured using a laser flash technique.^[23] Because annealing of irradiation damage begins to take place at temperatures above the irradiation temperature, measurements of thermal diffusivity were limited to 500°C (100°C below the average AGC-2 specimen irradiation temperature).

Plots of thermal diffusivity are shown in Figures A-133 through A-192. Discrete temperatures of 100, 300, and 500°C were statistically evaluated. Tables B-16a through B-18c contain values of the mean, standard deviation, and COV. Considering the complexities associated with measuring the thermal diffusivity of irradiated specimens, the COVs are reasonable, ranging between ~4% and ~8%. The high COV for the A3 matrix material may be explained from the fabrication history. A3 fuel compact matrix material is fabricated from a composite mixture of graphitic flake material and phenolic resins. In addition, the AGC-2 A3 matrix specimens were fabricated from a small, non-production sized batch that mixed the resins and graphitic flake material and individually cold pressed the mixture into solid specimen compacts. These compacts are then baked to a relatively low temperature of 1800°C, which is not high enough to induce graphitization of the mixture (a minimum of 2200°C is needed to begin graphitization). With inconsistencies due to the limited batch size, mixing, and/or individual die pressing of the mixture, it is not surprising that these specimens have larger thermal diffusivity variation. In addition, the higher variation in diffusivity of PCEA is most likely due to the higher level of microstructure defects from fabrication (increased porosity).

As stated earlier, the material property change dependence on dose and irradiation temperature have not been evaluated up to this point. Figure 10 and Figure 11 illustrate the ratio of irradiated to unirradiated thermal diffusivity as a function of dose and as a function of irradiation temperature, respectively, at 500°C for graphite type IG-110. Both plots for IG-110 and the other graphite types indicate that the general change in diffusivity is neither a function of dose or irradiation temperature. However, due to the singular nature of the specimen location in the experiment and the dose and temperature profiles along the axis of the experiment, it is not possible to separate the two. Specimens located in the center of the AGC-2 irradiation capsule experienced the highest radiation dose and temperature while those further from the centerline correspondingly received a lower dose at a lower irradiation temperature. With this correspondence between dose and temperature, there is no set of specimens with a variation in temperature for a constant dose and vice-versa. Therefore, the constant delta in diffusivity displayed in Figure 10 and Figure 11 is possibly a function of both temperature and dose. However, because they do display relatively constant values of diffusivity change (i.e., the property change has saturated), it may be possible to average all specimens of a particular type of graphite to evaluate other variables, as was done in Figure 12. Here the ratio of irradiated to unirradiated diffusivity is shown as a function of specimen temperature for seven graphite types. The plot shows that the greatest change in diffusivity occurs at lower temperatures. All graphite grades follow this similar trend. Detailed diffusivity dependency analysis including irradiation dose and irradiation temperature dependency will be addressed within the subsequent AGC-2 analysis report.

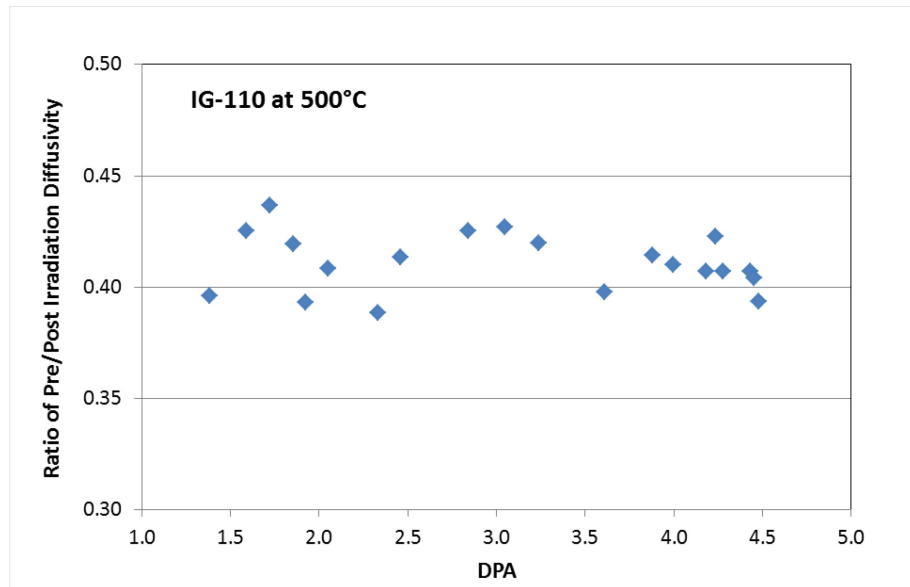


Figure 10. Ratio of irradiated diffusivity to unirradiated diffusivity for specimens of IG-110 at 500°C as a function of irradiation dose. Thermal diffusivity dependency on irradiation temperature is not presented.

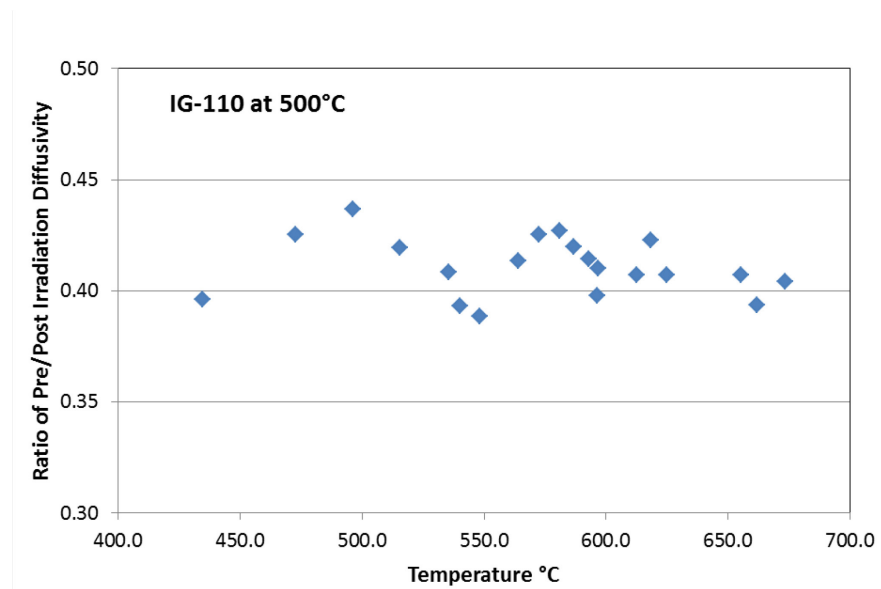


Figure 11. Ratio of irradiated diffusivity to unirradiated diffusivity for specimens of IG-110 at 500°C as a function of irradiation temperature. Thermal diffusivity dependency on irradiation dose is not presented.

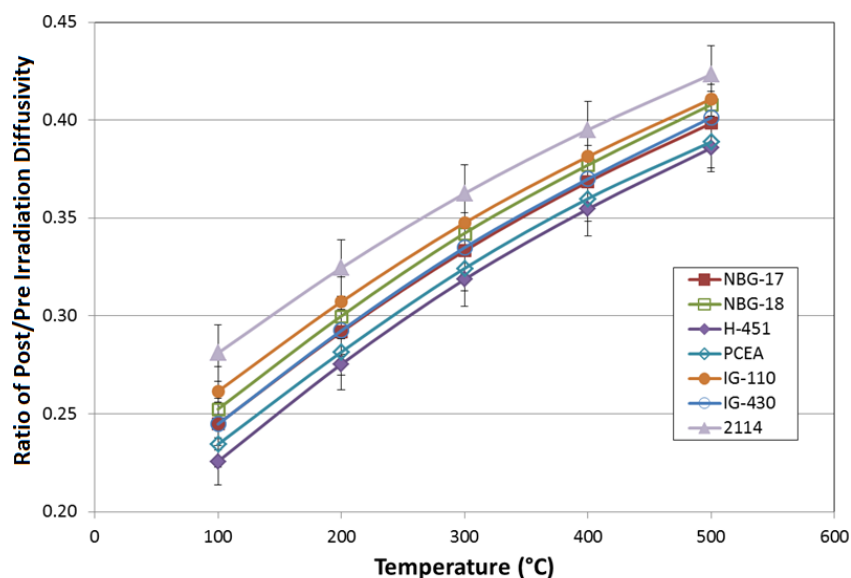


Figure 12. Ratio of irradiated diffusivity to unirradiated diffusivity as a function of specimen temperature for seven grades of graphite. Changes to thermal diffusivity resulting from irradiation dose and irradiation temperature are assumed to have been saturated allowing all graphite grades to be grouped together. The assumption that diffusivity change saturates will be validated within the subsequent AGC-2 analysis report.

4.5 Coefficient of Thermal Expansion

CTE was measured using a linear dilatometer technique.^[23] Because annealing of irradiation damage begins to take place at temperatures above the irradiation temperature, measurements of thermal expansion were limited to 500°C (100°C below the average AGC-2 specimen irradiation temperature).

Mean CTE data are plotted in Figures A-85 through A-108. A statistical evaluation of the CTE data was performed at three discrete temperatures (i.e., 100, 300, and 500°C) for each graphite type. Again, the dashed lines in these plots indicate the upper and lower IQR limits. There are no outliers to consider.

Tables B-5 through B-7 (see Appendix B) list the mean, standard deviation, and COV values for data evaluated at the discrete temperatures. As shown, COV values range from ~8% to 16%. This relatively large scatter in the data may be a result of the variation in stress levels of the different specimens.

Figure 13 and Figure 14 illustrate an increase in CTE as a function of dose and irradiation temperature, respectively, for graphite type IG-110 at 500°C. As is common in all the data, there is a near singular relationship between the irradiation temperature and dose for a given location in the experiment. Therefore, specimens at a given temperature will have a very narrow range of doses, and specimens at a given dose will have a very narrow range of temperatures. Because there are only a few (2–6) specimens at similar channel positions within the capsule, it is difficult to separate the variables of dose and irradiation temperature. Fortunately, the general trend for CTE change seems to demonstrate very little dependence on increasing dose or irradiation temperature for all specimens tested, as seen in Figure 13 and Figure 14.

While the change to CTE appears to saturate with increasing dose and irradiation temperature, it can be observed that stress appears to increase CTE values rather markedly in irradiated specimens. As applied stress is increased, significant changes in CTE are noted. Detailed CTE dependency on irradiation dose and irradiation temperature will be addressed within the subsequent AGC-2 analysis report.

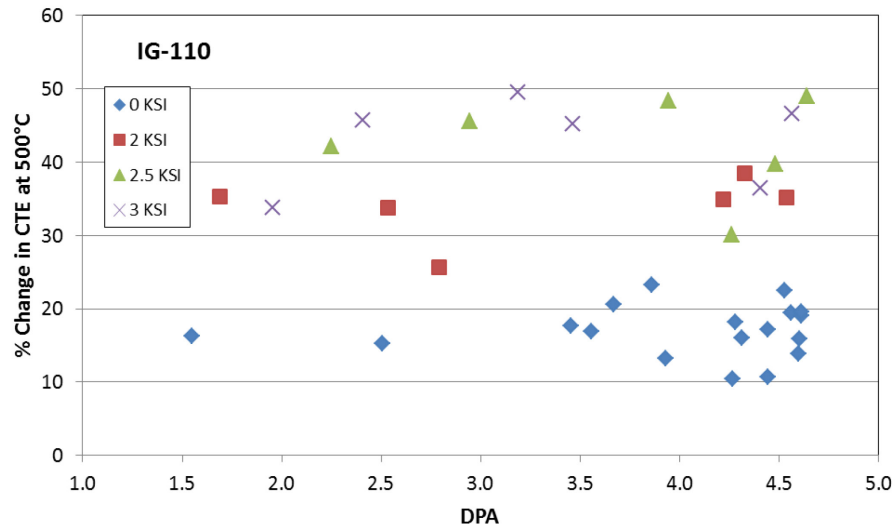


Figure 13. Percent increase in CTE at 500°C for graphite grade IG-110 as a function of irradiation dose for four different stress levels. CTE dependency on irradiation temperature is not presented.

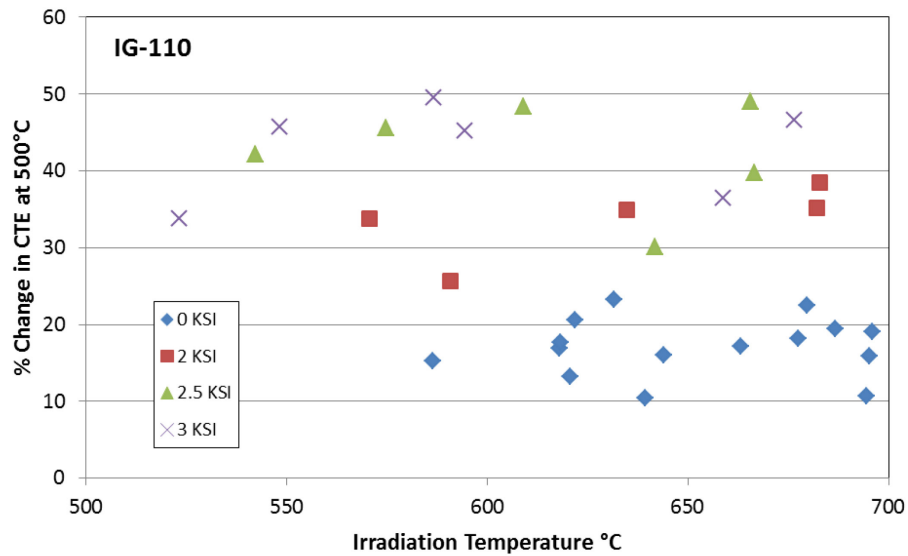


Figure 14. Percent increase in CTE at 500°C for graphite grade IG-110 as a function of irradiation temperature for four different stress levels. CTE dependency on irradiation dose is not presented.

Figure 15 illustrates the average increase in CTE as a function of temperature for stressed and unstressed specimens of the six major graphite grades. Each data point is averaged over all specimen doses and irradiation temperatures for each graphite grade. Specimens that were mechanically loaded are averaged over stress values of 13.8 MPa, 17.2 MPa, or 20.7 MPa (2 ksi, 2.5 ksi and 3 ksi, respectively). The measured CTE values for all stressed creep specimens can be seen to be considerably higher than the unstressed control specimens of the same grade. This indicates that stress has a significant effect on the CTE of irradiated graphite and will be analyzed further in the subsequent AGC-2 analysis report.

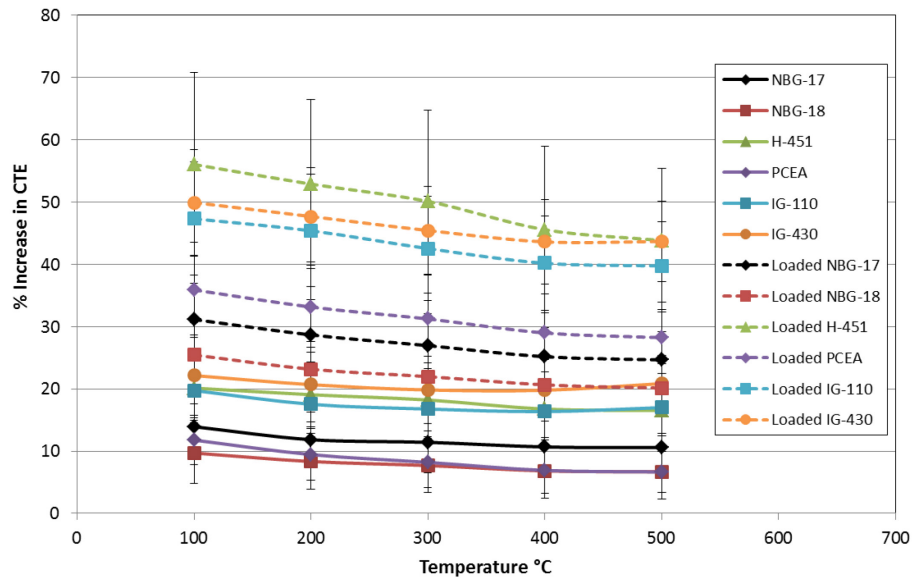


Figure 15. Percent increase in CTE for six different grades of graphite as a function of temperature for stressed and unstressed conditions. Changes to CTE resulting from irradiation dose and temperature are assumed to have been saturated allowing all graphite grades to be grouped together. The assumption that CTE change saturates will be validated within the subsequent AGC-2 analysis report.

5. REFERENCES

1. T. Burchell, R. Bratton, and W. Windes, "NGNP Graphite Selection and Acquisition Strategy," ORNL/TM 2007/153, September 2007.
2. R. L. Bratton and T. D. Burchell, 2005, "NGNP Graphite Testing and Qualification Specimen Selection Strategy," INL/EXT 05 00269, Idaho National Laboratory, May 2005.
3. PLN 2497, 2010, Graphite Technology Development Plan, Rev. 1, Idaho National Laboratory, October 2010.
4. TFR 645, 2010, Advanced Graphite Capsule AGC 2 Experiment Test Train, Rev. 0, Idaho National Laboratory, July 2010.
5. T. Burchell and R. Bratton, 2005, "Graphite Irradiation Creep Capsule AGC 1 Experimental Plan," ORNL/TM 2005/505, Oak Ridge National Laboratory, May 2005.
6. INL Drawing 600786, 2009, "ATR Advanced Graphite Capsule (AGC 2) Graphite Specimen Machining Details," Rev. 1, Idaho National Laboratory, March 2009.
7. INL Drawing 600786, 2012, "ATR Advanced Graphite Capsule (AGC 2) Graphite Specimen Machining Details," Rev. 2, Idaho National Laboratory, July 2012.

8. INL Drawing 600787, 2010, "ATR Advanced Graphite Capsule (AGC 2) Experiment Graphite Specimen Cut Out Diagrams," Rev. 3, Idaho National Laboratory, July 2010.
9. DWG 601266, 2012, ATR Advanced Graphite Capsule Number 2 (AGC 2) Capsule Facility Assemblies, Rev. 2, Idaho National Laboratory, July 2012.
10. DWG 601258, 2012, ATR Advanced Graphite Capsule 2 (AGC 2) Graphite Specimen Holder Assemblies and Details, Rev. 1, Idaho National Laboratory, July 2012.
11. DWG 600001, 2009, ATR TMIST-1 Oxidation Experiment In-Vessel Installation, Rev. 2, Idaho National Laboratory, March 2009.
12. J. R. Parry, 2010, "Engineering Calculations and Analysis Report: Reactor Physics Projections for the AGC 2 Experiment Irradiated in the ATR South Flux Trap," ECAR 1050, Rev. 0, Idaho National Laboratory, October 13, 2010.
13. T. Burchell, 2009, "A Revised AGC 1 Creep Capsule Layout," ORNL/TM 2009/009, Oak Ridge National Laboratory, January 2009.
14. T. Burchell, J. Strizak, and M. Williams, 2011, "AGC 1 Specimen Preirradiation Data Report," ORNL/TM 2010/285, Oak Ridge National Laboratory, August 2011.
15. T. Reed, 2012, "AGC 1 Individual Fluence, Temperature, and Load Calculation and Tabulation," ECAR 1943, Idaho National Laboratory, September 2012.
16. T. Reed, 2012, "AGC 1 As Run Thermal Results," ECAR 1944, Idaho National Laboratory, September 2012.
17. L. Hull, 2012, "AGC-2 Irradiation Data Qualification Final Report," INL/EXT 12 26248, July 2012.
18. TFR 645, 2010, Advanced Graphite Capsule AGC 2 Experiment Test Train, Rev. 0, Idaho National Laboratory, July 2010.
19. D. Swank, 2010, "AGC 2 Graphite Preirradiation Data Package," INL/EXT 10 19588, Rev. 0, Idaho National Laboratory, August 2010.
20. R. G. Ambrosek, "Thermal Projections for AGC 2," ECAR 1161, Idaho National Laboratory.
21. M. Davenport, 2010, Engineering Work Instructions for Assembling the AGC-2 Experiment, Quality Assurance Record: QA# 137268, October 2010.
22. W. Windes, 2014, "AGC 2 Disassembly Report," INL/EXT 14 32060, May 2014.
23. D. Swank, AGC 2 Graphite Specimen Postirradiation Characterization Plan," PLN 4657, Rev. 0, Idaho National Laboratory,
24. J. E. Brocklehurst and R. G. Brown, "Constant Stress Irradiation Creep Experiments on Graphite In Br 2" Carbon, Volume 7, Issue 4, August 1969.
25. W. J. Gray, "Constant Stress Irradiation-Induced Compressive Creep of Graphite at High Fluences," Carbon, Volume 11, Issue 4, August 1973.
26. ASTM 769-09, Standard Test Method for Sonic Velocity in Manufactured Carbon and Graphite Materials for Use in Obtaining Young's Modulus, American Society for Testing and Materials International, 2009
27. ASTM-769-98 (reapproved 2005), Standard Test Method for Sonic Velocity in Manufactured Carbon and Graphite Materials for Use in Obtaining Young's Modulus, American Society for Testing and Materials International, 2005

Appendix A

AGC-2 Post-Irradiation Data

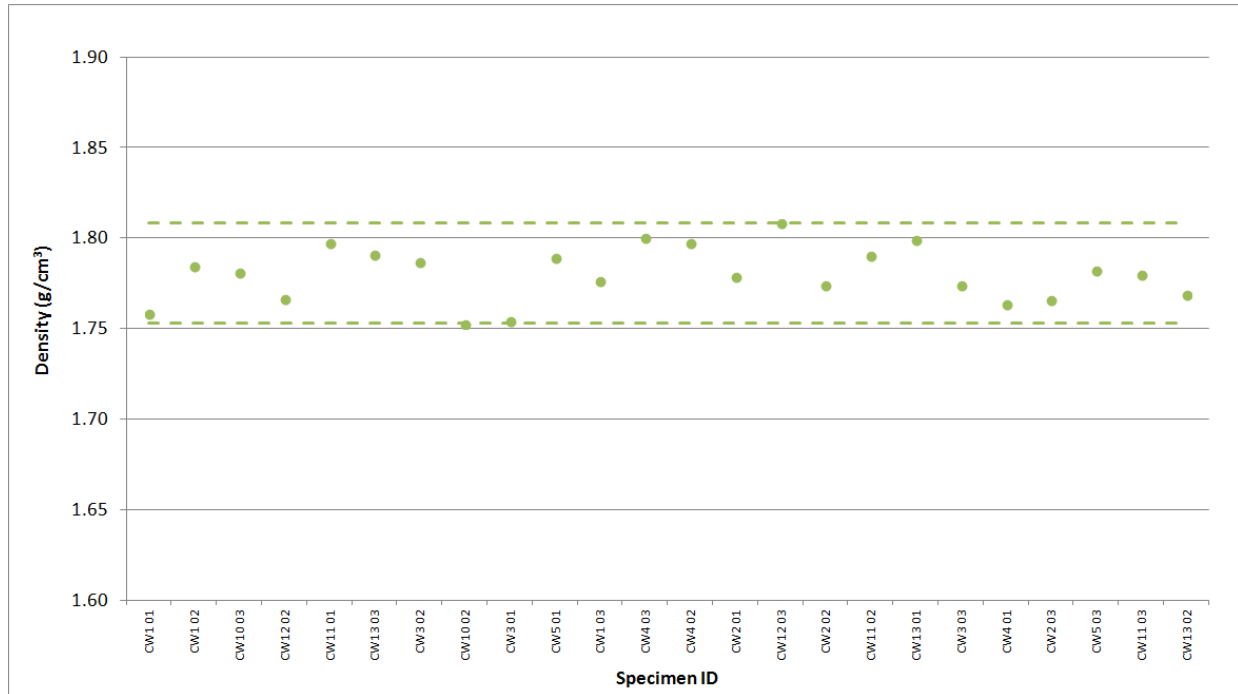


Figure A-1. H-451 Creep Density.

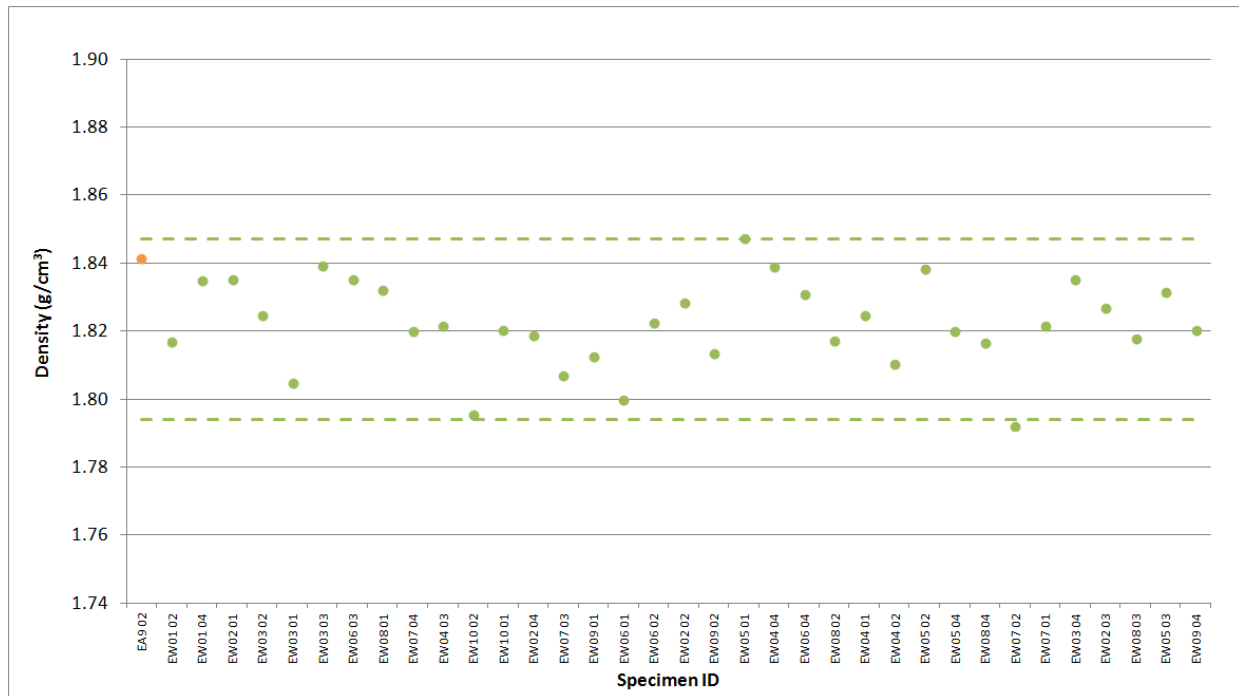


Figure A-2. IG-110 Creep Density.

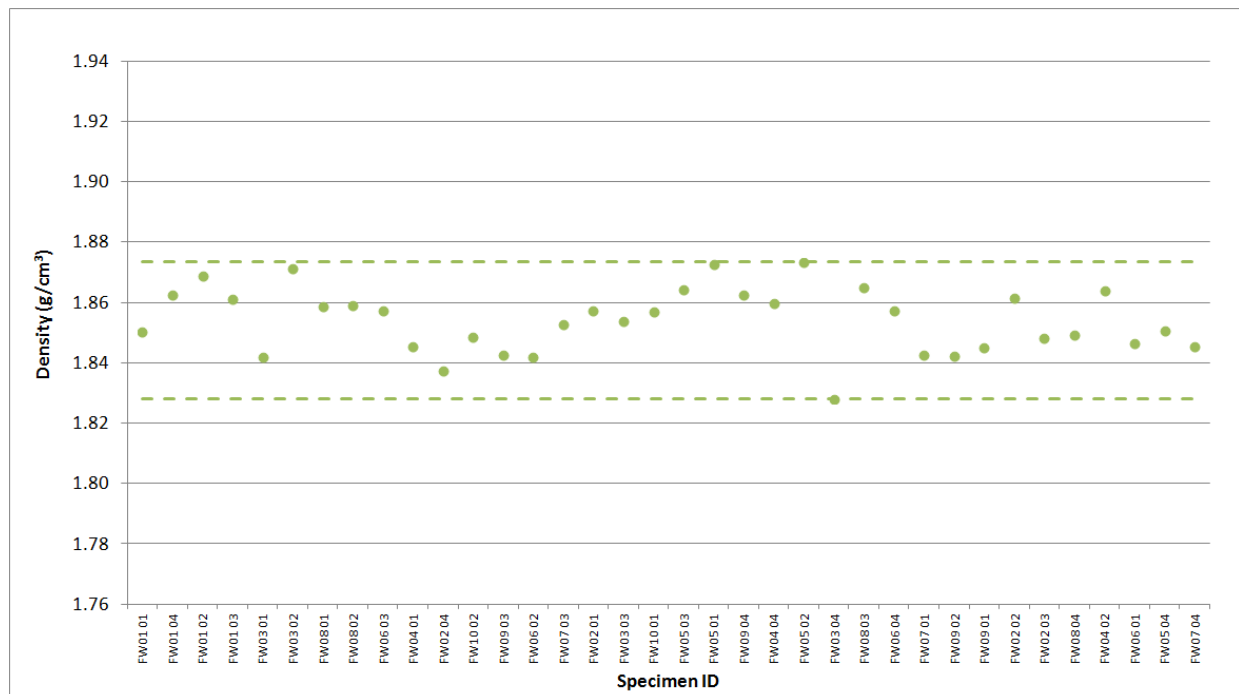


Figure A-3. IG-430 Creep Density.

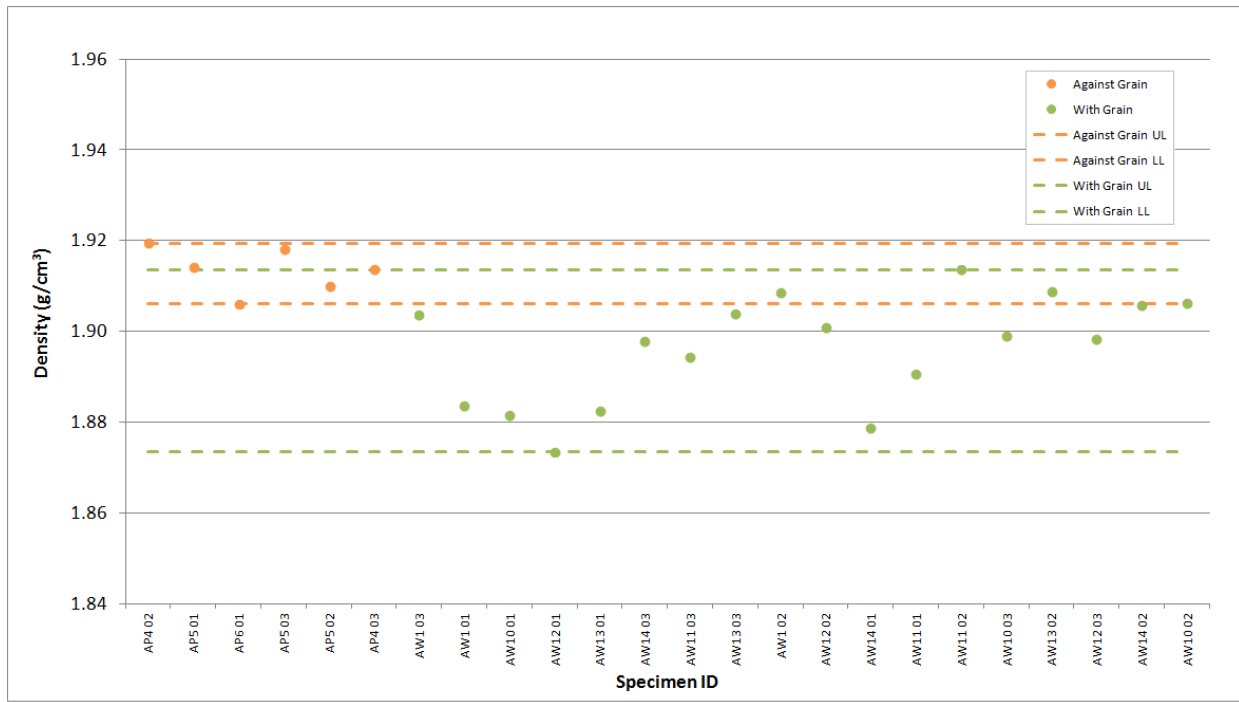


Figure A-4. NBG-17 Creep Density.

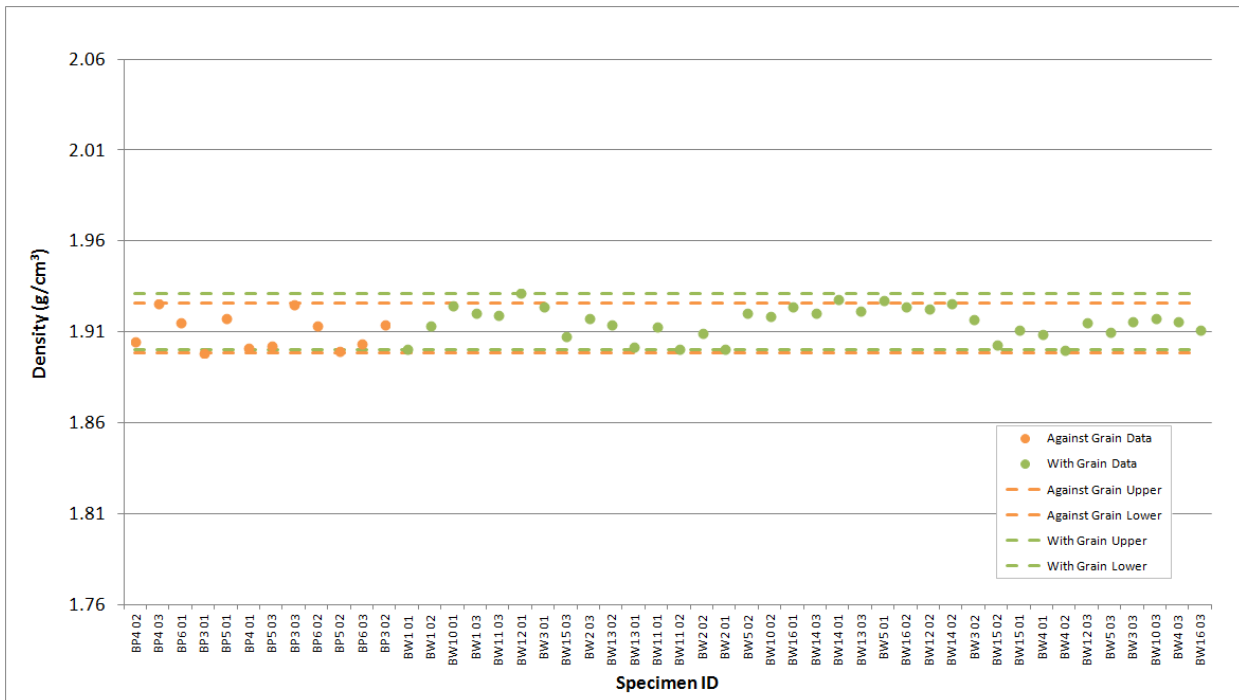


Figure A-5. NBG-18 Creep Density.

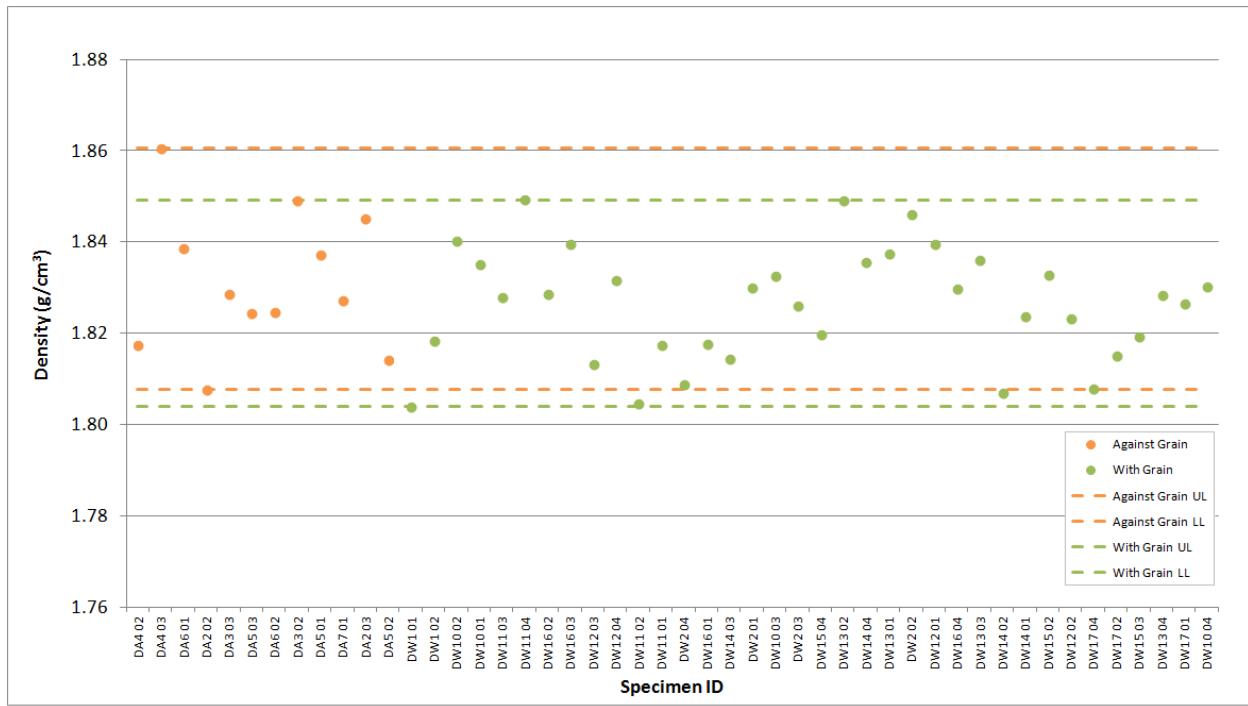


Figure A-6. PCEA Creep Density.

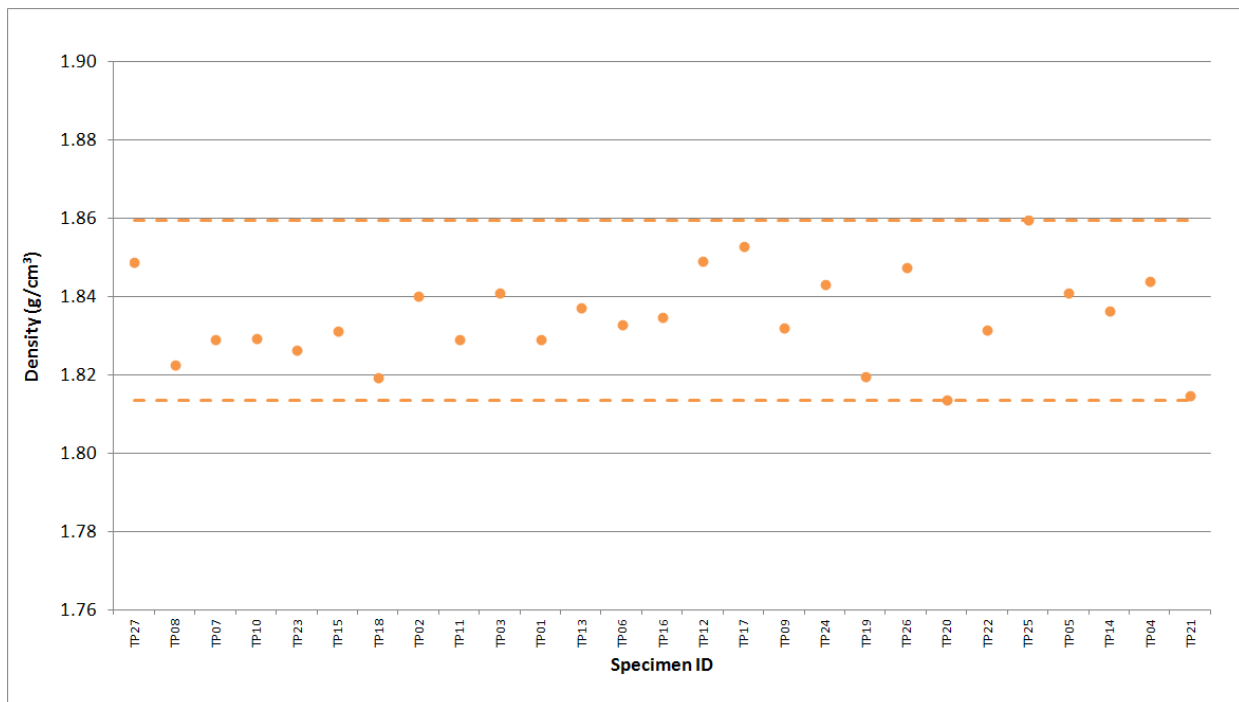


Figure A-7. 2114 Piggyback Density.

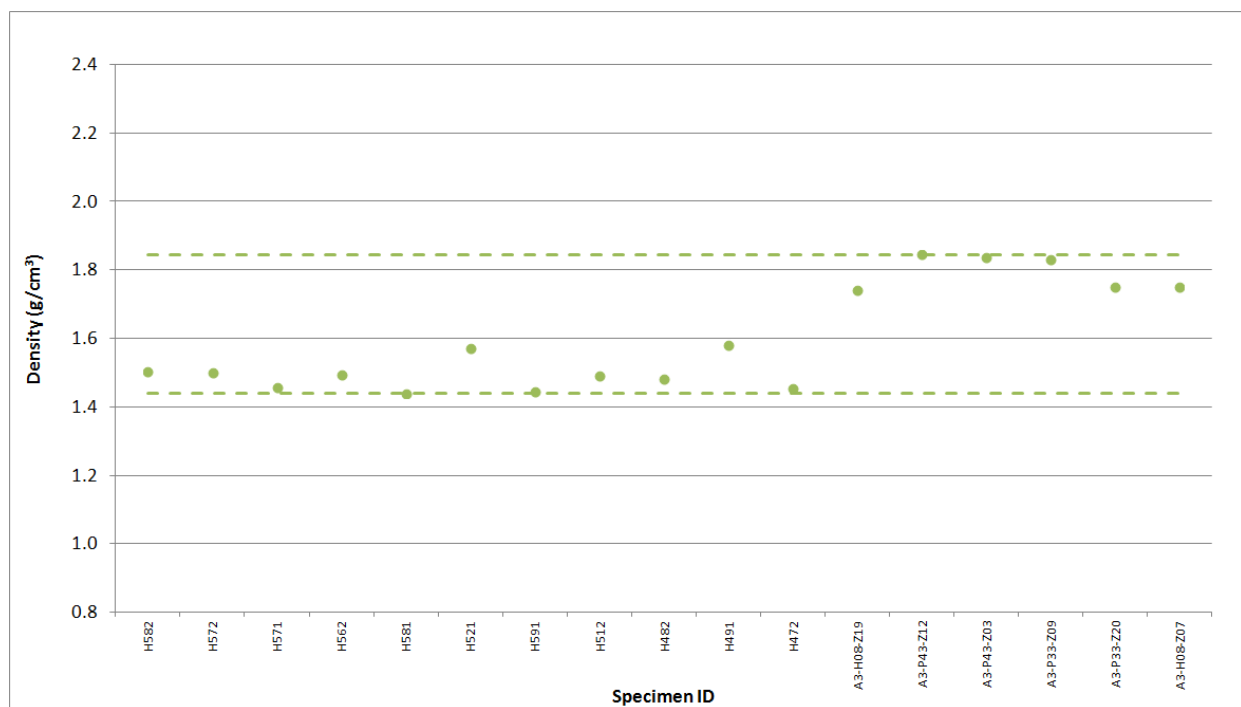


Figure A-8. A3 Piggyback Density.

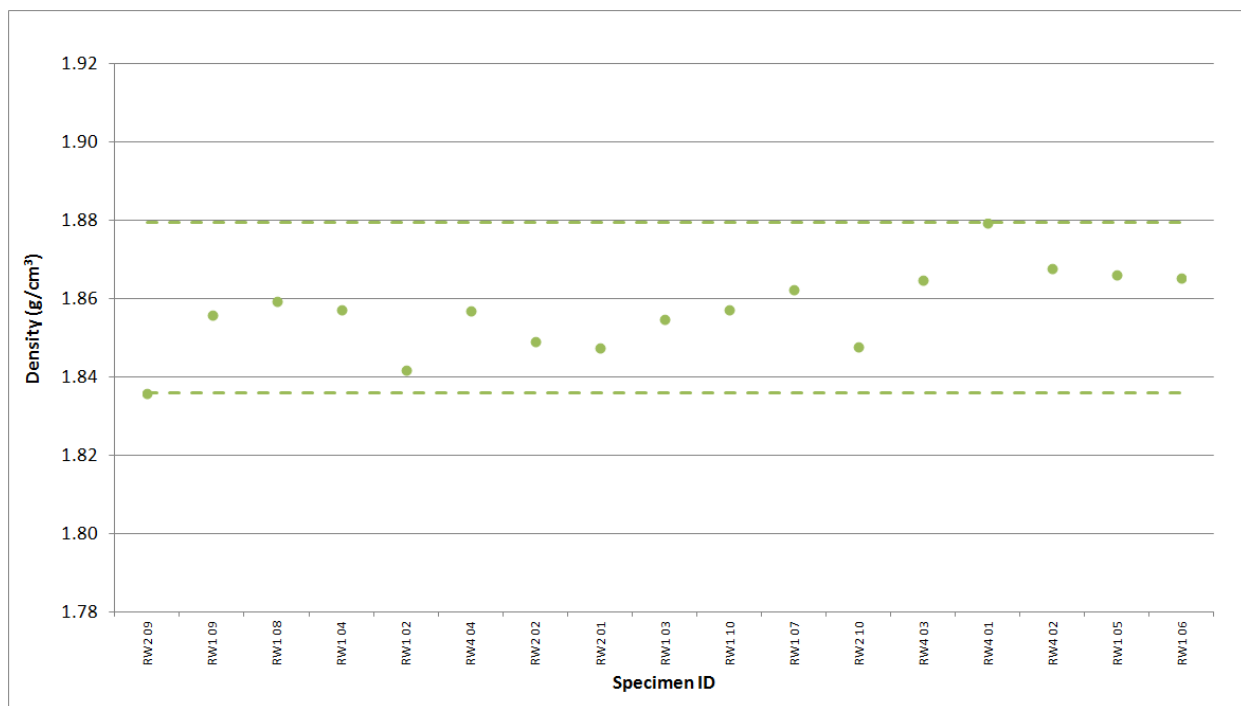


Figure A-9. BAN Piggyback Density.

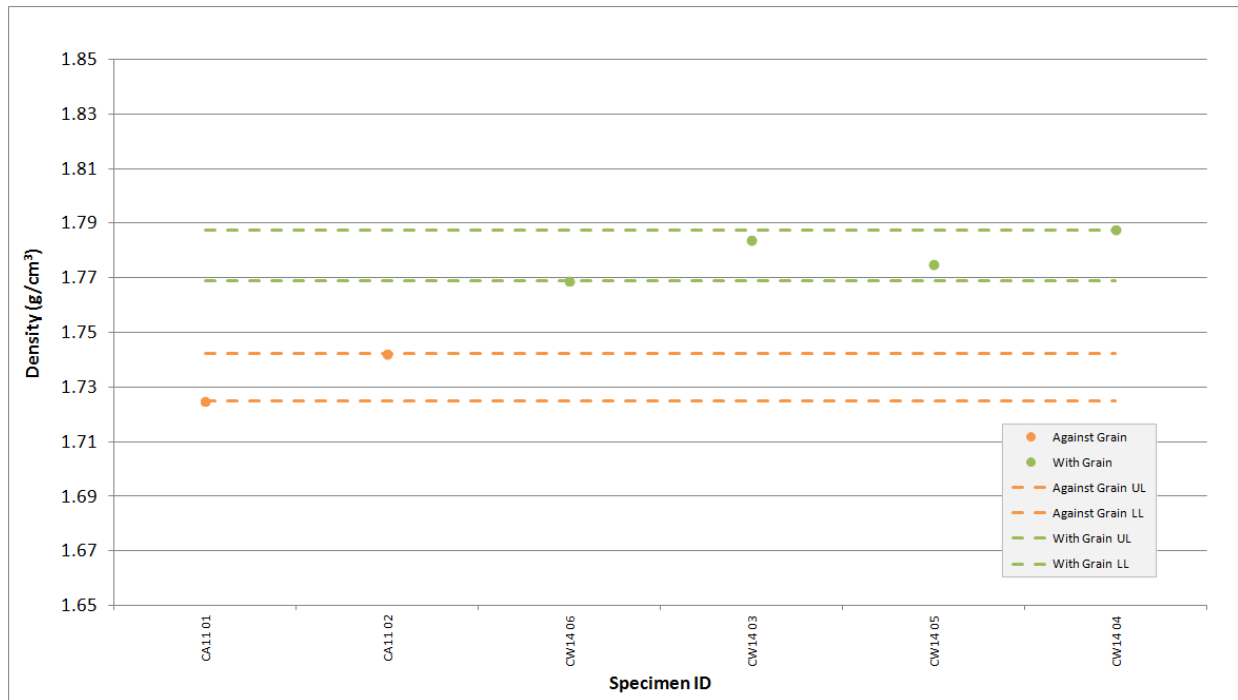


Figure A-10. H-451 Piggyback Density.

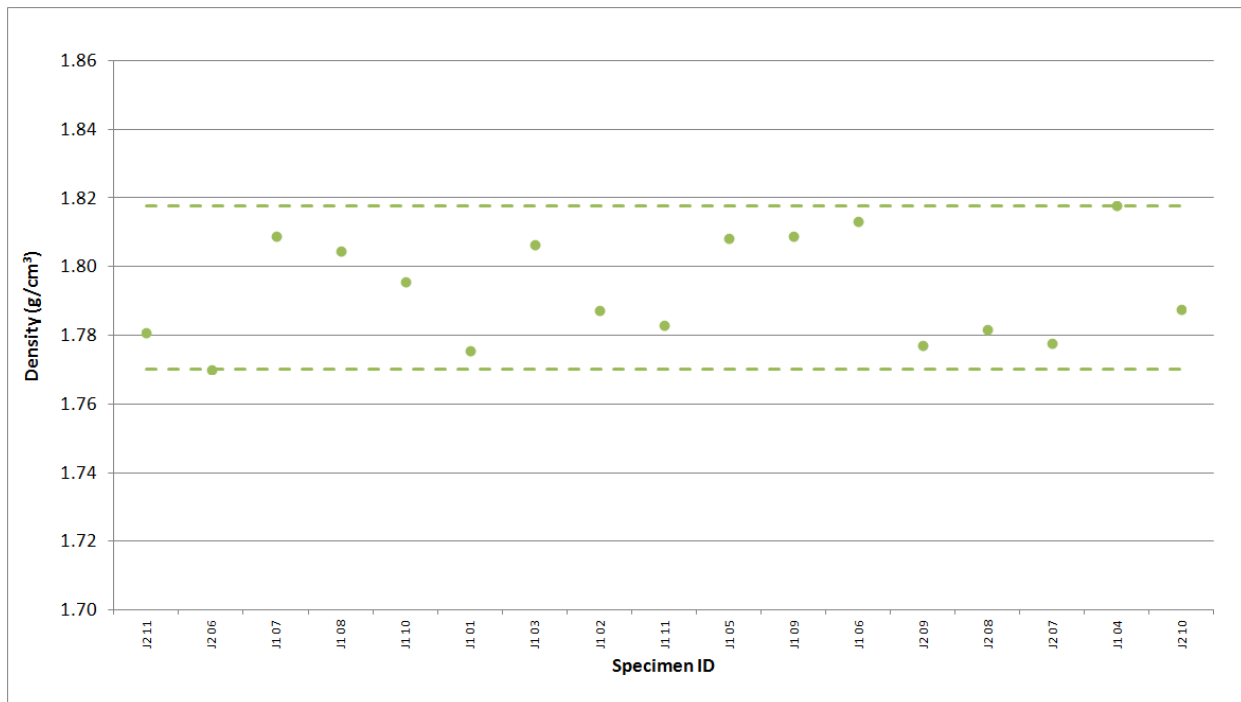


Figure A-11. HLM Piggyback Density.

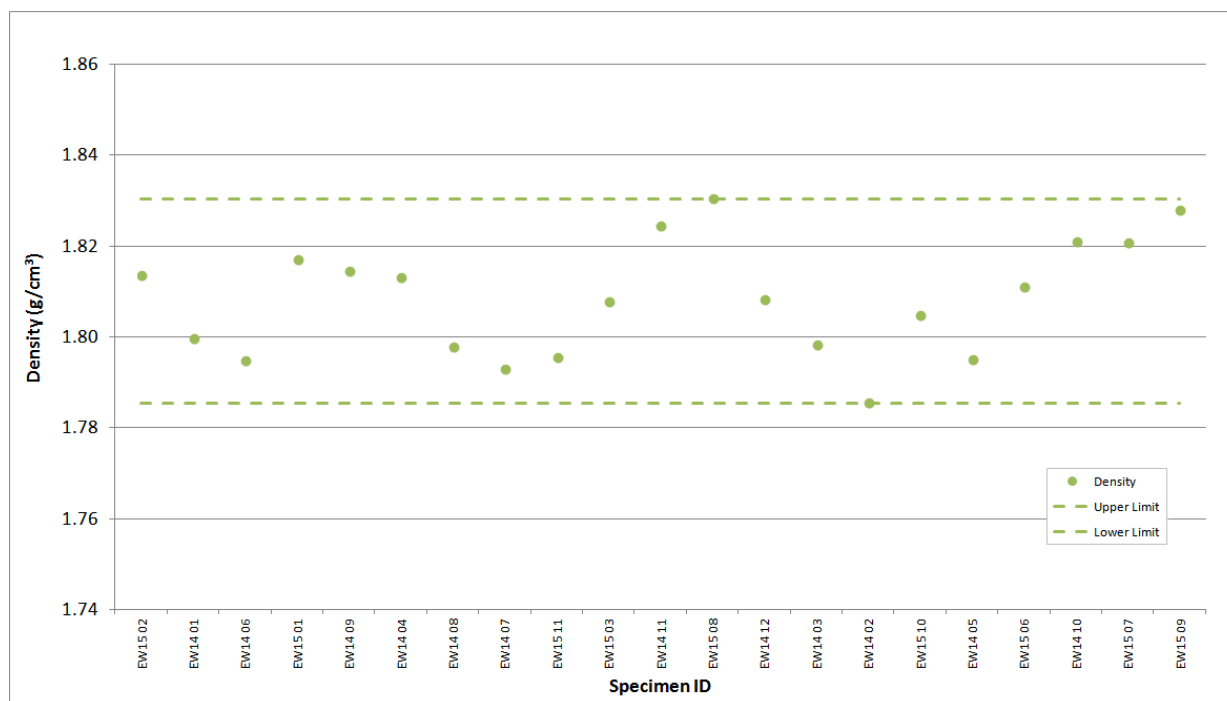


Figure A-12. IG-110 Piggyback Density.

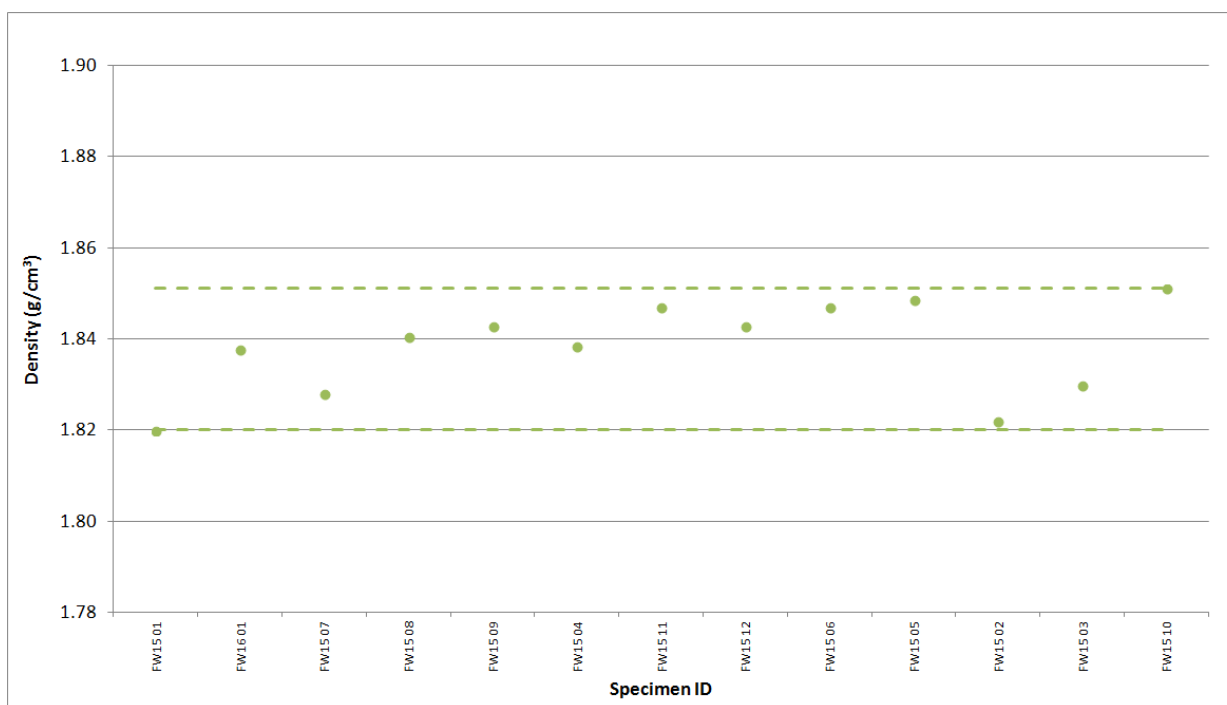


Figure A-13. IG-430 Piggyback Density.

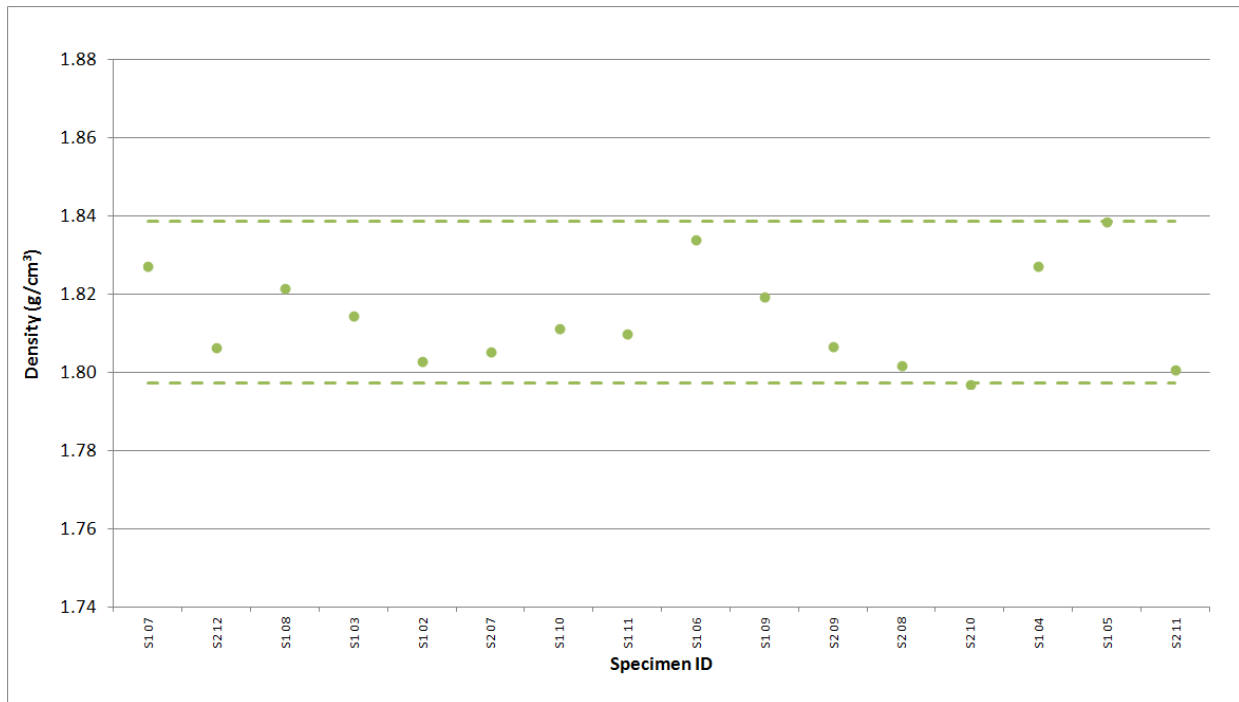


Figure A-14. NBG-10 Piggyback Density.

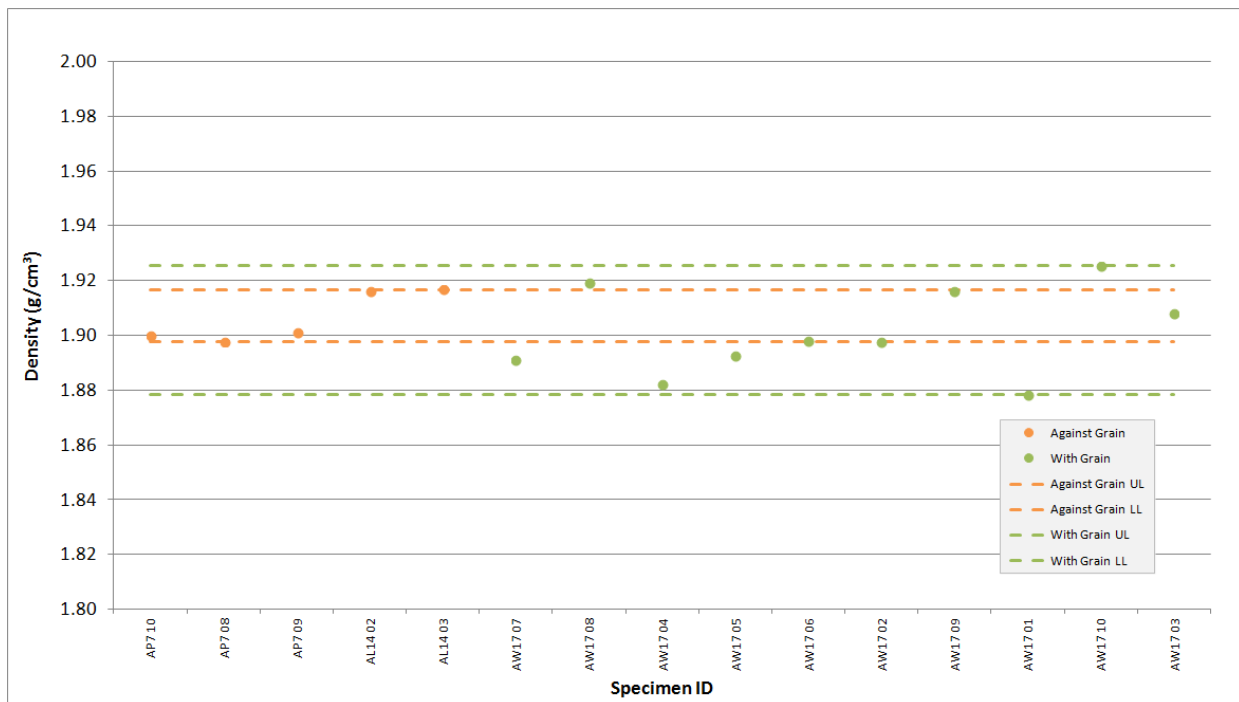


Figure A-15. NBG-17 Piggyback Density.

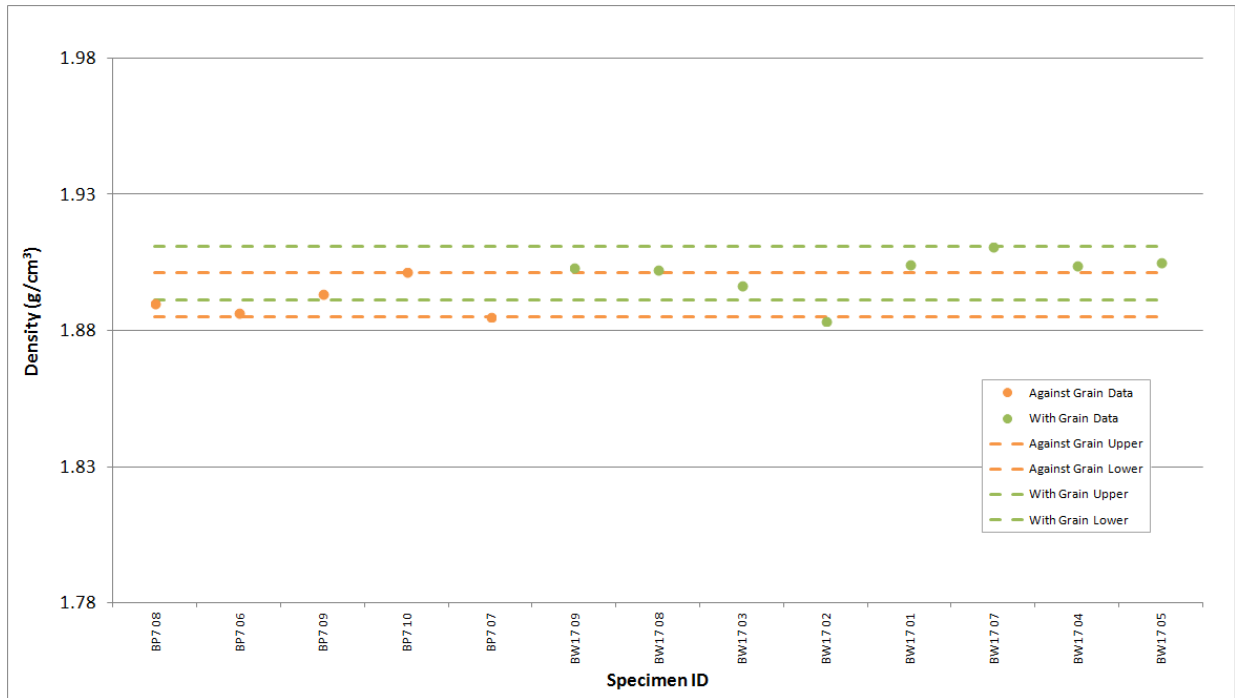


Figure A-16. NBG-18 Piggyback Density.

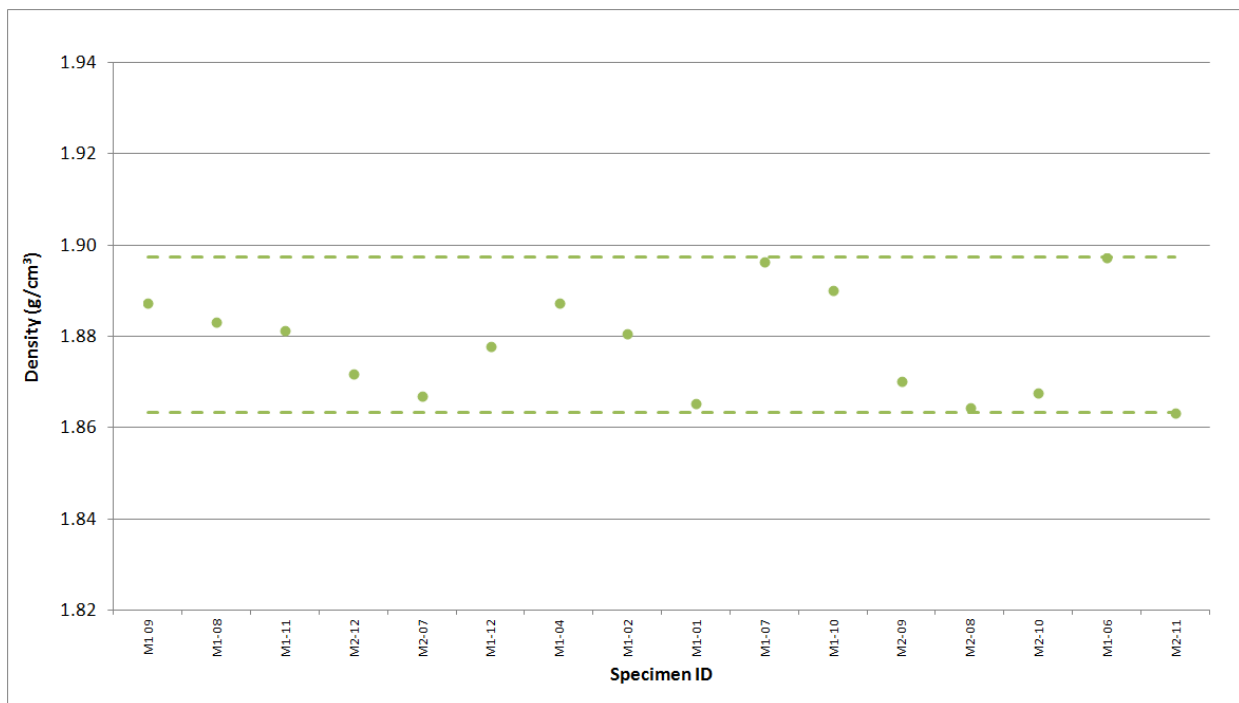


Figure A-17. NBG-25 Piggyback Density.

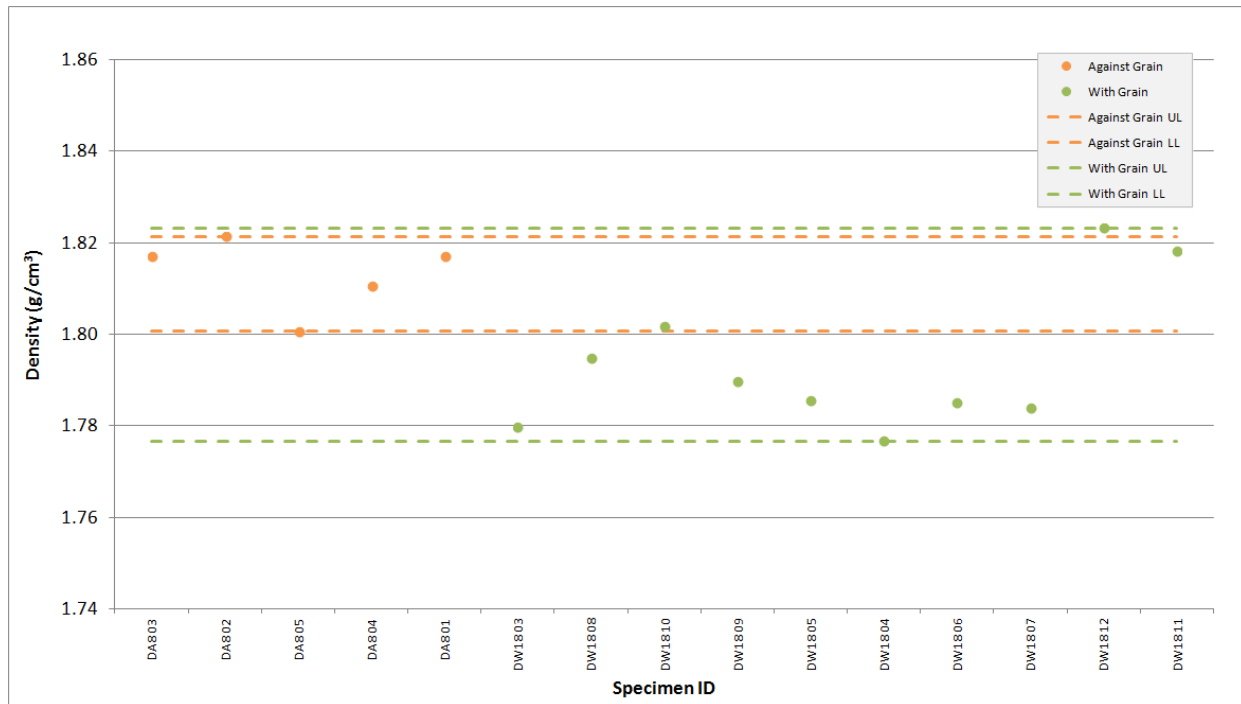


Figure A-18. PCEA Piggyback Density.

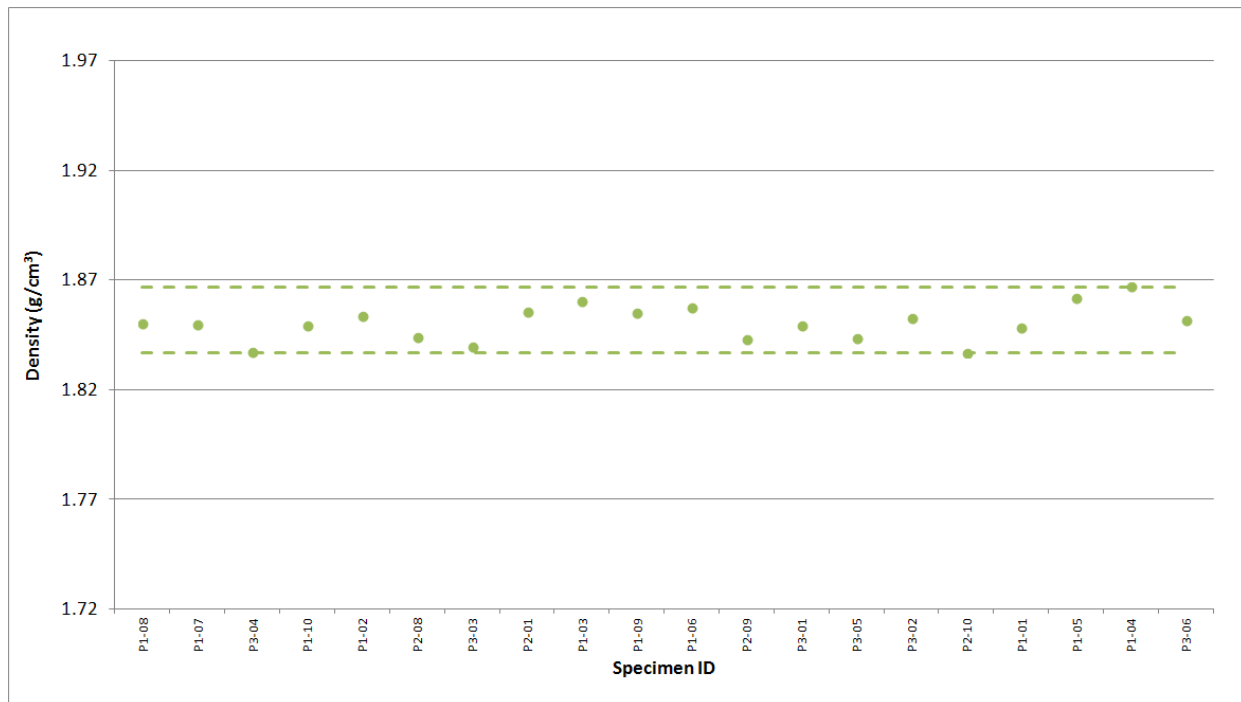


Figure A-19. PCIB Piggyback Density.

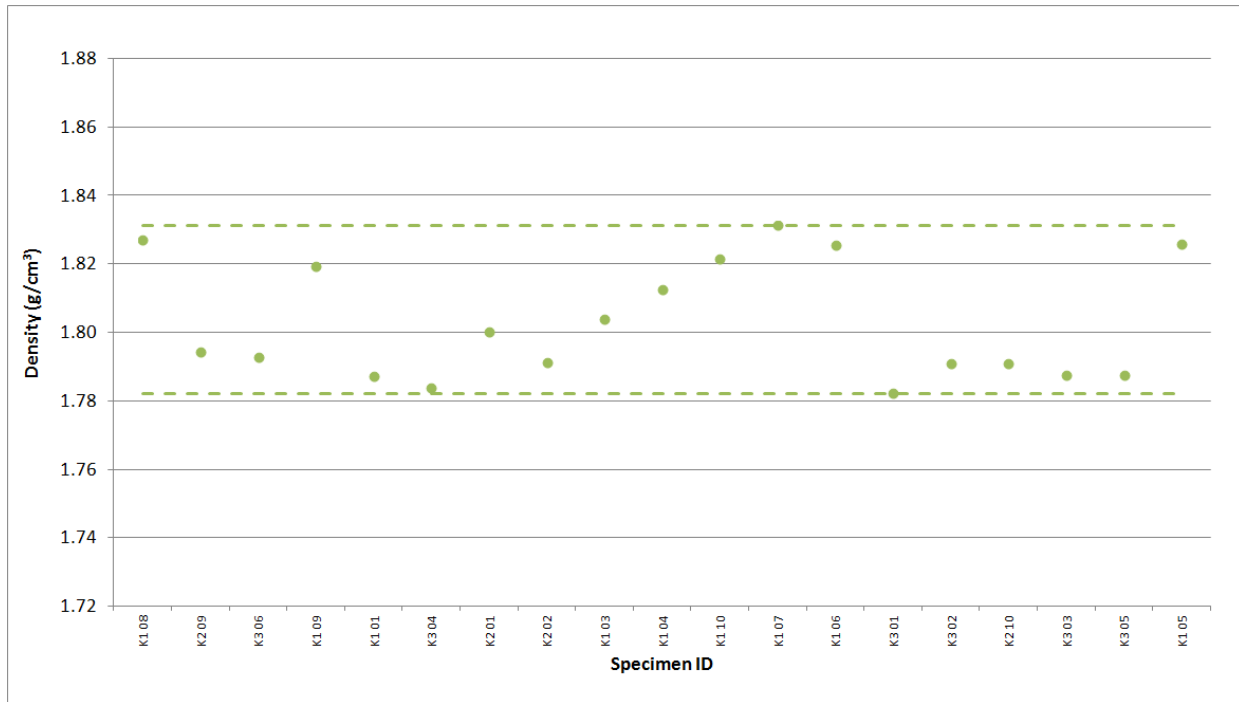


Figure A-20. PGX Piggyback Density.

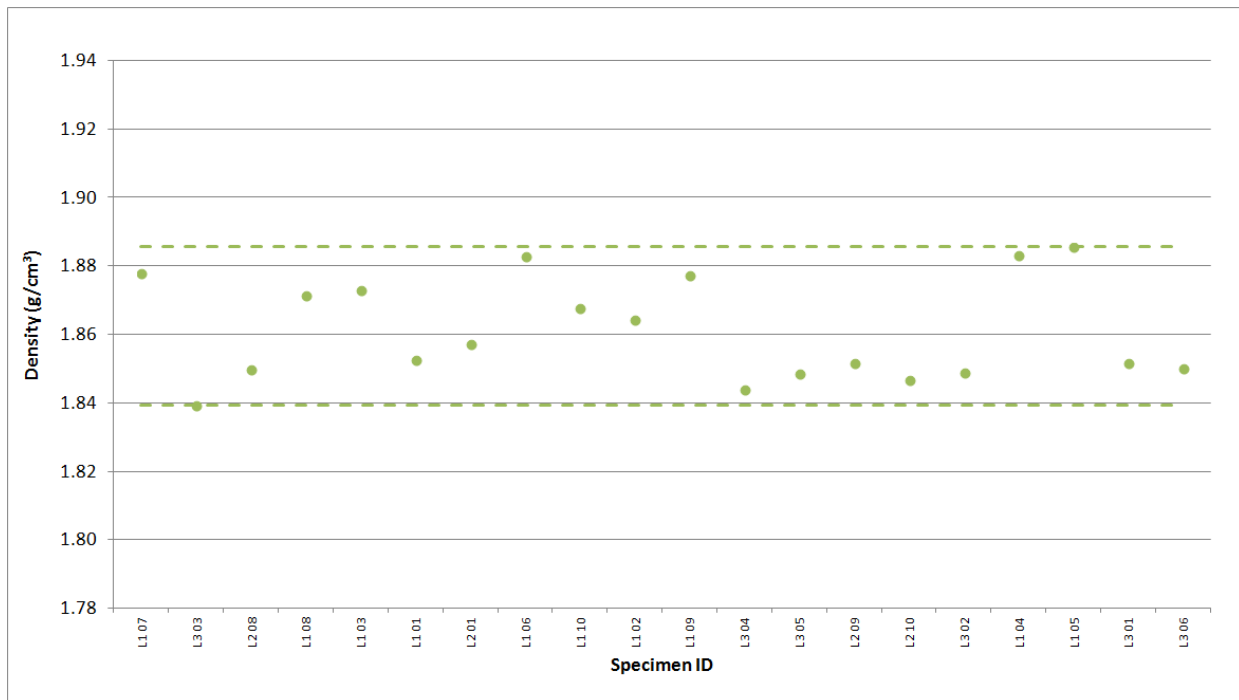


Figure A-21. PPEA Piggyback Density.

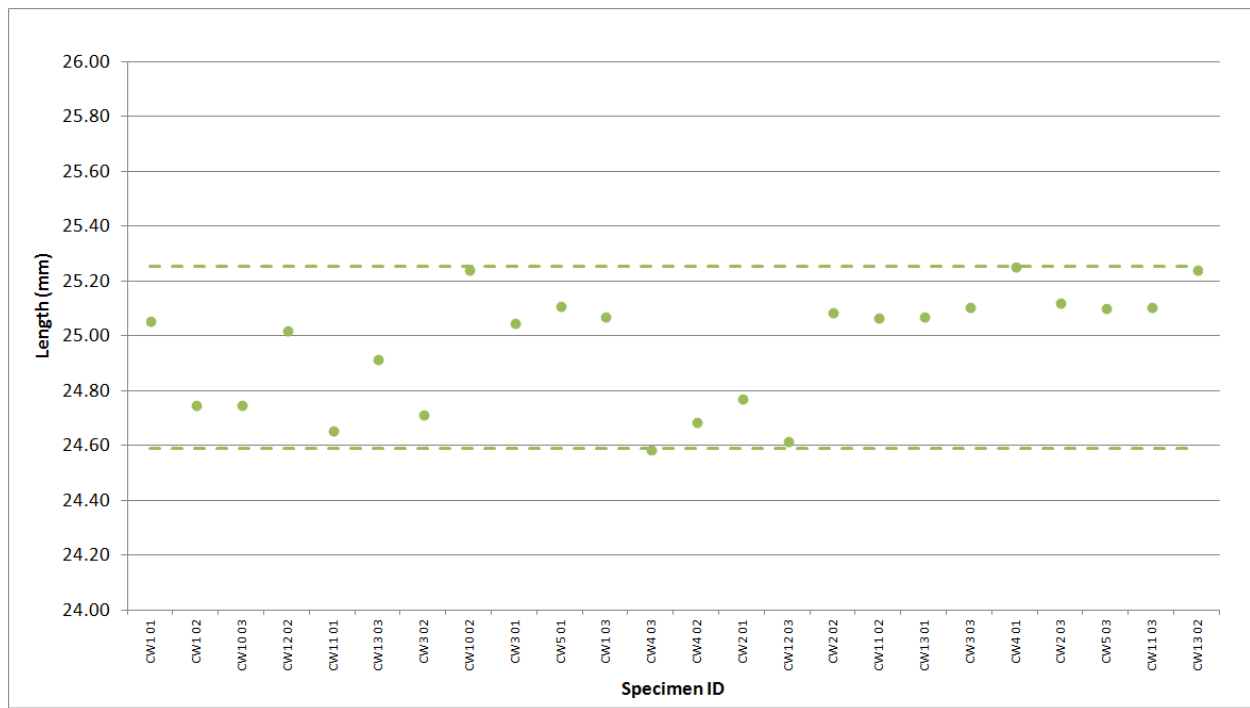


Figure A-22. H-451 Creep Length.

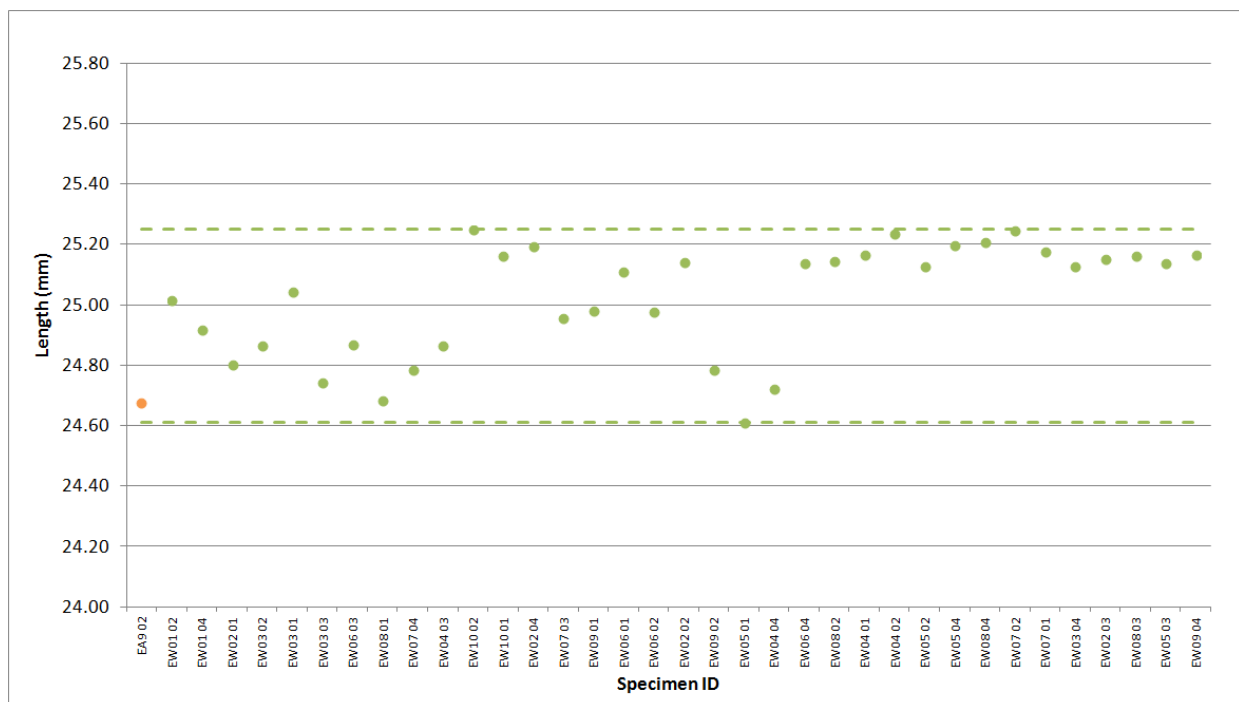


Figure A-23. IG-110 Creep Length.

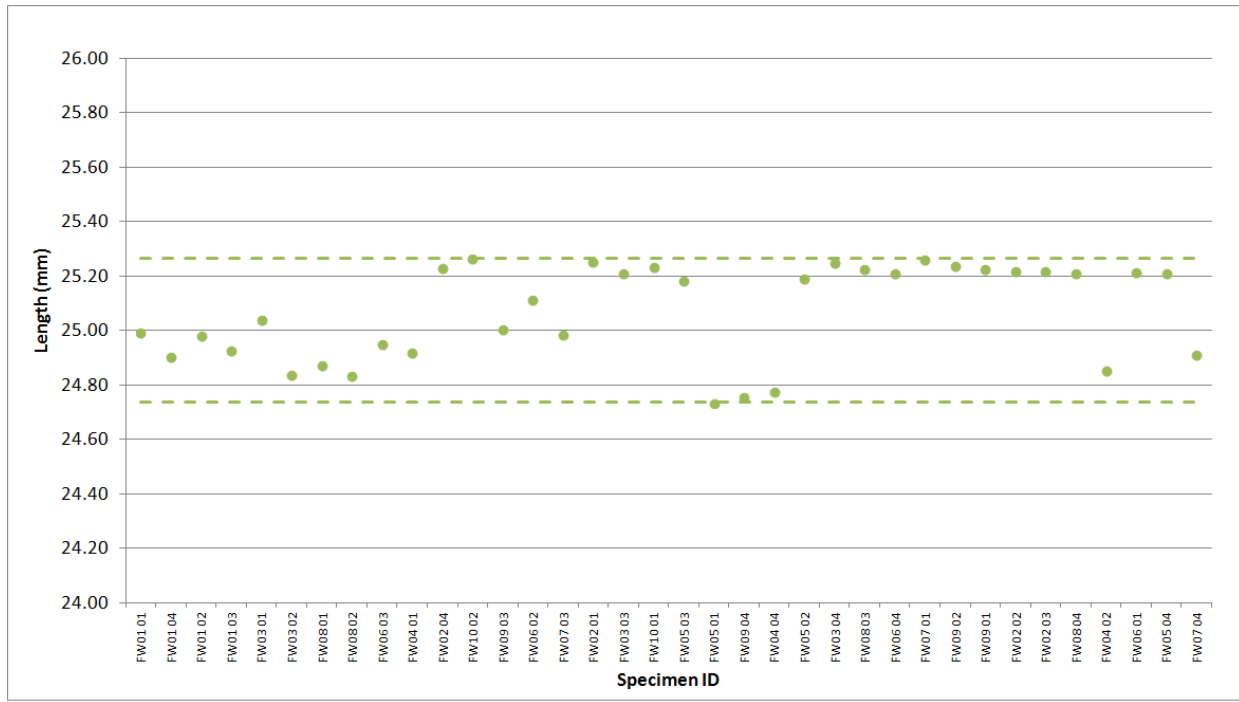


Figure A-24. IG-430 Creep Length.

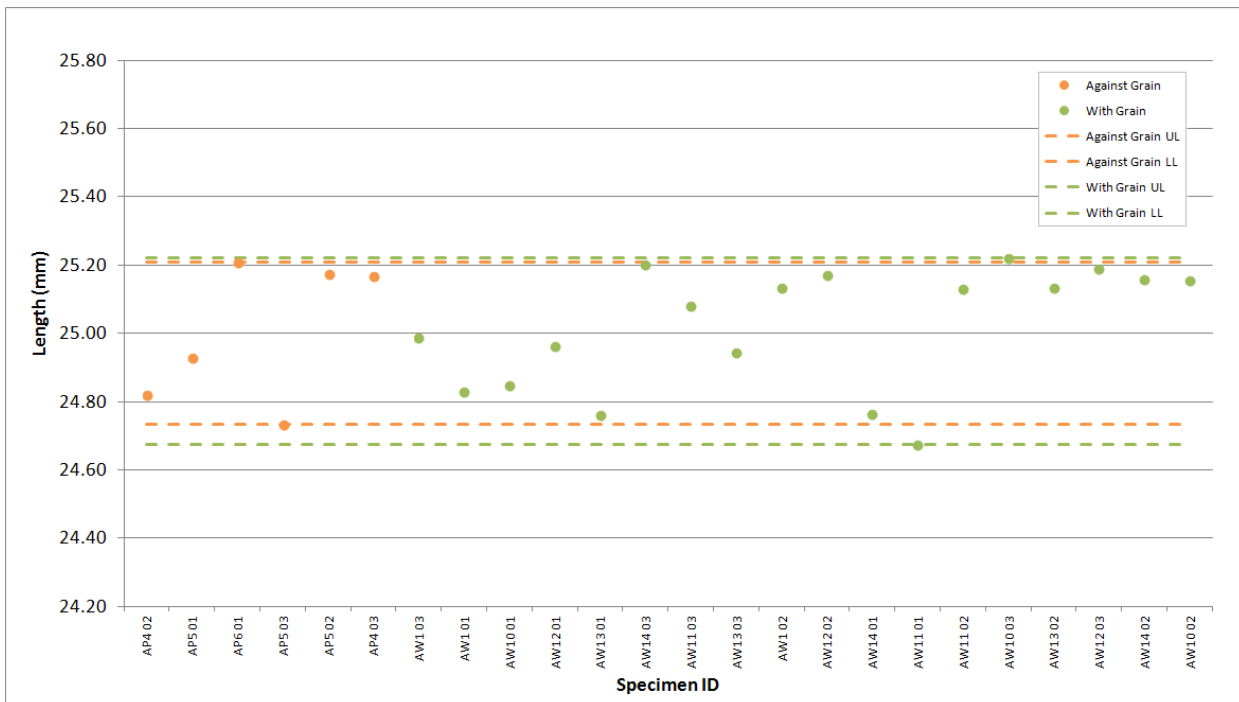


Figure A-25. NBG-17 Creep Length.

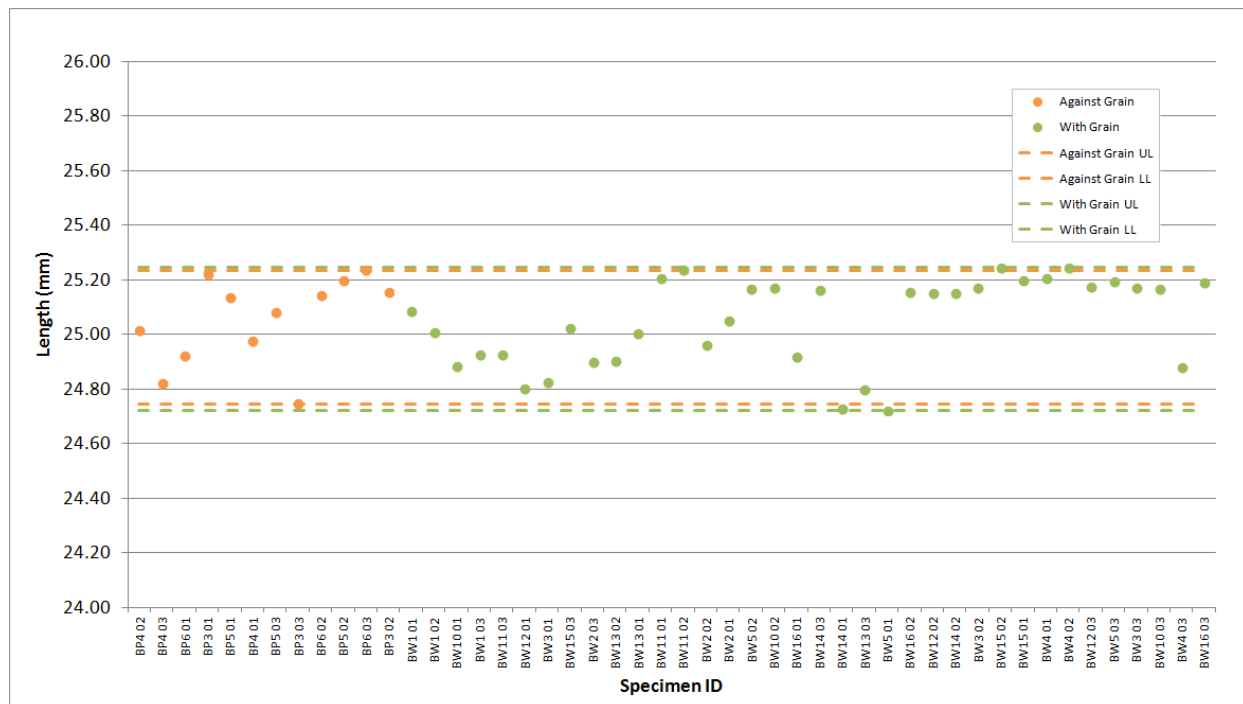


Figure A-26. NBG-18 Creep Length.

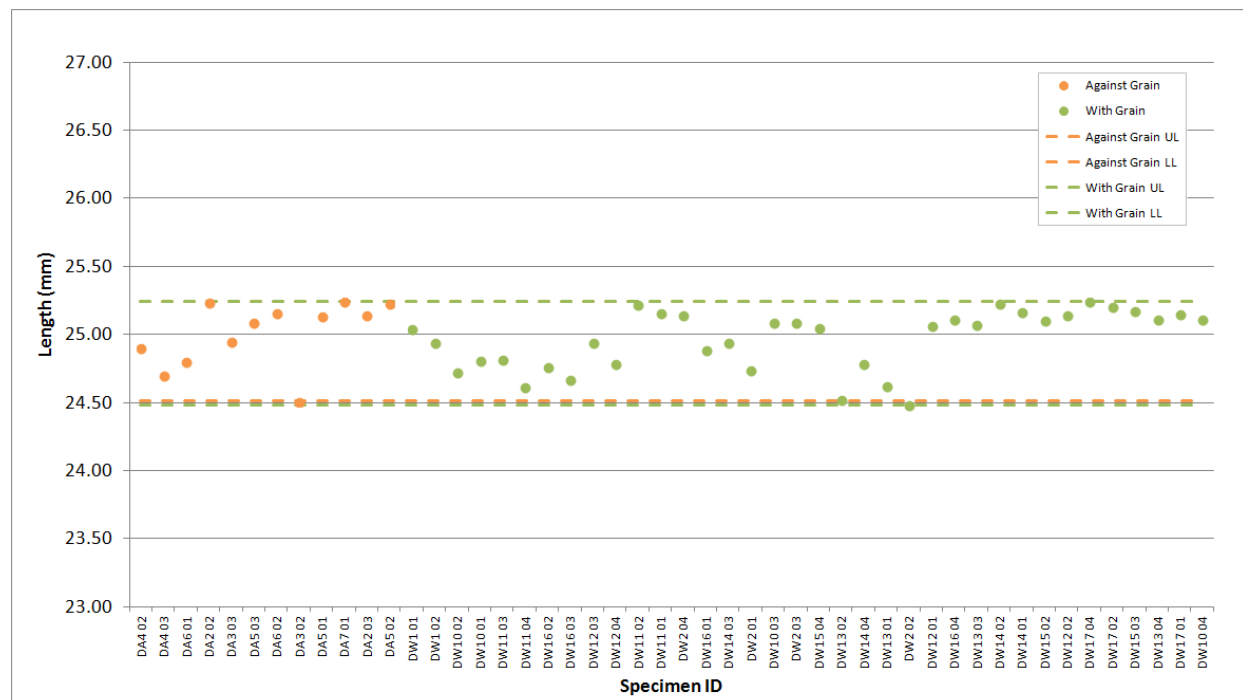


Figure A-27. PCEA Creep Length.

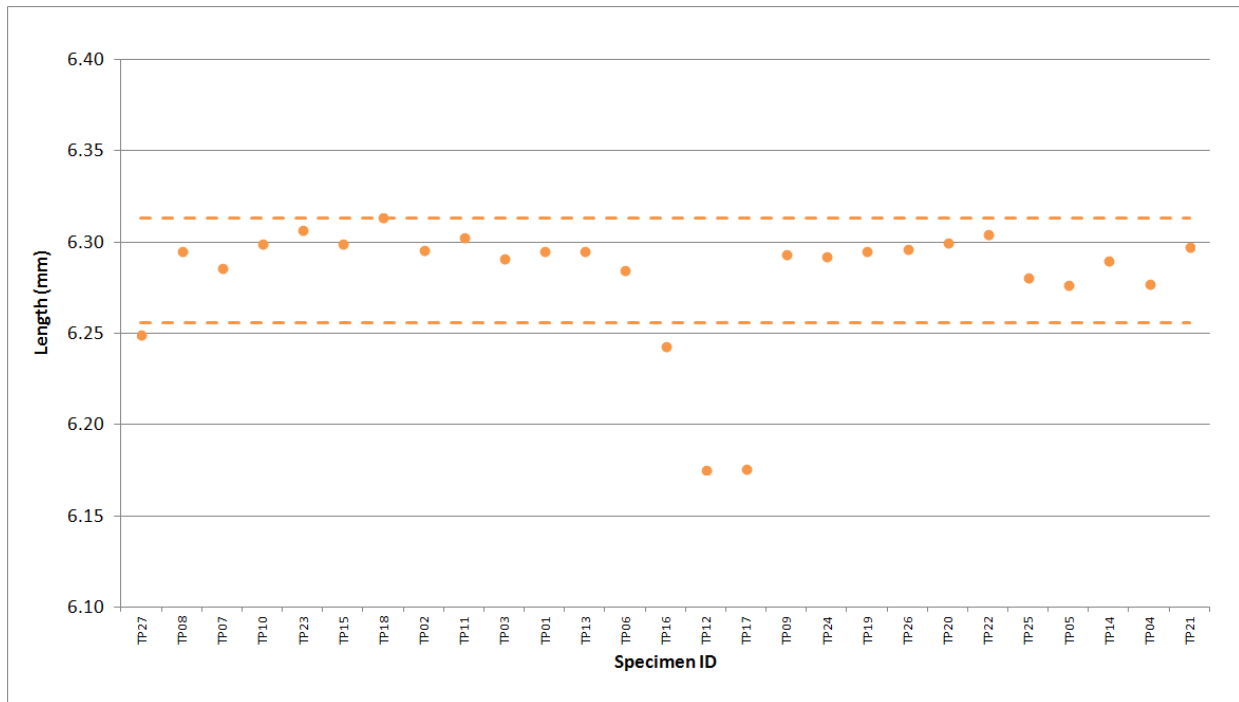


Figure A-28. 2114 Piggyback Length.

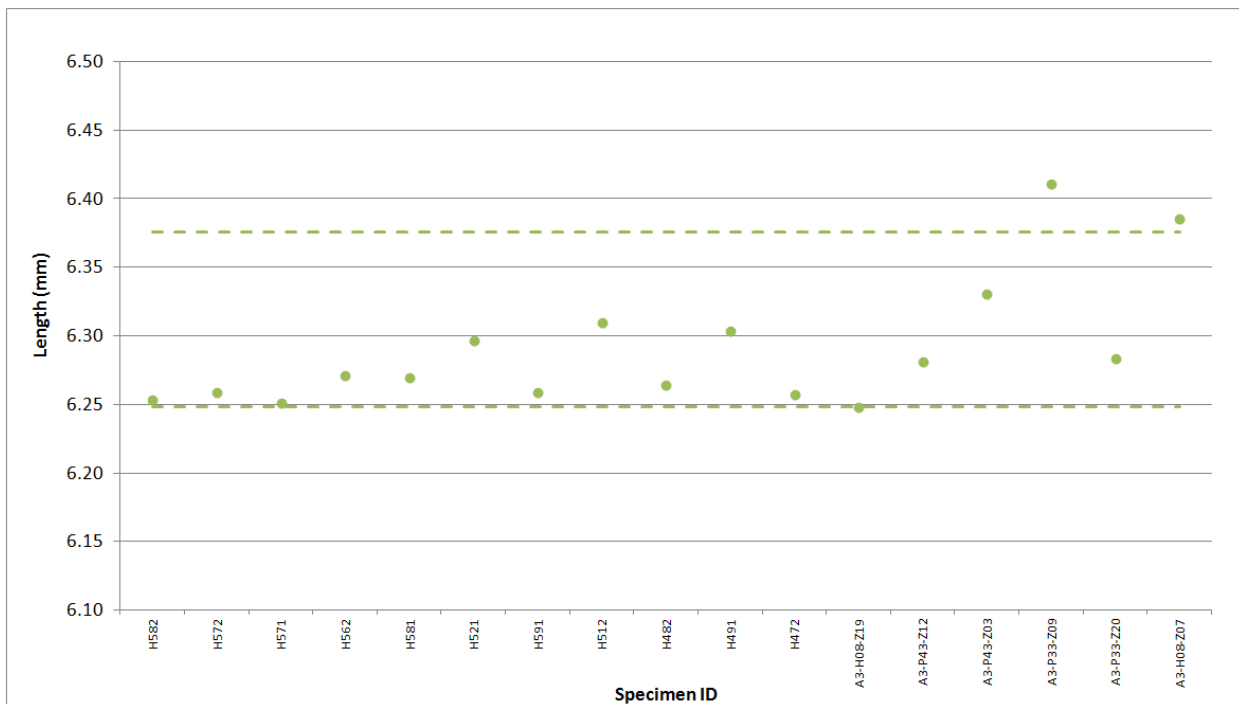


Figure A-29. A3 Piggyback Length.

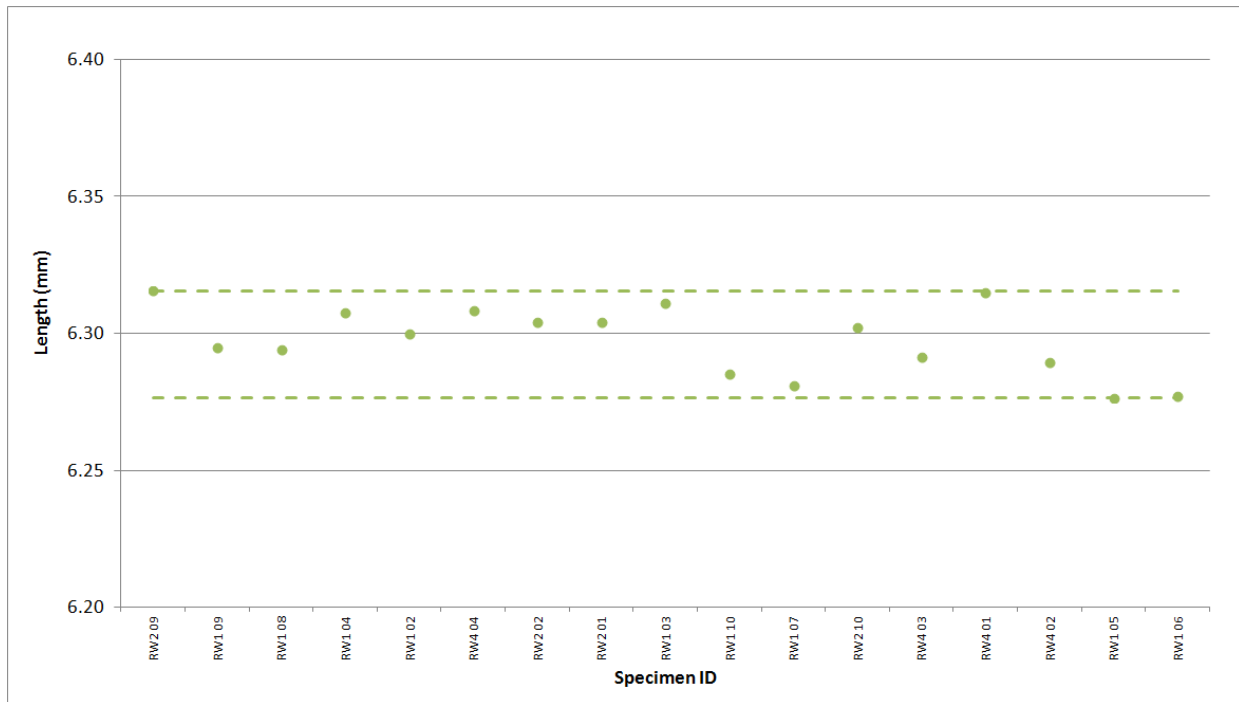


Figure A-30. BAN Piggyback Length.

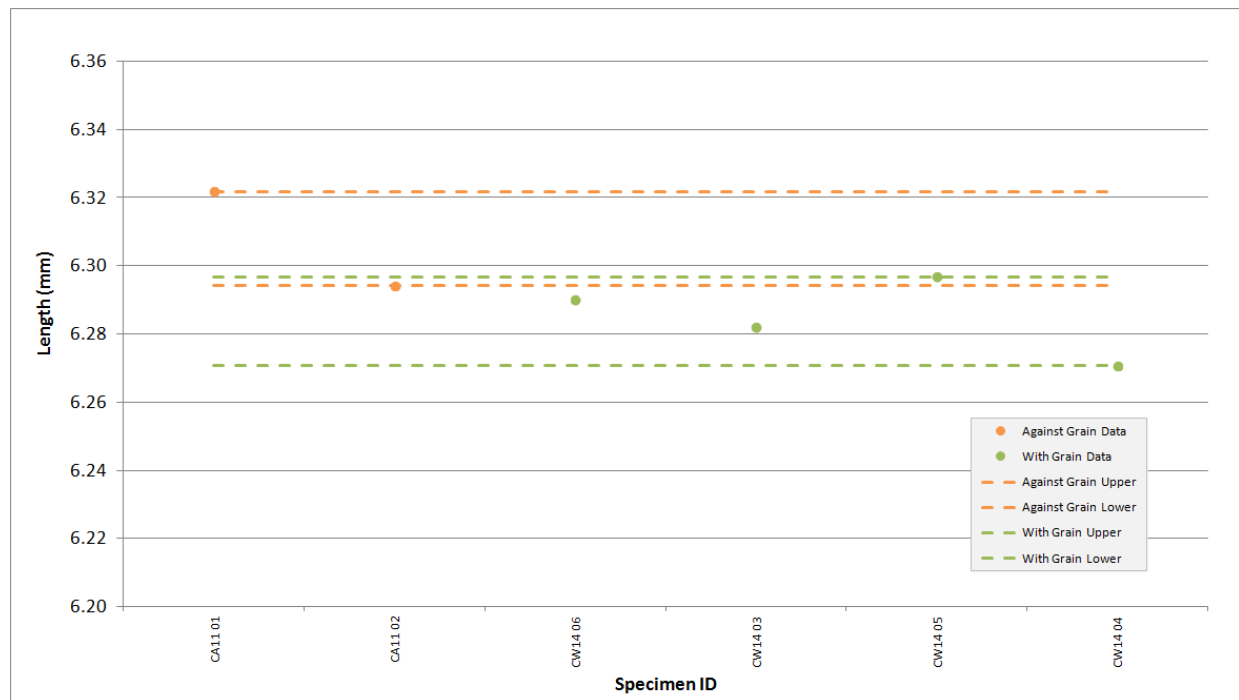


Figure A-31. H-451 Piggyback Length.

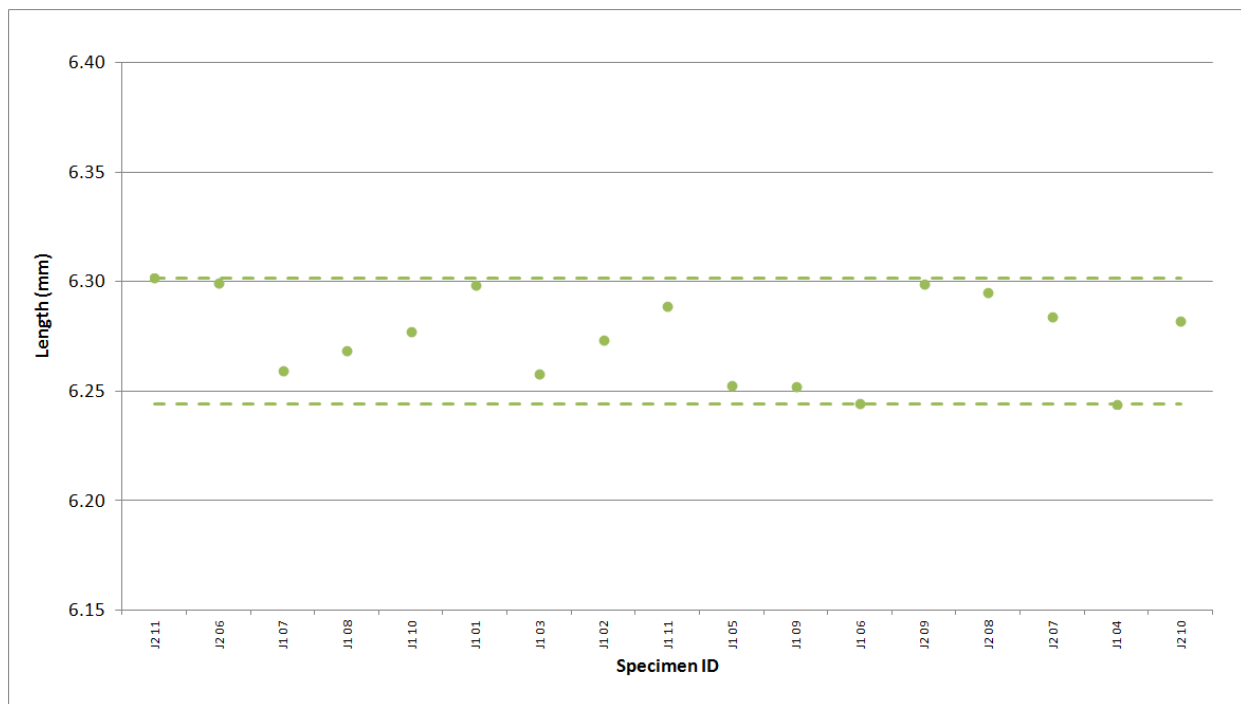


Figure A-32. HLM Piggyback Length.

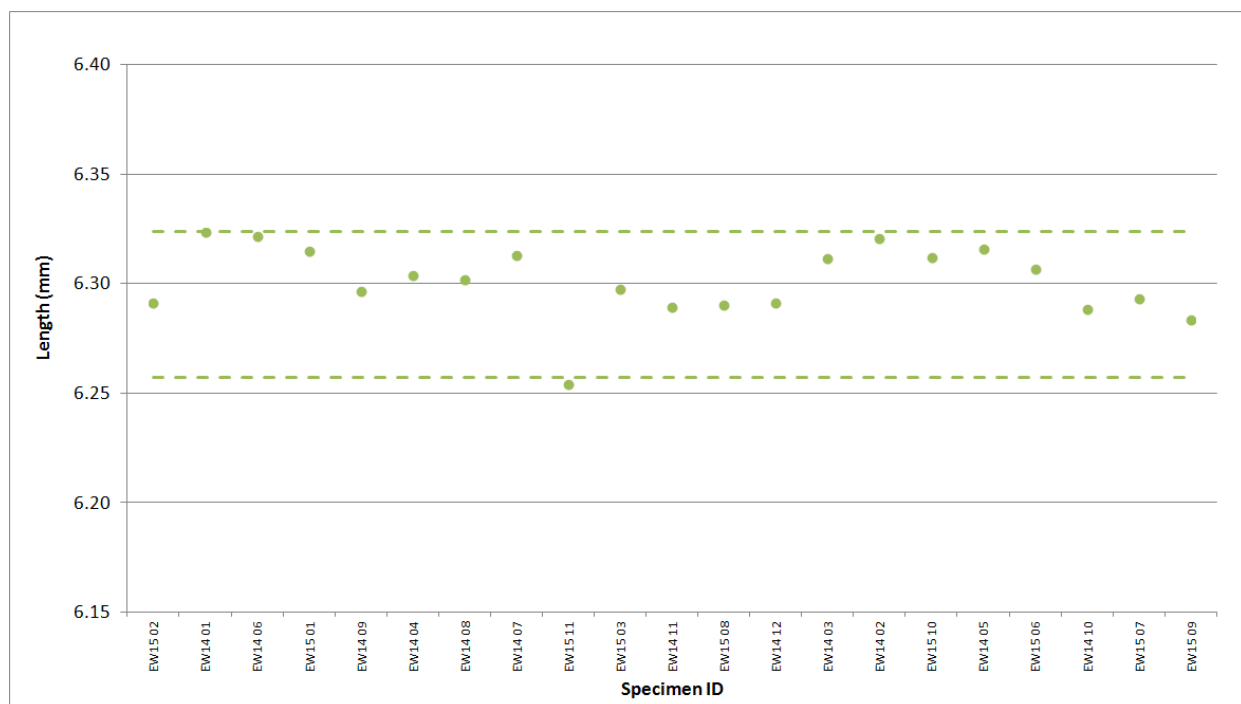


Figure A-33. IG-110 Piggyback Length.

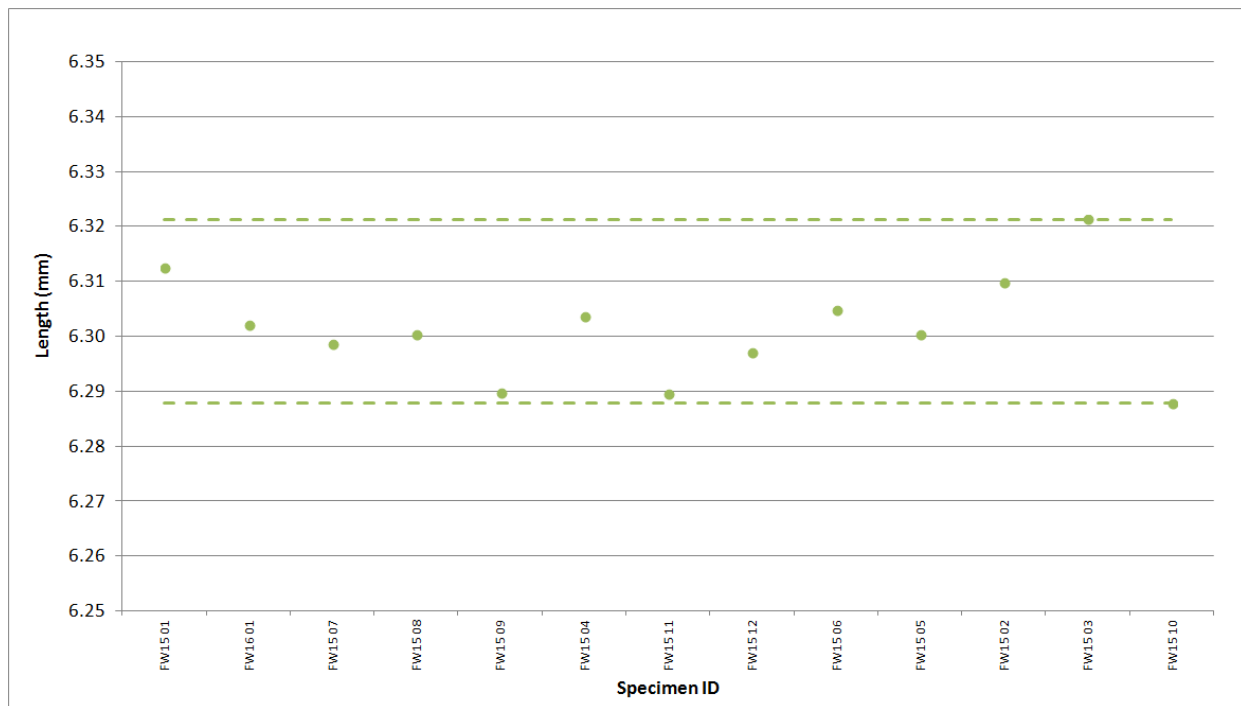


Figure A-34. IG-430 Piggyback Length.

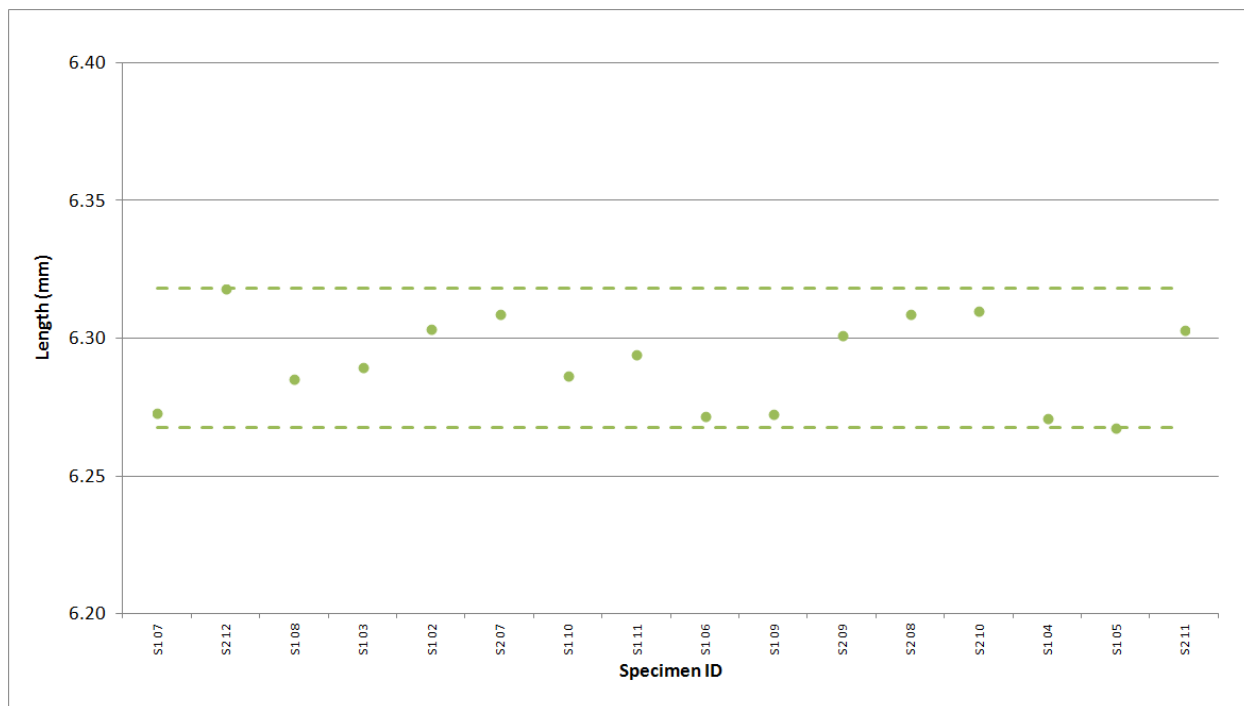


Figure A-35. NBG-10 Piggyback Length.

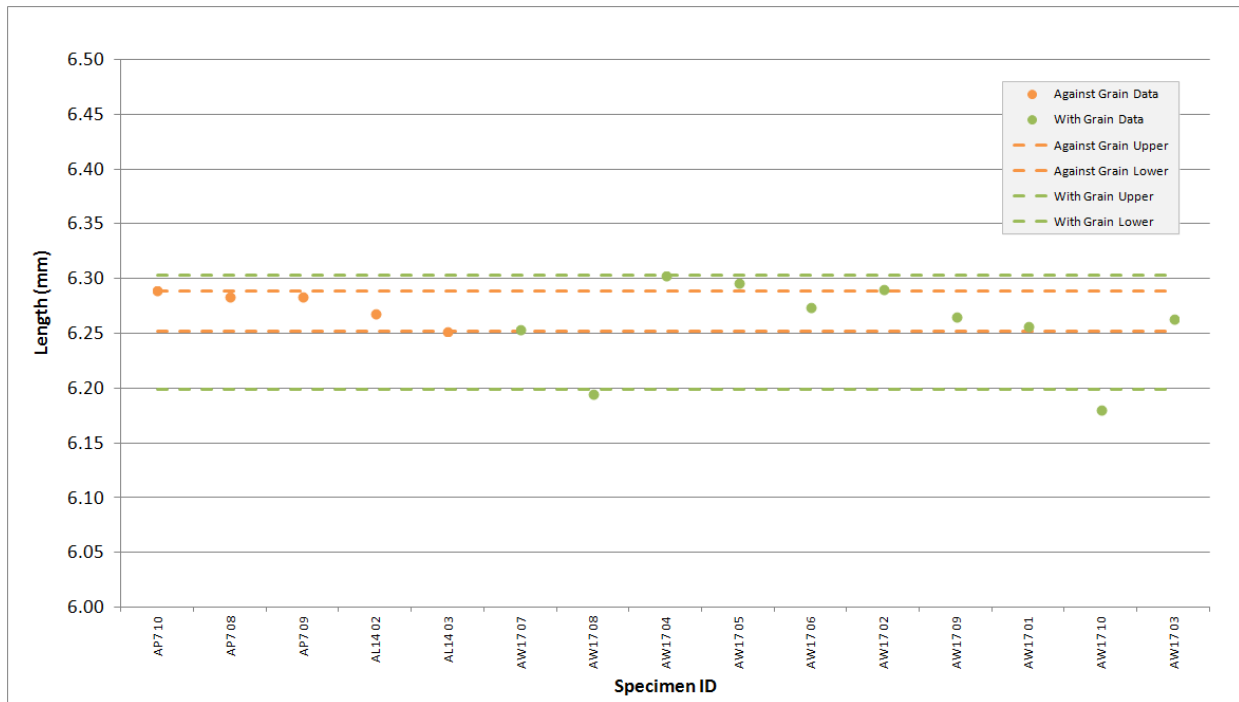


Figure A-36. NBG-17 Piggyback Length.

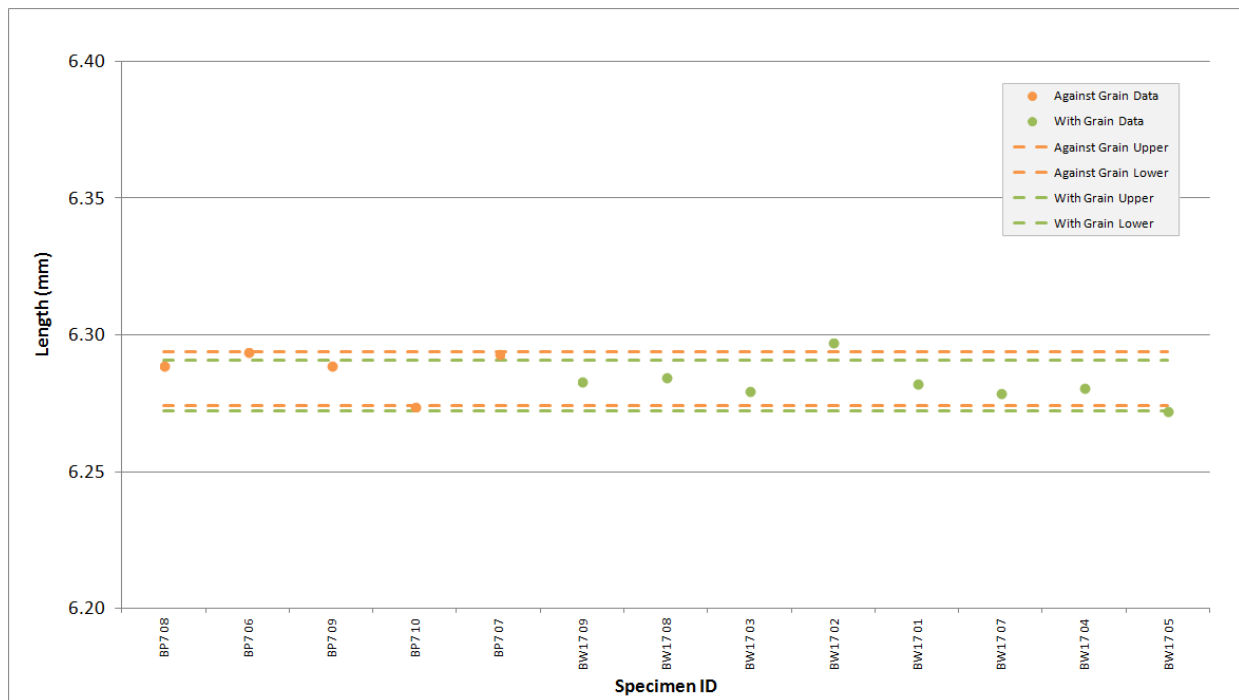


Figure A-37. NBG-18 Piggyback Length.

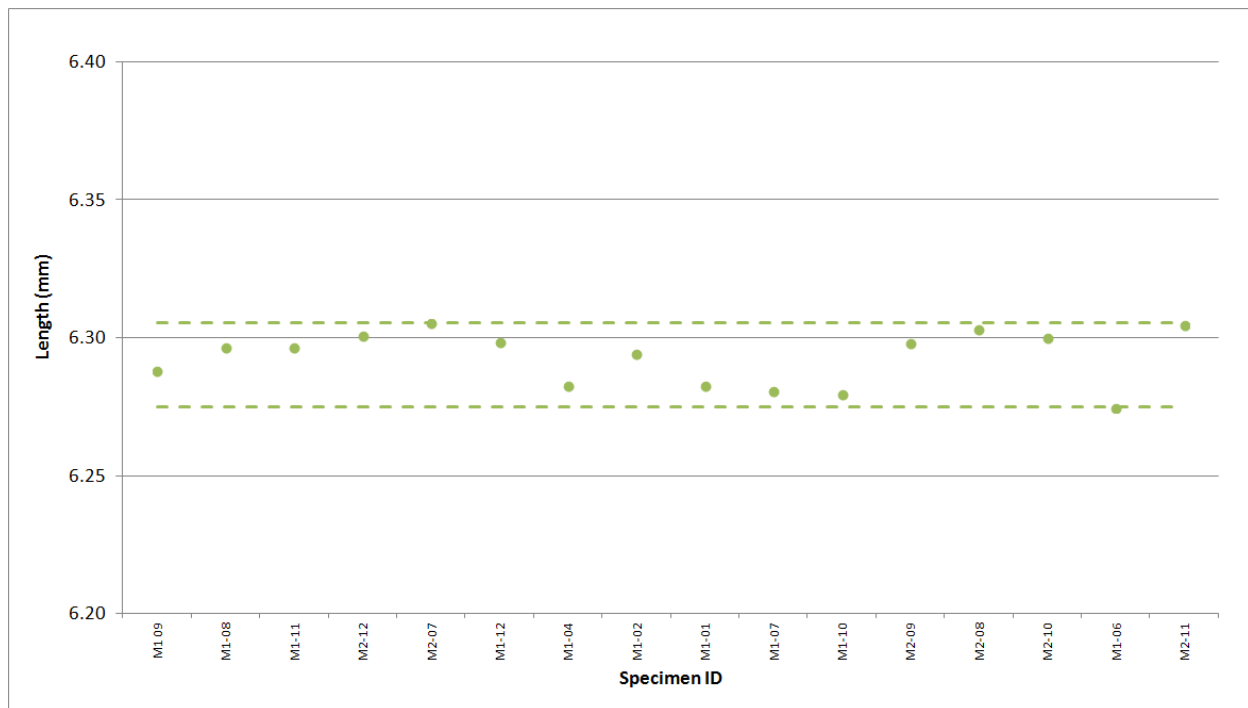


Figure A-38. NBG-25 Piggyback Length.

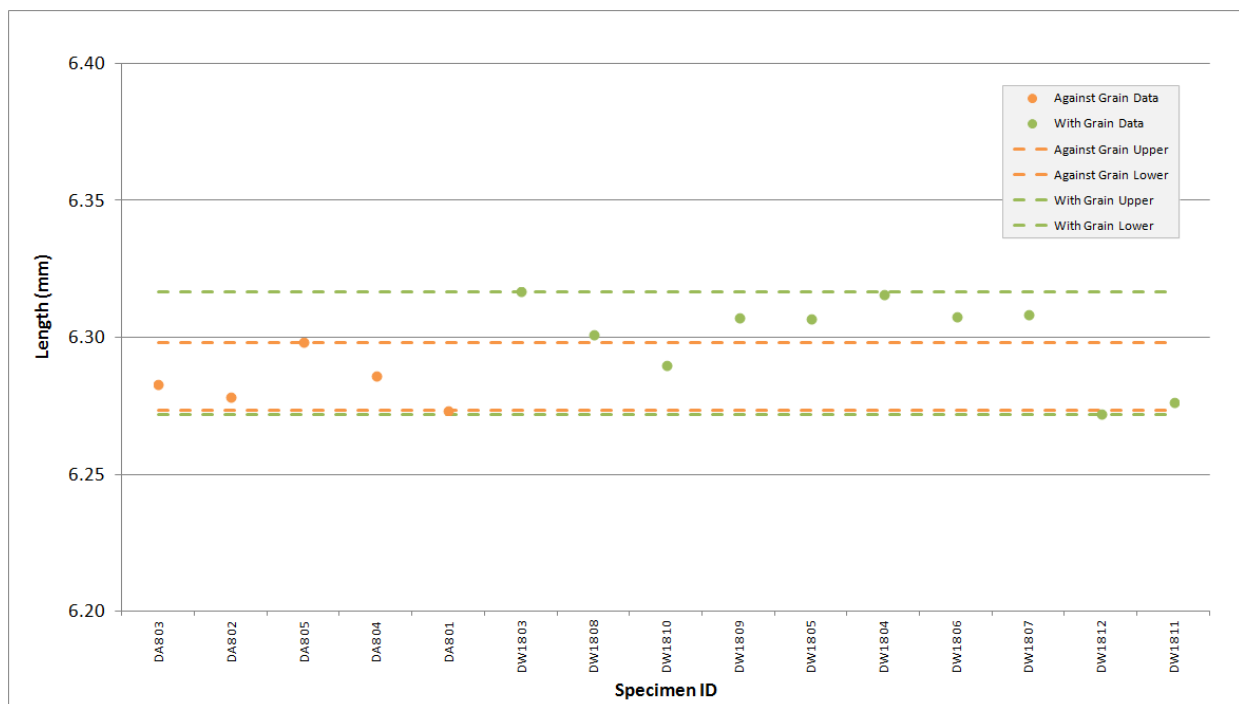


Figure A-39. PCEA Piggyback Length.

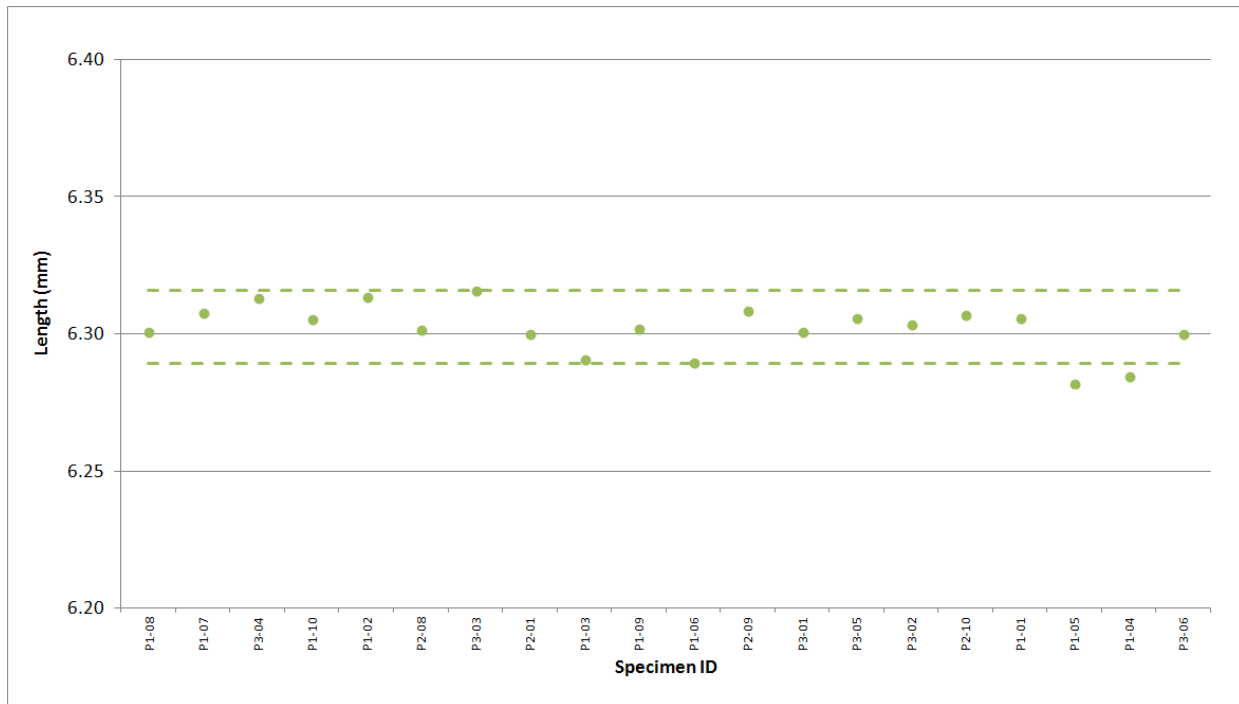


Figure A-40. PCIB Piggyback Length.

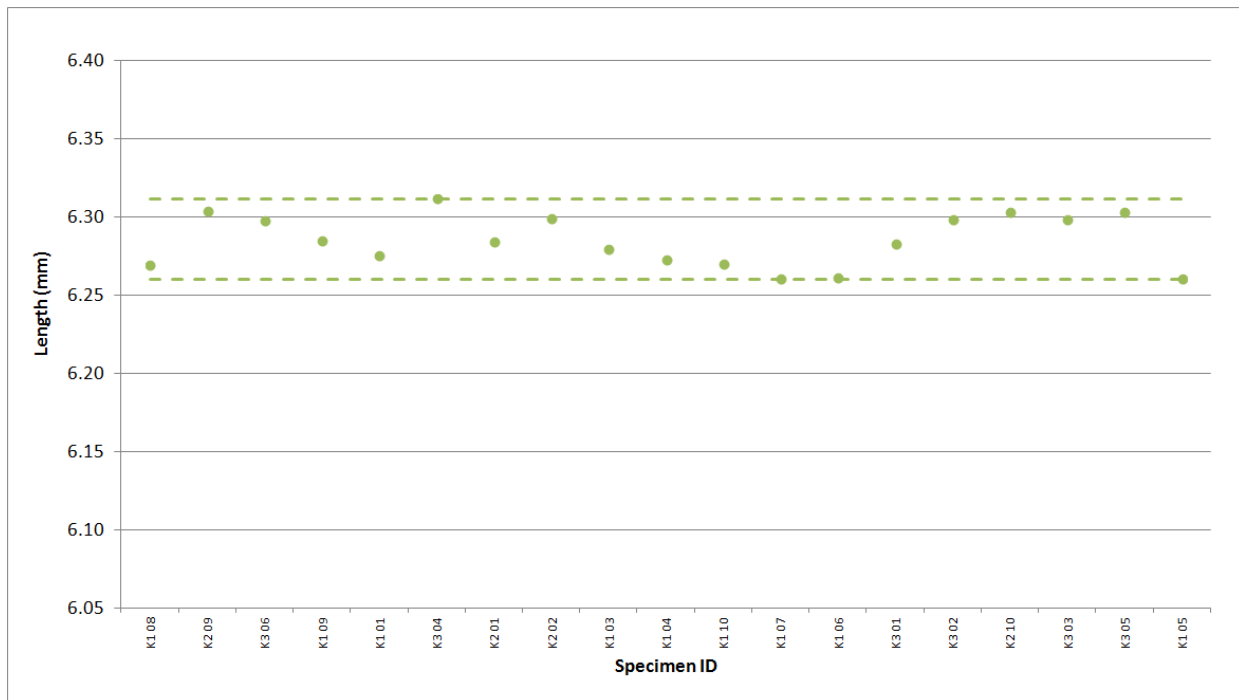


Figure A-41. PGX Piggyback Length.

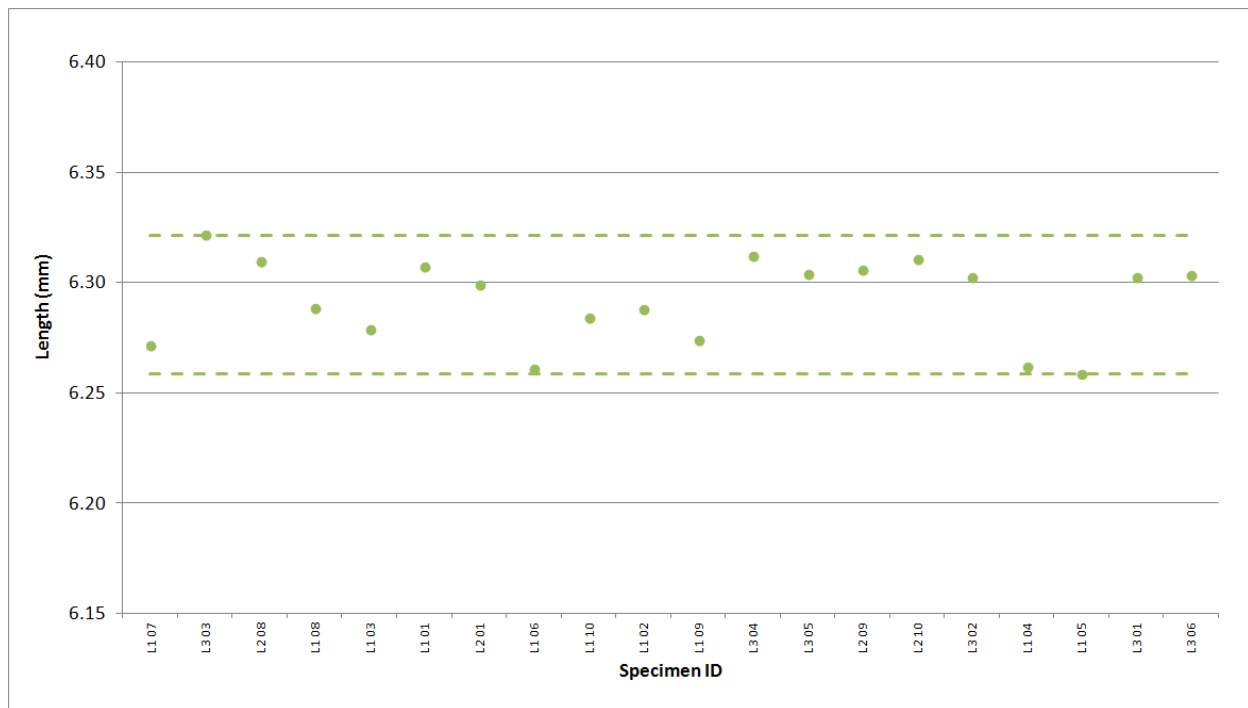


Figure A-42. PPEA Piggyback Length.

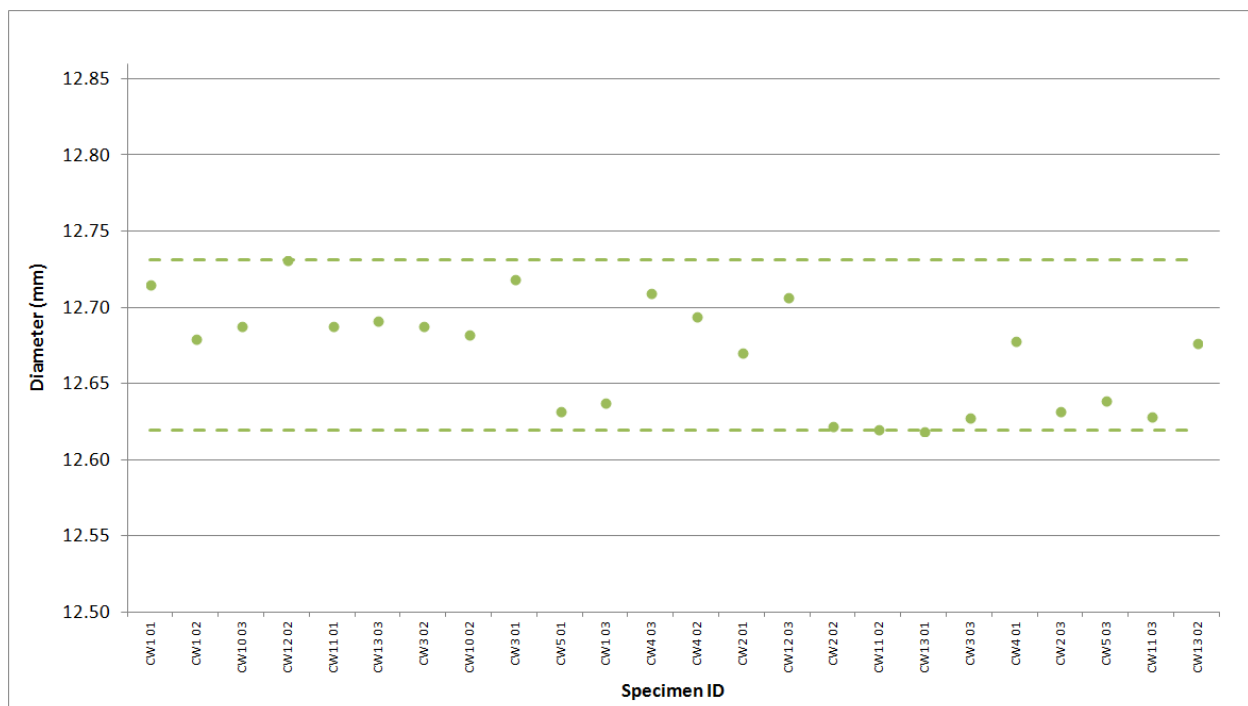


Figure A-43. H-451 Creep Diameter.

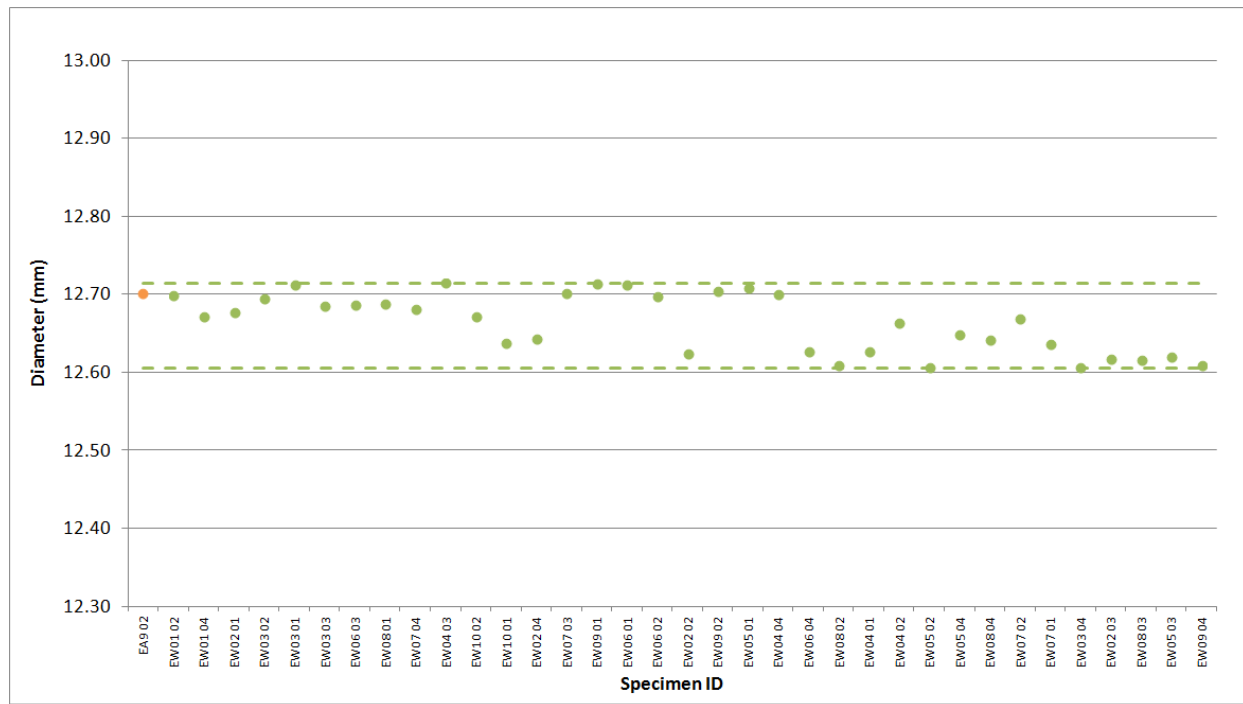


Figure A-44. IG-110 Creep Diameter.

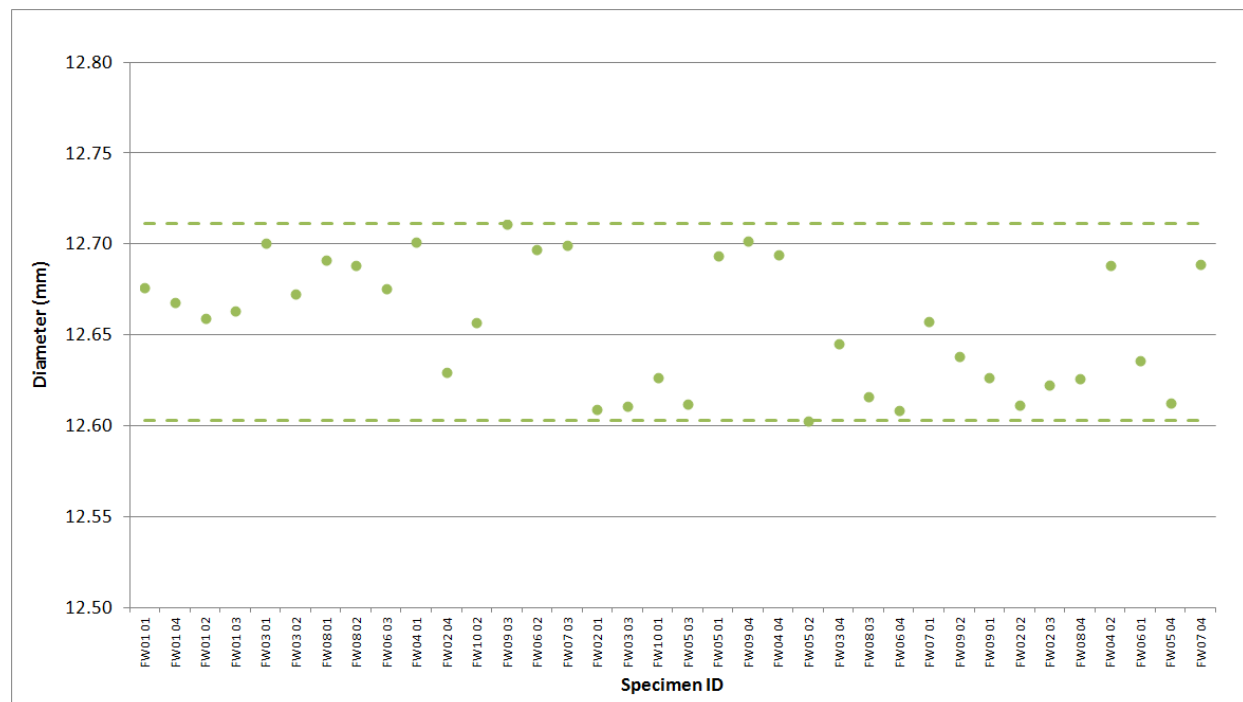


Figure A-45. IG-430 Creep Diameter.

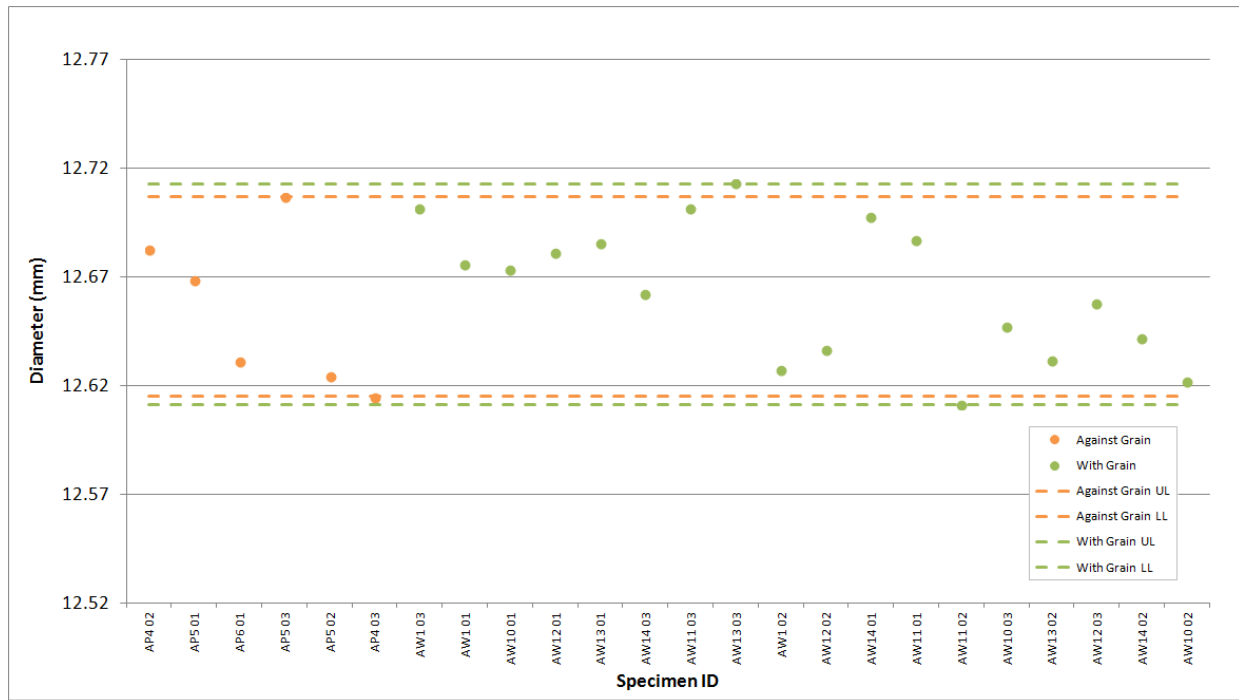


Figure A-46. NBG-17 Creep Diameter.

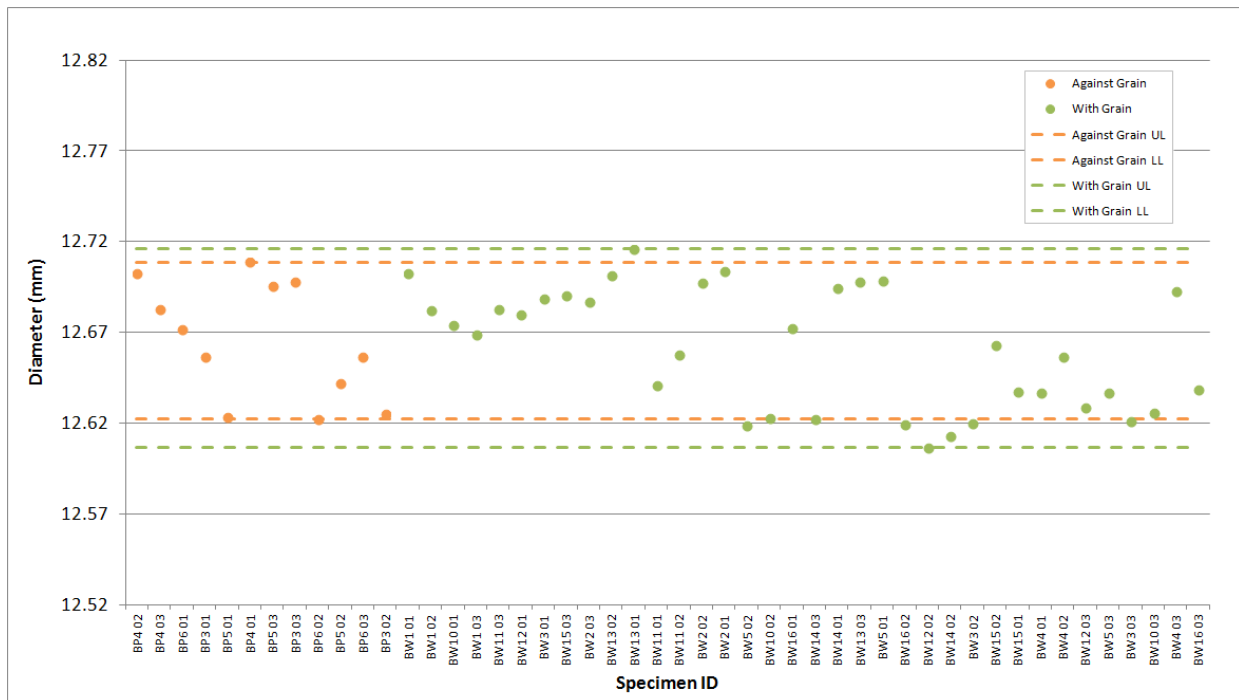


Figure A-47. NBG-18 Creep Diameter.

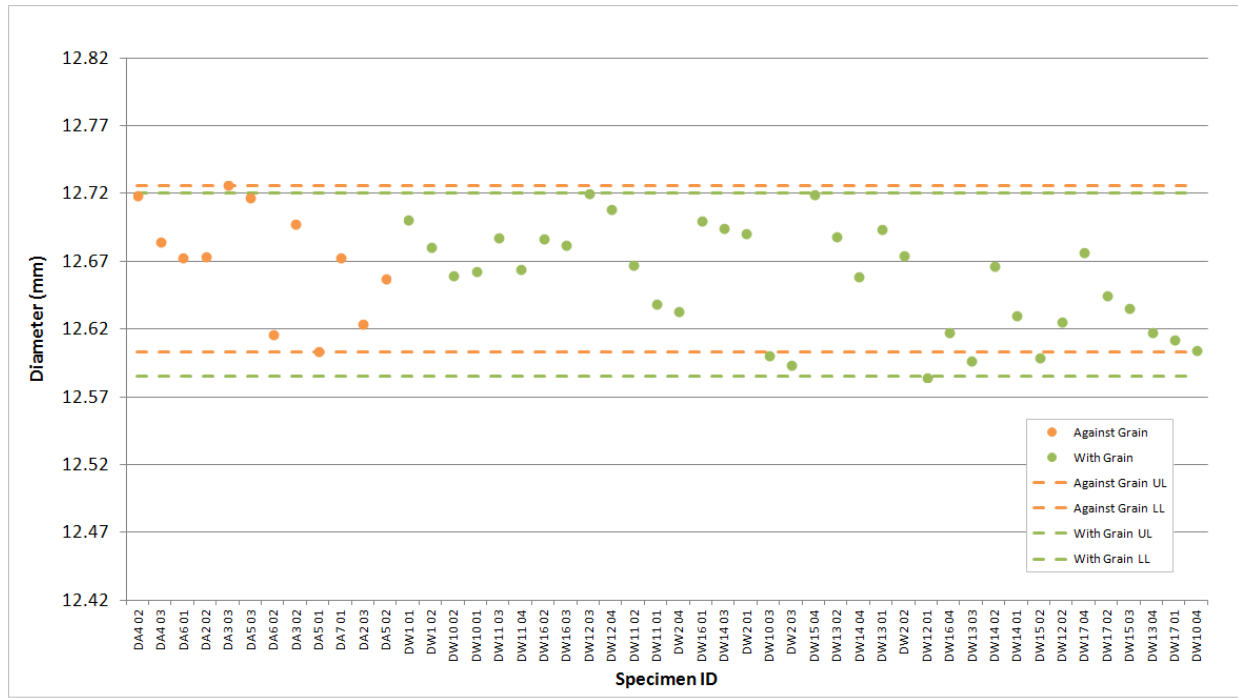


Figure A-48. PCEA Creep Diameter.

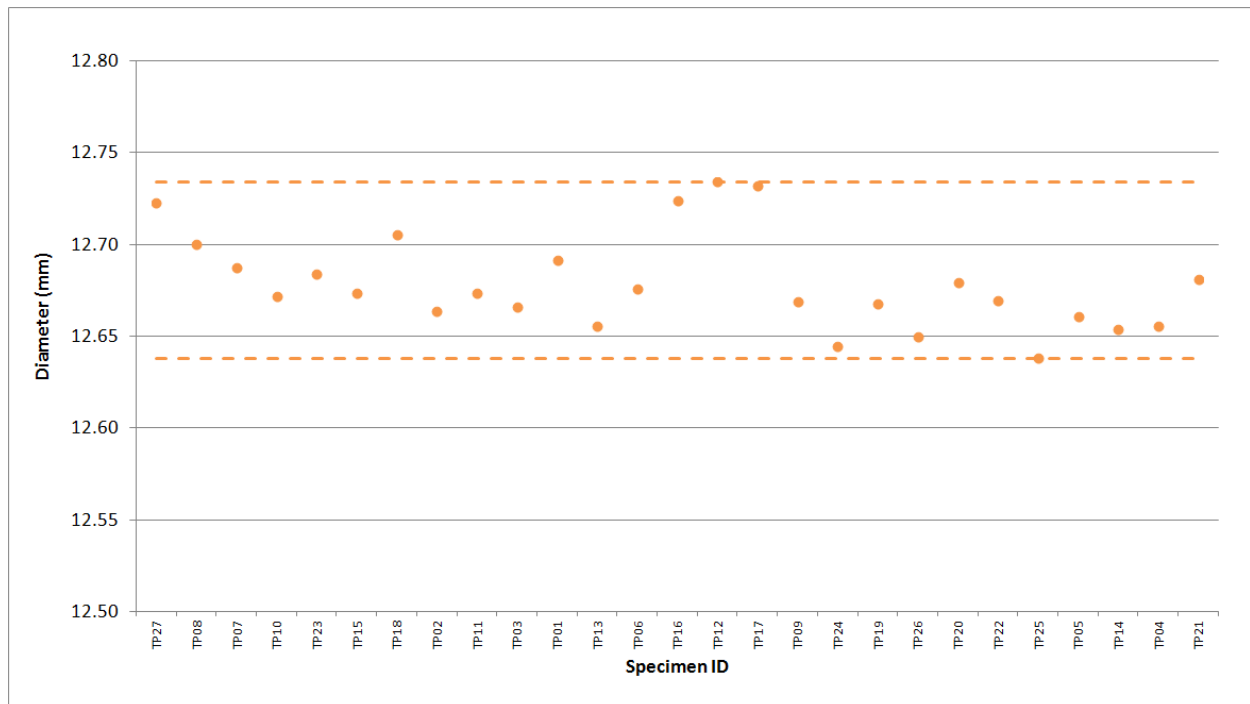


Figure A-49. 2114 Piggyback Diameter.

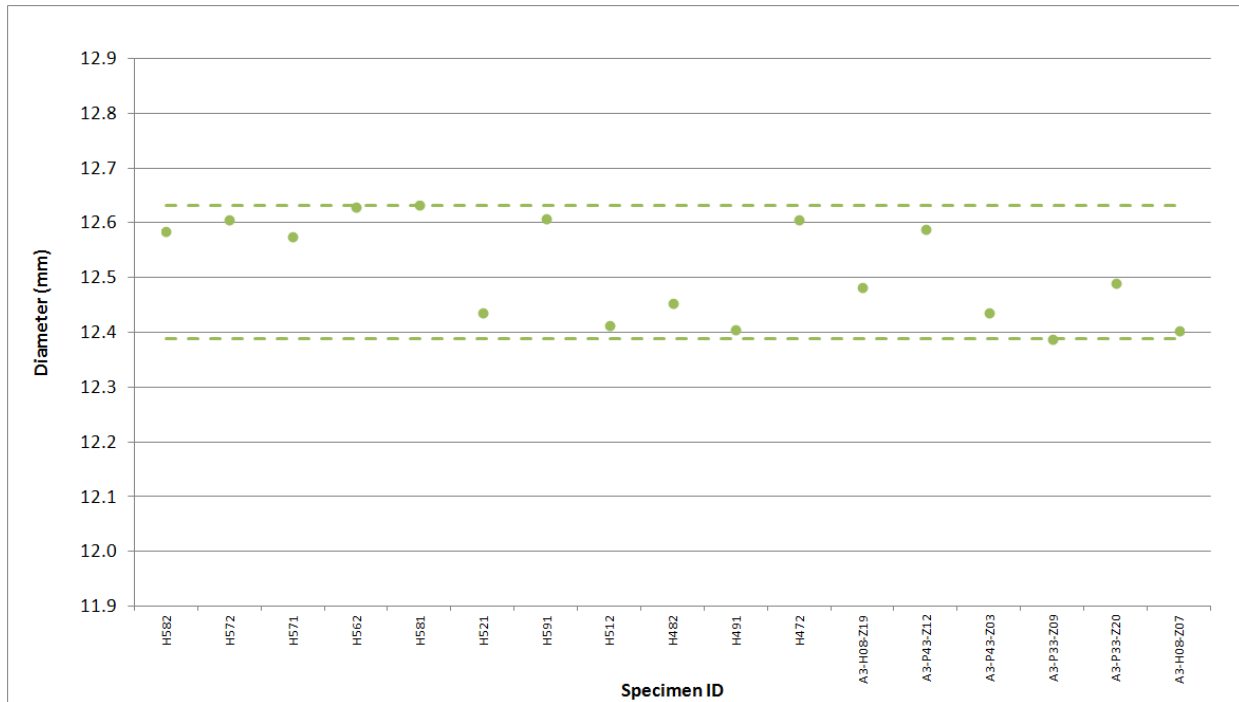


Figure A-50. A3 Piggyback Diameter.

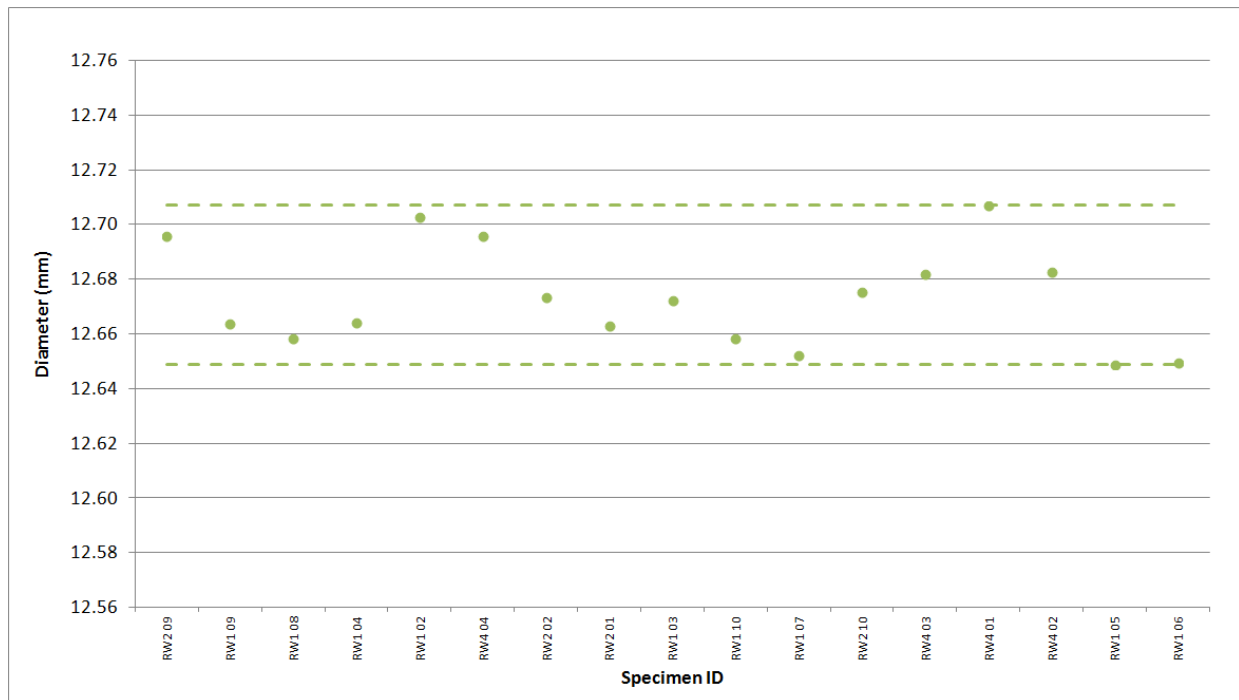


Figure A-51. BAN Piggyback Diameter.

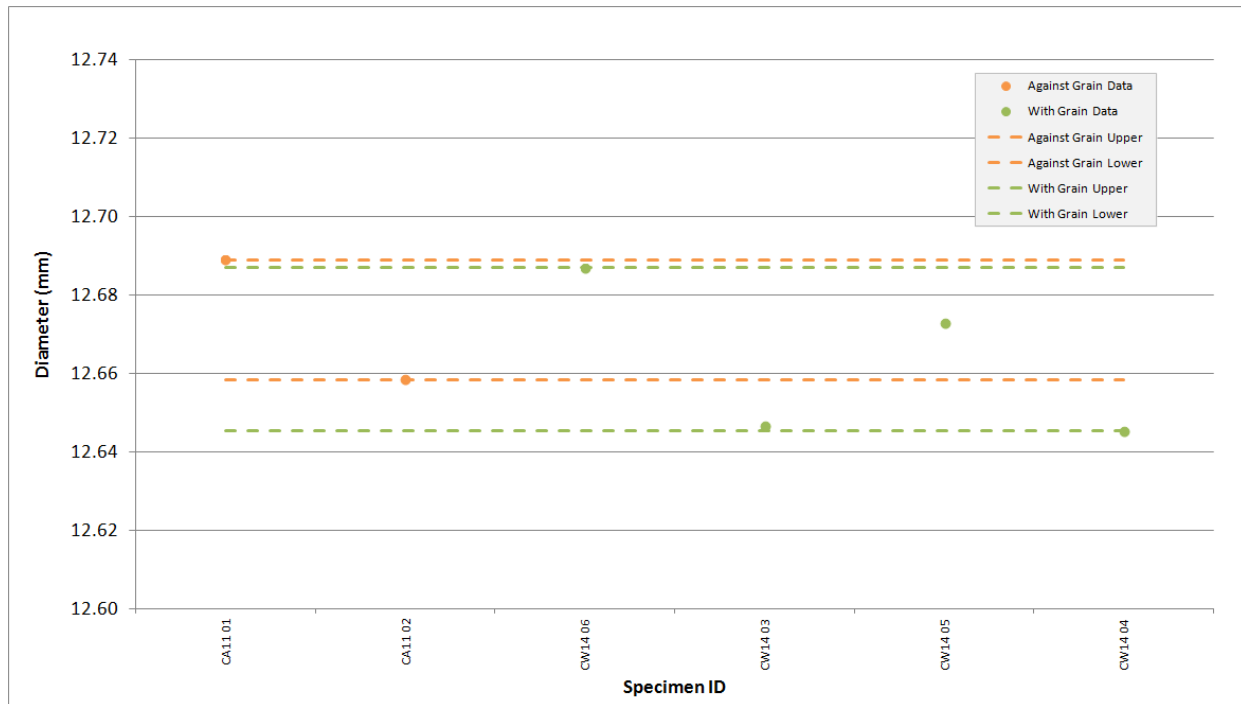


Figure A-52. H-451 Piggyback Diameter.

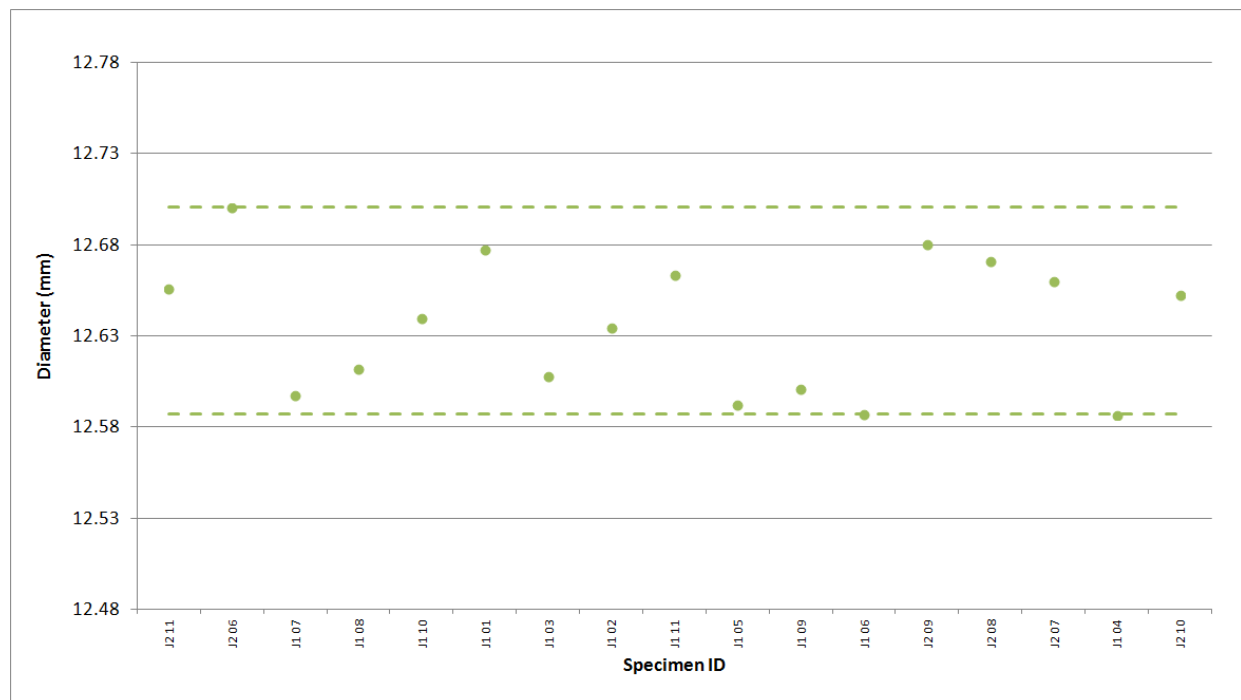


Figure A-53. HLM Piggyback Diameter.

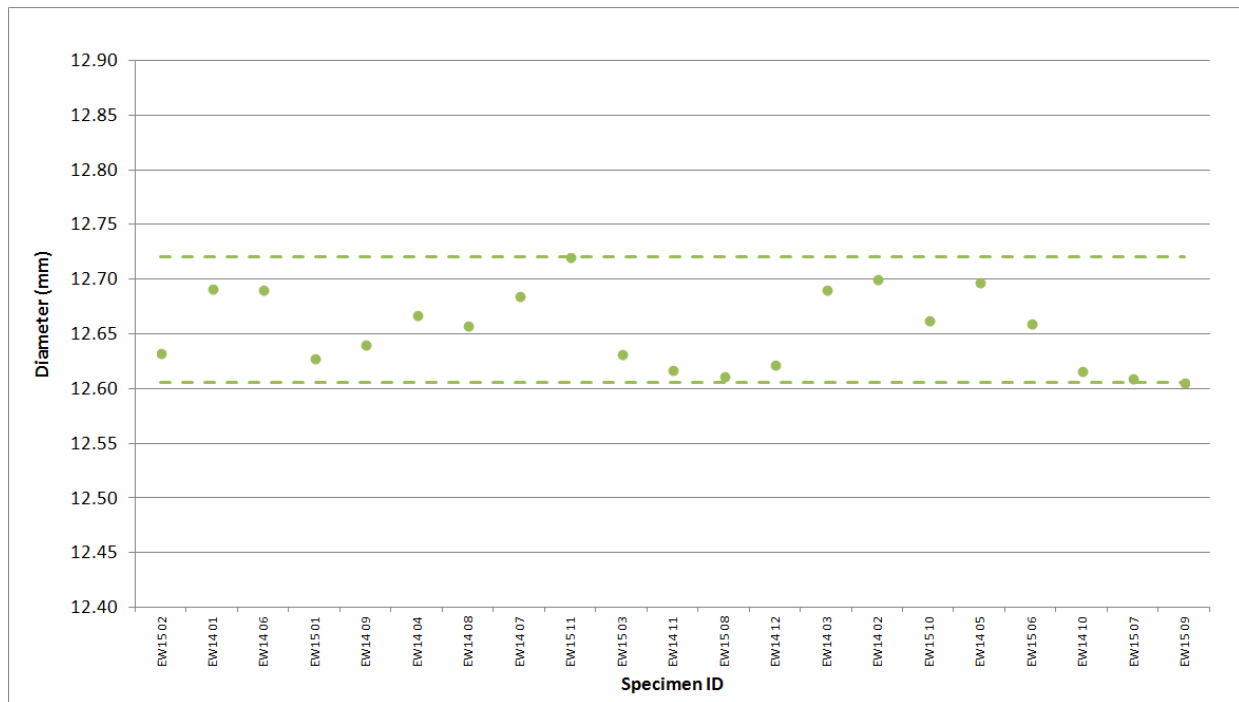


Figure A-54. IG-110 Piggyback Diameter.

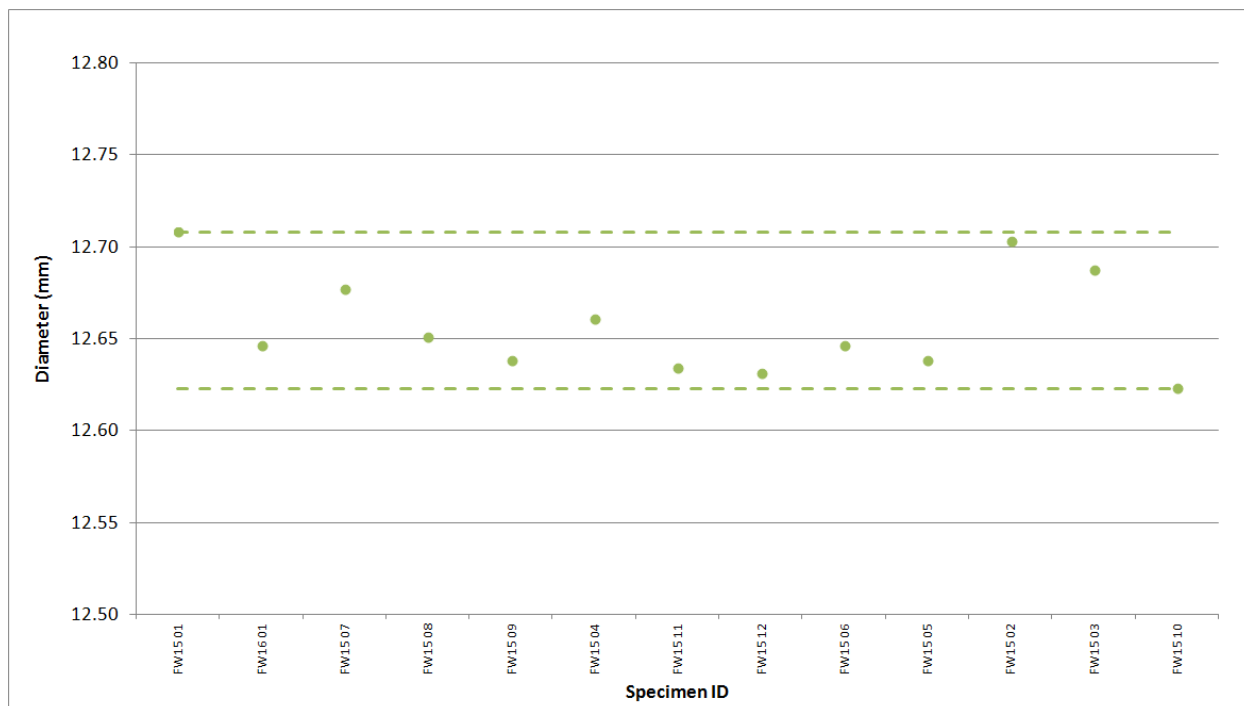


Figure A-55. IG-430 Piggyback Diameter.

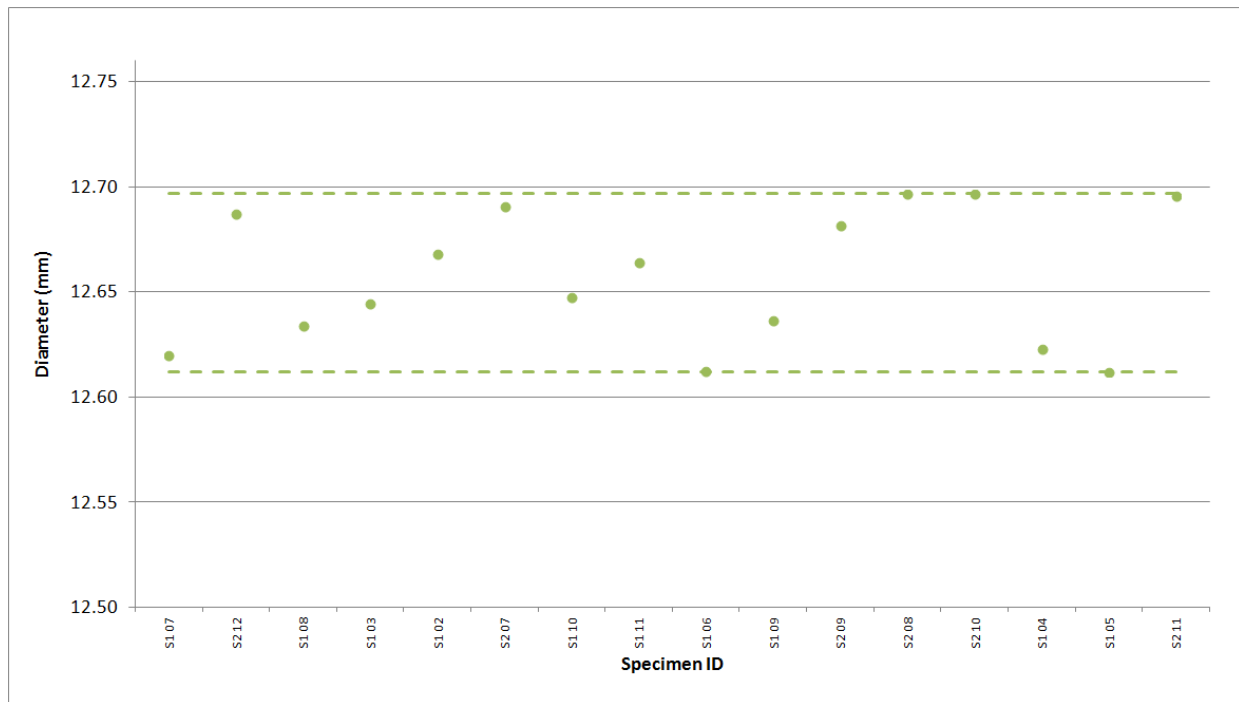


Figure A-56. NBG-10 Piggyback Diameter.

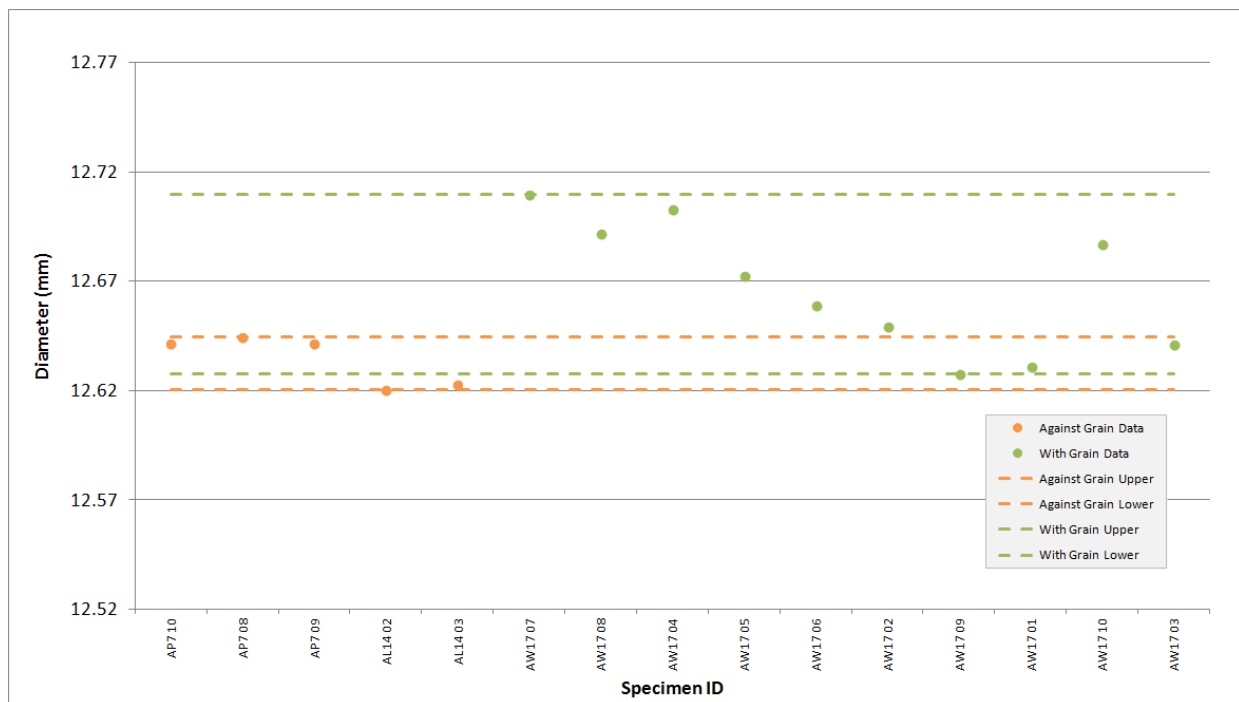


Figure A-57. NBG-17 Piggyback Diameter.

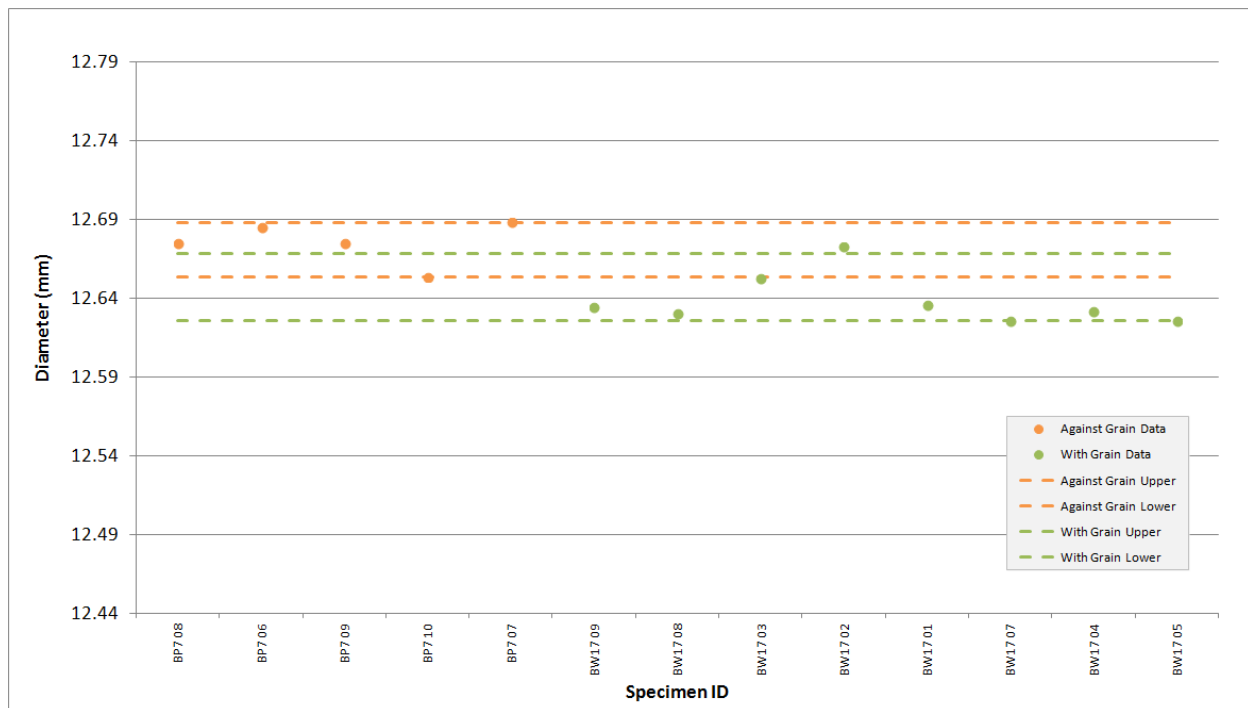


Figure A-58. NBG-18 Piggyback Diameter.

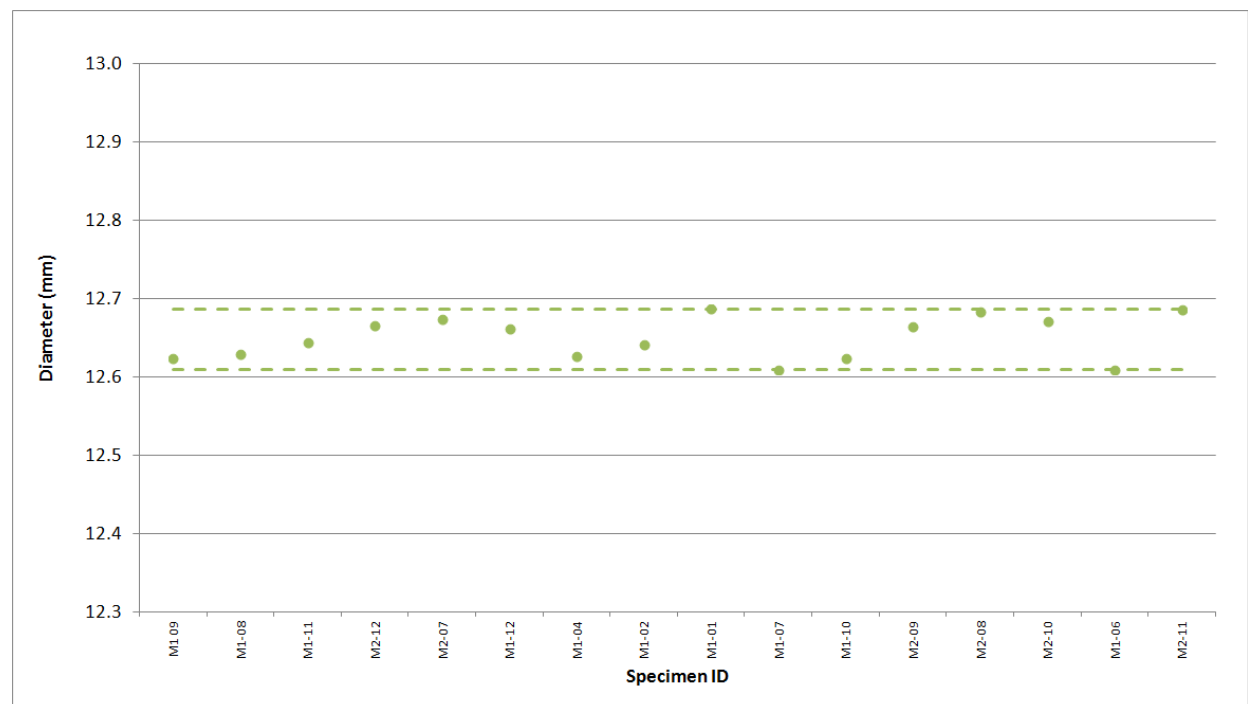


Figure A-59. NBG-25 Piggyback Diameter.

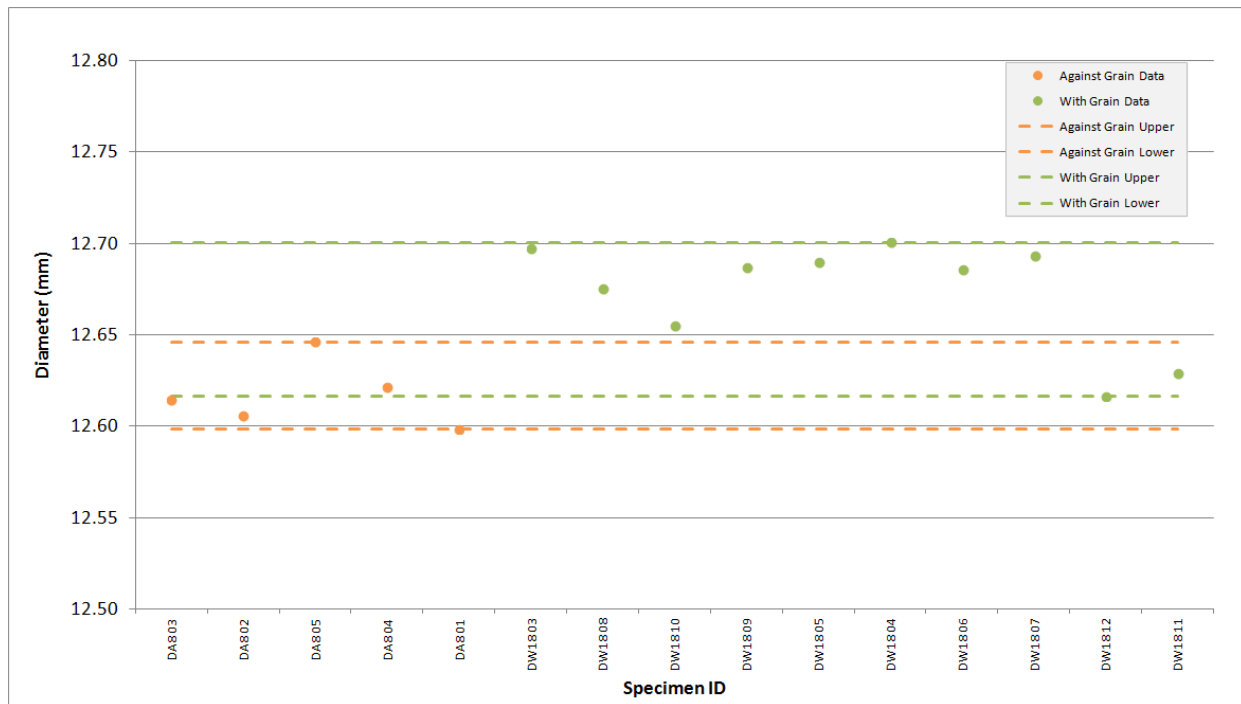


Figure A-60. PCEA Piggyback Diameter.

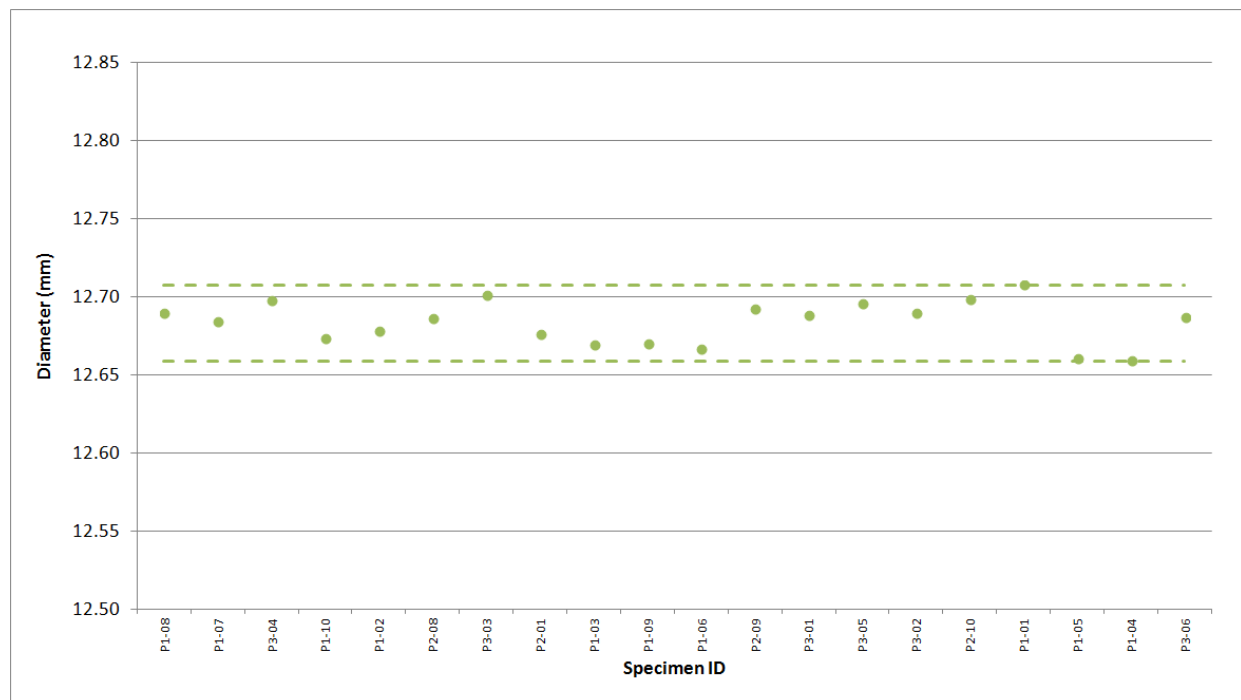


Figure A-61. PCIB Piggyback Diameter.

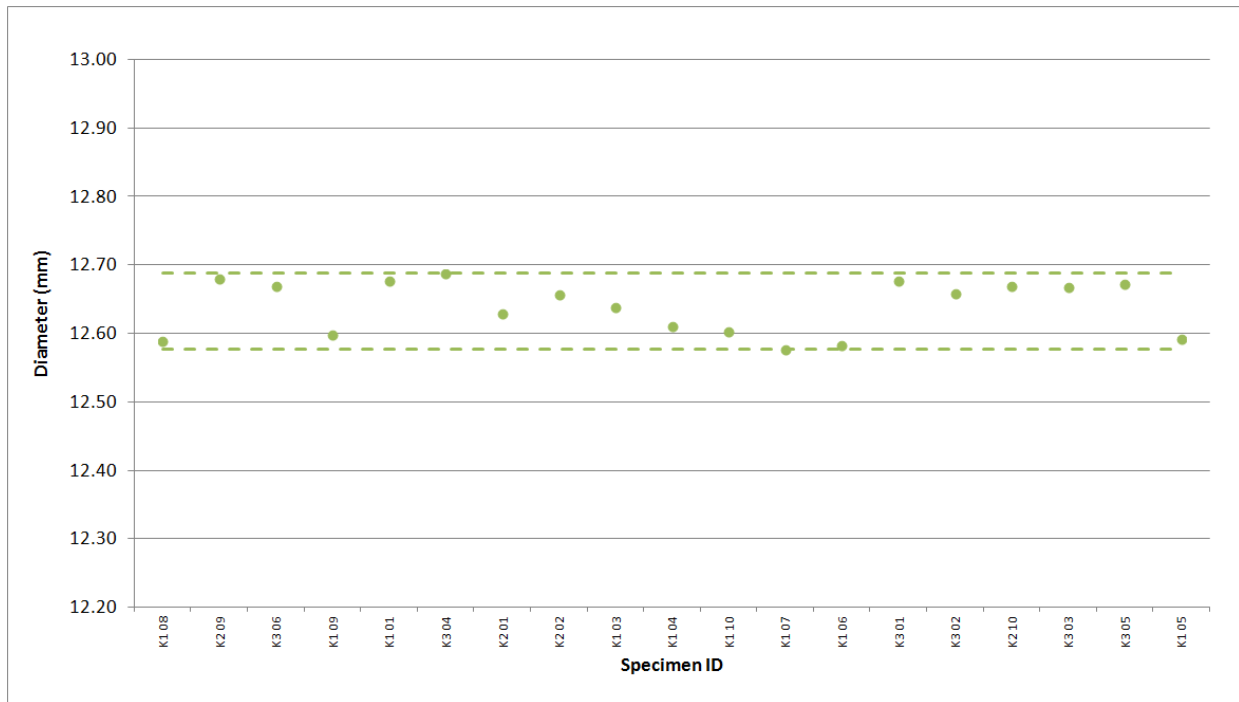


Figure A-62. PGX Piggyback Diameter.

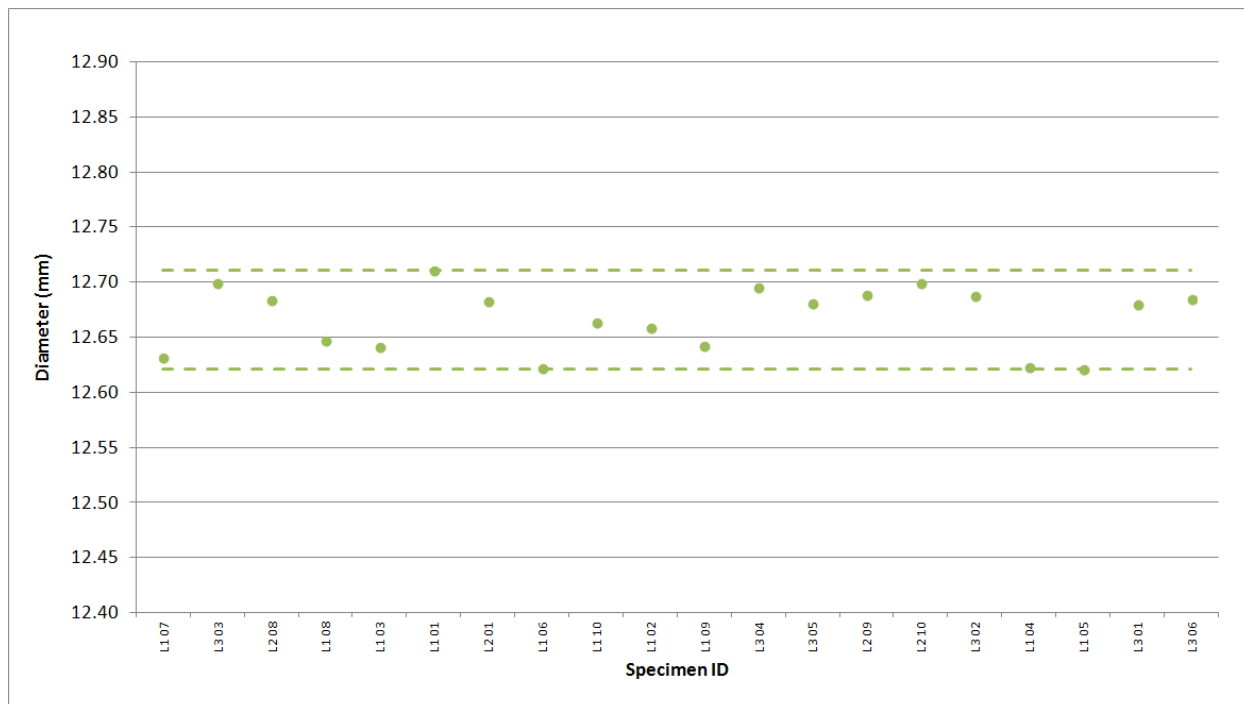


Figure A-63. PPEA Piggyback Diameter.

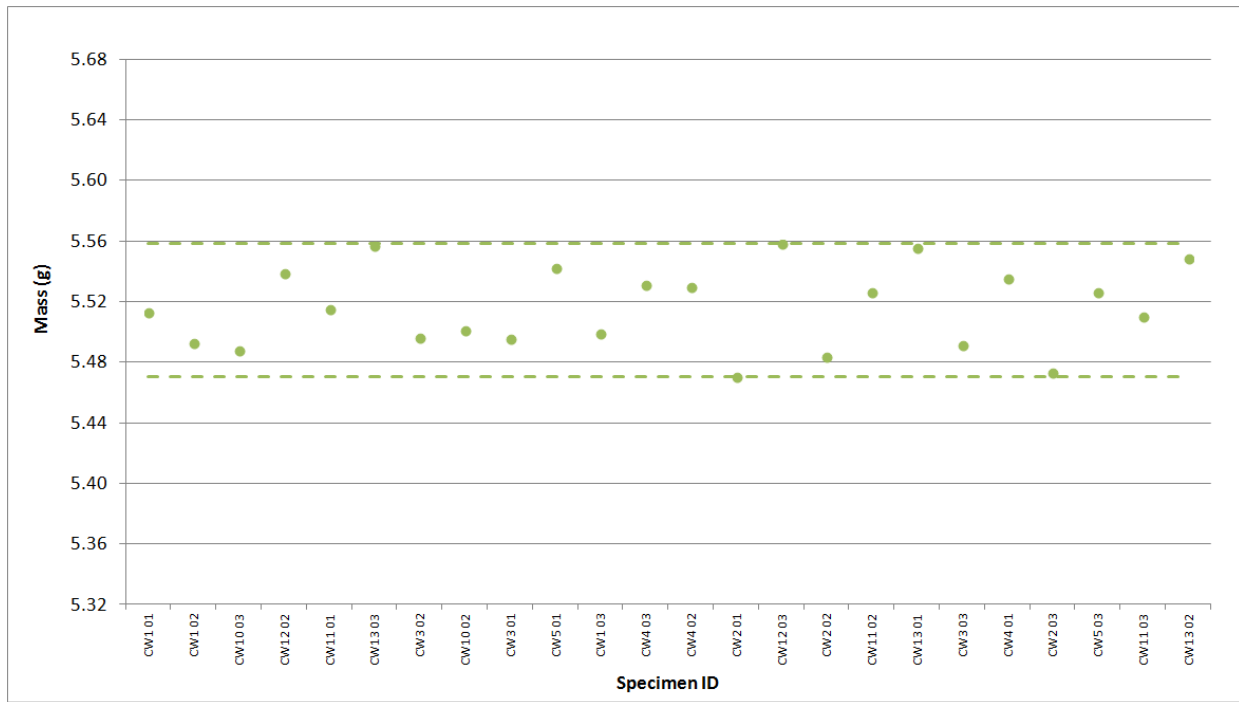


Figure A-64. H-451 Creep Mass.

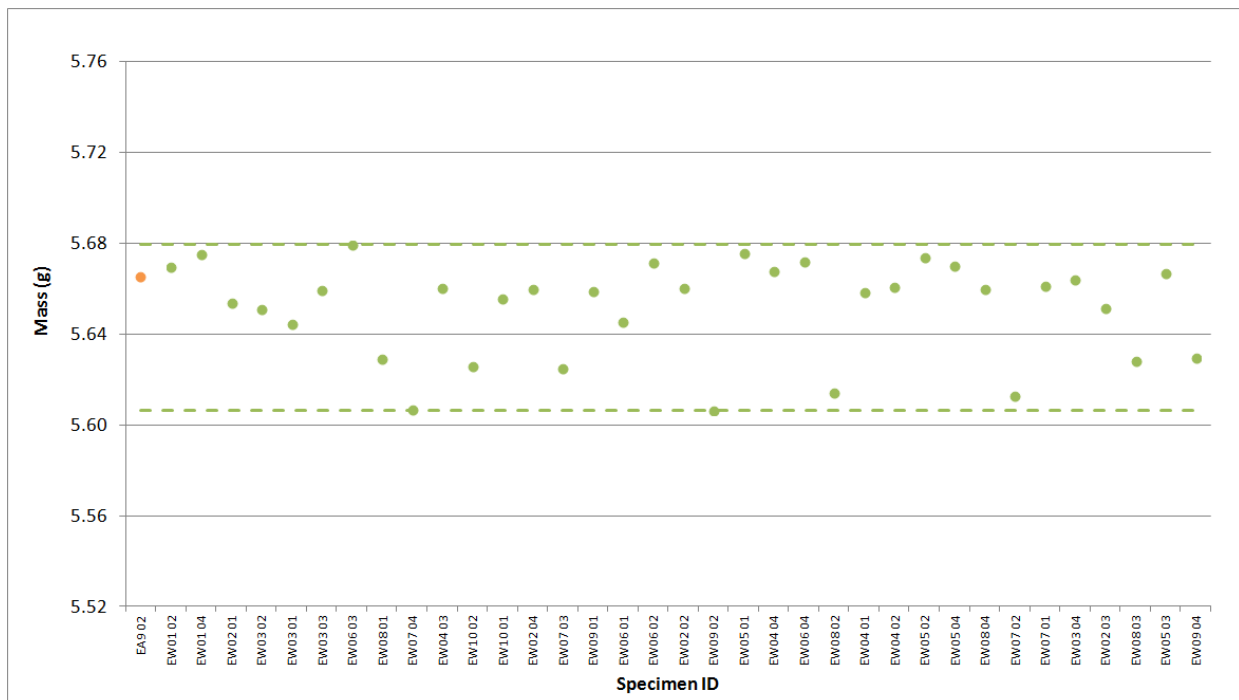


Figure A-65. IG-110 Creep Mass.

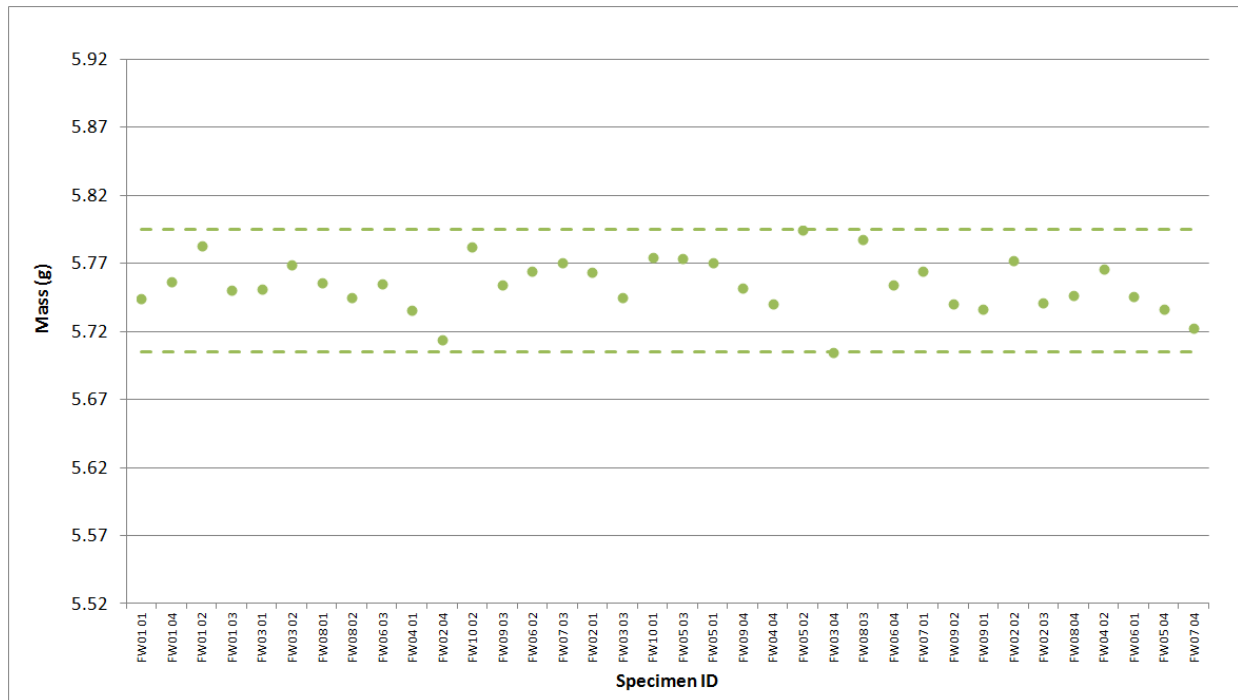


Figure A-66. IG-430 Creep Mass.

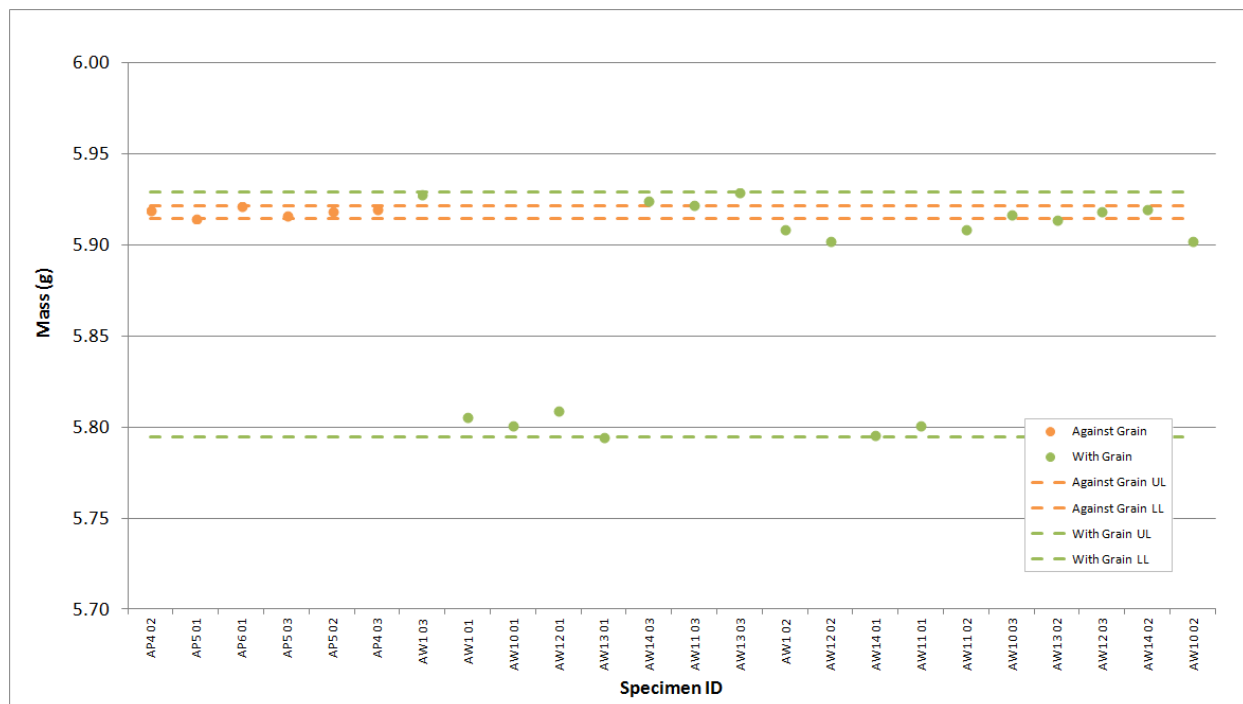


Figure A-67. NBG-17 Creep Mass.

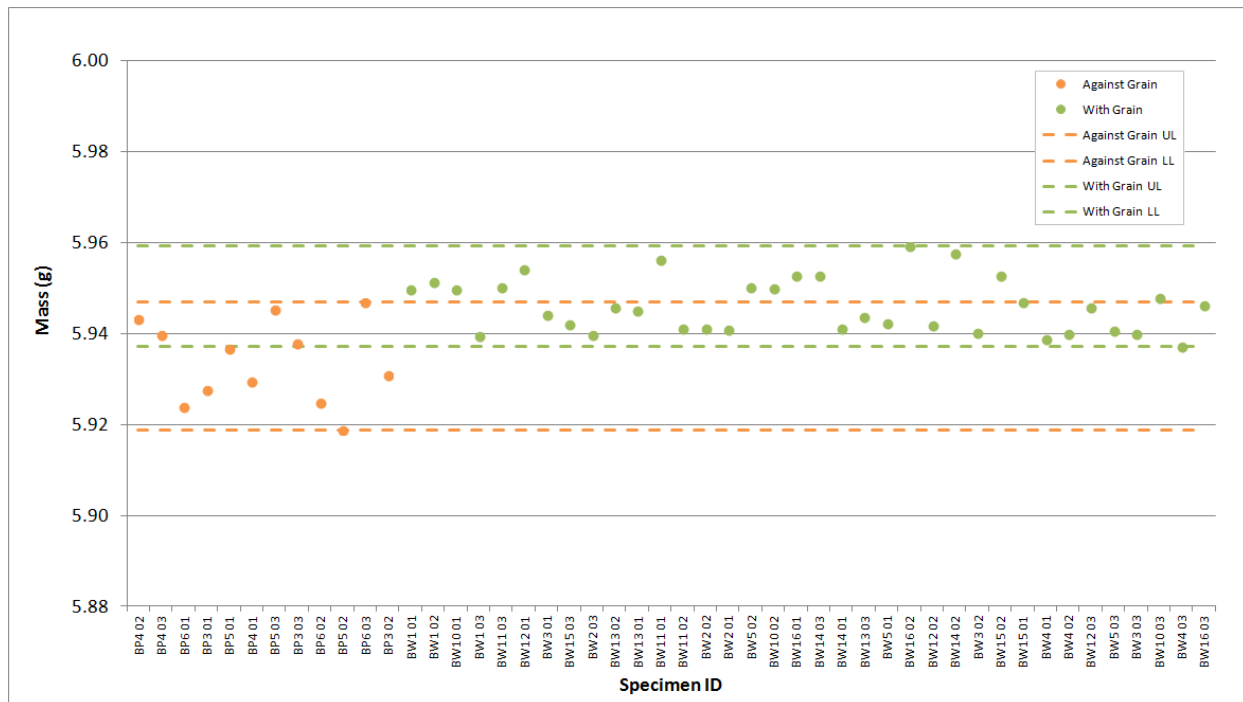


Figure A-68. NBG-18 Creep Mass.



Figure A-69. PCEA Creep Mass.

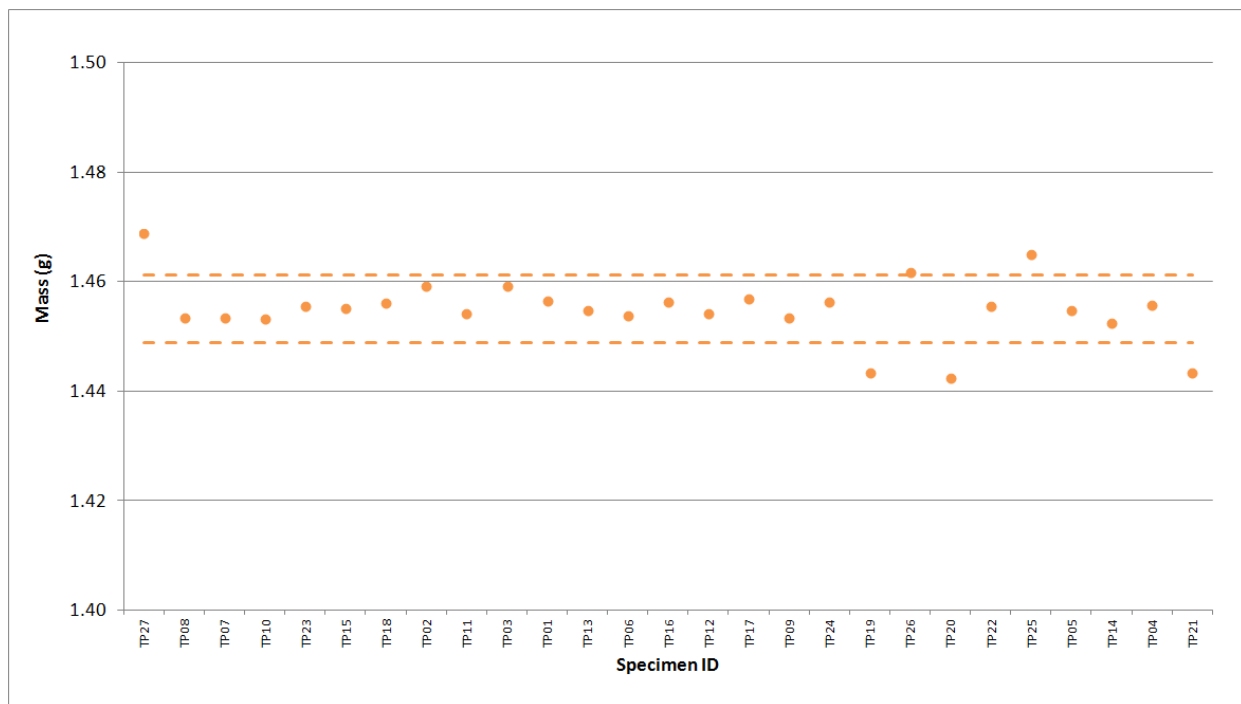


Figure A-70. 2114 Piggyback Mass.

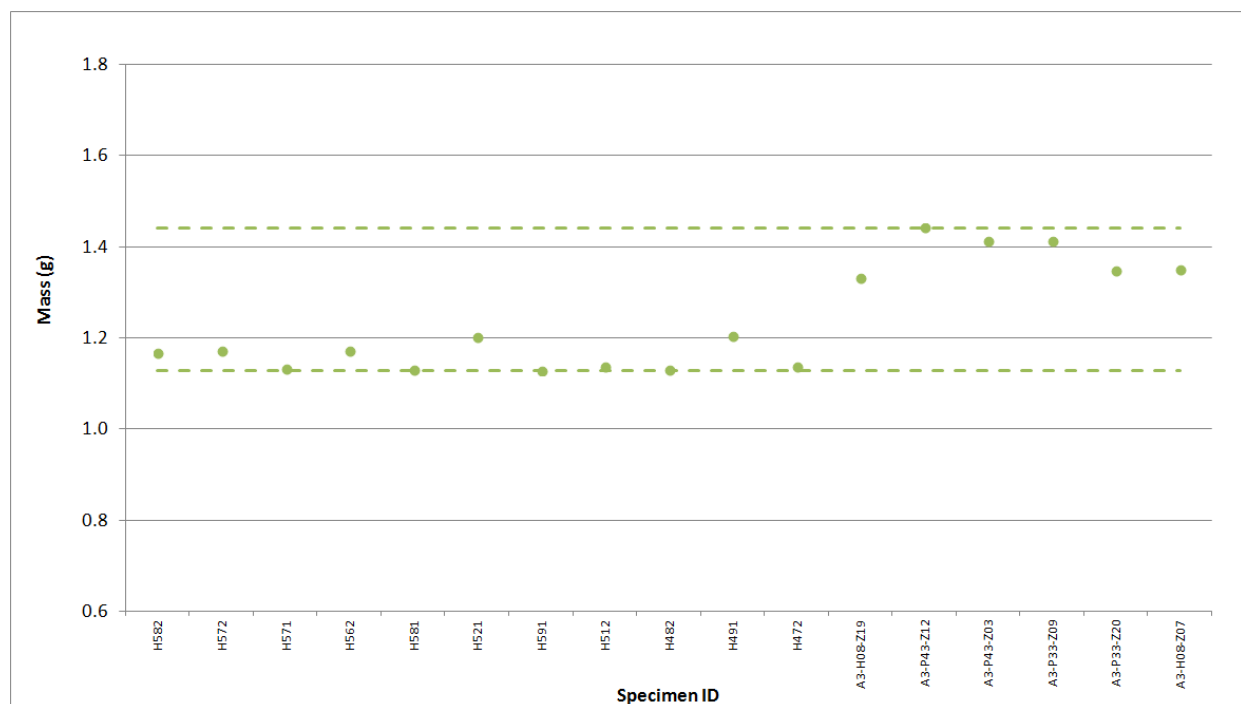


Figure A-71. A3 Piggyback Mass.

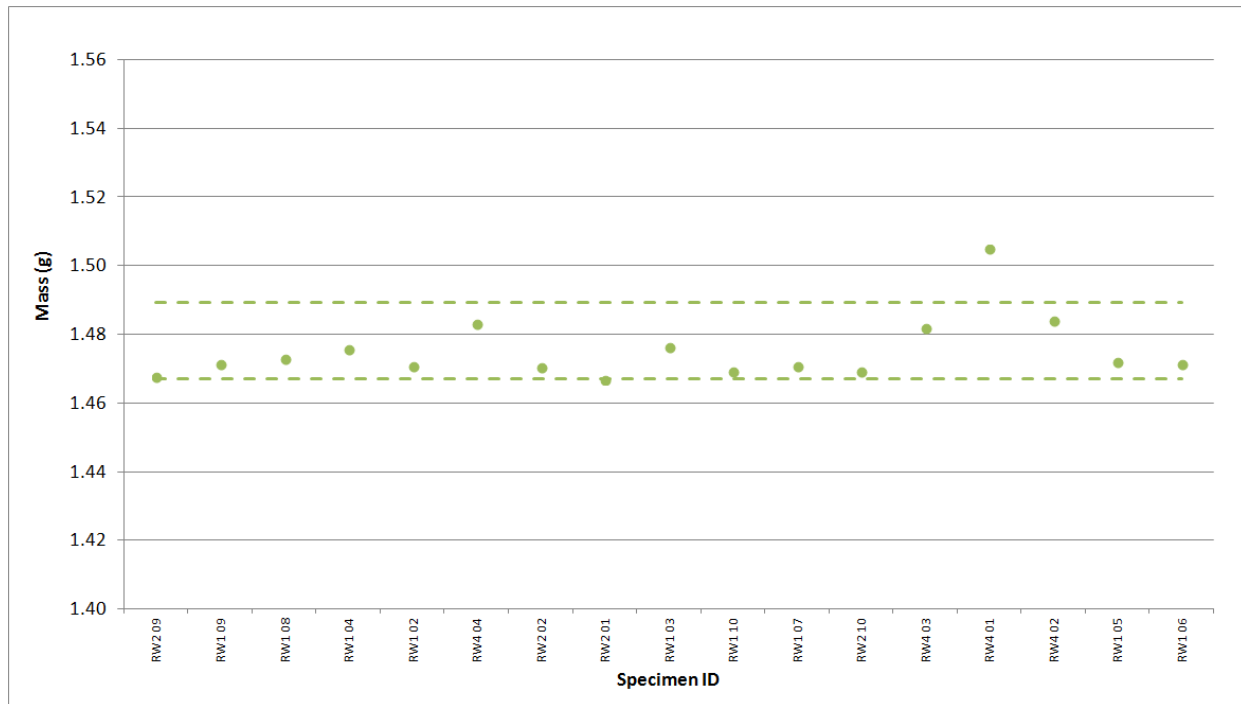


Figure A-72. BAN Piggyback Mass.

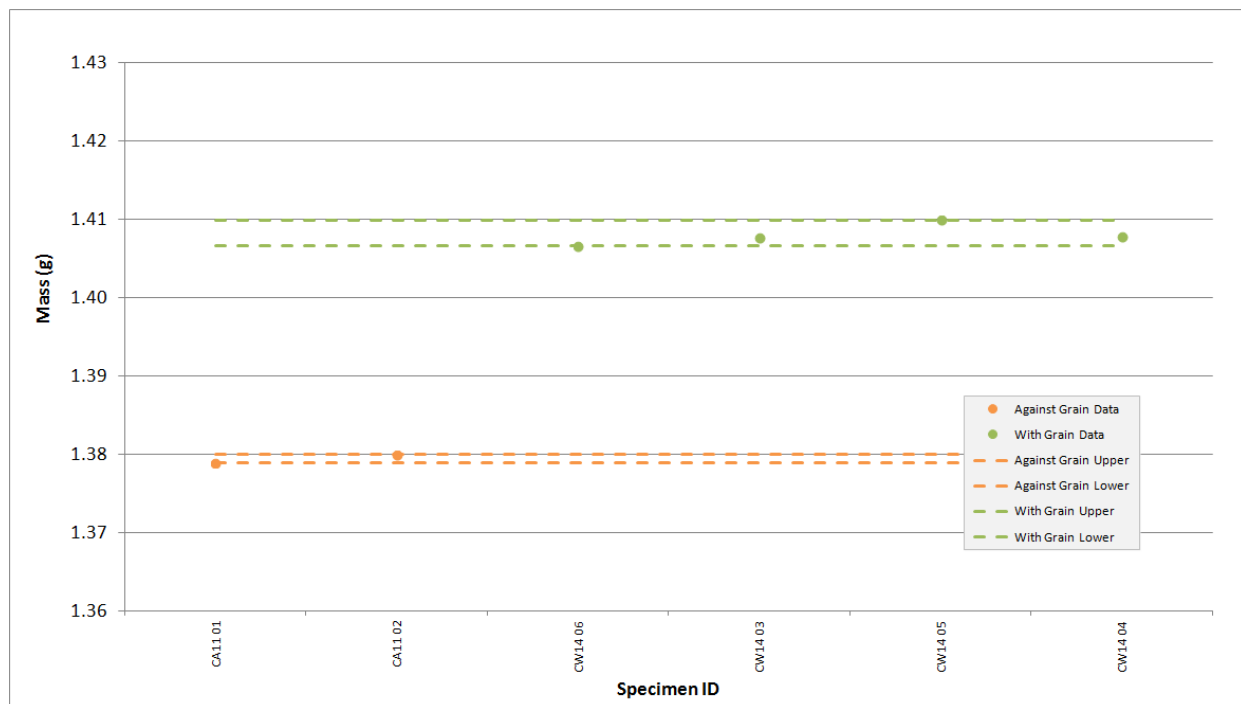


Figure A-73. H-451 Piggyback Mass.

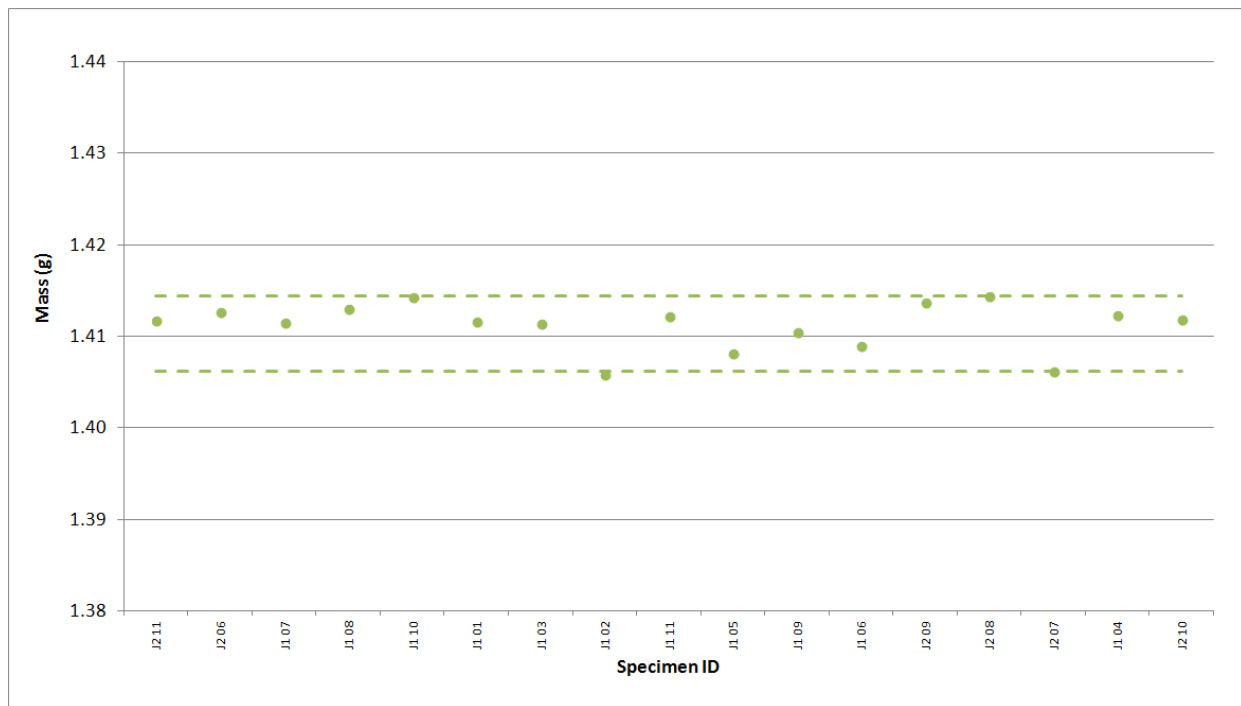


Figure A-74. HLM Piggyback Mass.

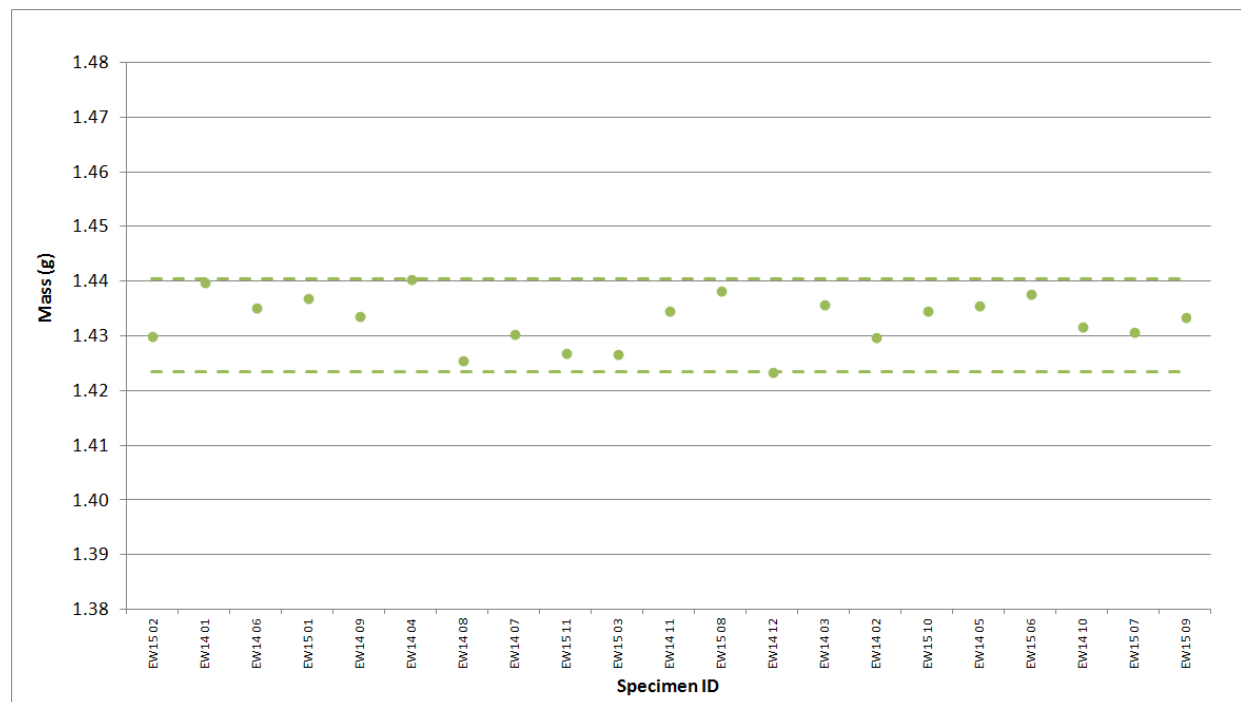


Figure A-75. IG-110 Piggyback Mass.

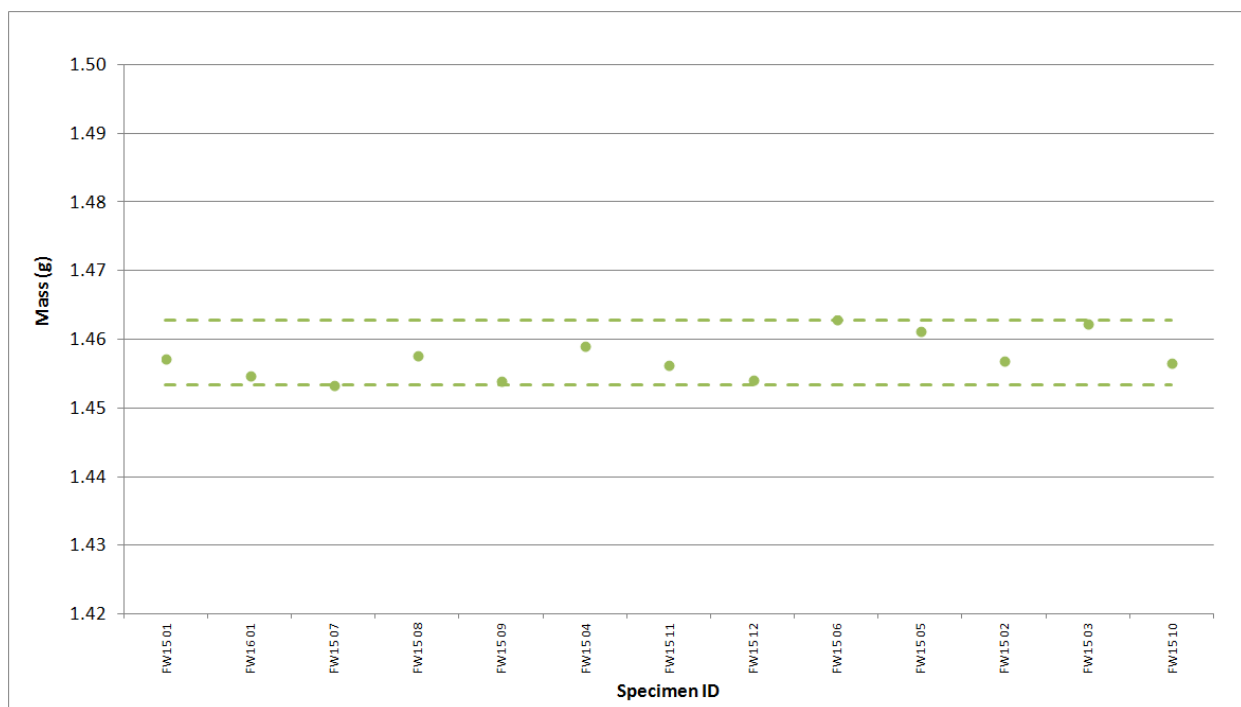


Figure A-76. IG-430 Piggyback Mass.

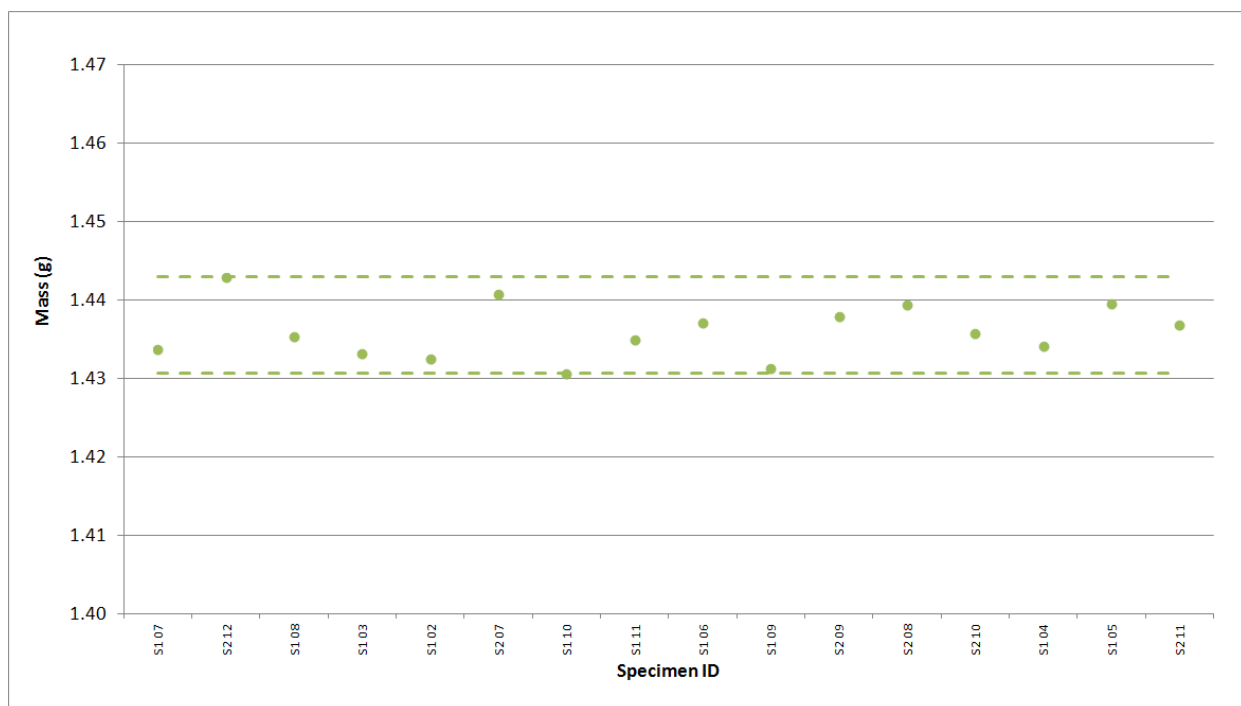


Figure A-77. NBG-10 Piggyback Mass.

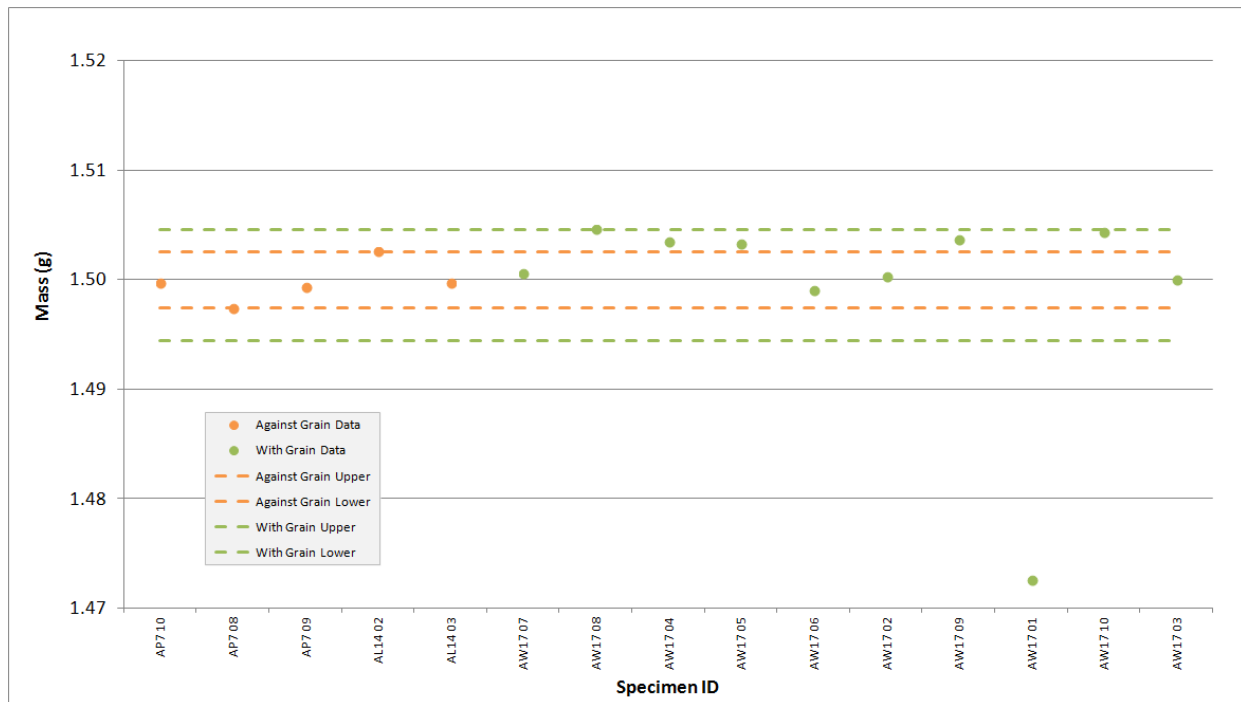


Figure A-78. NBG-17 Piggyback Mass.

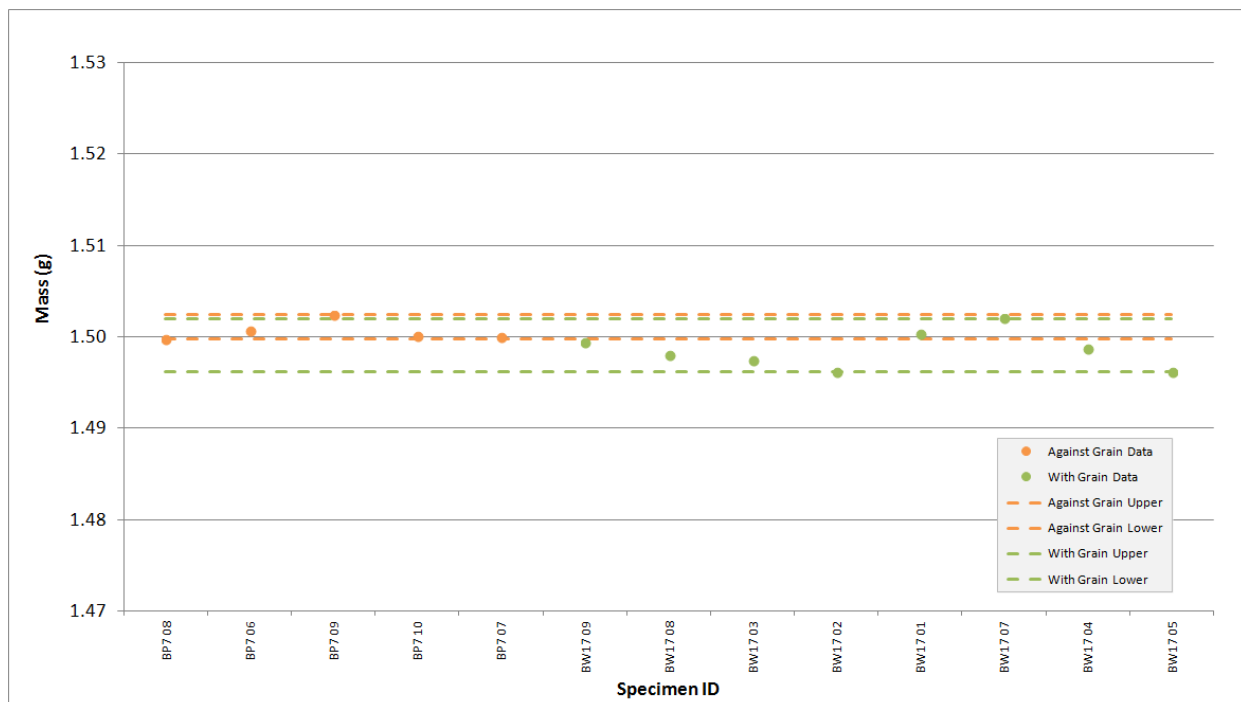


Figure A-79. NBG-18 Piggyback Mass.

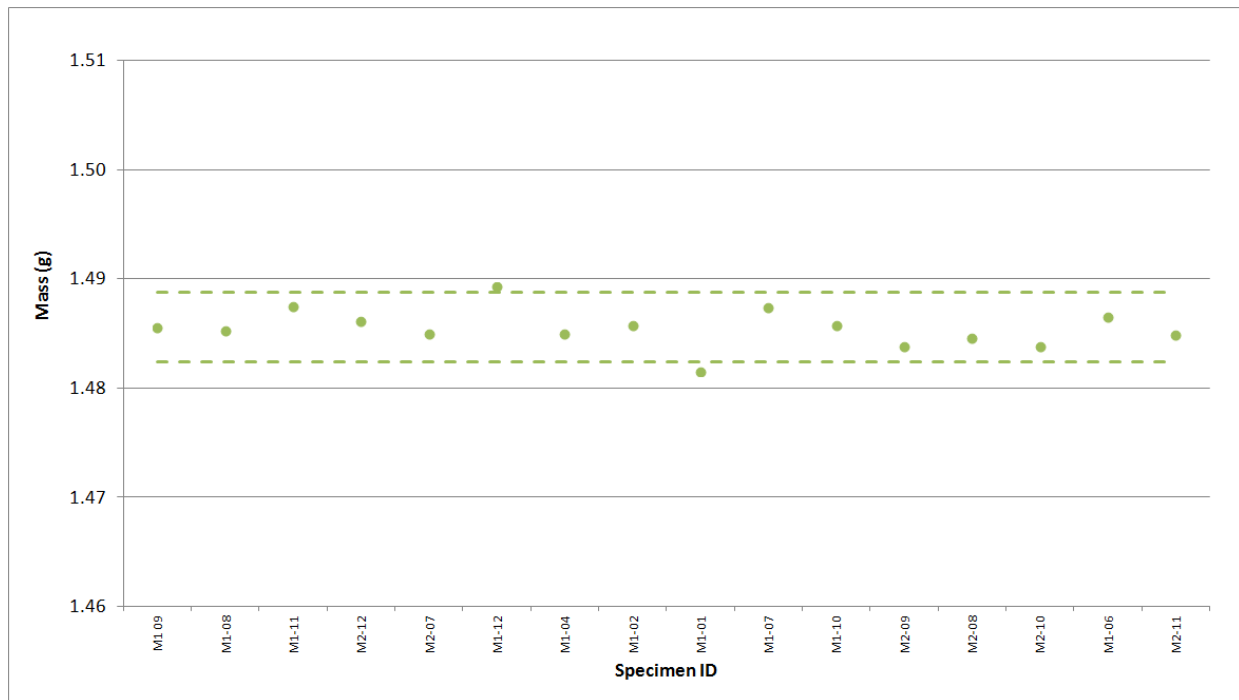


Figure A-80. NGB-25 Piggyback Mass.

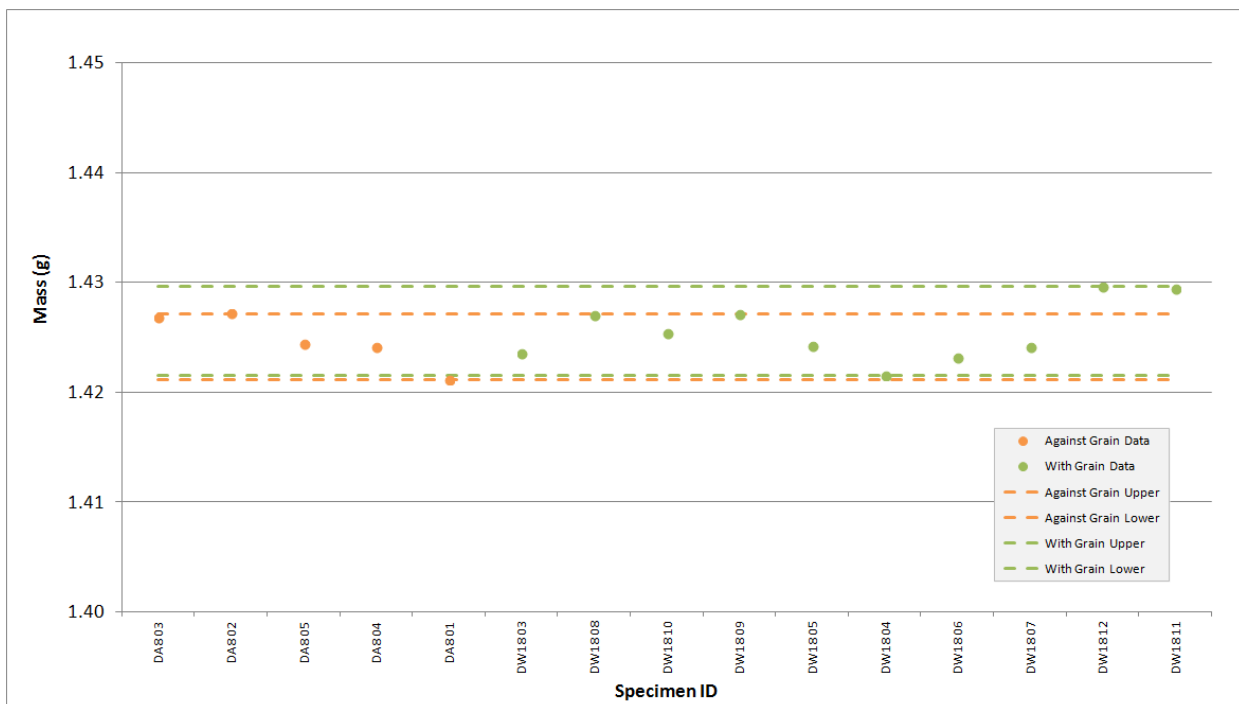


Figure A-81. PCEA Piggyback Mass.

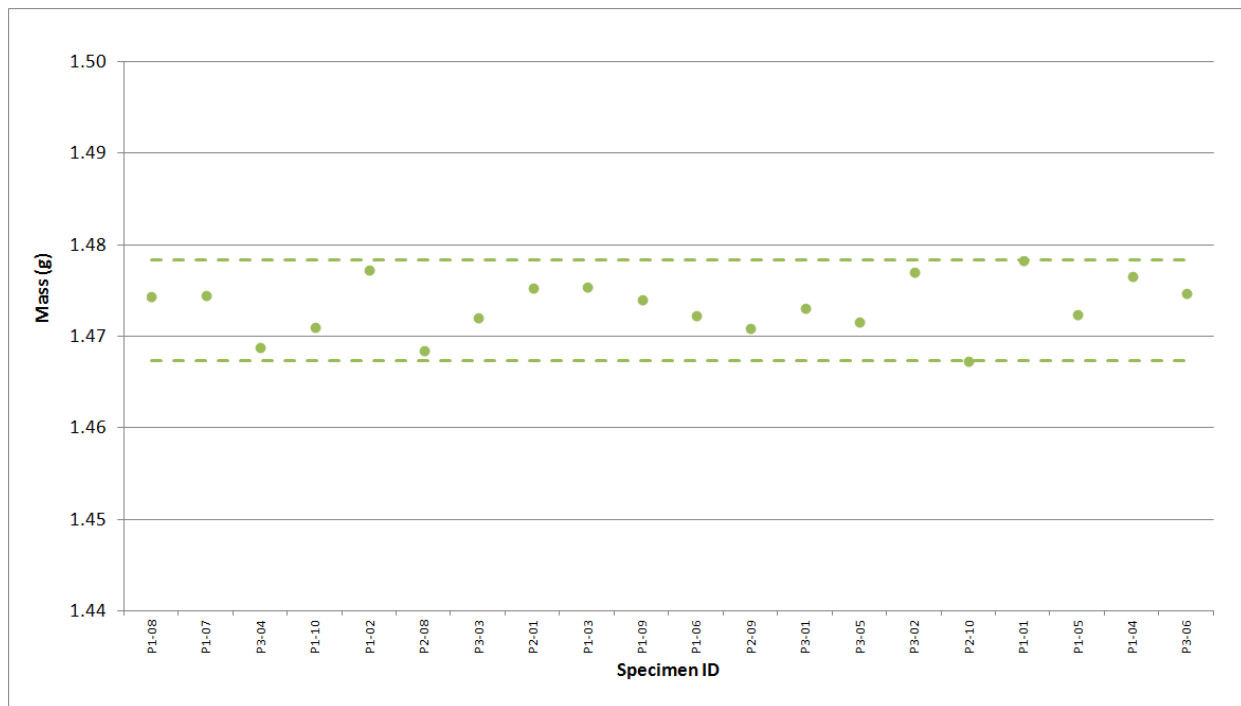


Figure A-82. PCIB Piggyback Mass.

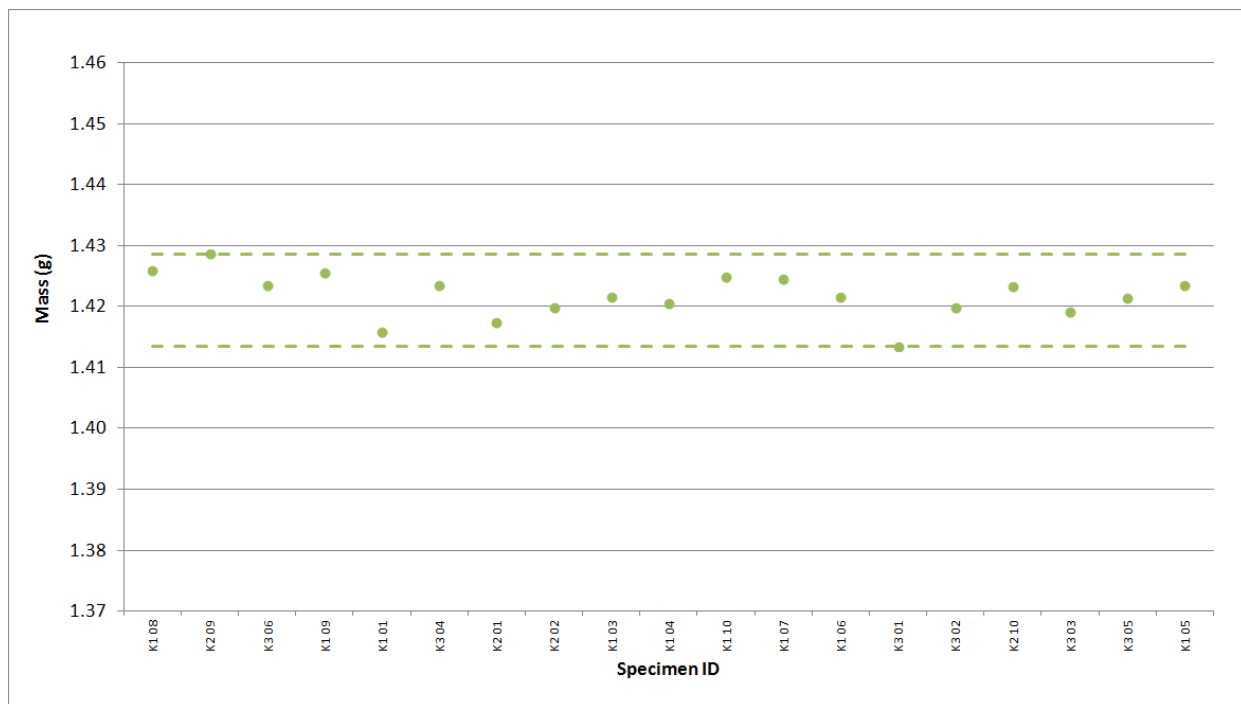


Figure A-83. PGX Piggyback Mass.

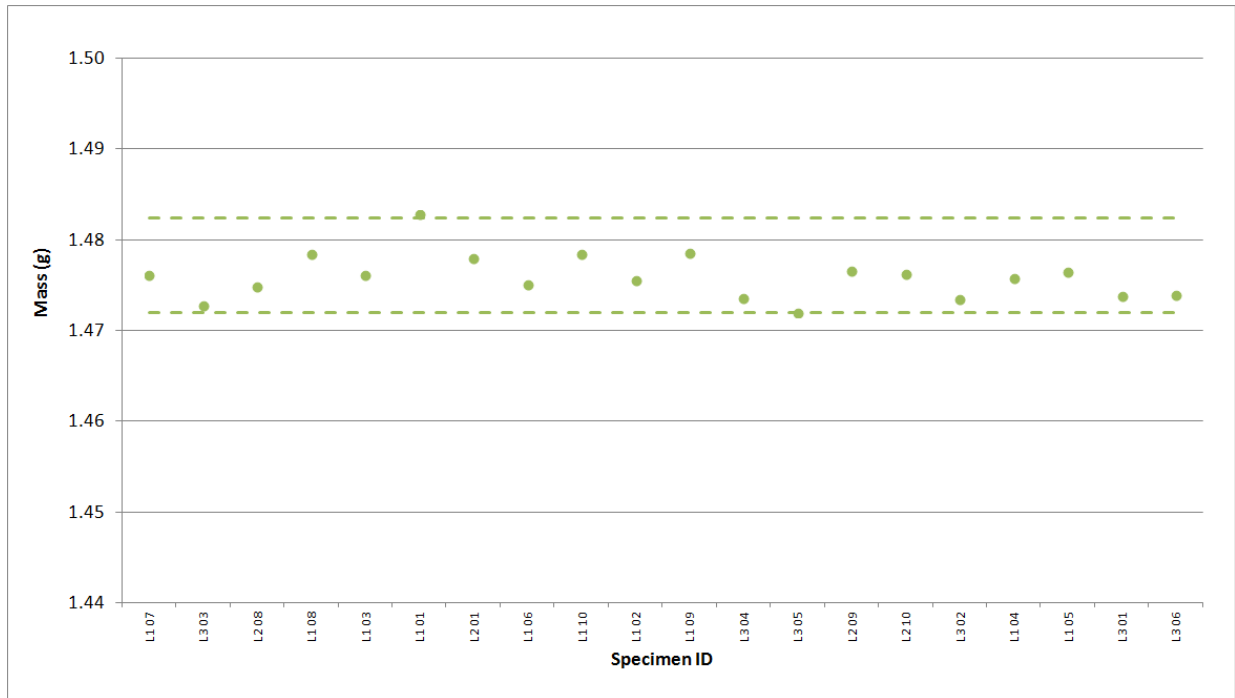


Figure A-84. PPEA Piggyback Mass.

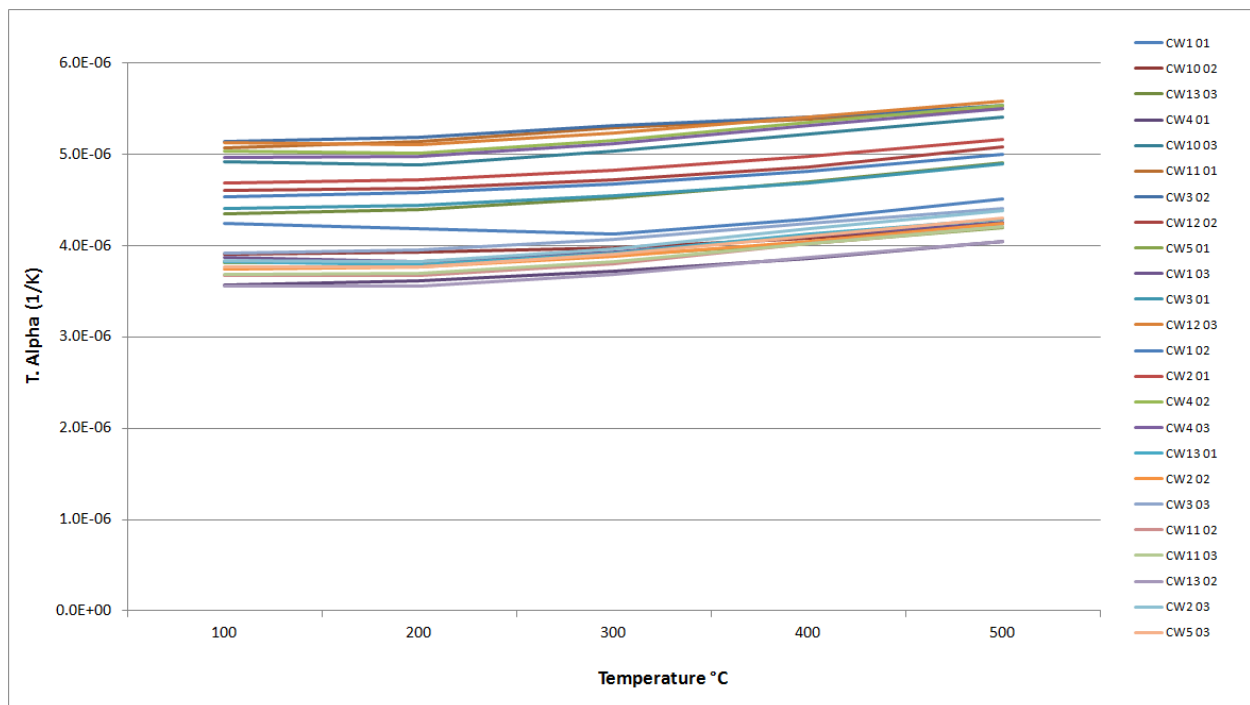


Figure A-85. H-451 Creep Coefficient of Thermal Expansion.

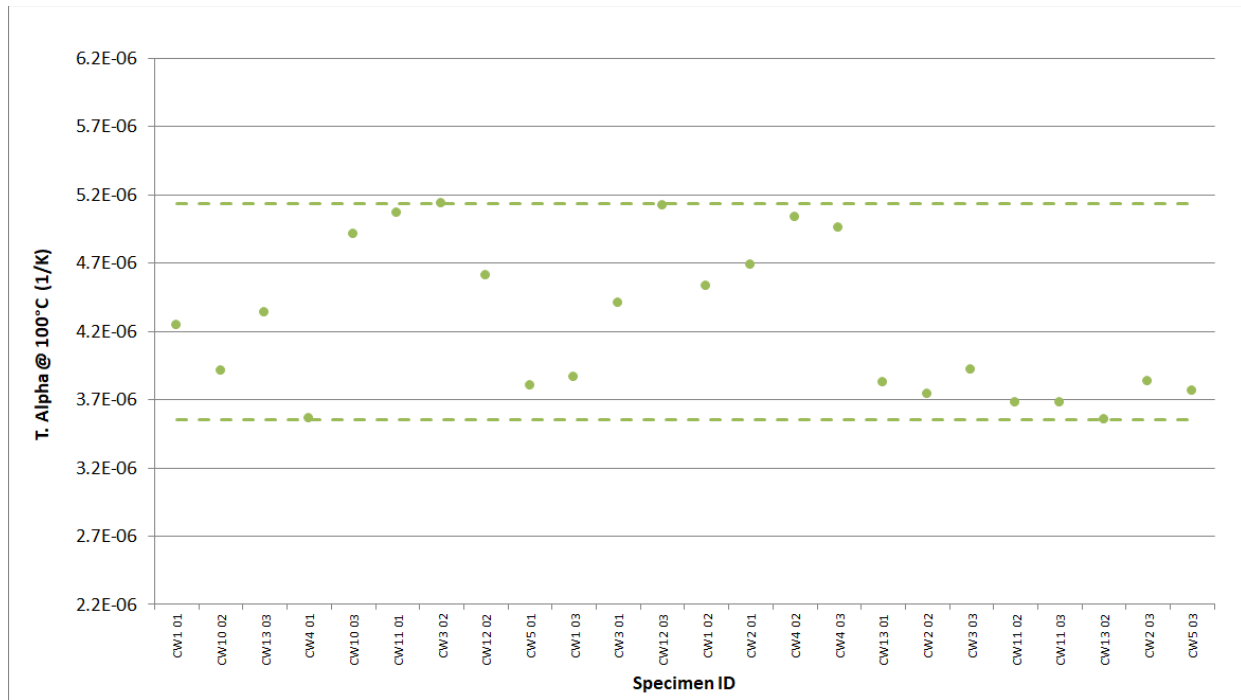


Figure A-86. H-451 Creep Coefficient of Thermal Expansion @ 100°C.

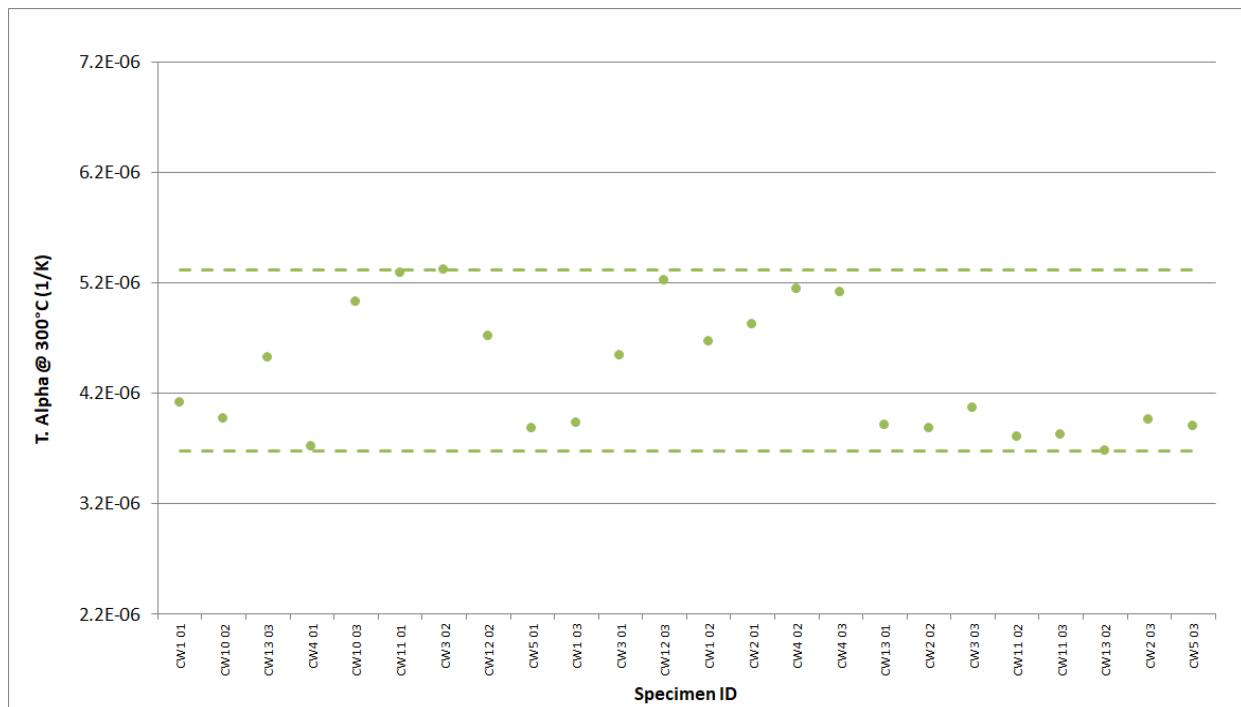


Figure A-87. H-451 Creep Coefficient of Thermal Expansion @ 300°C.

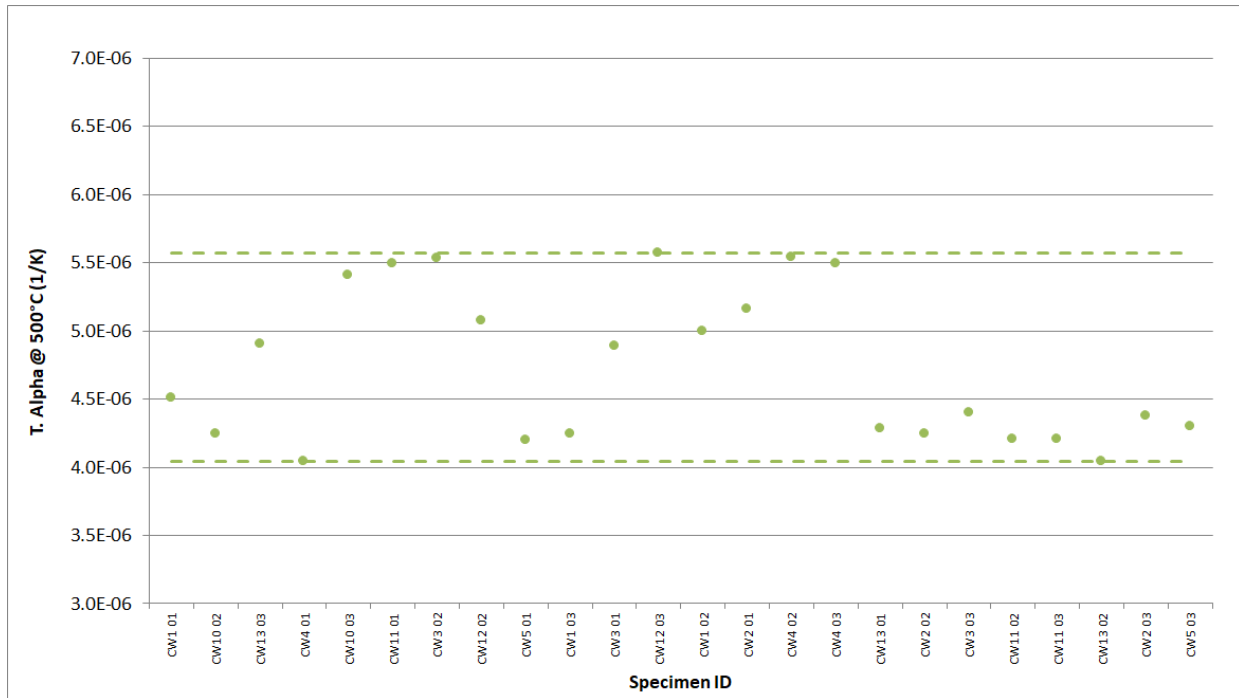


Figure A-88. H-451 Creep Coefficient of Thermal Expansion @ 500°C .

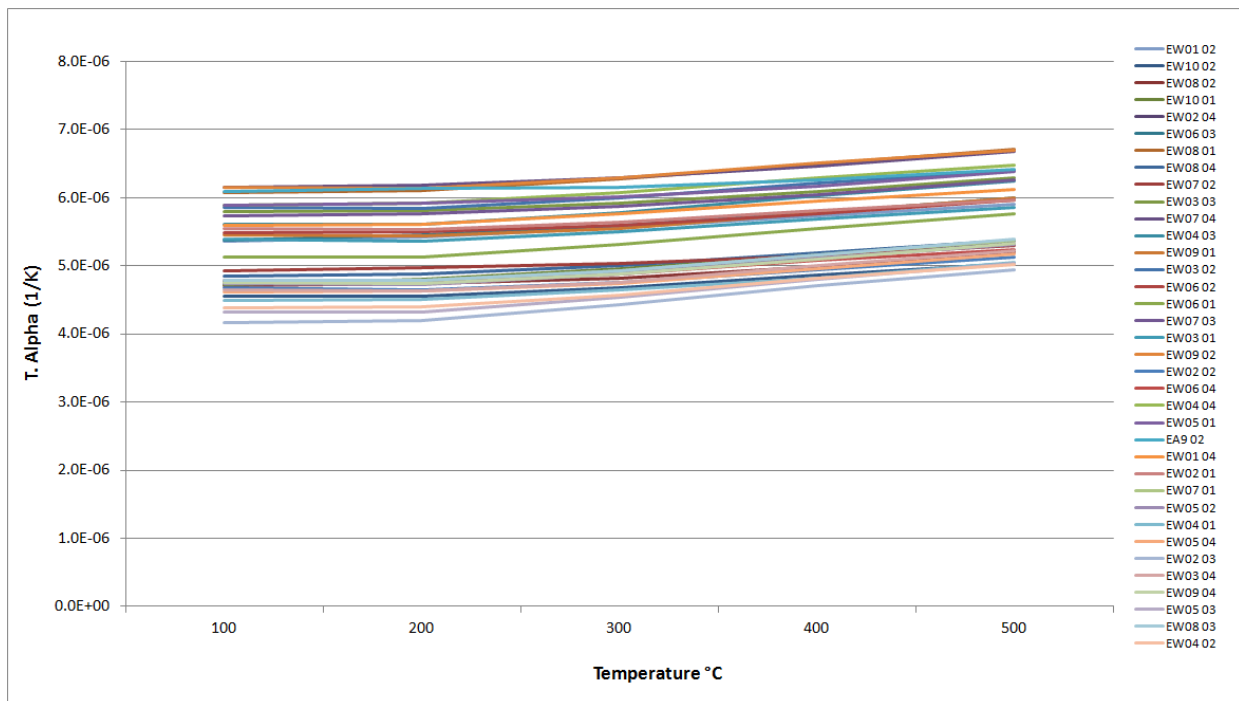


Figure A-89. IG-110 Creep Coefficient of Thermal Expansion.

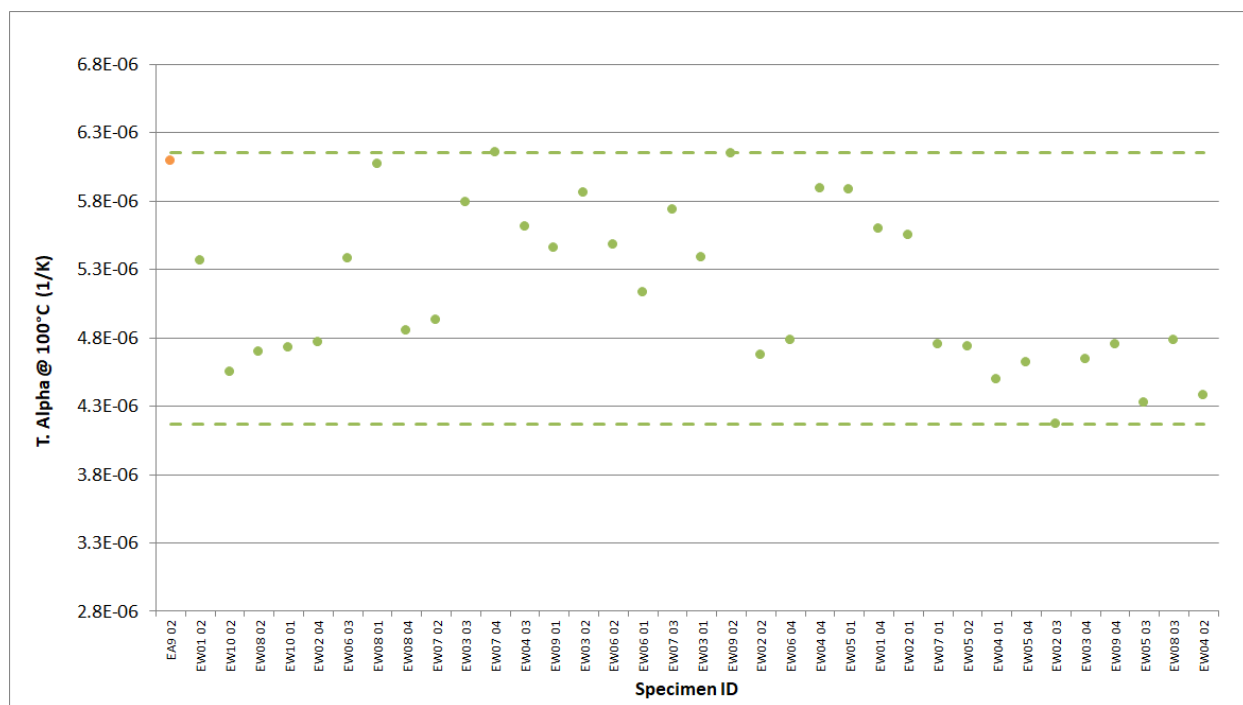


Figure A-90. IG-110 Creep Coefficient of Thermal Expansion @ 100°C.

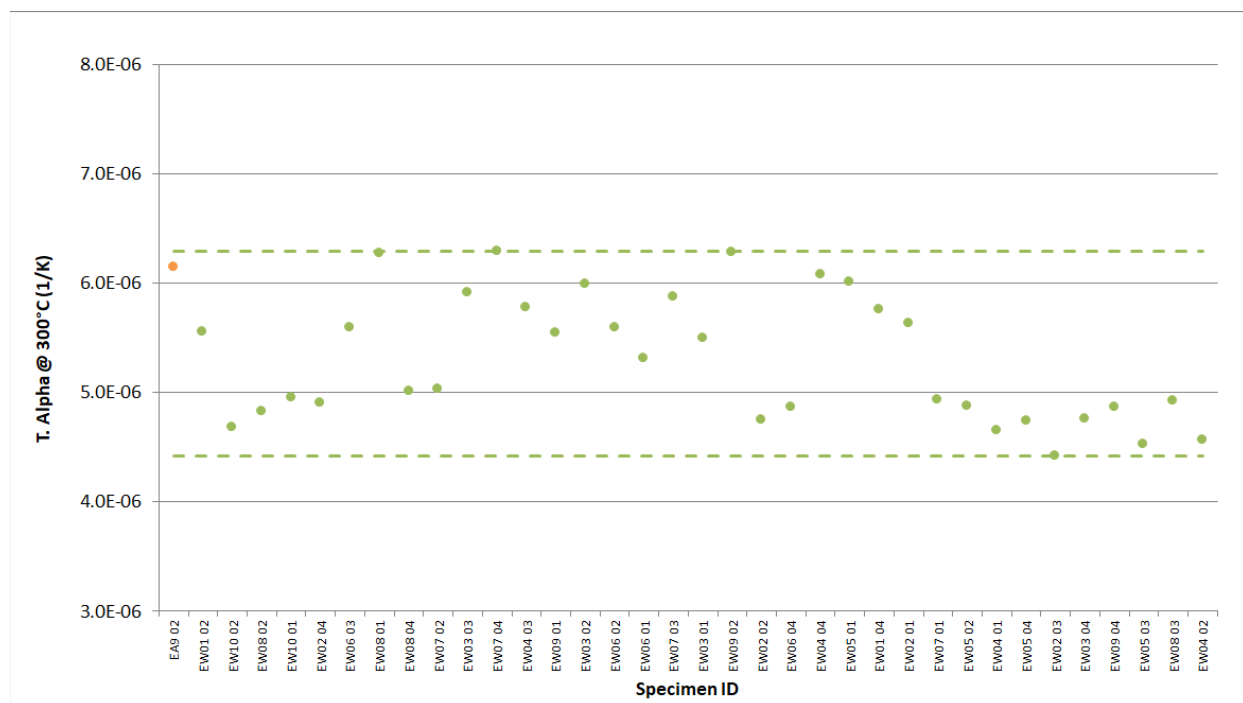


Figure A-91. IG-110 Creep Coefficient of Thermal Expansion @ 300°C.

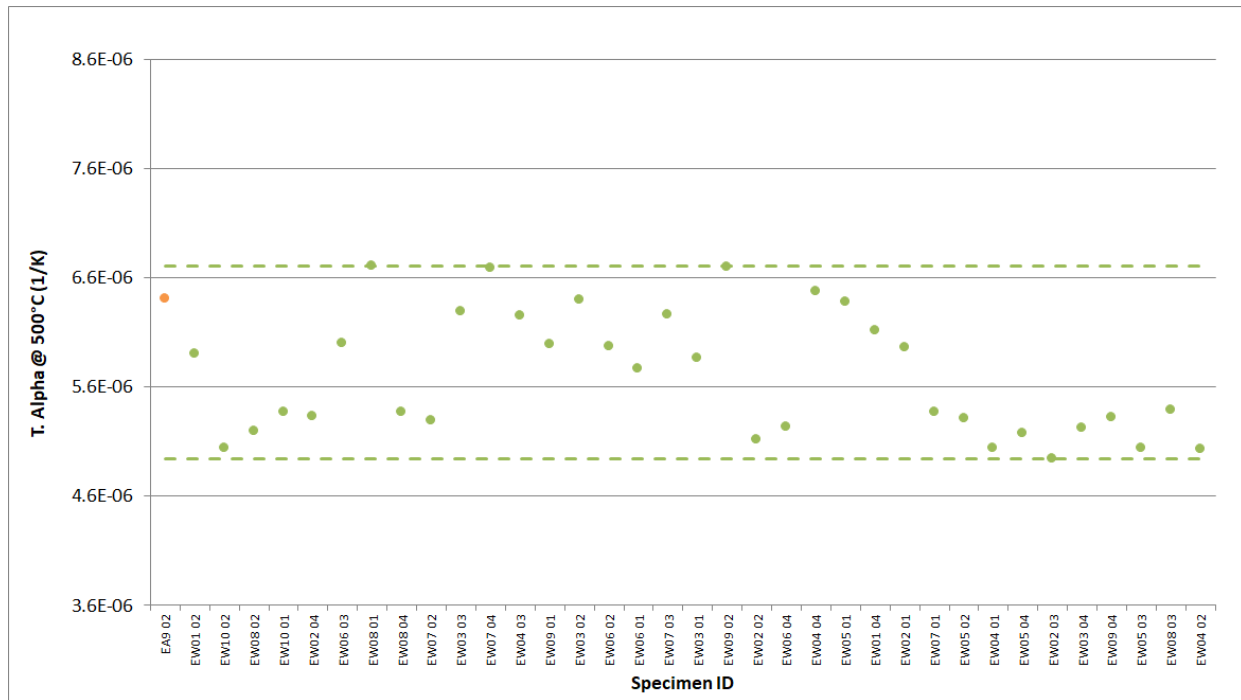


Figure A-92. IG-110 Creep Coefficient of Thermal Expansion @ 500°C.

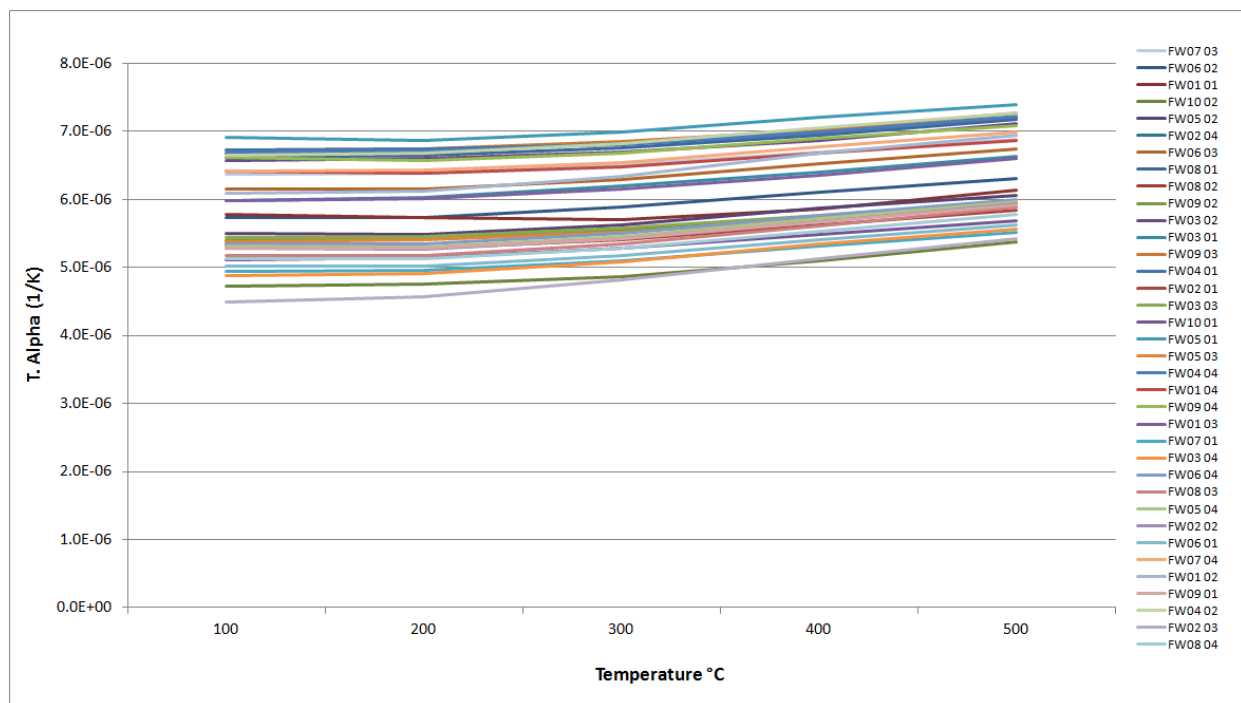


Figure A-93. IG-430 Creep Coefficient of Thermal Expansion.

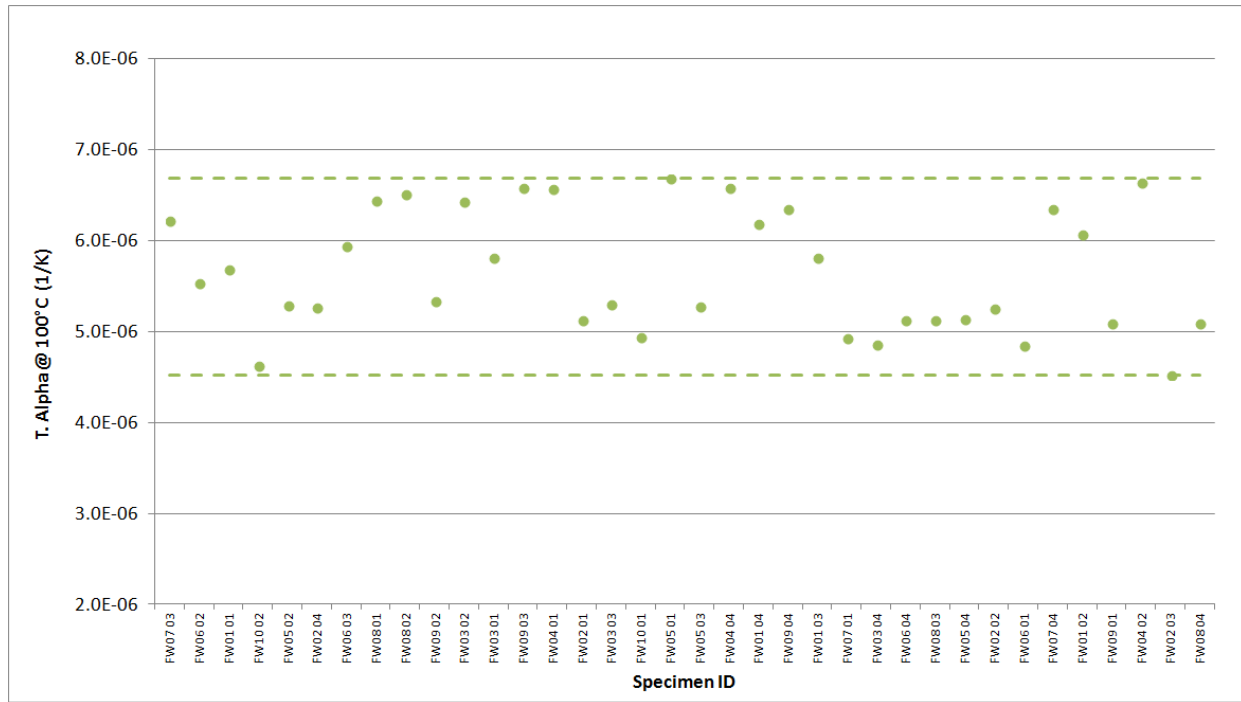


Figure A-94. IG-430 Creep Coefficient of Thermal Expansion @ 100°C.

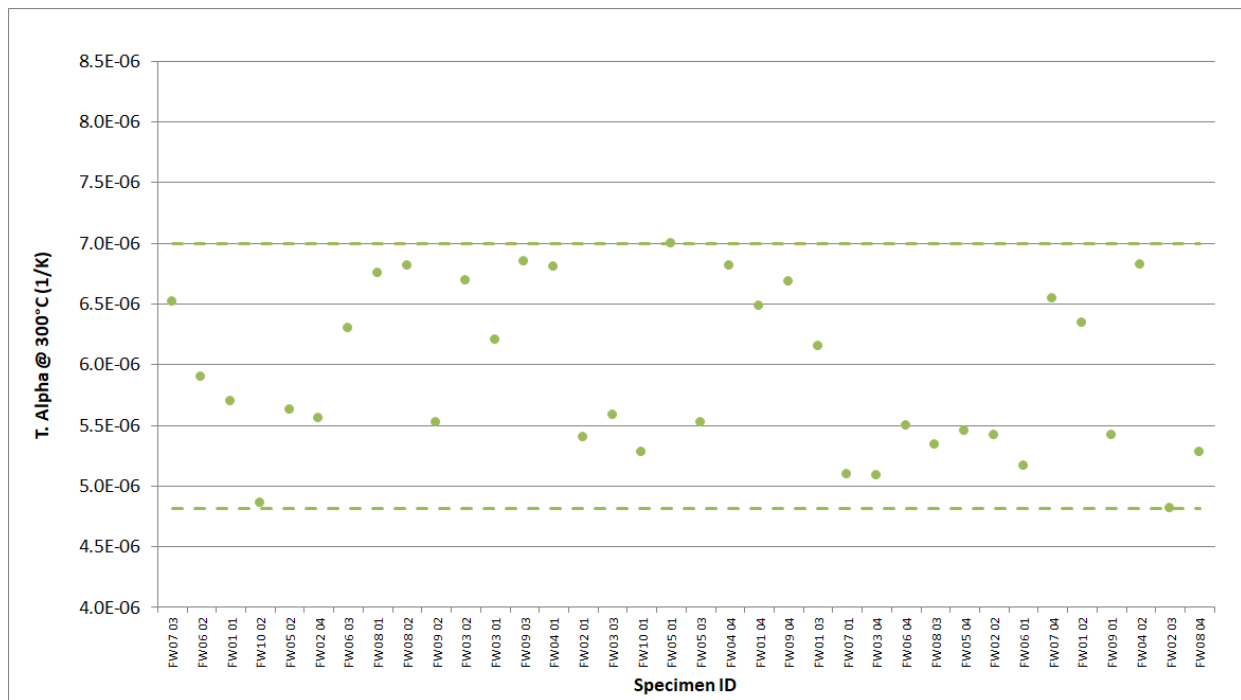


Figure A-95. IG-430 Creep Coefficient of Thermal Expansion @ 300°C.

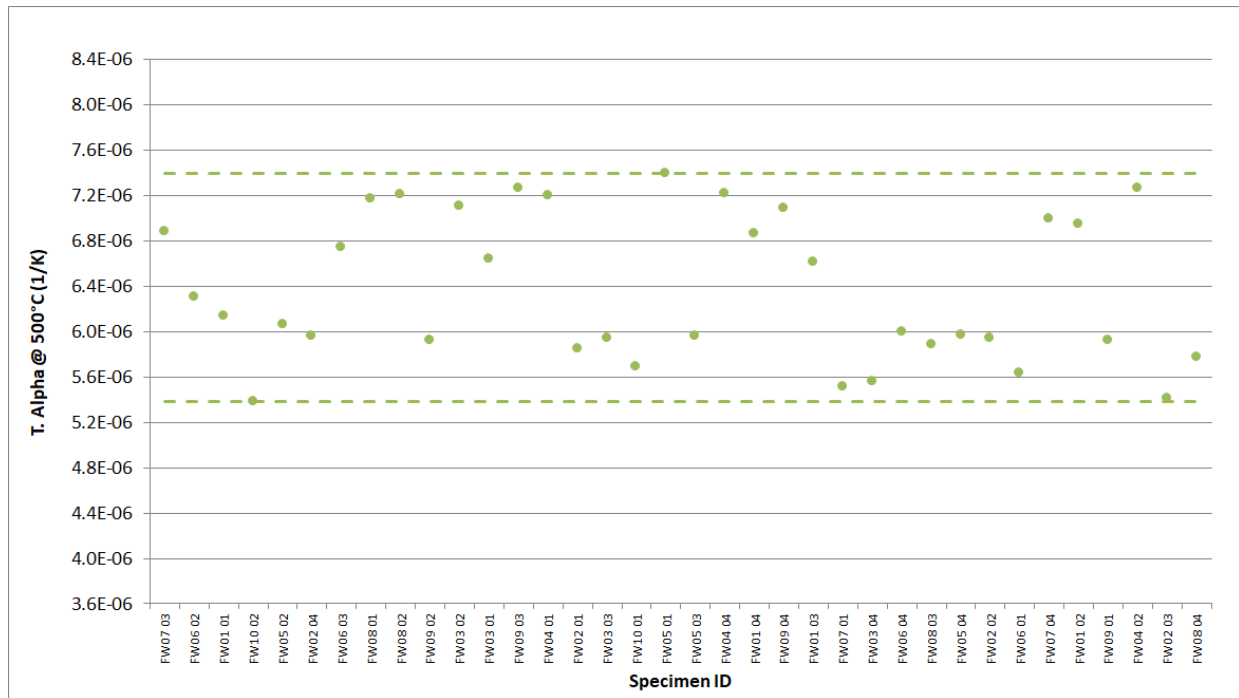


Figure A-96. IG-430 Creep Coefficient of Thermal Expansion @ 500°C.

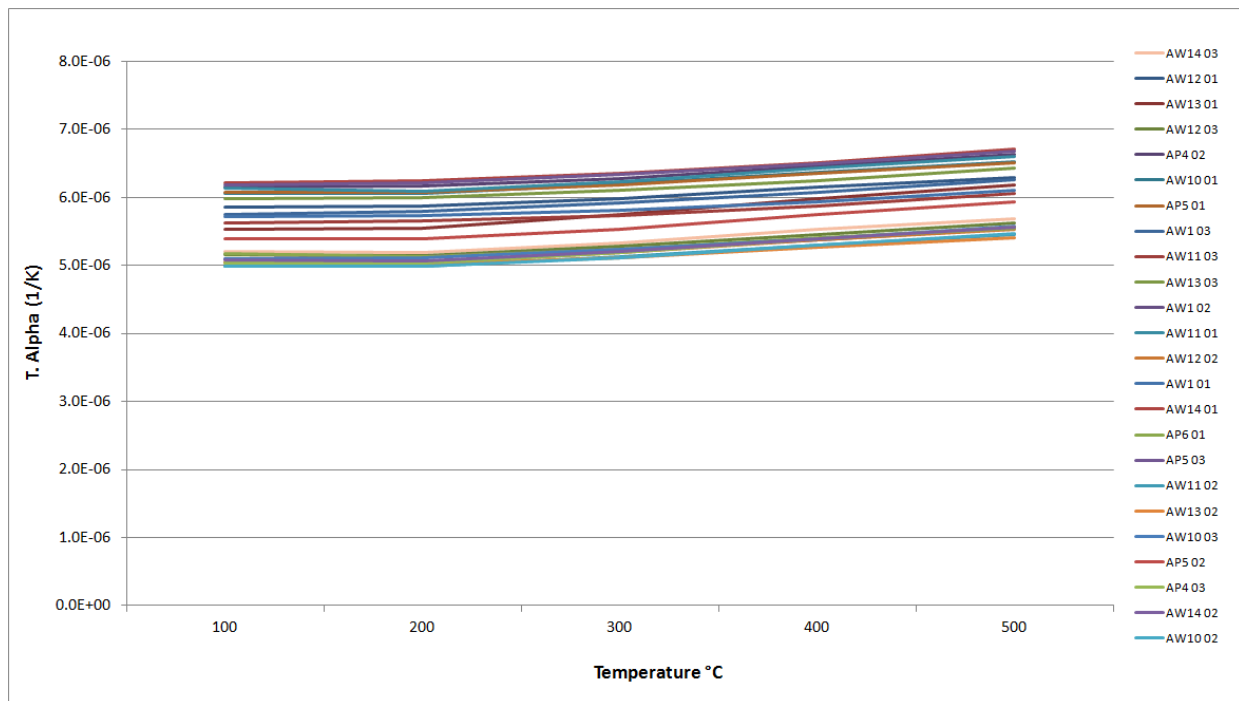


Figure A-97. NBG-17 Creep Coefficient of Thermal Expansion.

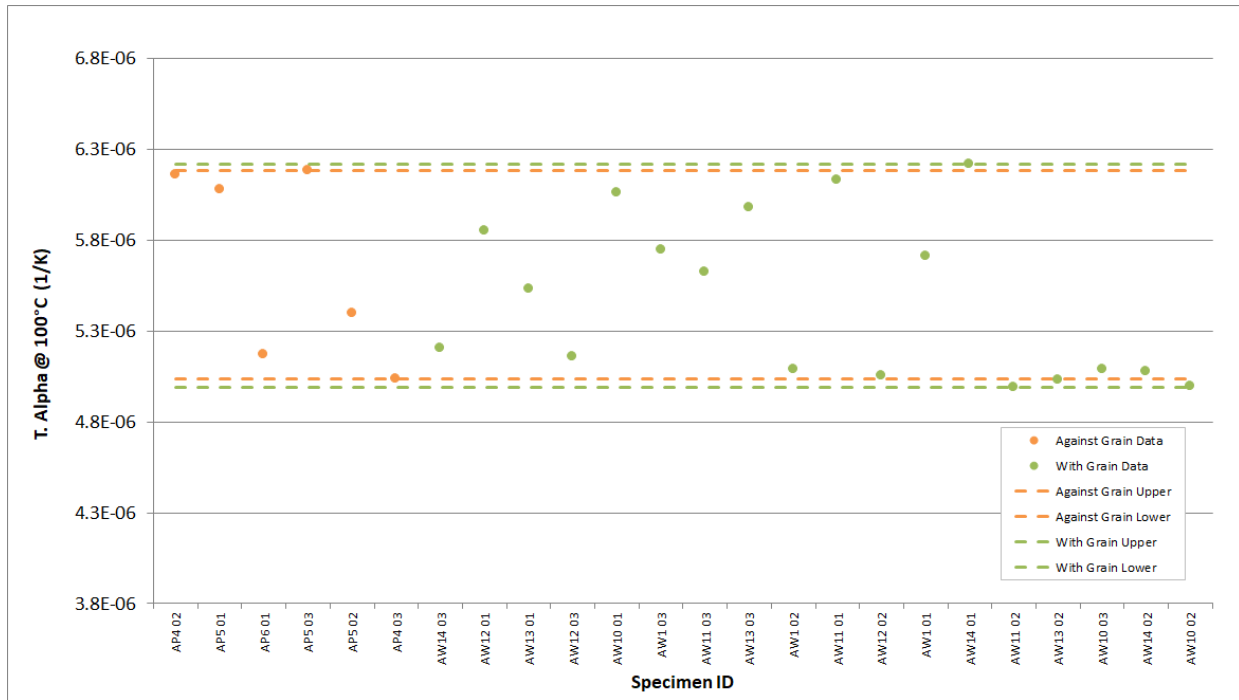


Figure A-98. NBG-17 Creep Coefficient of Thermal Expansion @ 100°C.

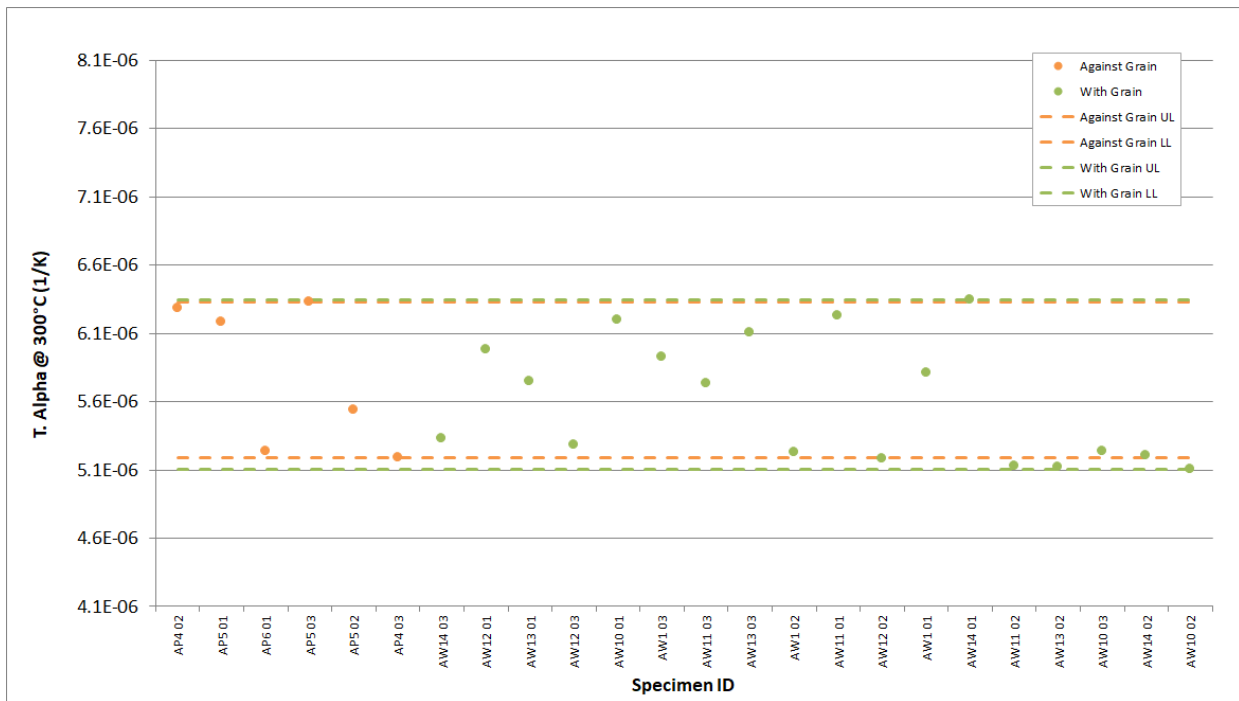


Figure A-99. NBG-17 Creep Coefficient of Thermal Expansion @ 300°C.

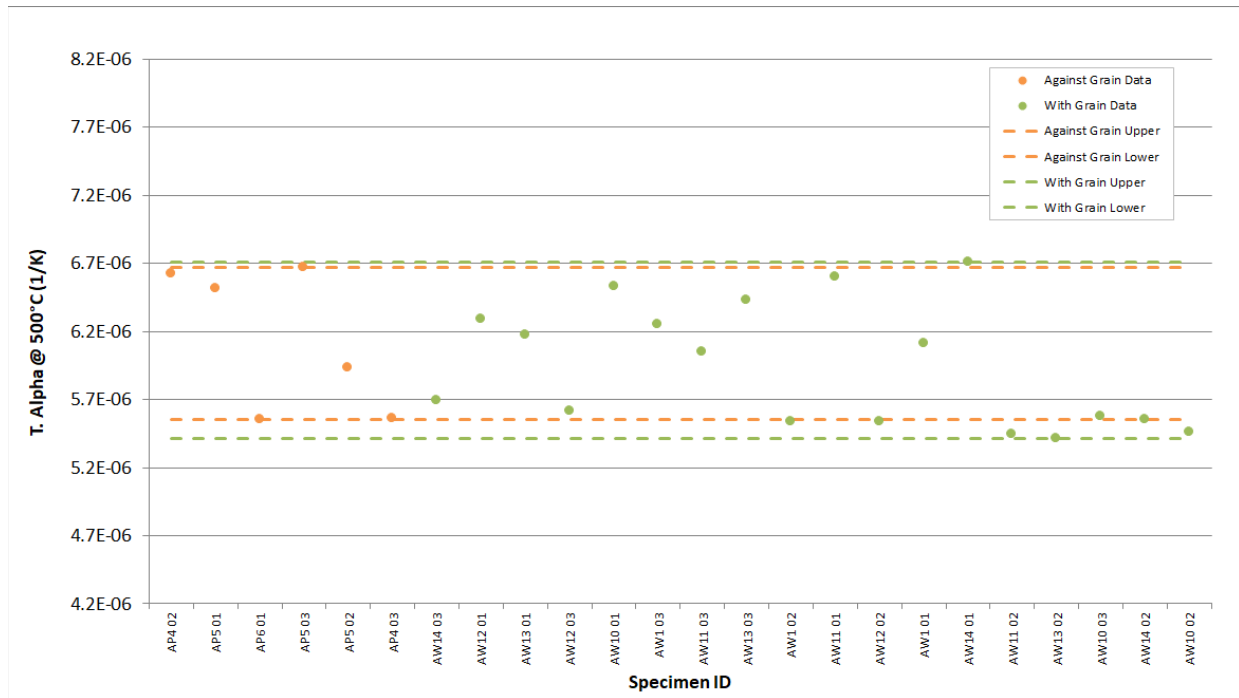


Figure A-100. NBG-17 Creep Coefficient of Thermal Expansion @ 500°C.

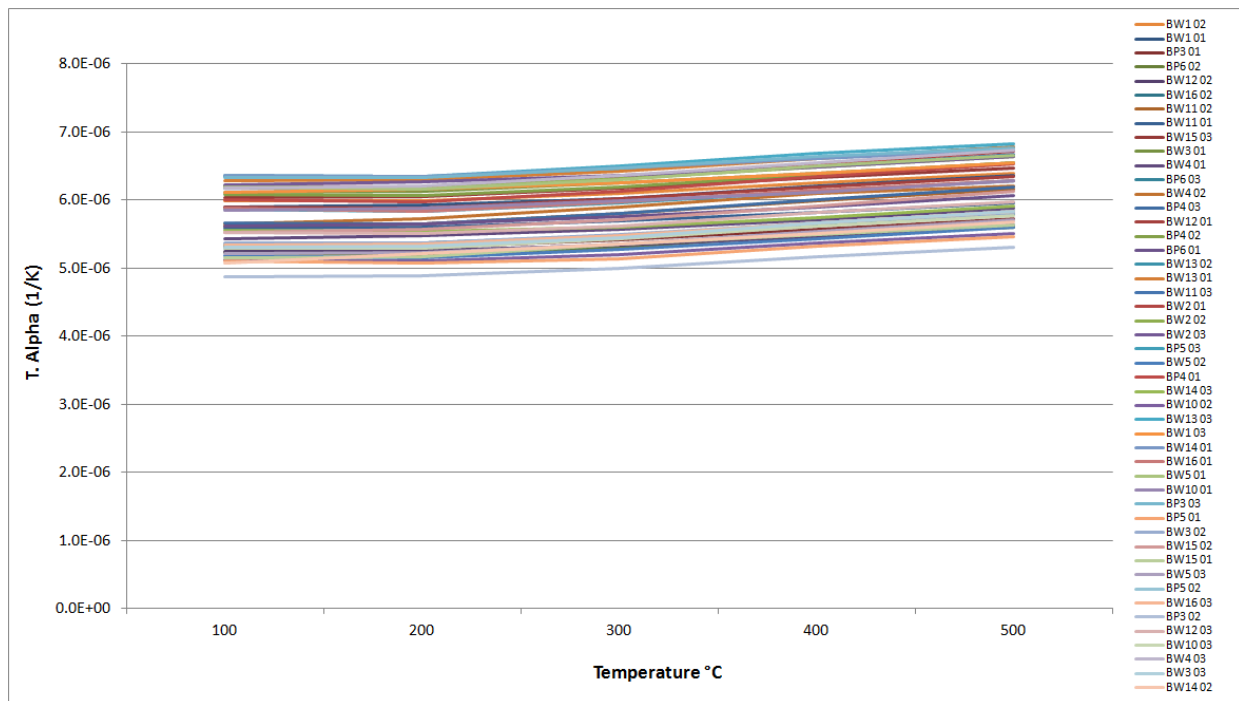


Figure A-101. NBG-18 Creep Coefficient of Thermal Expansion.

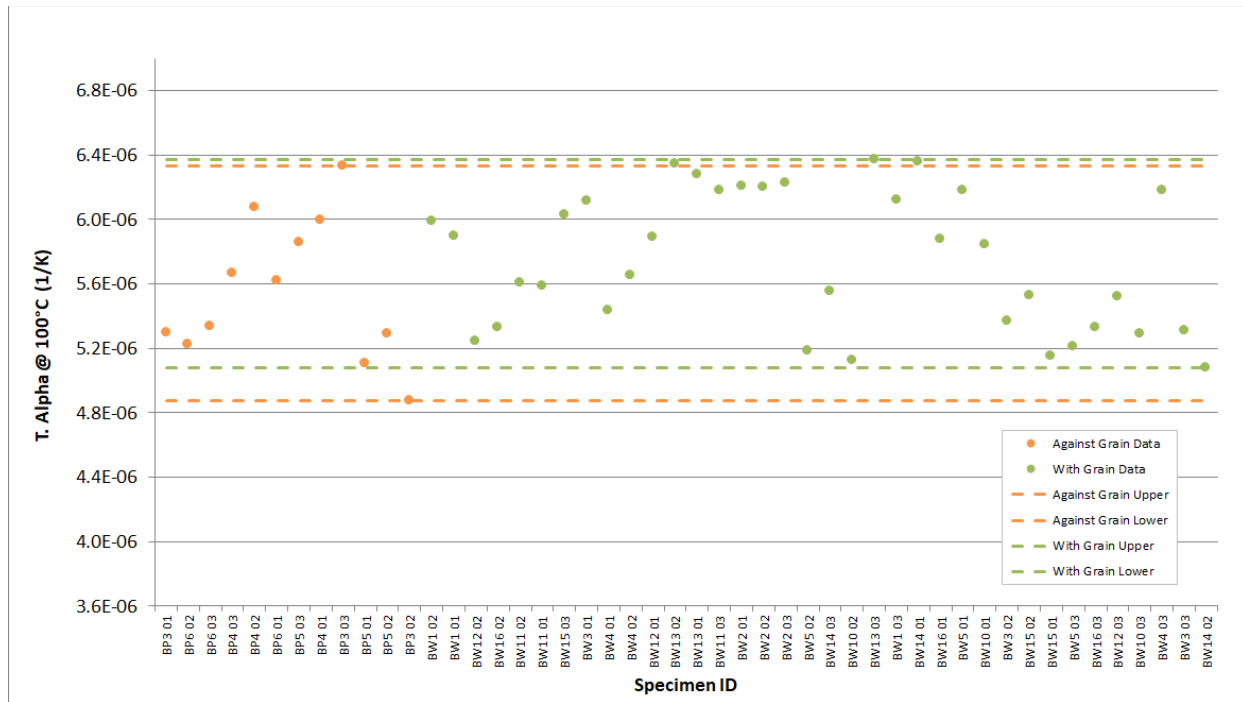


Figure A-102. NBG-18 Creep Coefficient of Thermal Expansion @ 100°C.

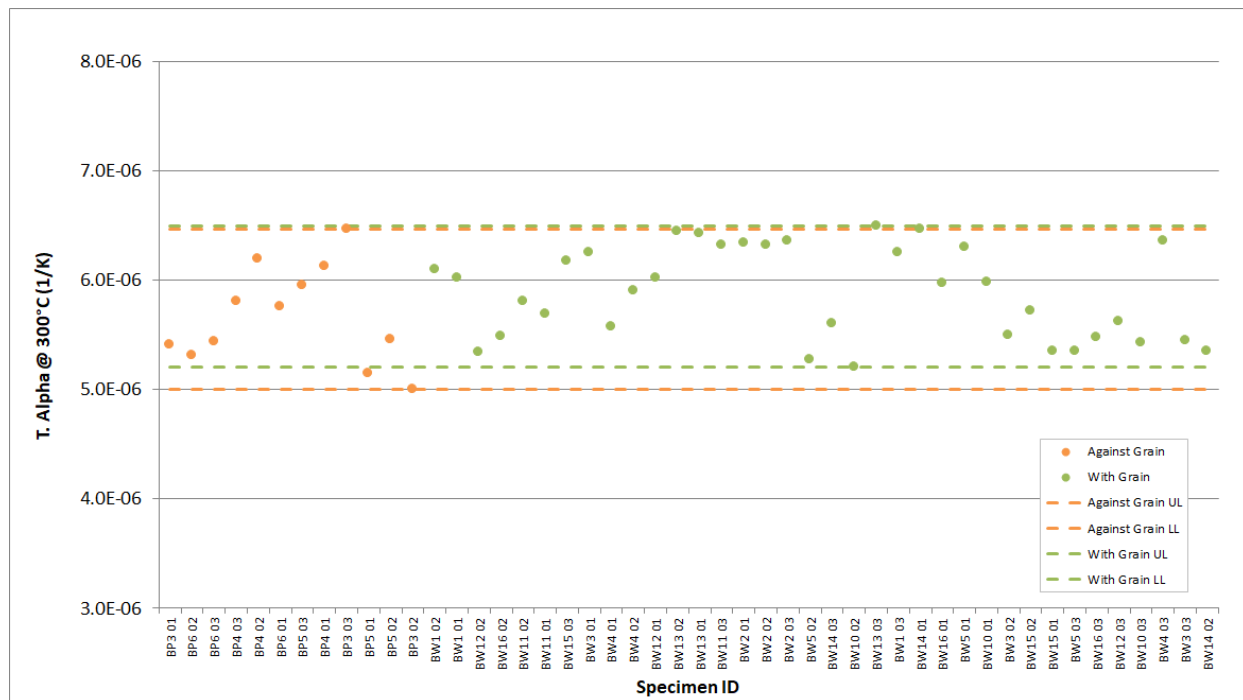


Figure A-103. NBG-18 Creep Coefficient of Thermal Expansion @ 300°C.

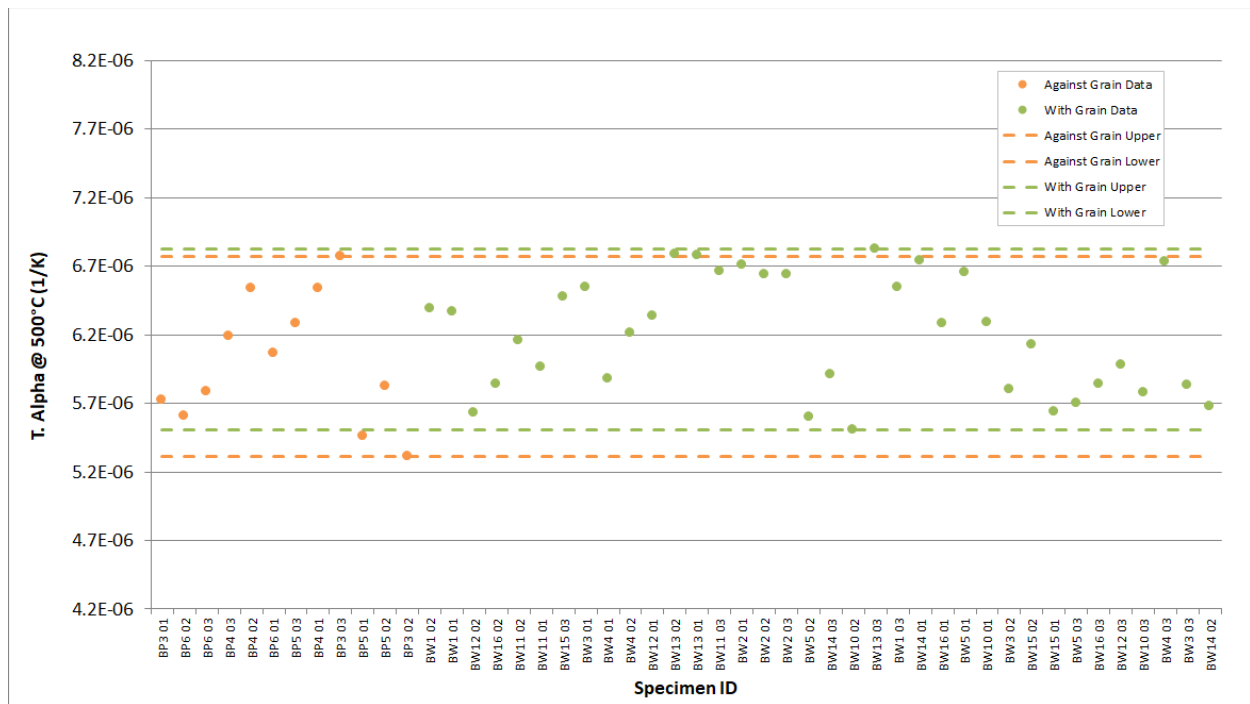


Figure A-104. NBG-18 Creep Coefficient of Thermal Expansion @ 500°C.

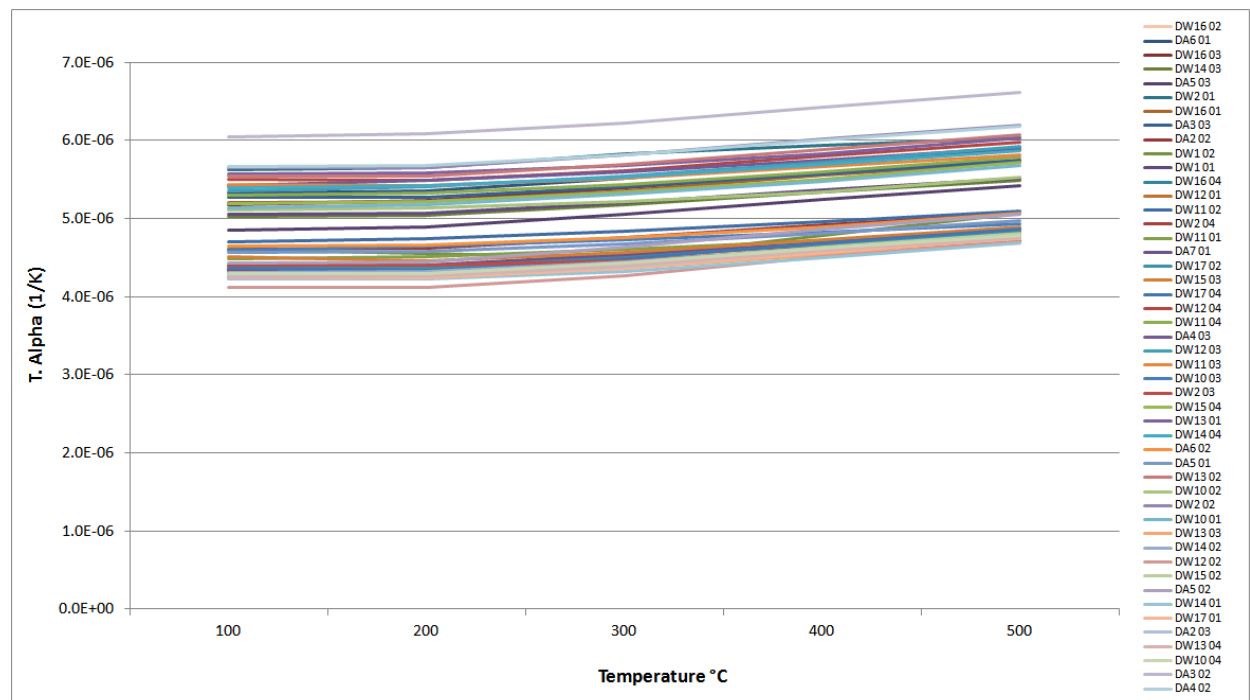


Figure A-105. PCEA Creep Coefficient of Thermal Expansion.



Figure A-106. PCEA Creep Coefficient of Thermal Expansion @ 100°C.

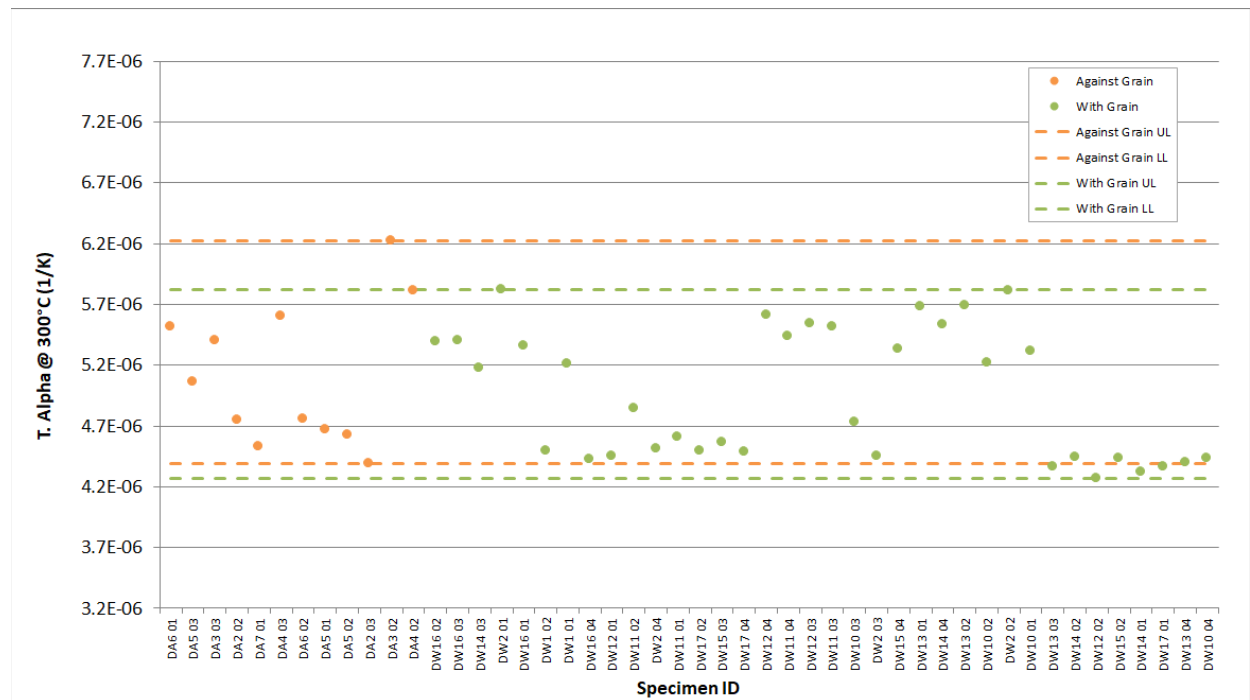


Figure A-107. PCEA Creep Coefficient of Thermal Expansion @ 300°C.

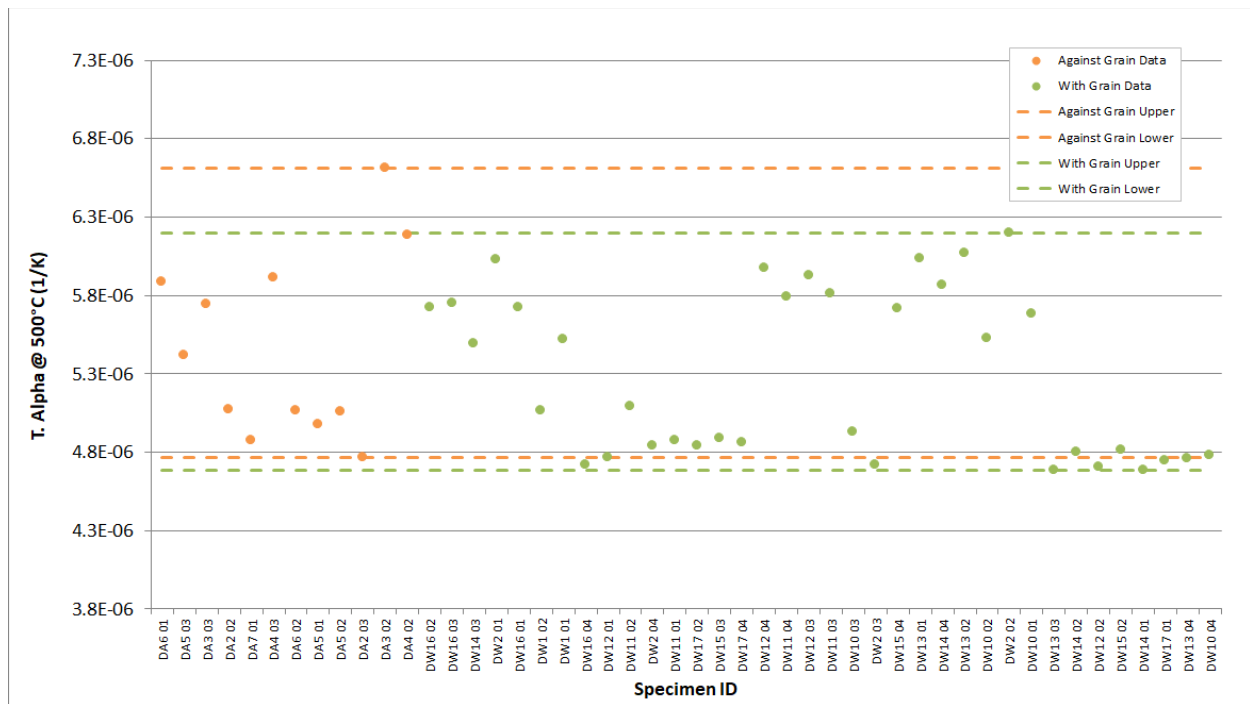


Figure A-108. PCEA Creep Coefficient of Thermal Expansion @ 500°C.

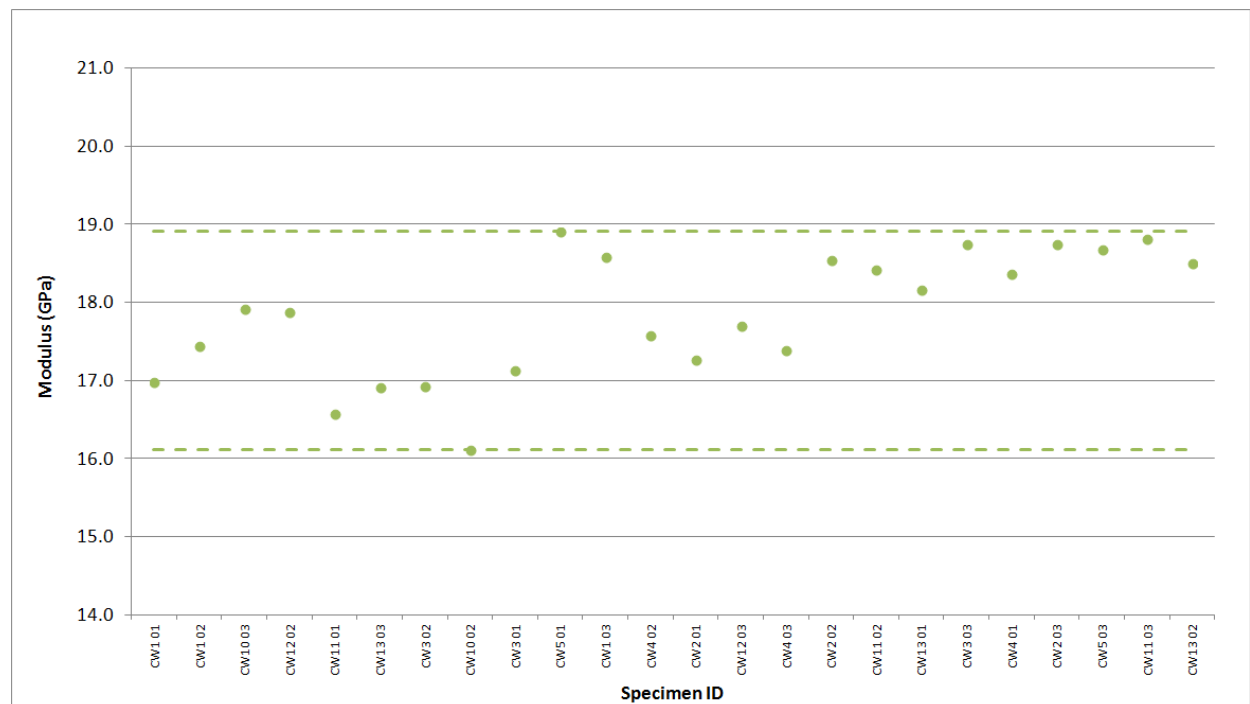


Figure A-109. H-451 Creep Modulus by Sonic Resonance.

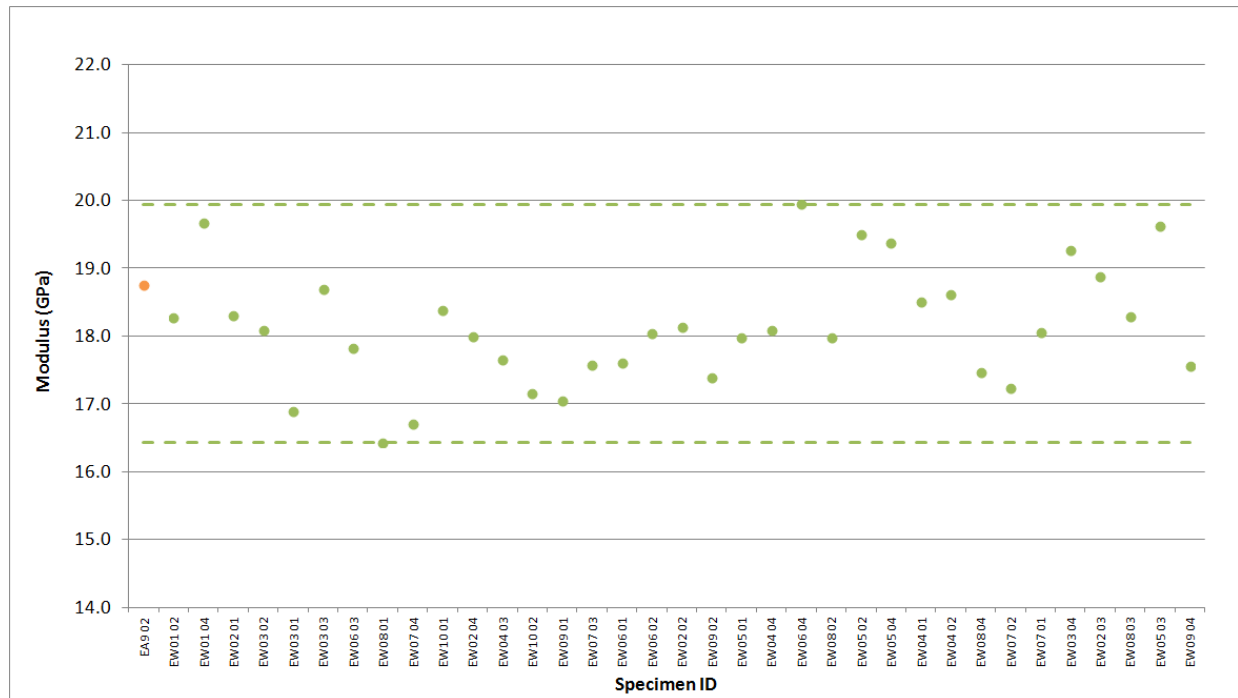


Figure A-110. IG-110 Creep Modulus by Sonic Resonance.

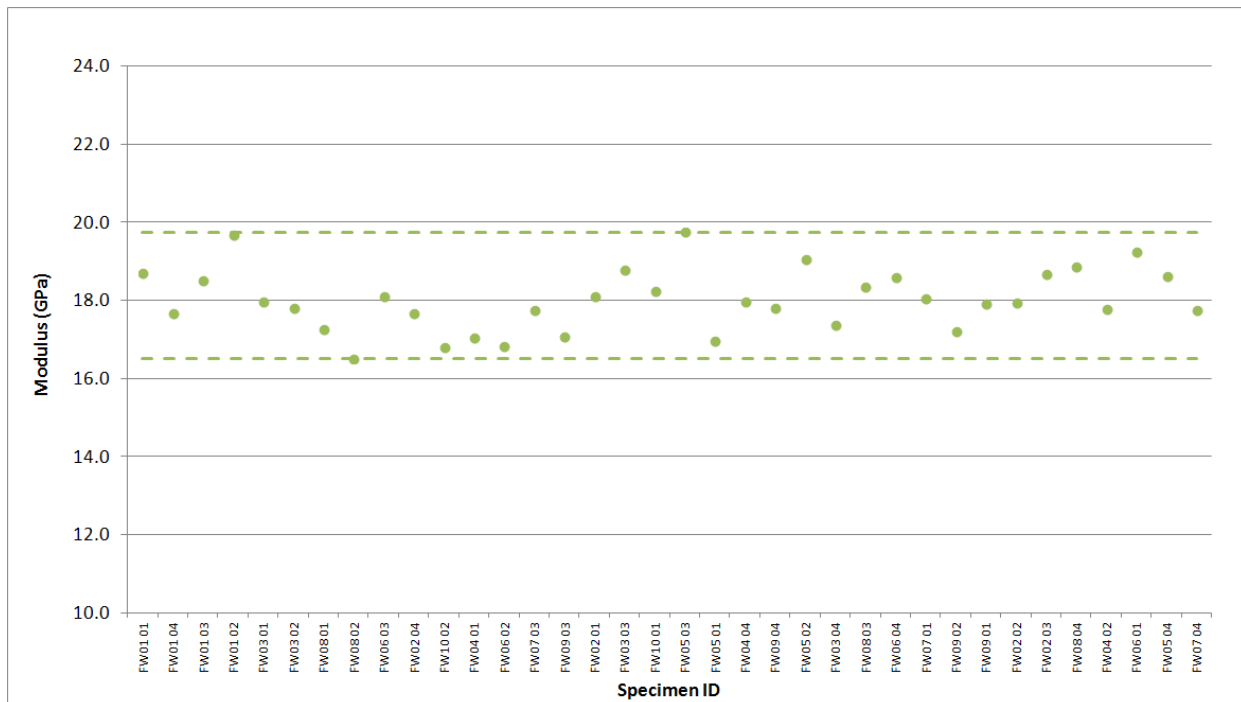


Figure A-111. IG-430 Creep Modulus by Sonic Resonance.

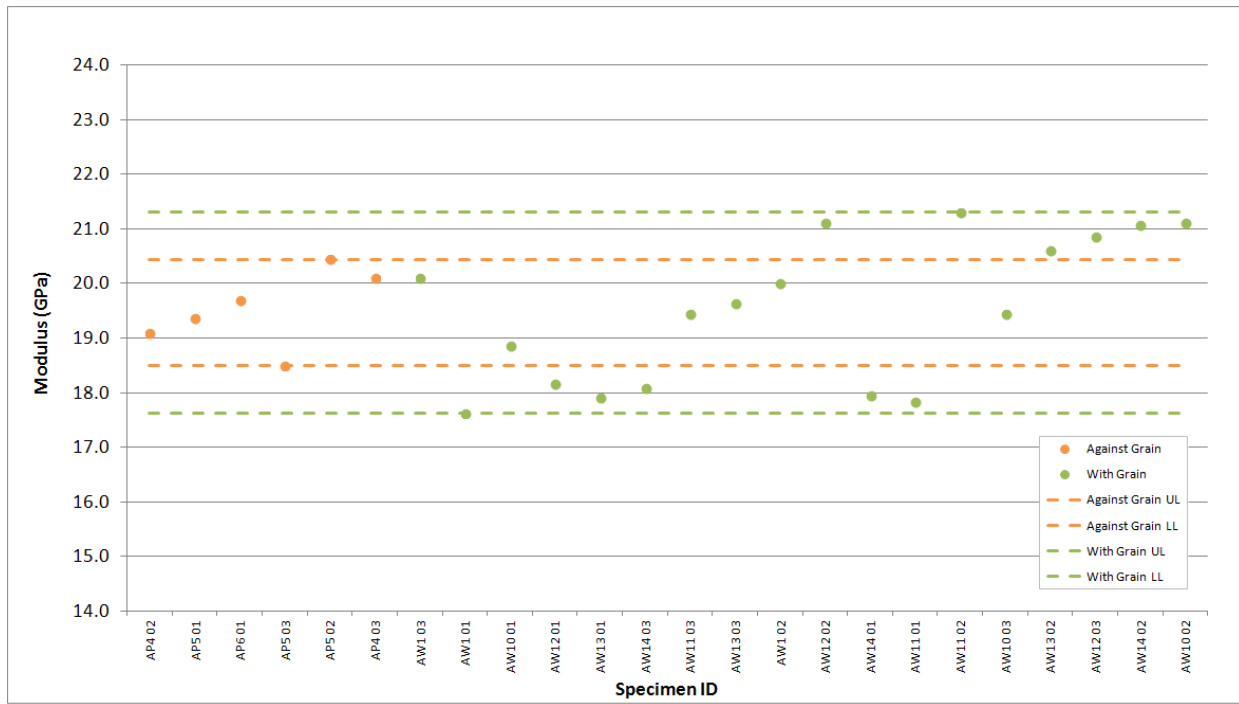


Figure A-112. NBG-17 Creep Modulus by Sonic Resonance.

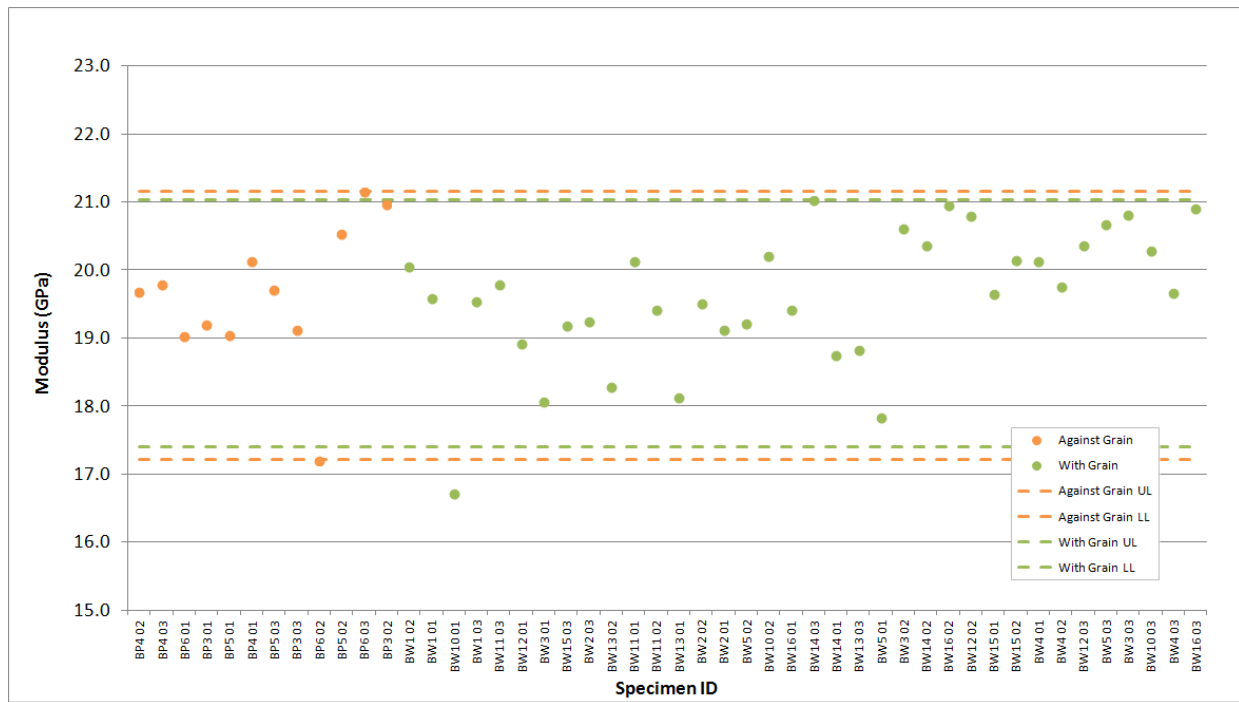


Figure A-113. NBG-18 Creep Modulus by Sonic Resonance.

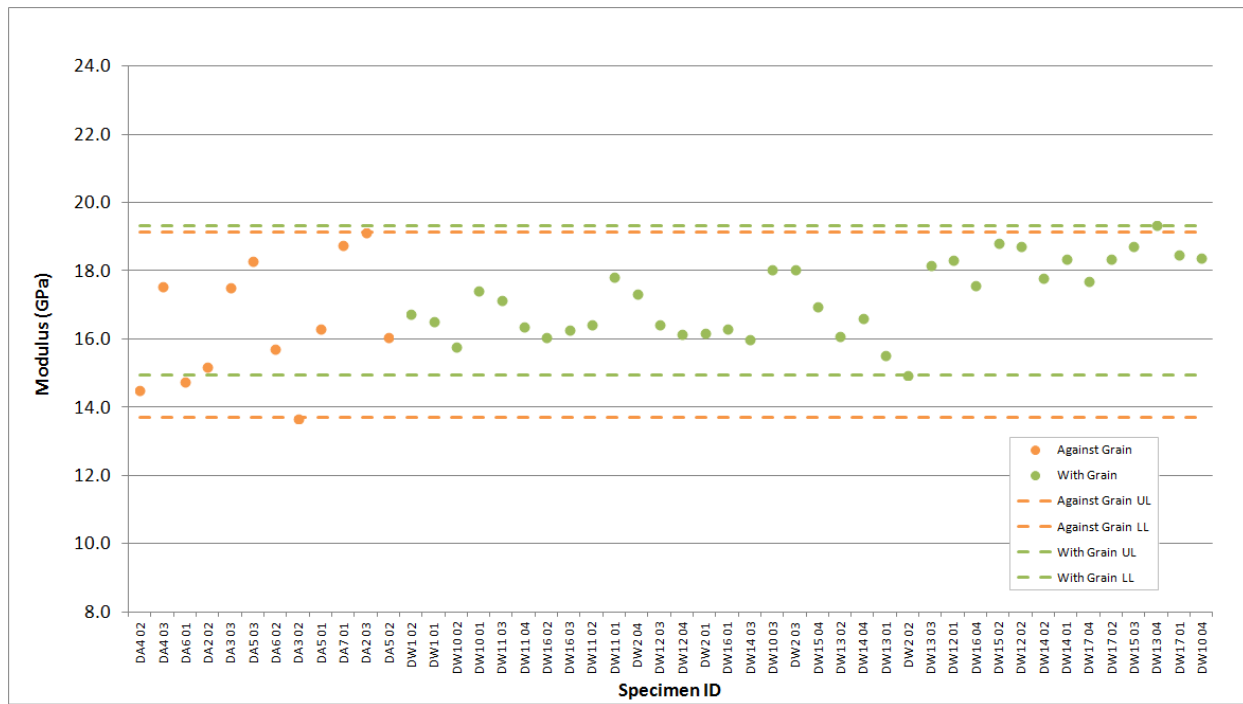


Figure A-114. PCEA Creep Modulus by Sonic Resonance.

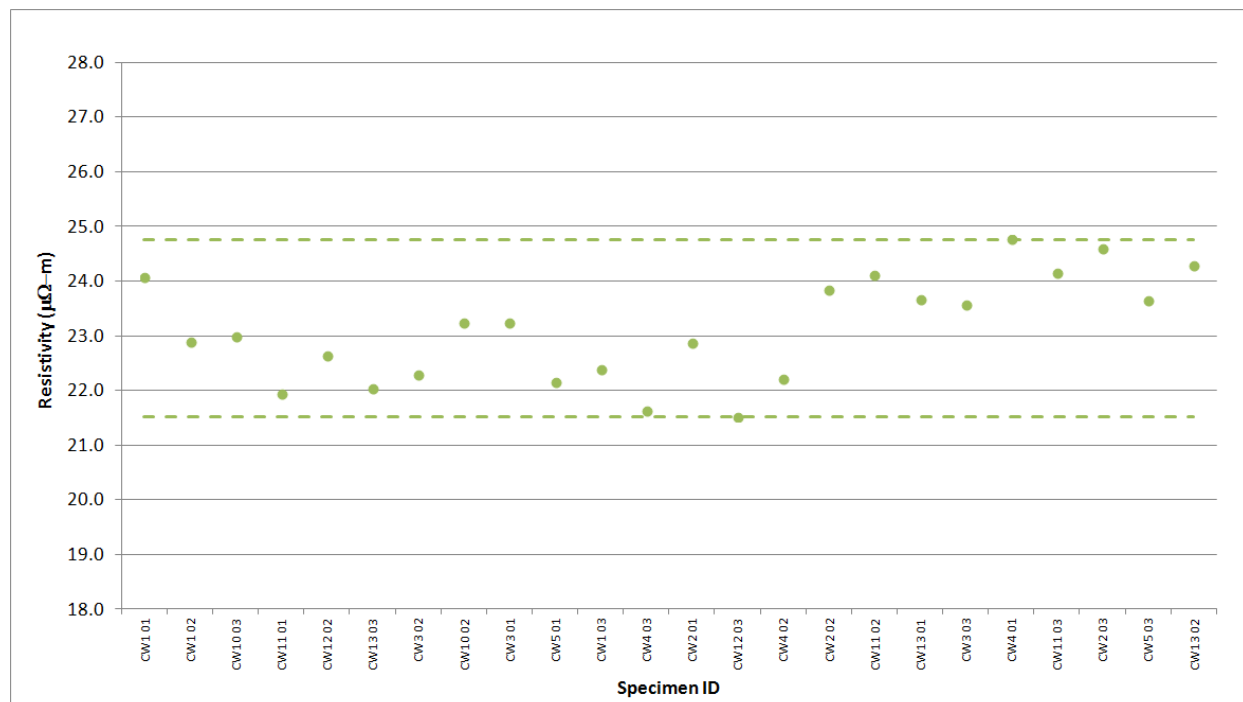


Figure A-115. H-451 Creep Resistivity.

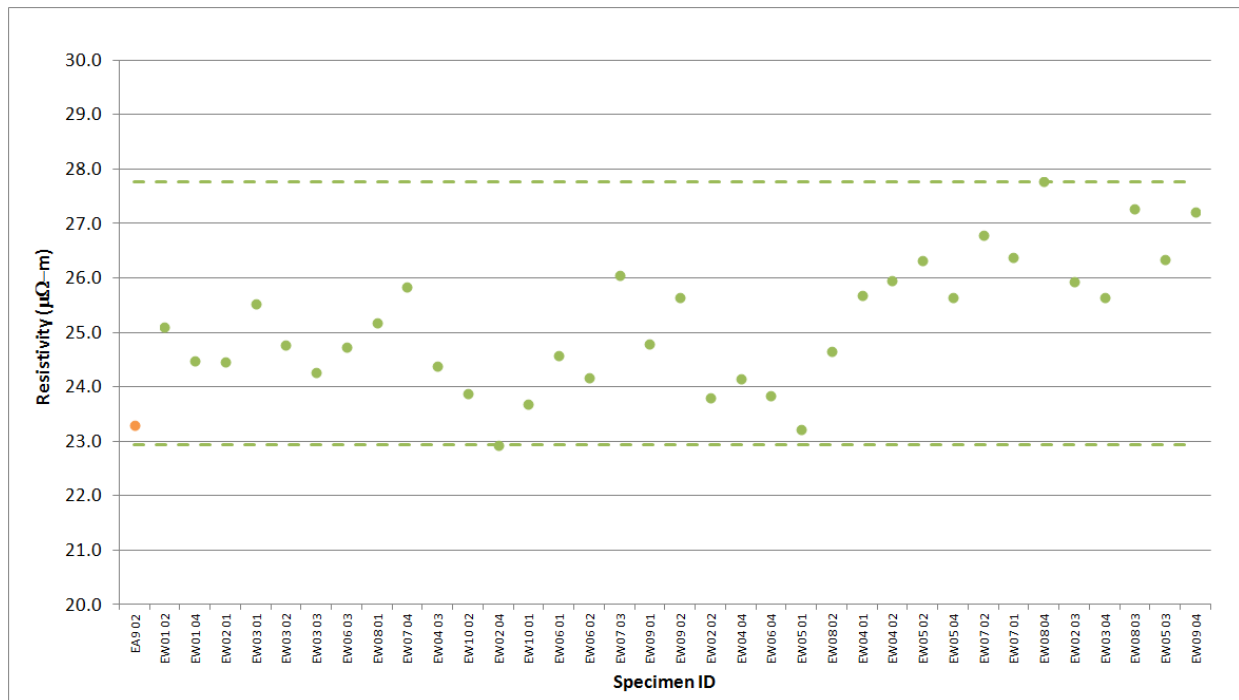


Figure A-116. IG-110 Creep Resistivity.

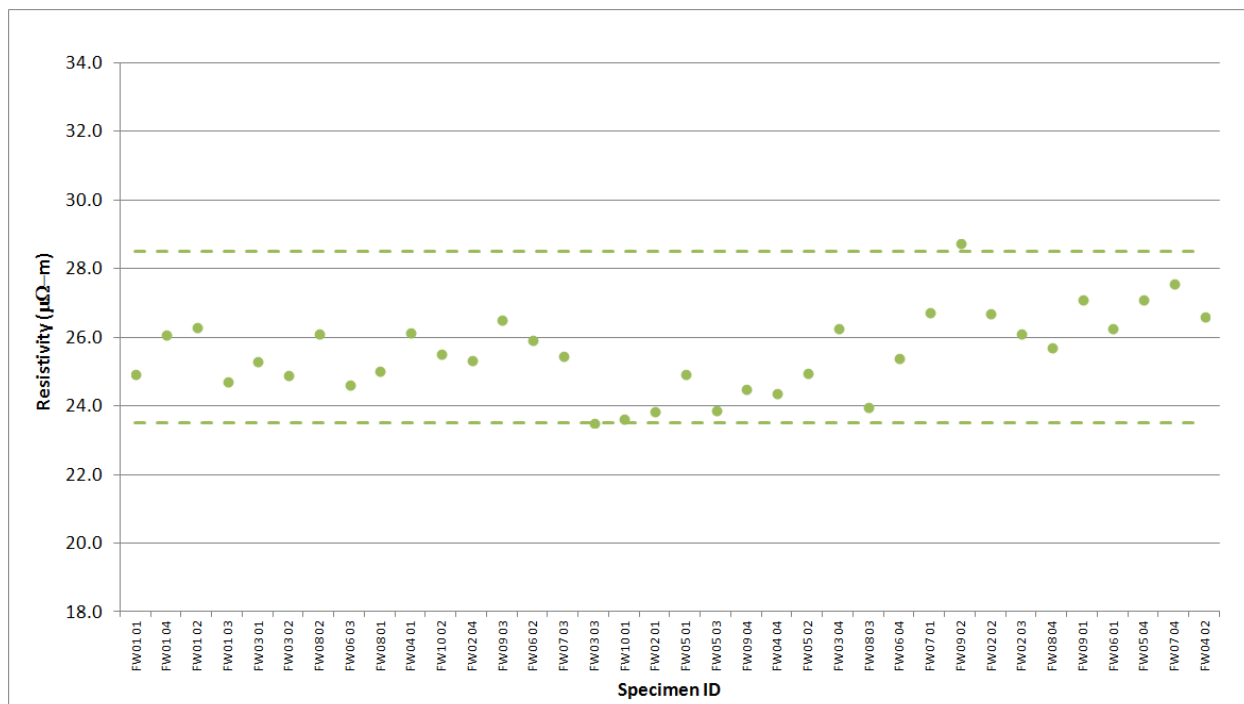


Figure A-117. IG-430 Creep Resistivity.

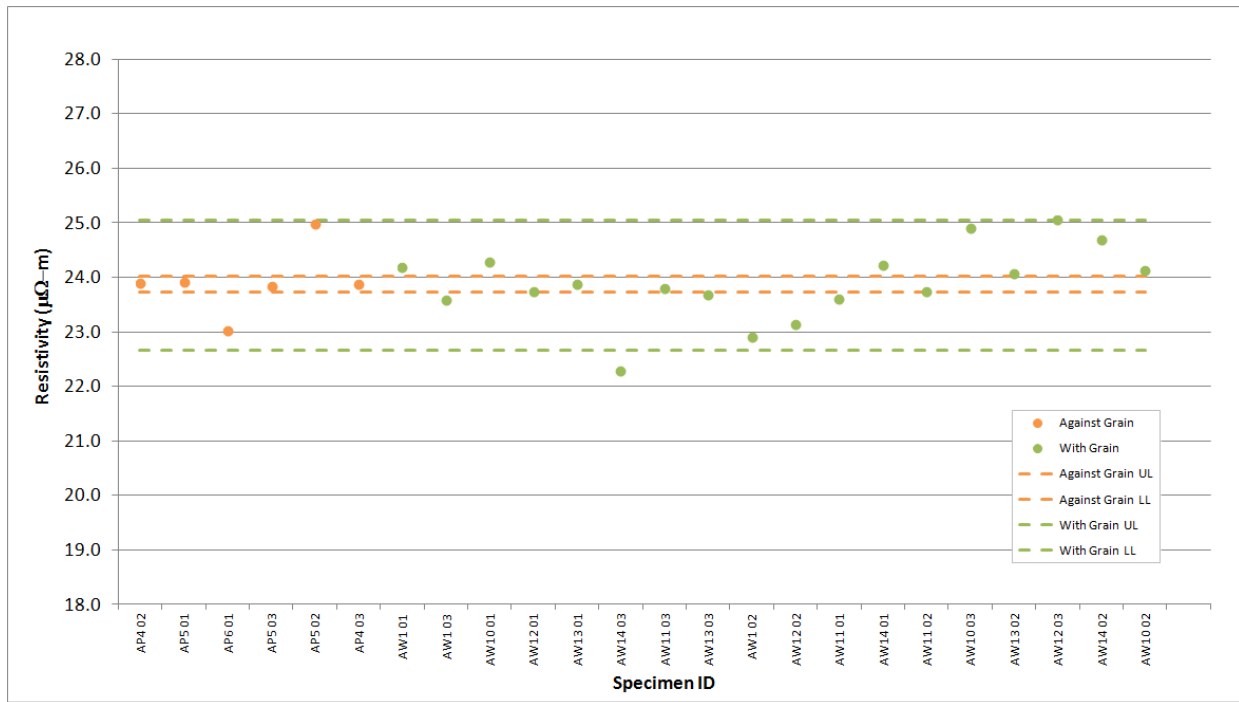


Figure A-118. NBG-17 Creep Resistivity.

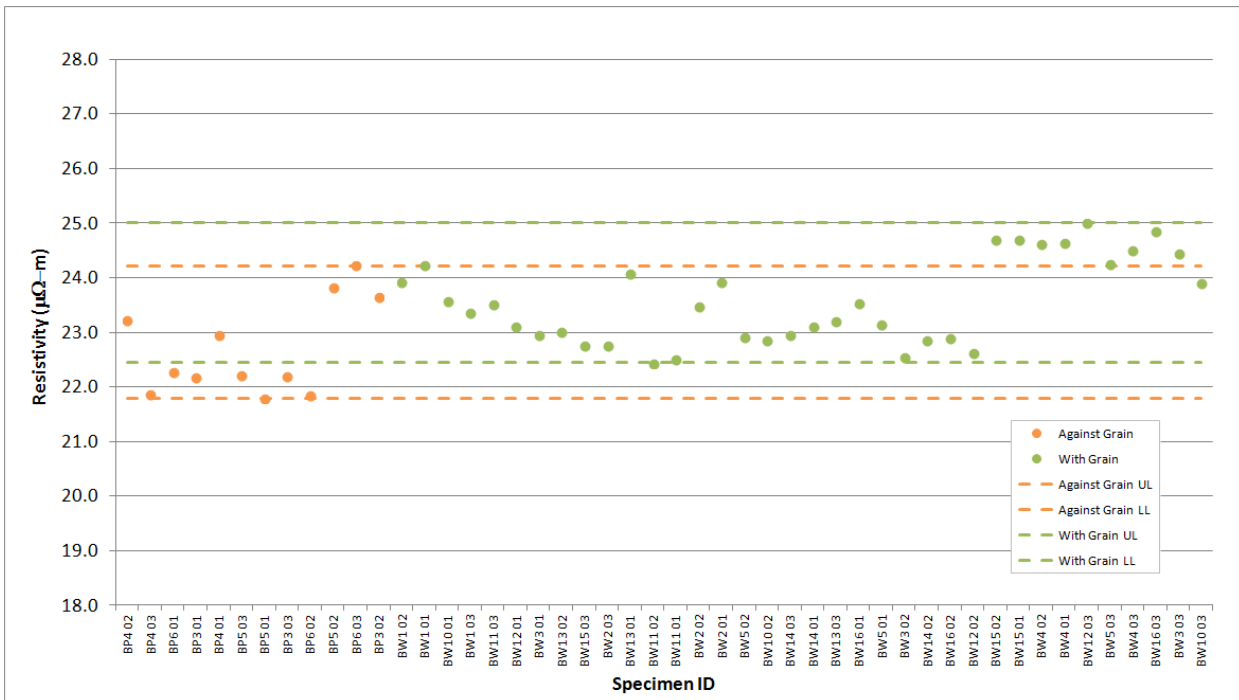


Figure A-119. NBG-18 Creep Resistivity.

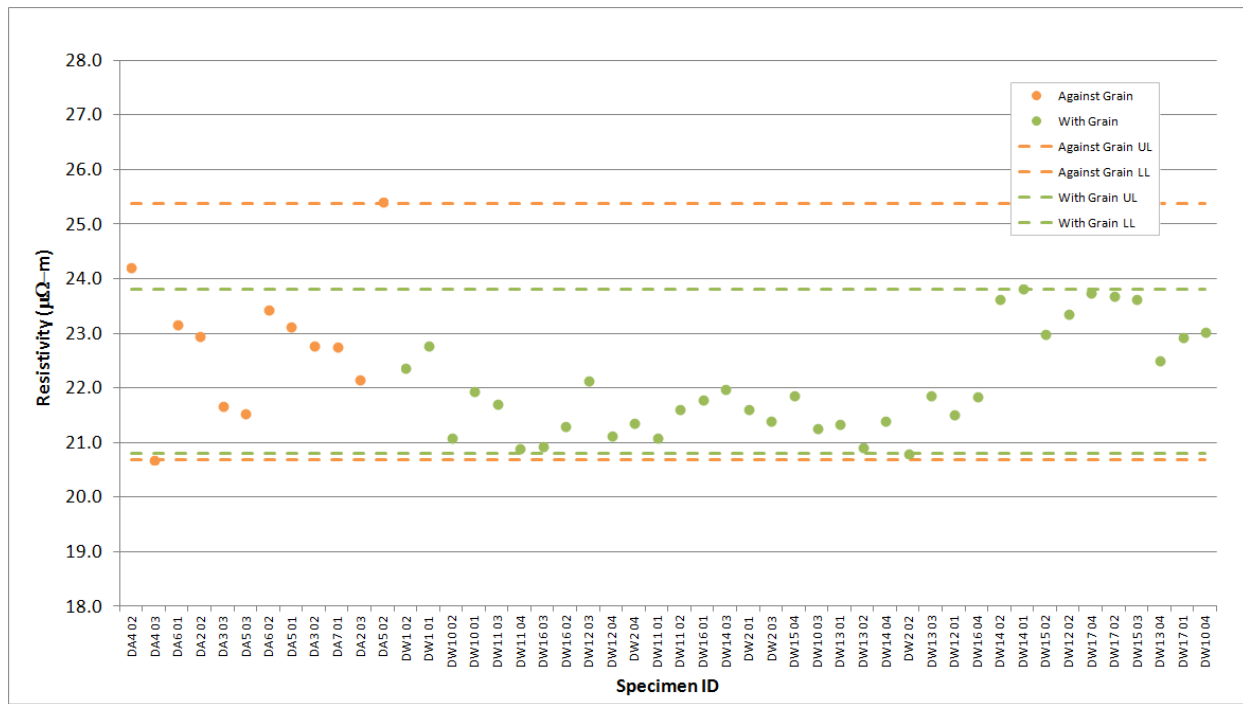


Figure A-120. PCEA Creep Resistivity.

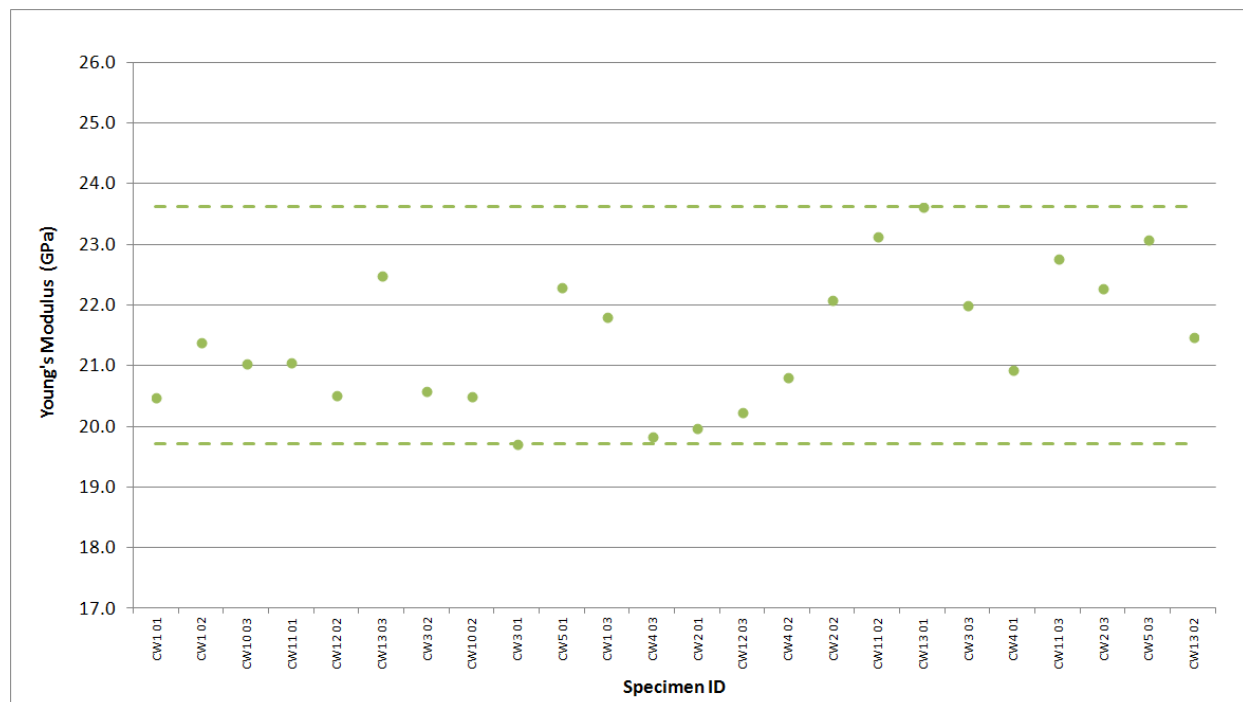


Figure A-121. H-451 Creep Young's Modulus by Sonic Velocity.

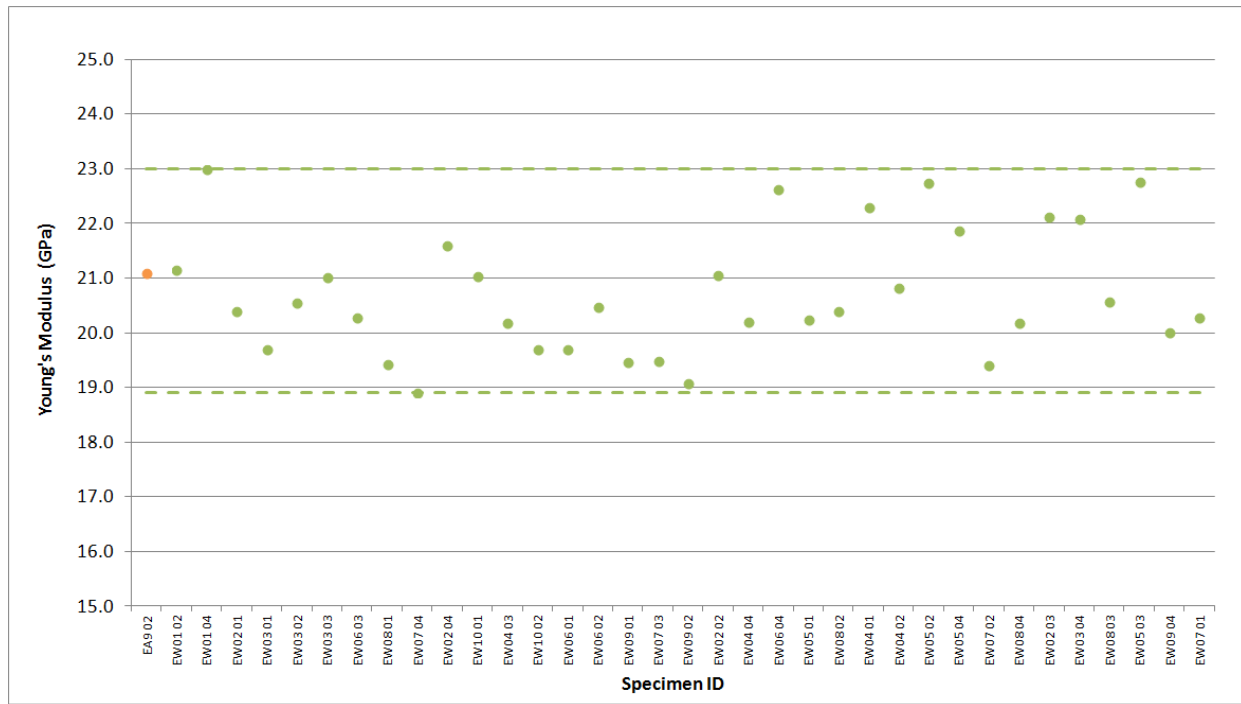


Figure A-122. IG-110 Creep Young's Modulus by Sonic Velocity.

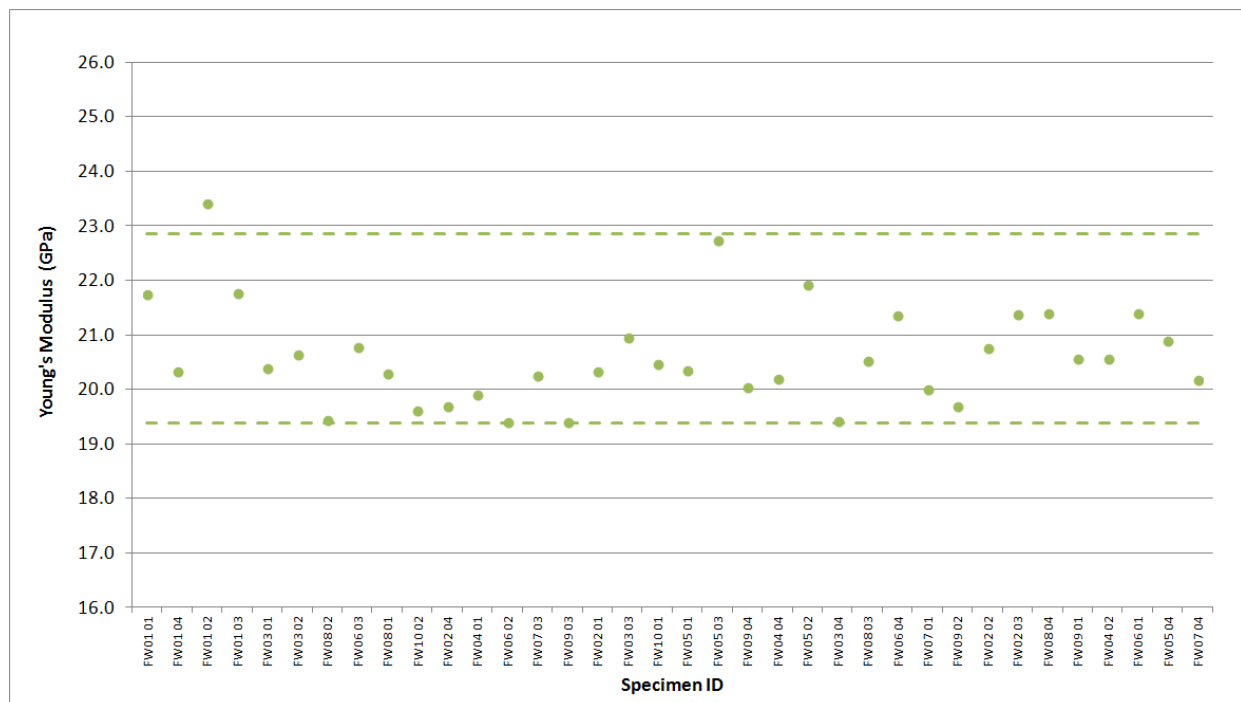


Figure A-123. IG-430 Creep Young's Modulus by Sonic Velocity.

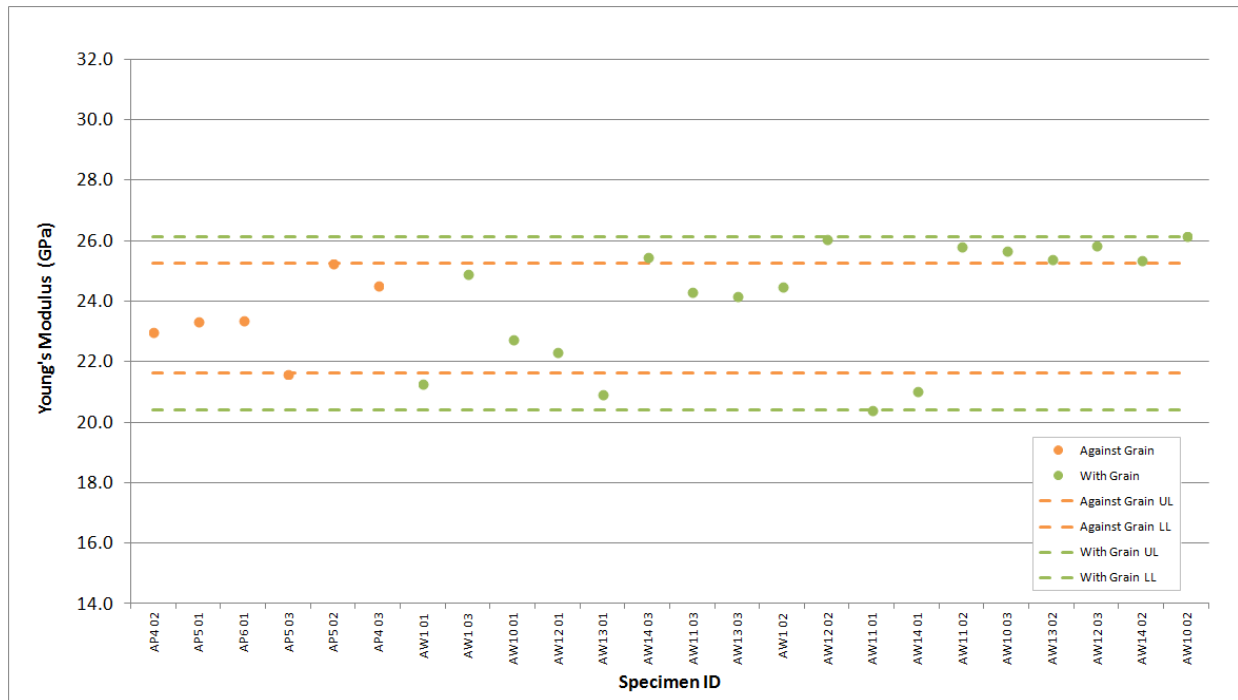


Figure A-124. NBG-17 Creep Young's Modulus by Sonic Velocity.

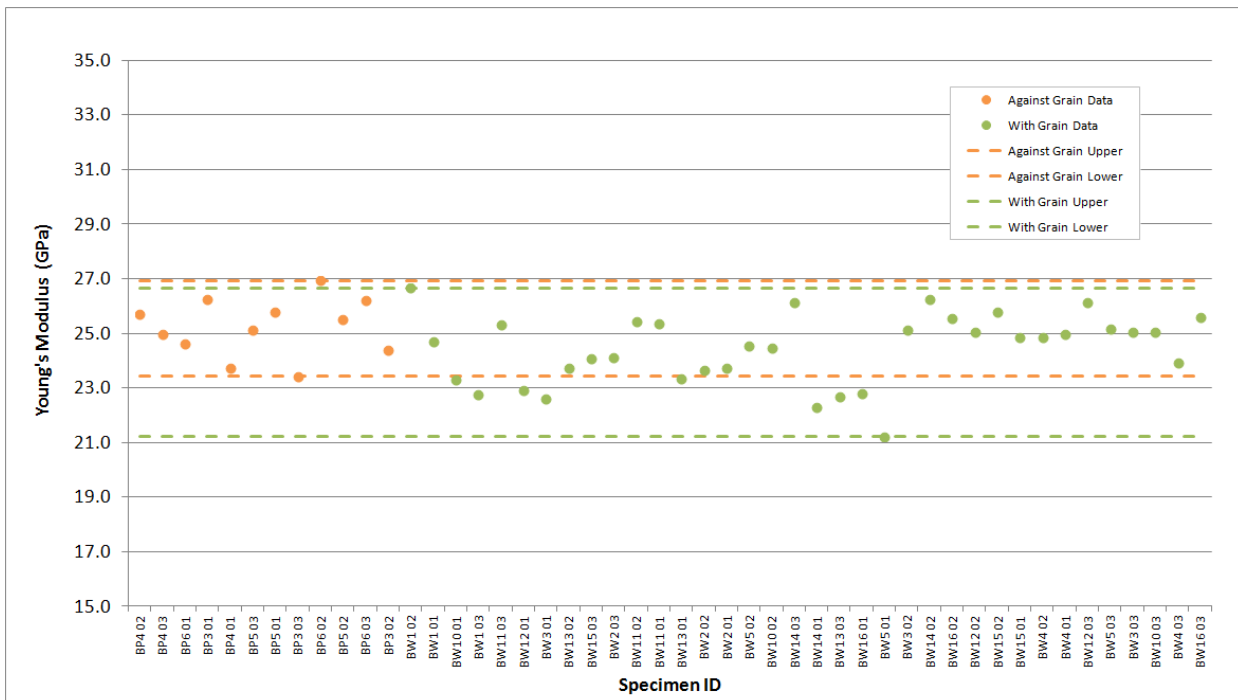


Figure A-125. NBG-18 Creep Young's Modulus by Sonic Velocity.

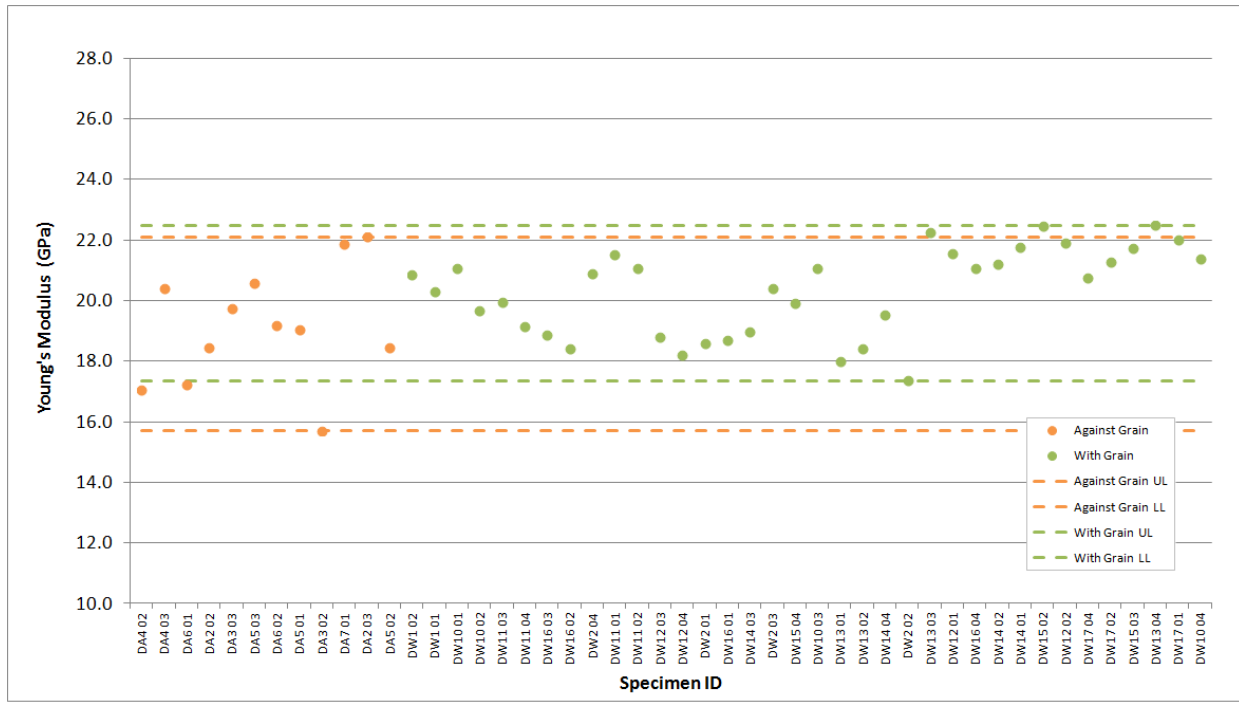


Figure A-126. PCEA Creep Young's Modulus by Sonic Velocity.

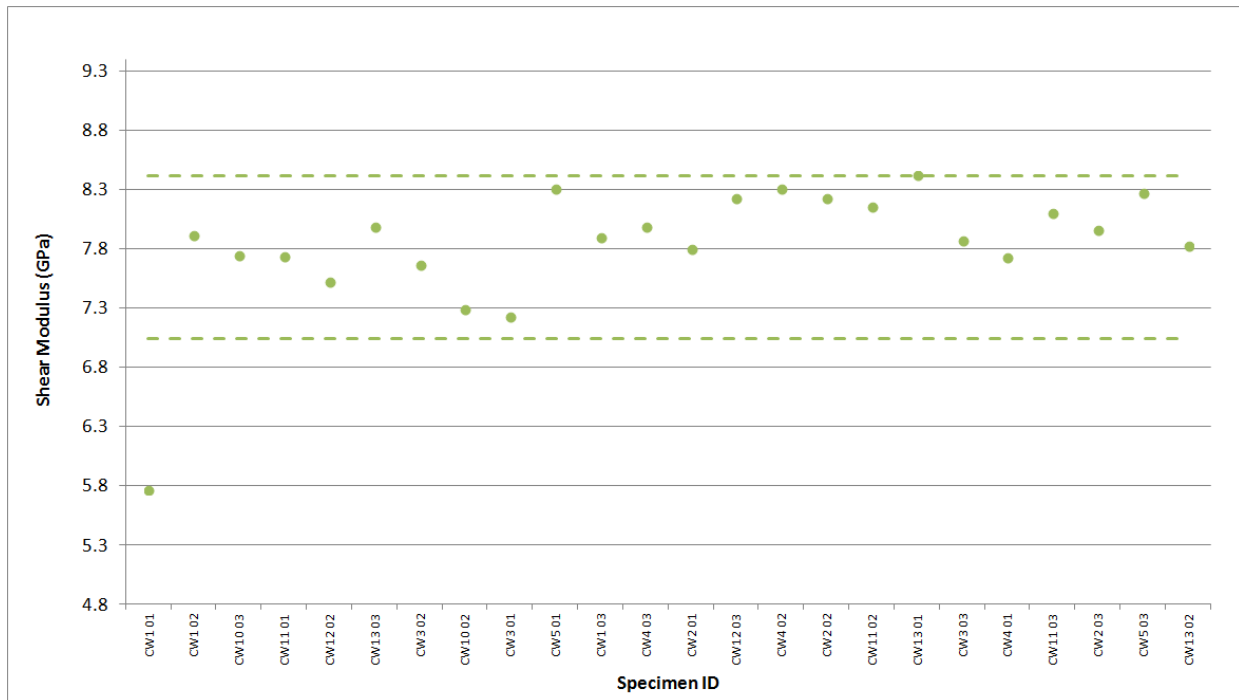


Figure A-127. H-451 Creep Shear Modulus by Sonic Velocity.

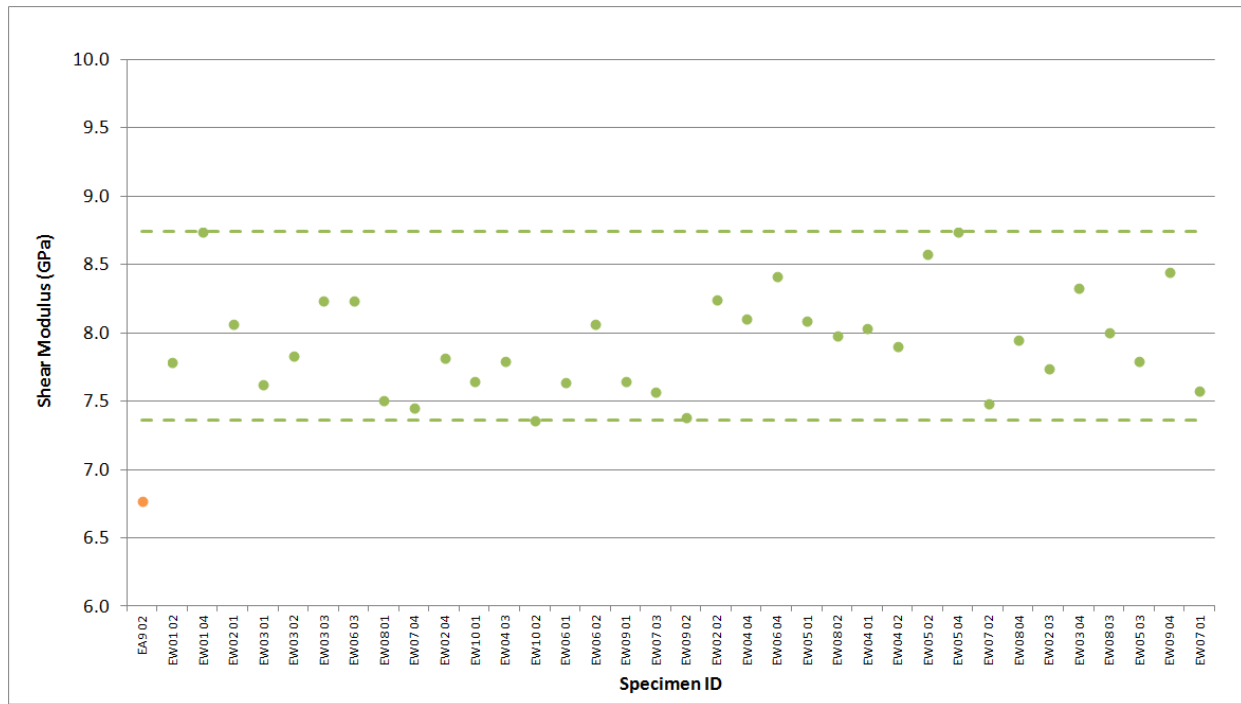


Figure A-128. IG-110 Creep Shear Modulus by Sonic Velocity.

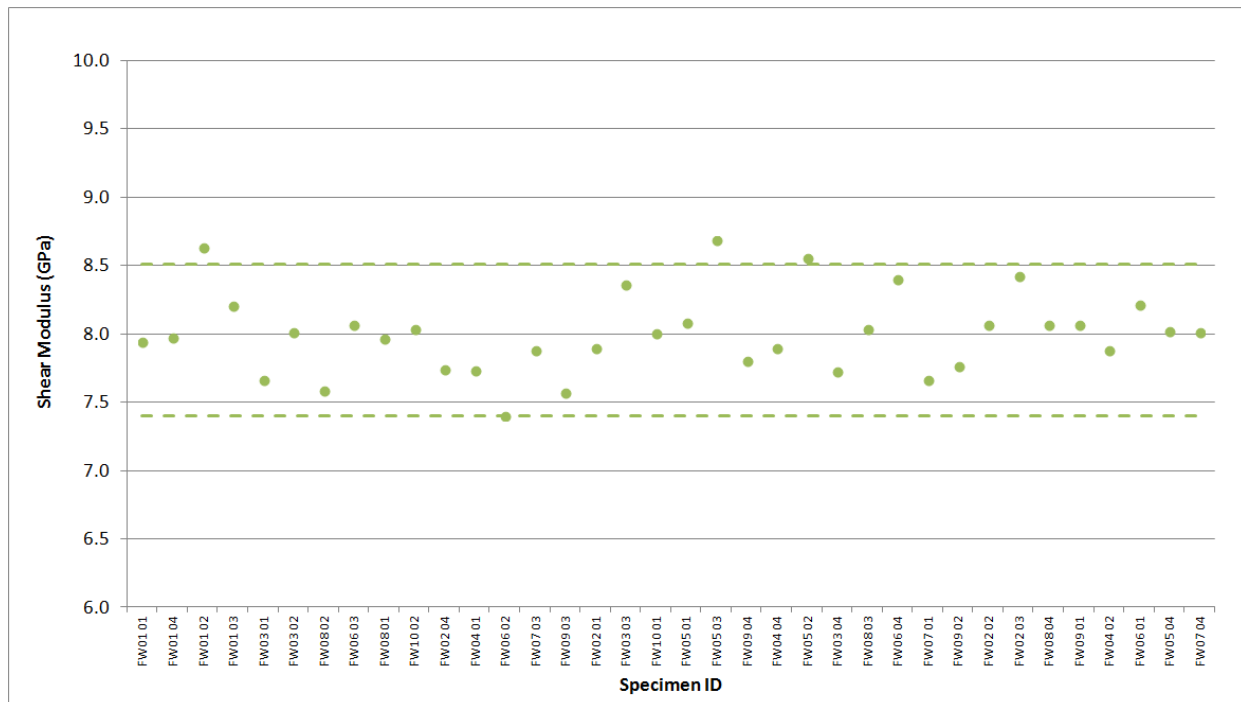


Figure A-129. IG-430 Creep Shear Modulus by Sonic Velocity.

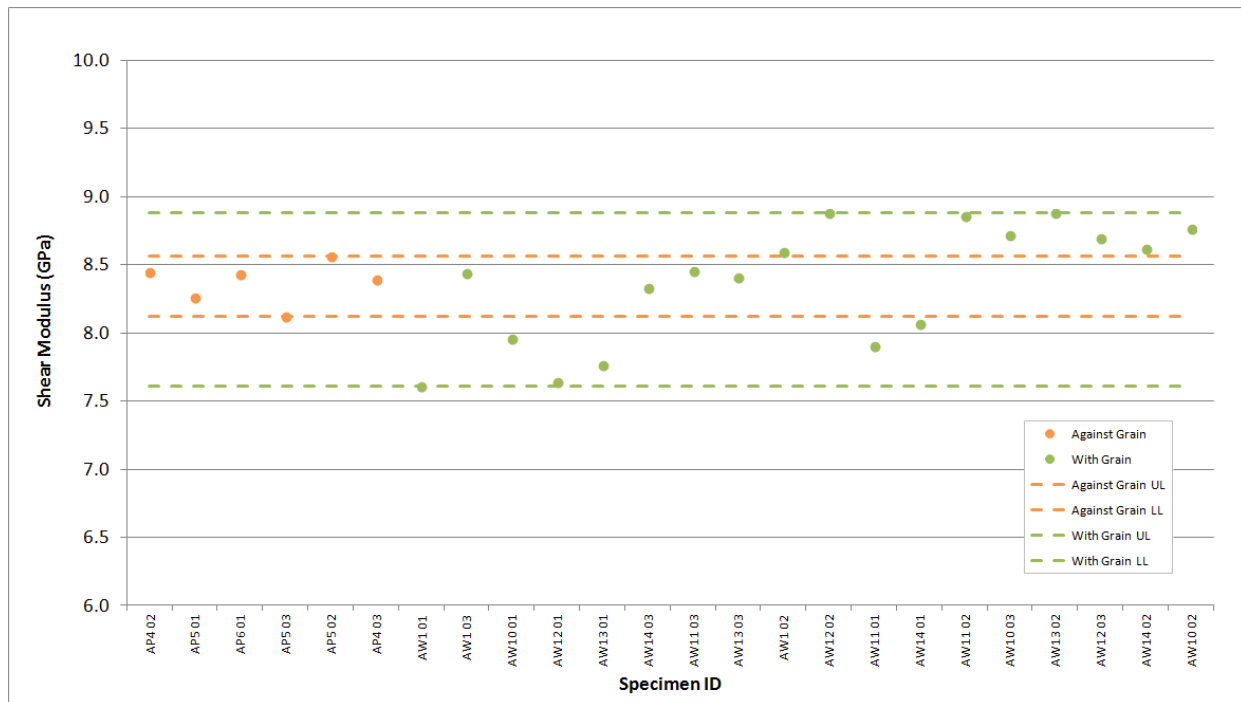


Figure A-130. NBG-17 Creep Shear Modulus by Sonic Velocity.

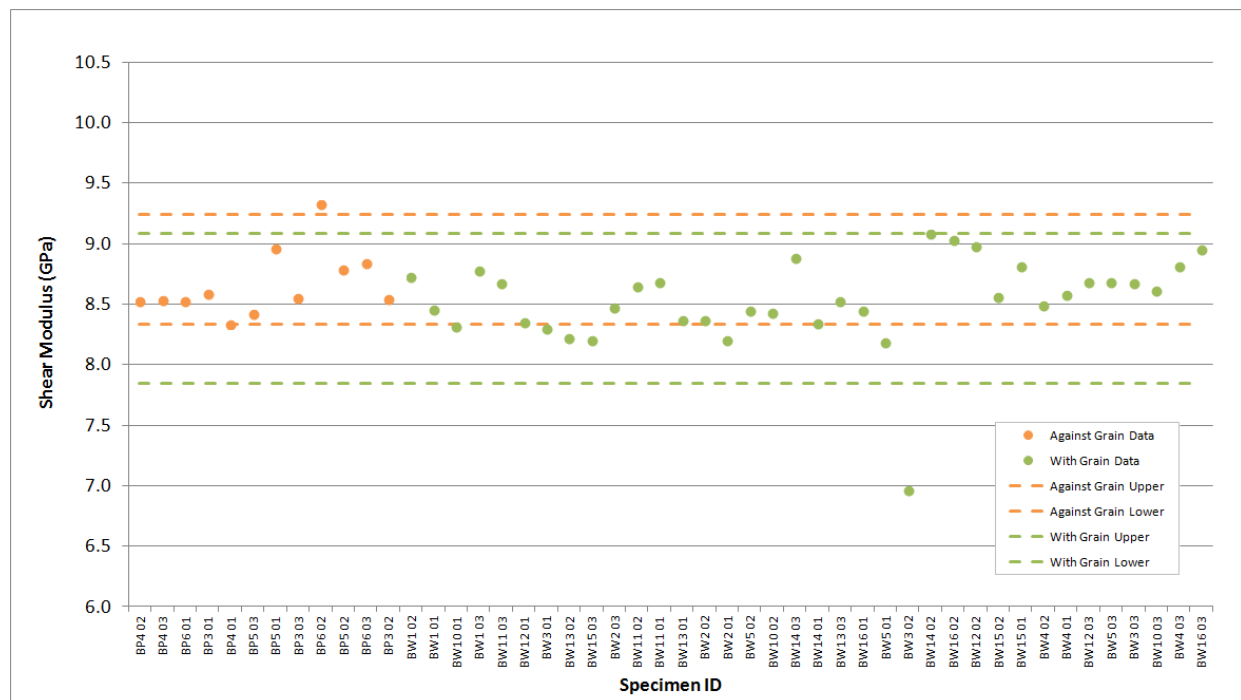


Figure A-131. NBG-18 Creep Shear Modulus by Sonic Velocity.

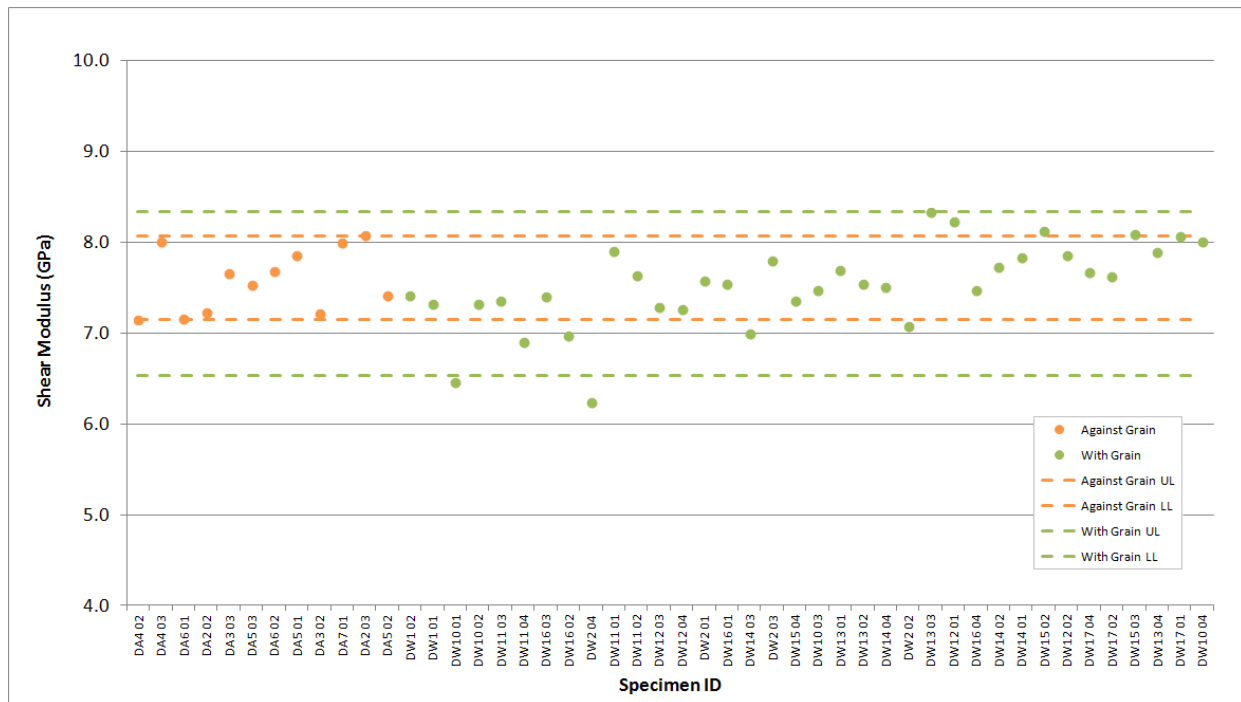


Figure A-132. PCEA Creep Shear Modulus by Sonic Velocity.

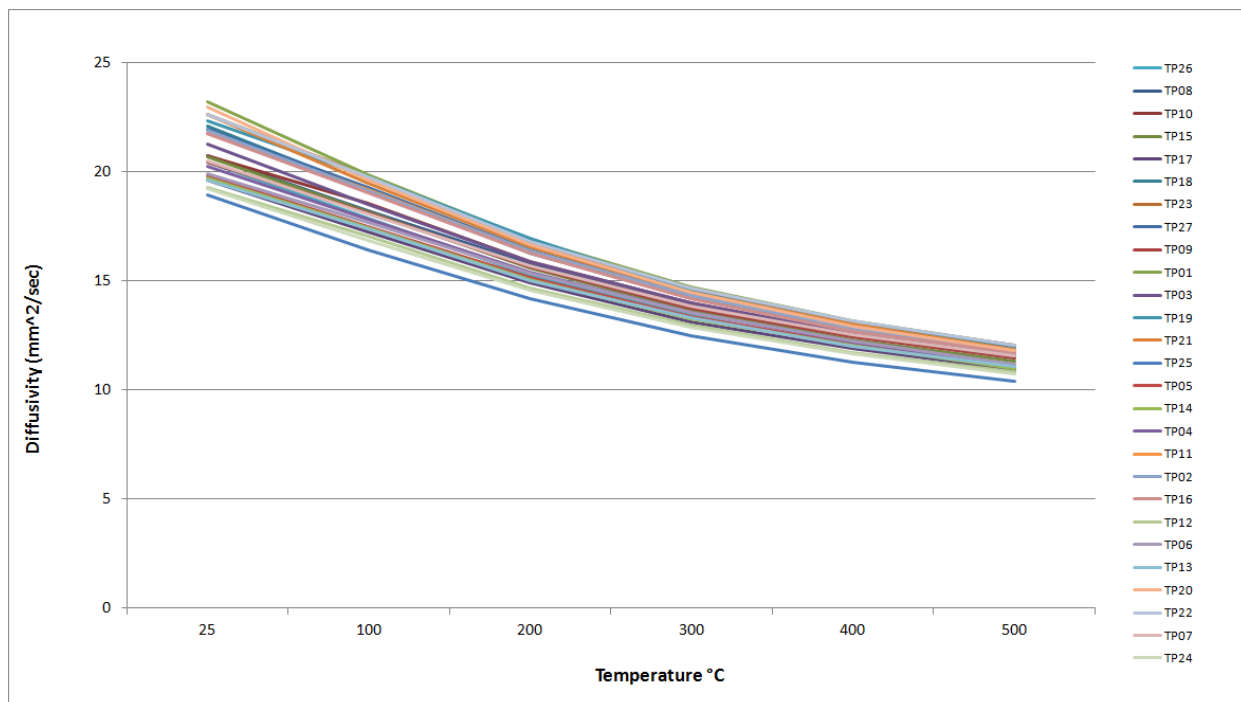


Figure A-133. 2114 Piggyback Diffusivity.

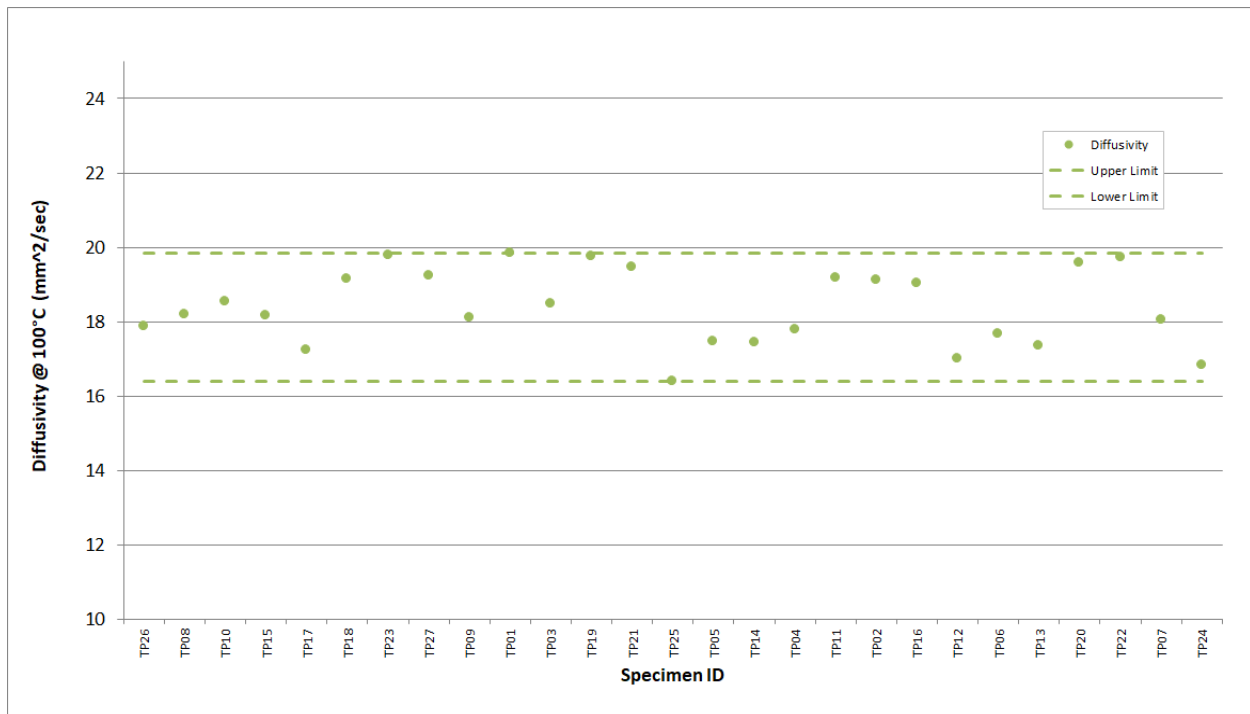


Figure A-134. 2114 Piggyback Diffusivity @ 100°C.

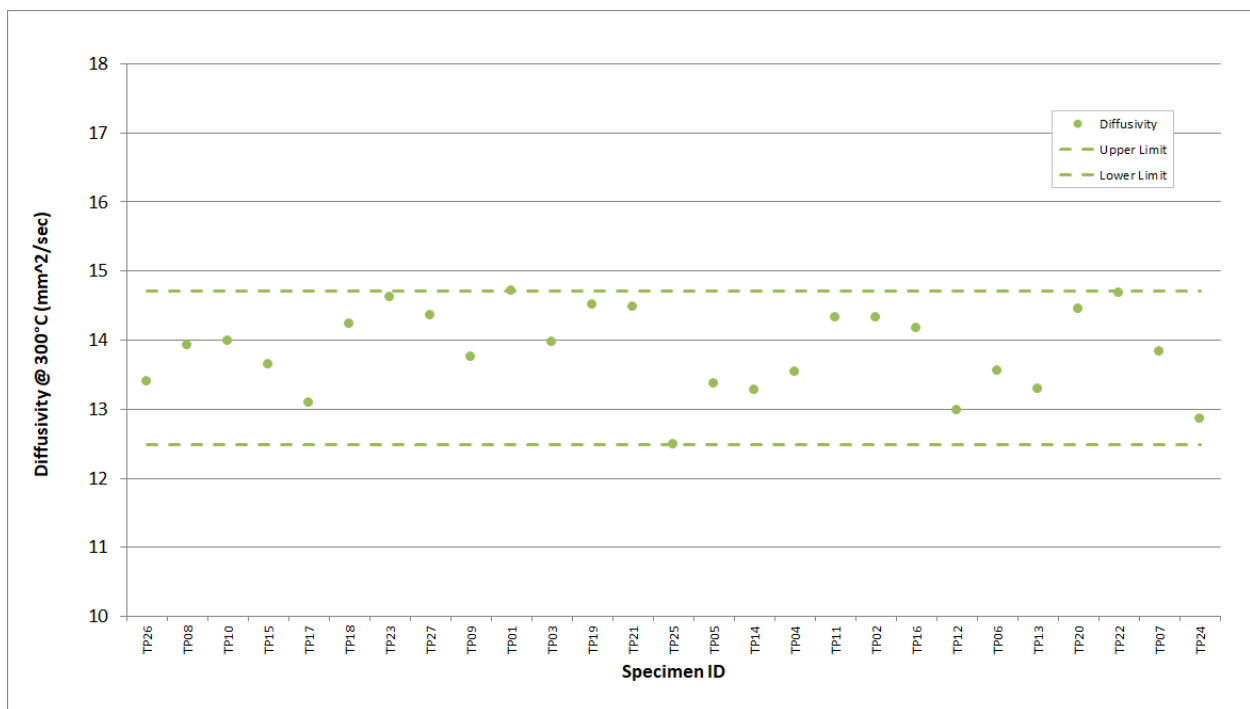


Figure A-135. 2114 Piggyback Diffusivity @ 300°C.

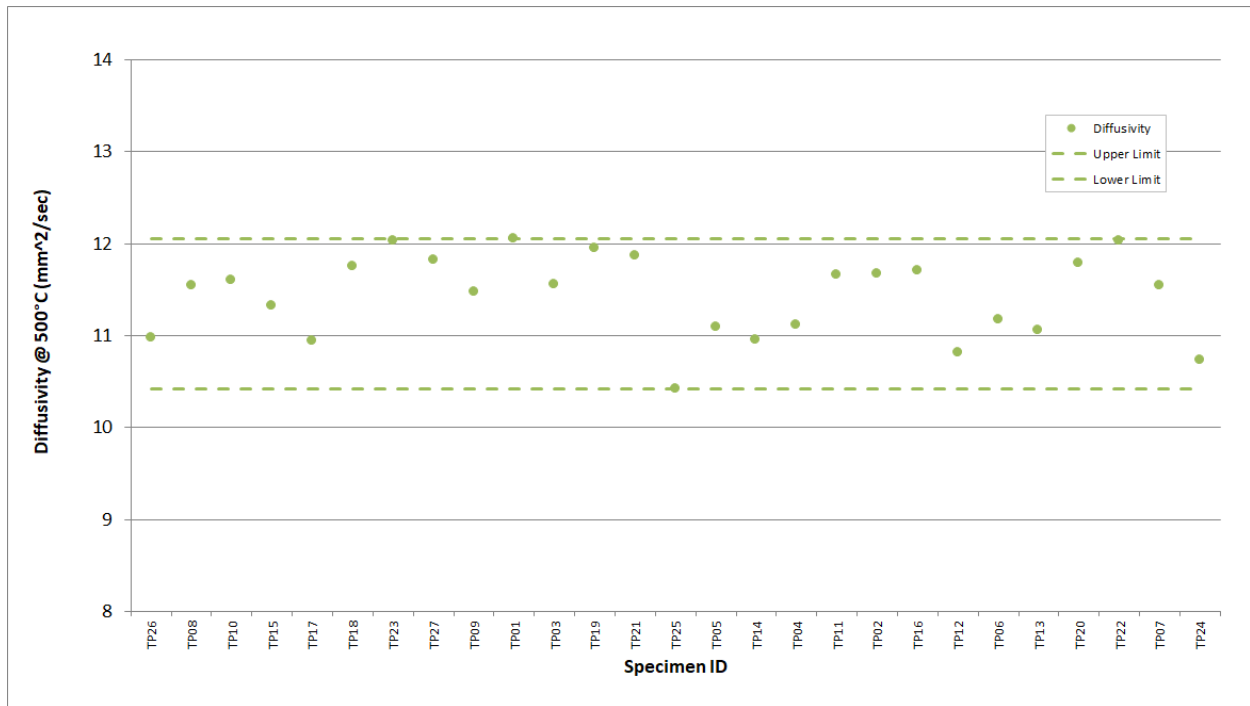


Figure A-136. 2114 Piggyback Diffusivity @ 500°C.

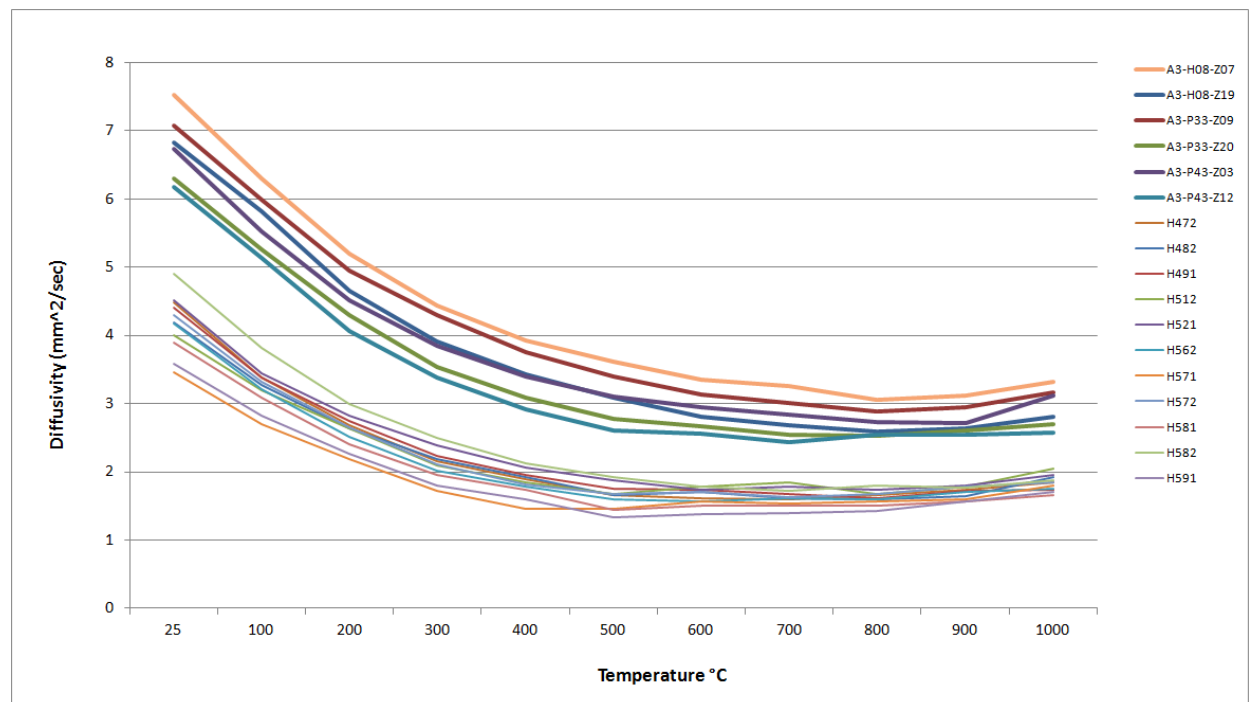


Figure A-137. A3 Piggyback Diffusivity.

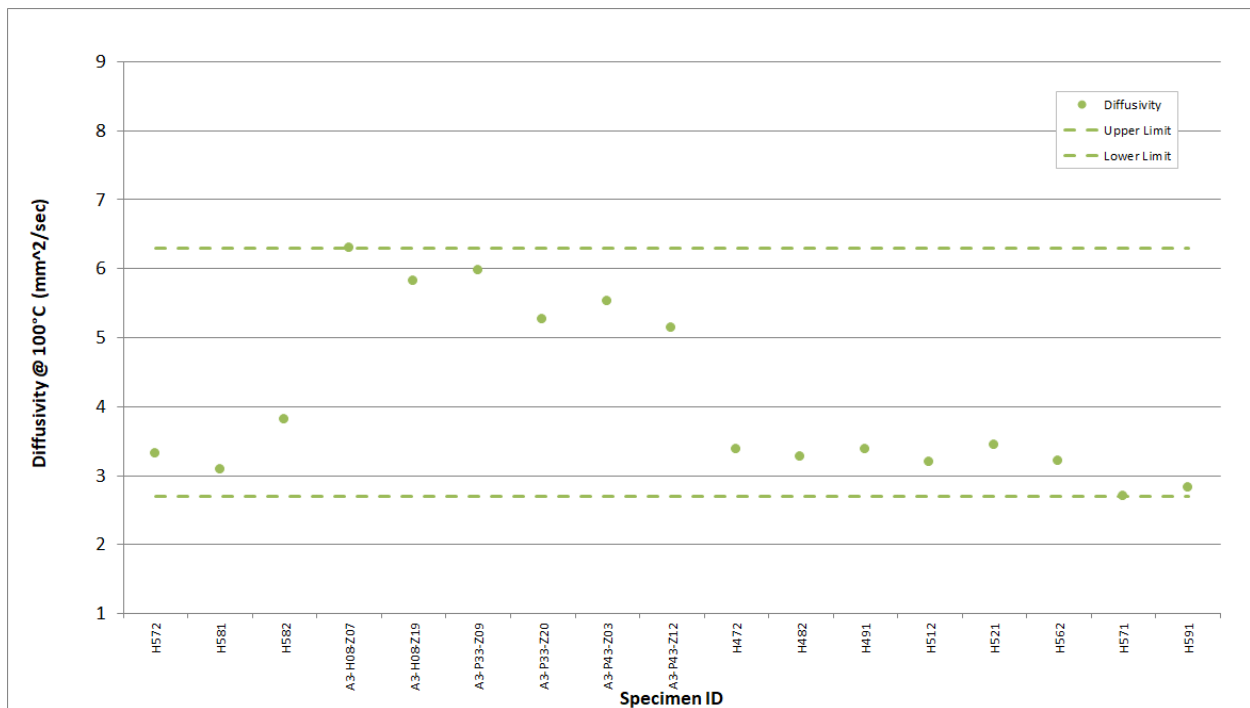


Figure A-138. A3 Piggyback Diffusivity @ 100°C.

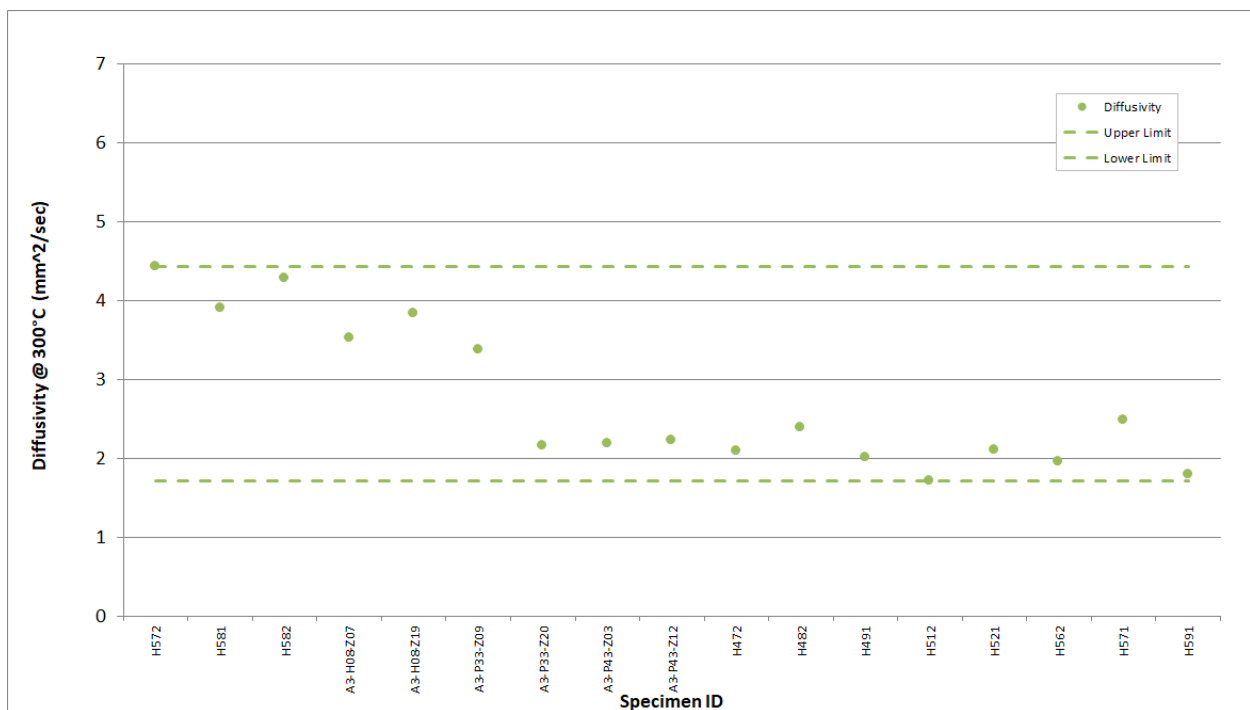


Figure A-139. A3 Piggyback Diffusivity @ 300°C.

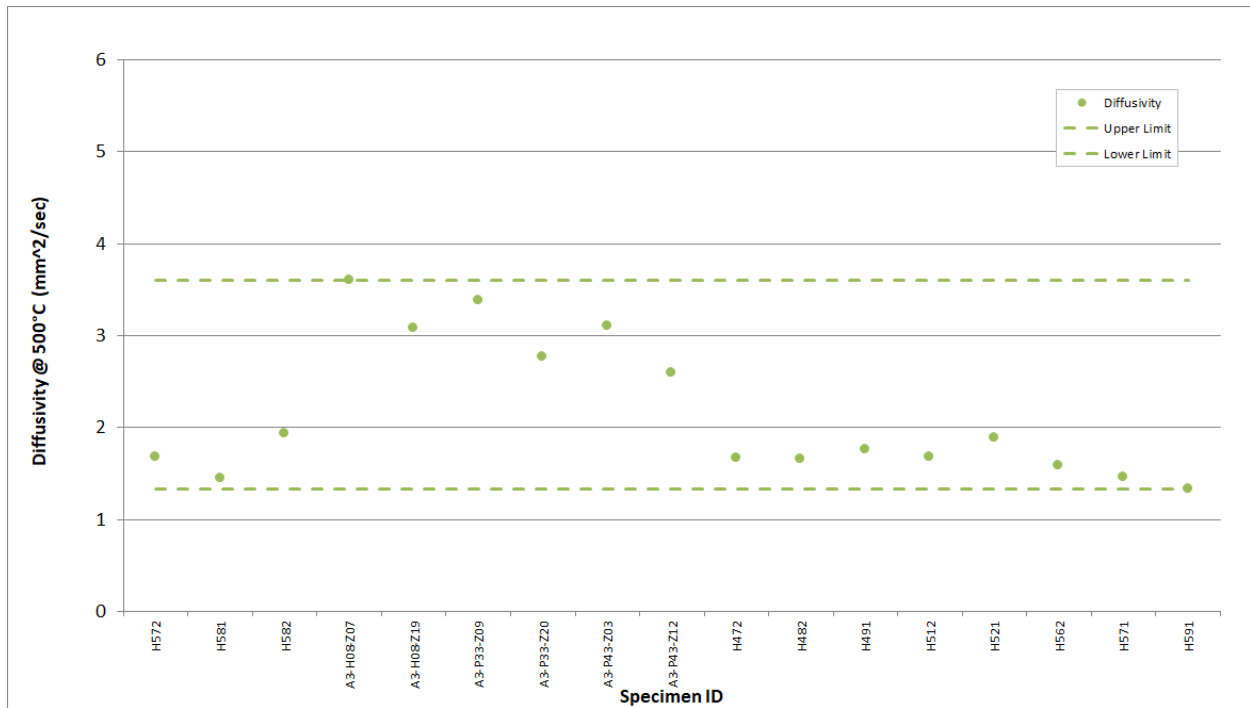


Figure A-140. A3 Piggyback Diffusivity @ 500°C.

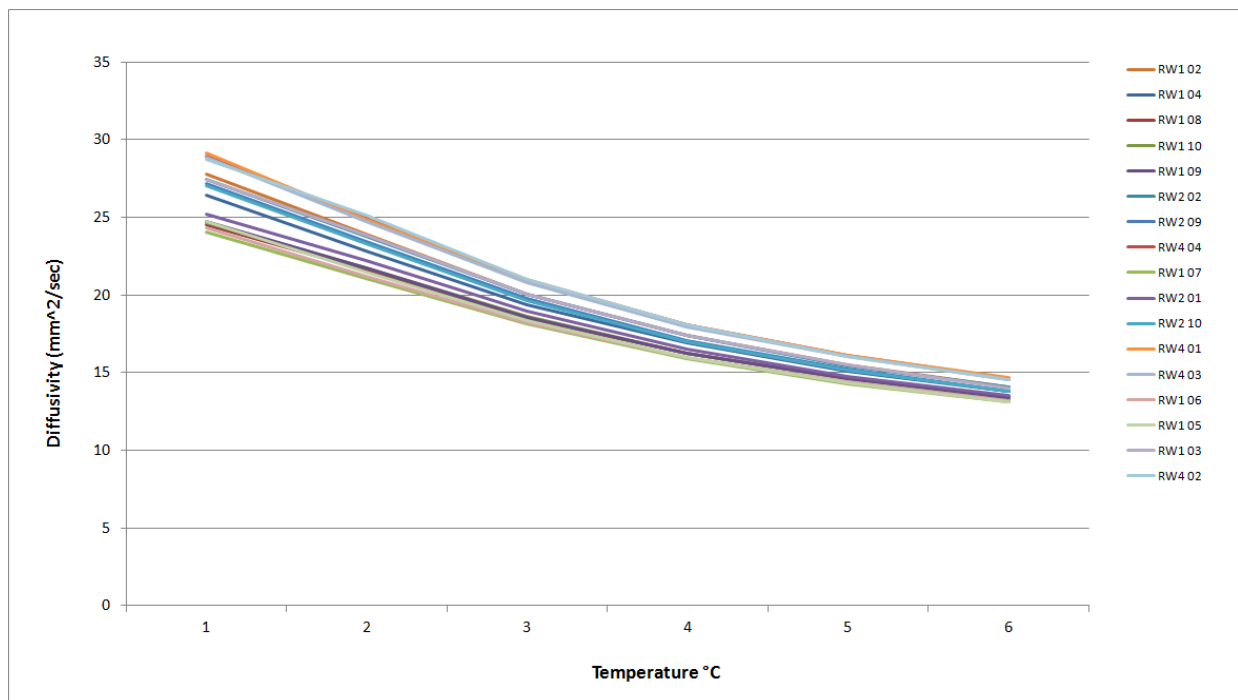


Figure A-141. BAN Piggyback Diffusivity.

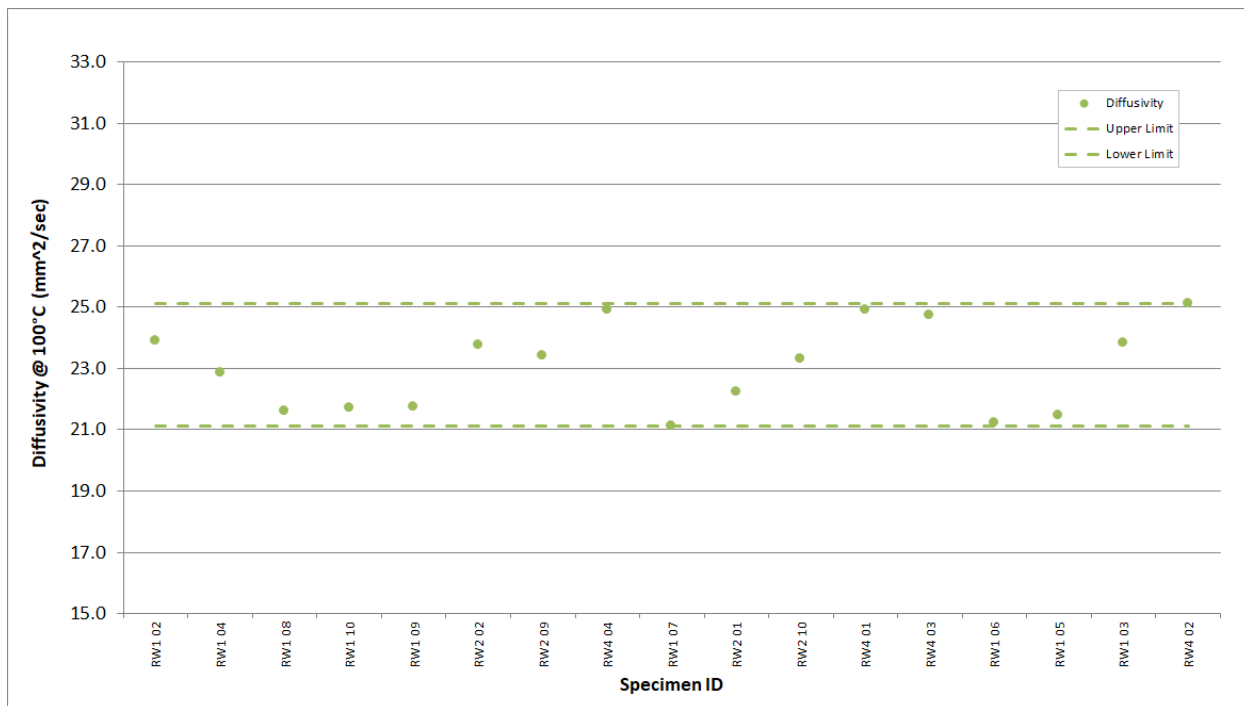


Figure A-142. BAN Piggyback Diffusivity @ 100°C.

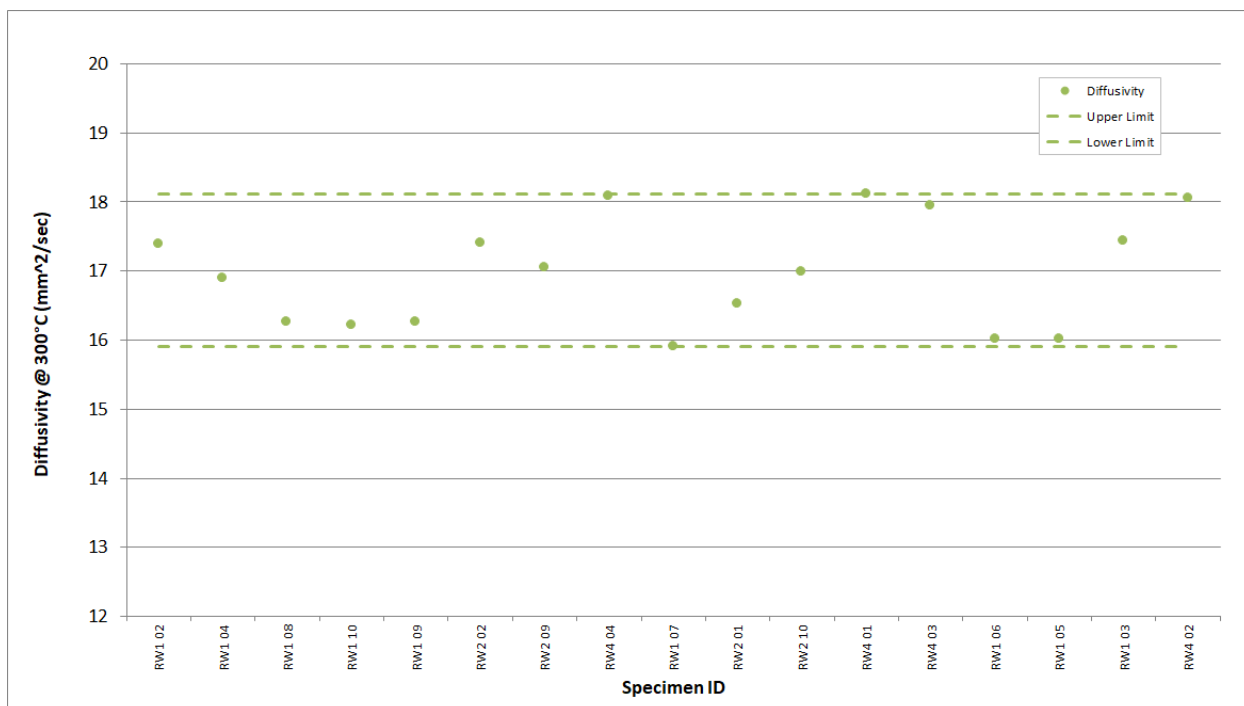


Figure A-143. BAN Piggyback Diffusivity @ 300°C.

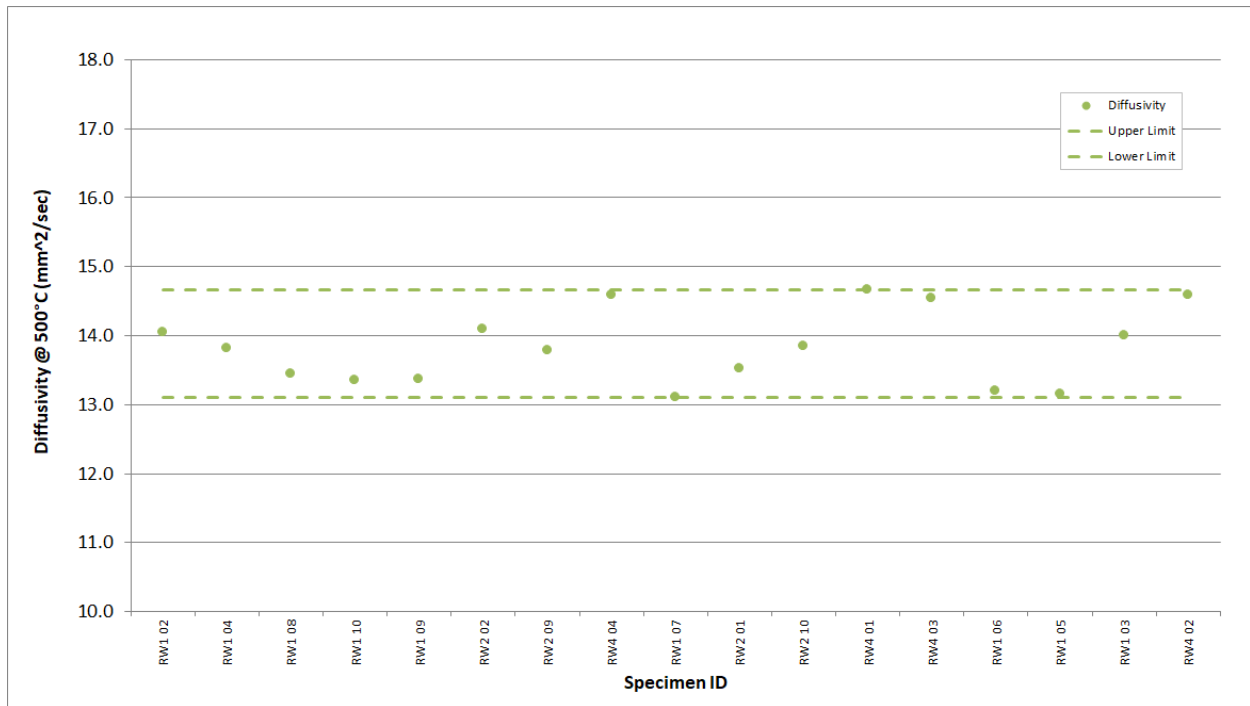


Figure A-144. BAN Piggyback Diffusivity @ 500°C.

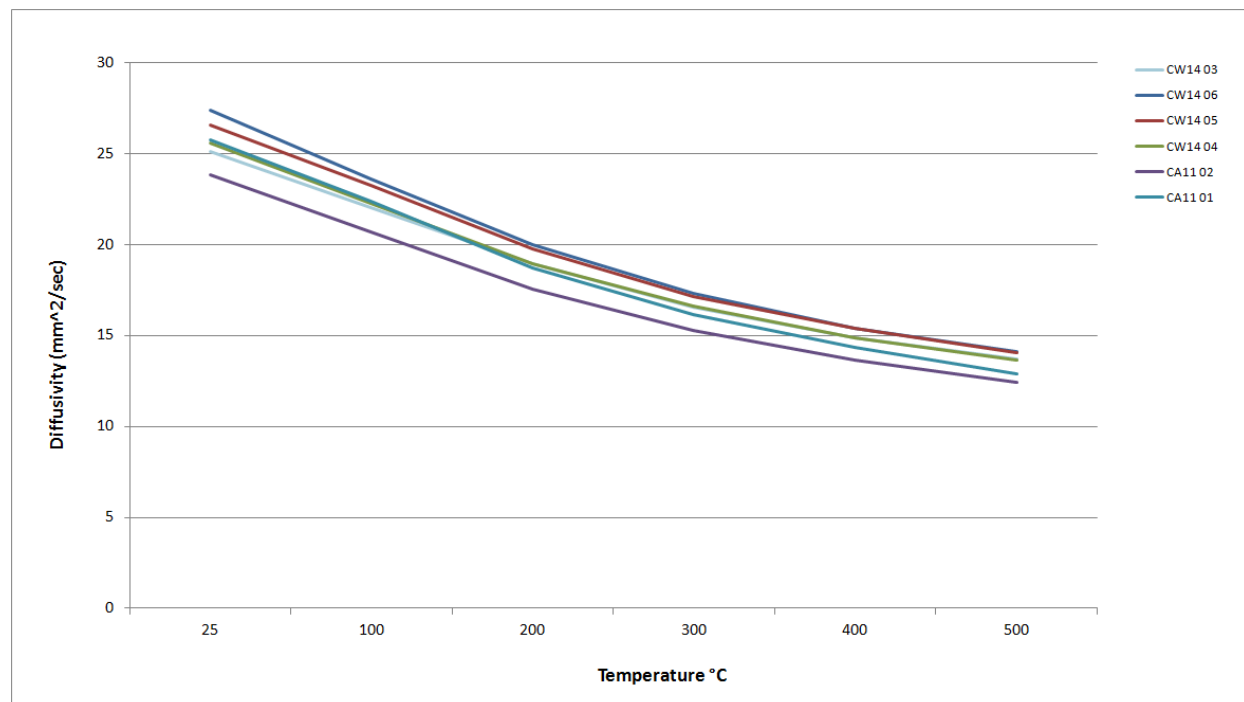


Figure A-145. H-451 Piggyback Diffusivity.

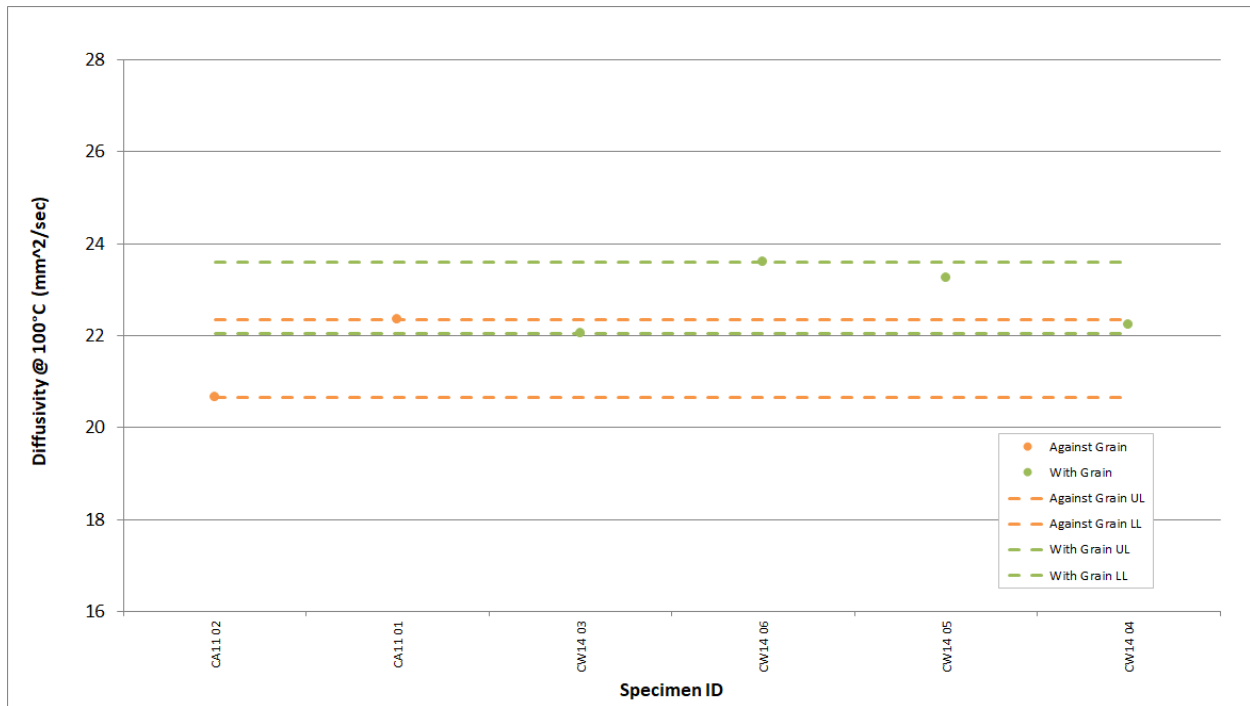


Figure A-146. H-451 Piggyback Diffusivity @ 100°C.

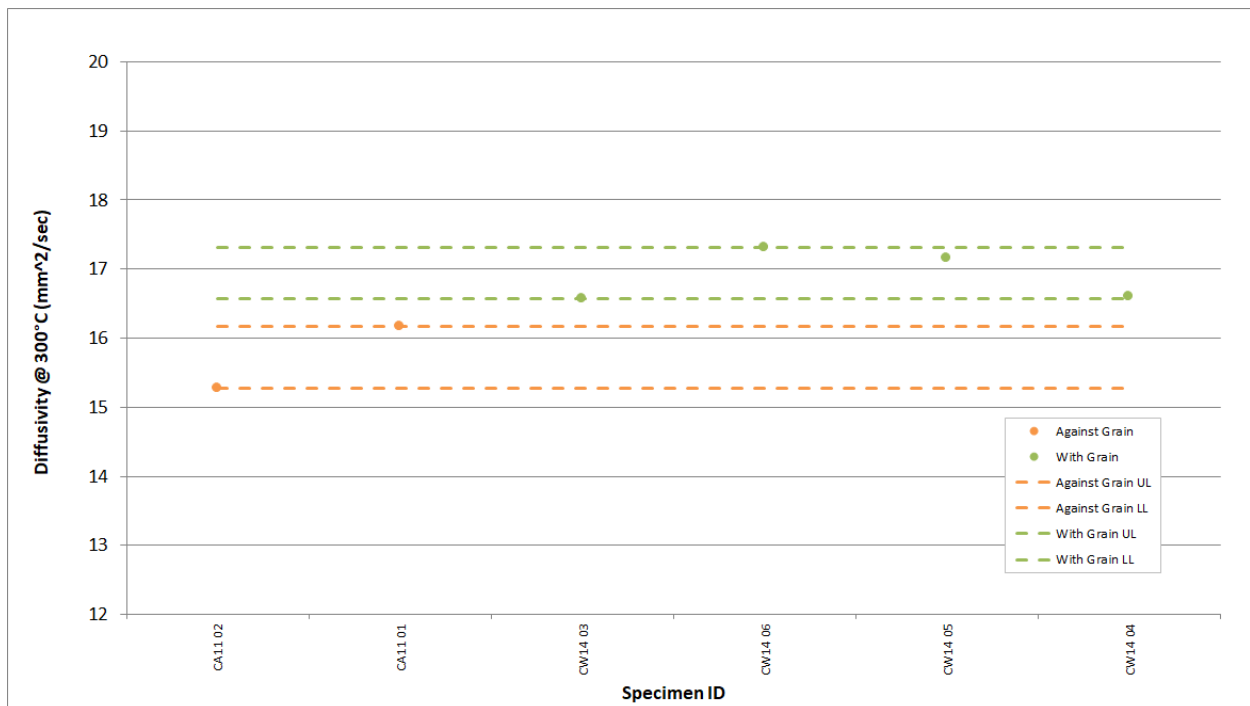


Figure A-147. H-451 Piggyback Diffusivity @ 300°C.

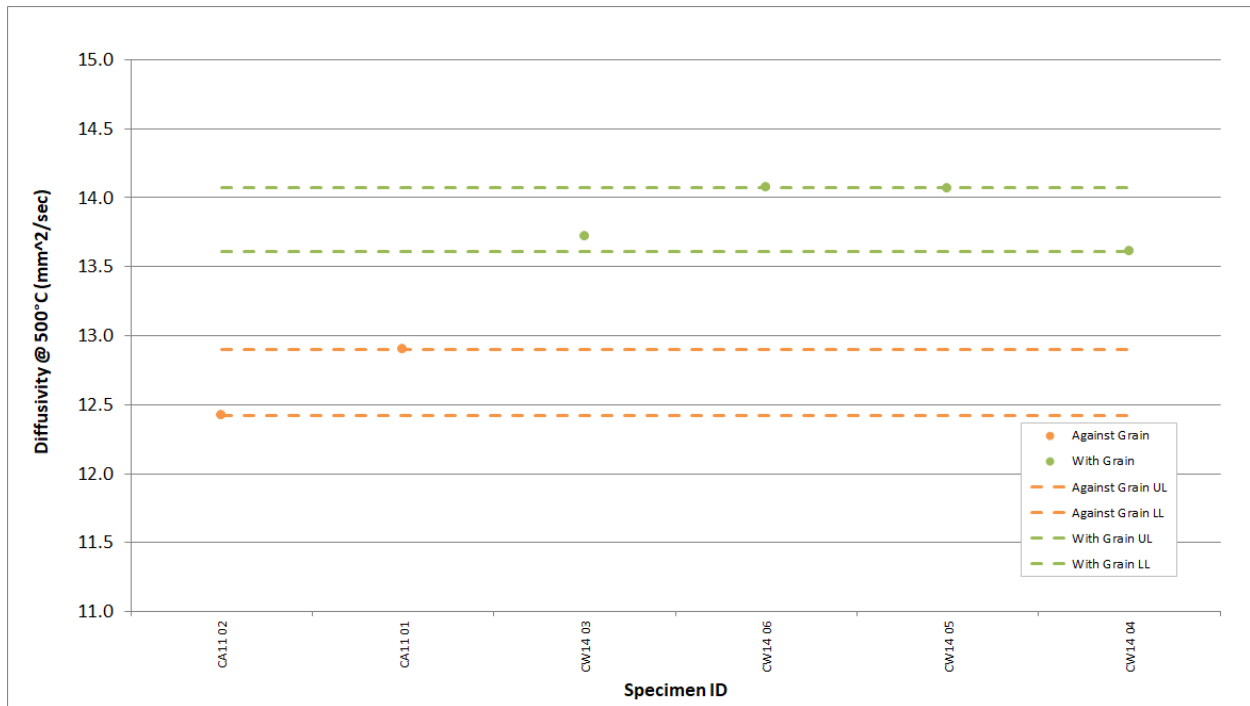


Figure A-148. H-451 Piggyback Diffusivity @ 500°C.

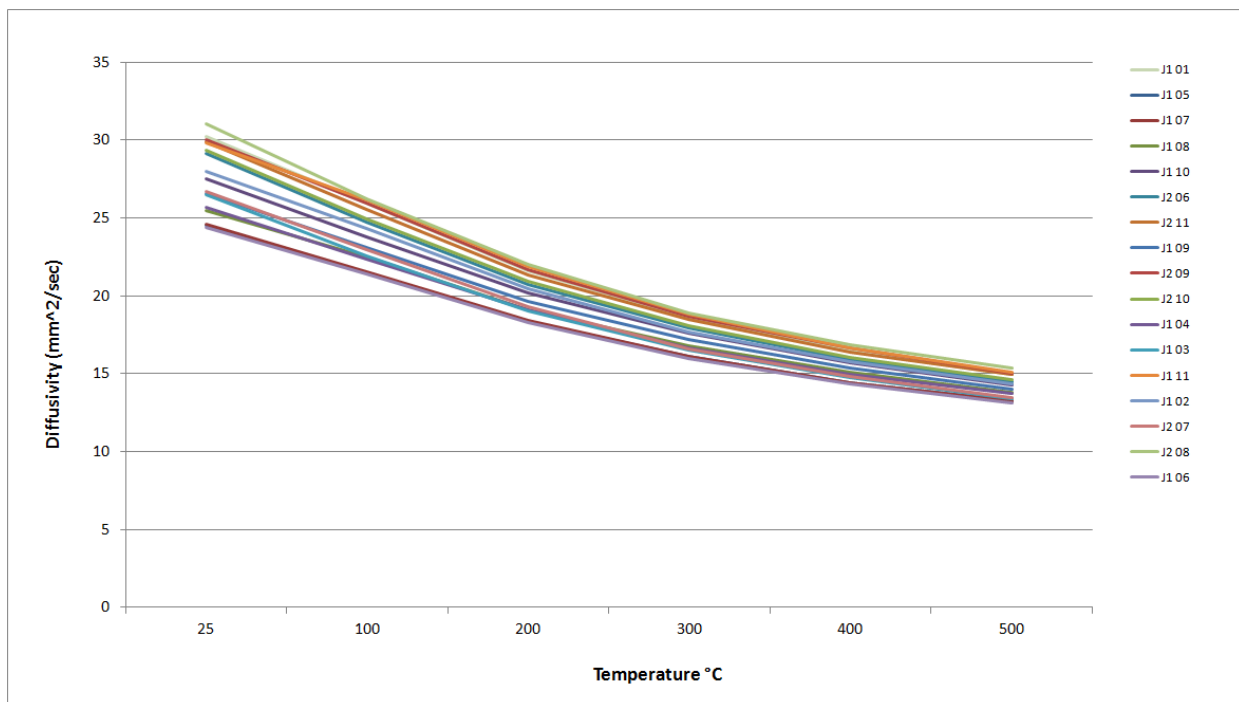


Figure A-149. HLM Piggyback Diffusivity.

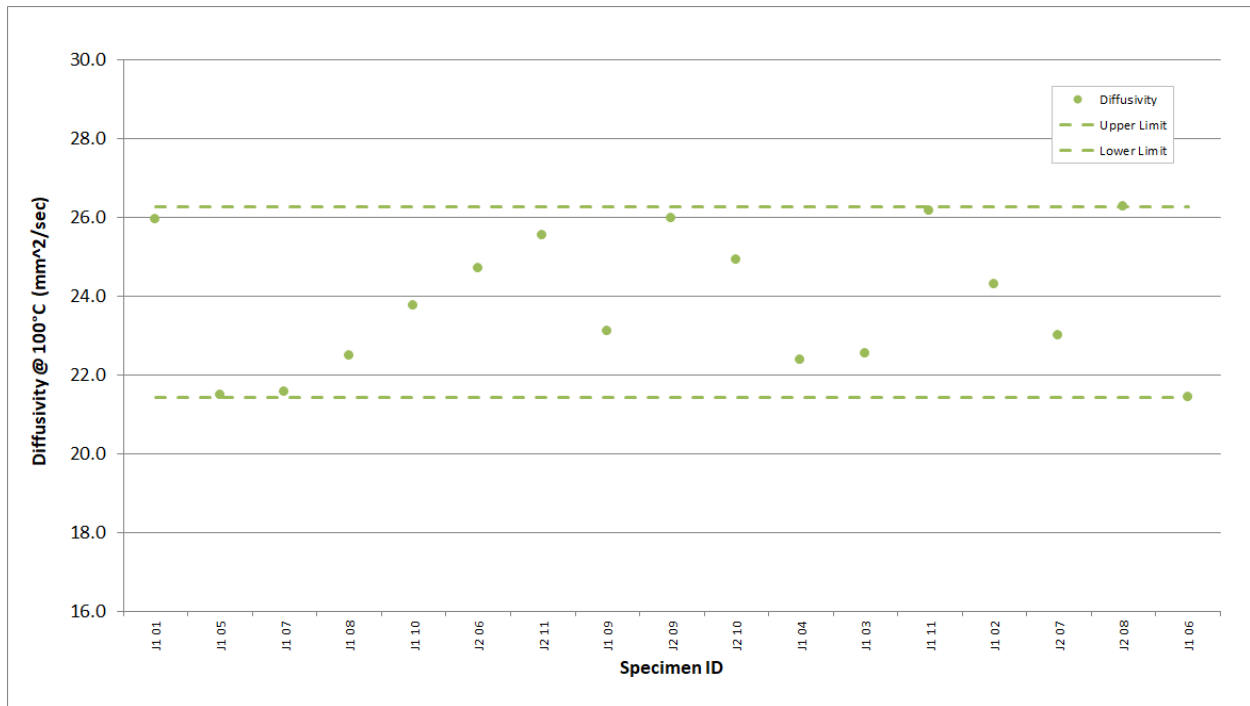


Figure A-150. HLM Piggyback Diffusivity @ 100°C.

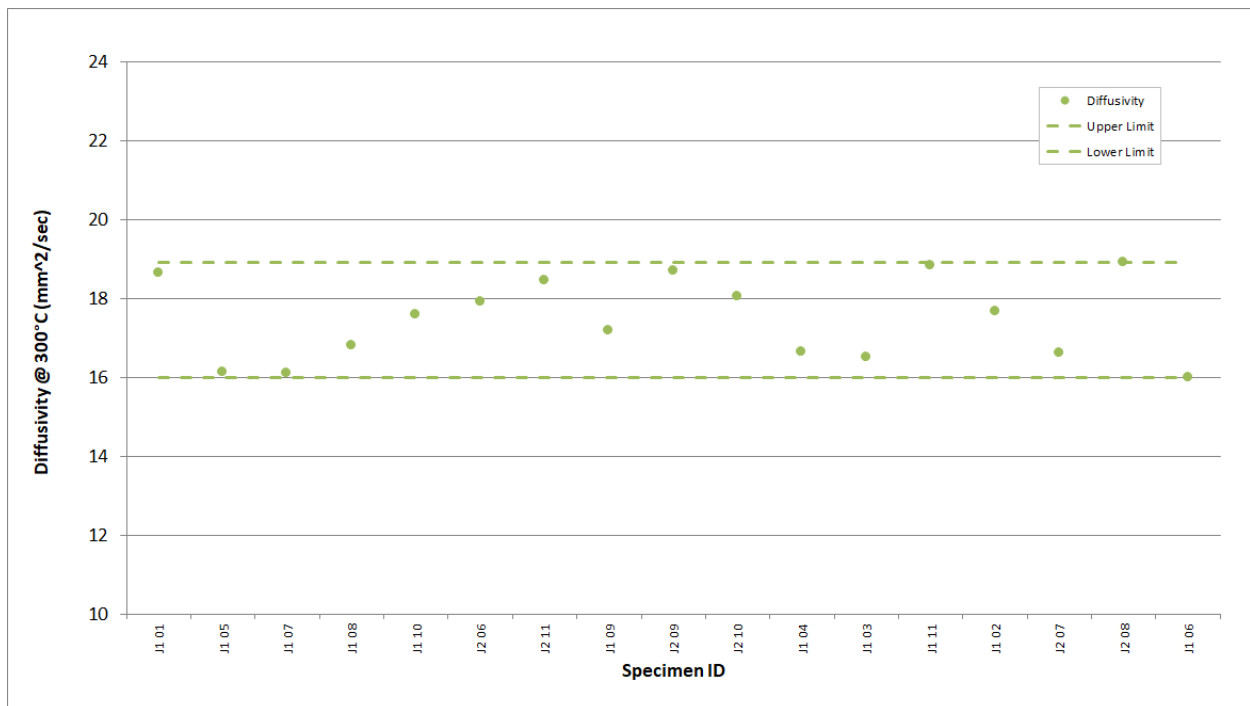


Figure A-151. HLM Piggyback Diffusivity @ 300°C.

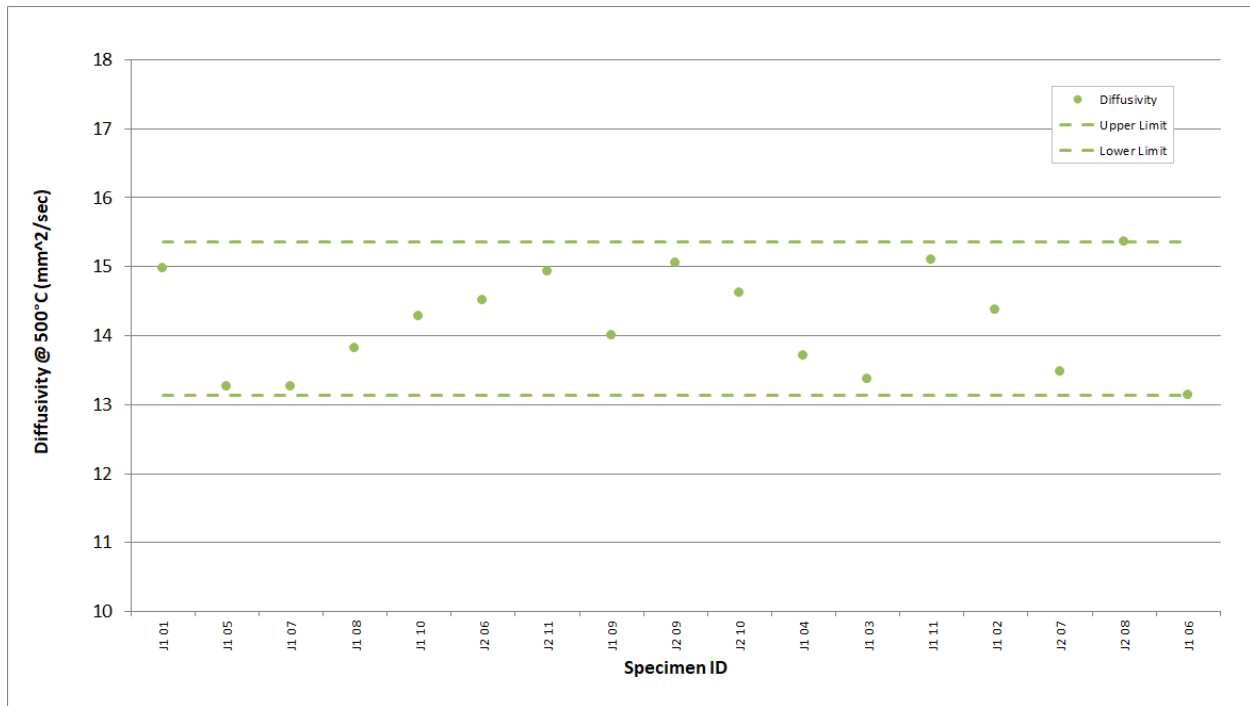


Figure A-152. HLM Piggyback Diffusivity @ 500°C.

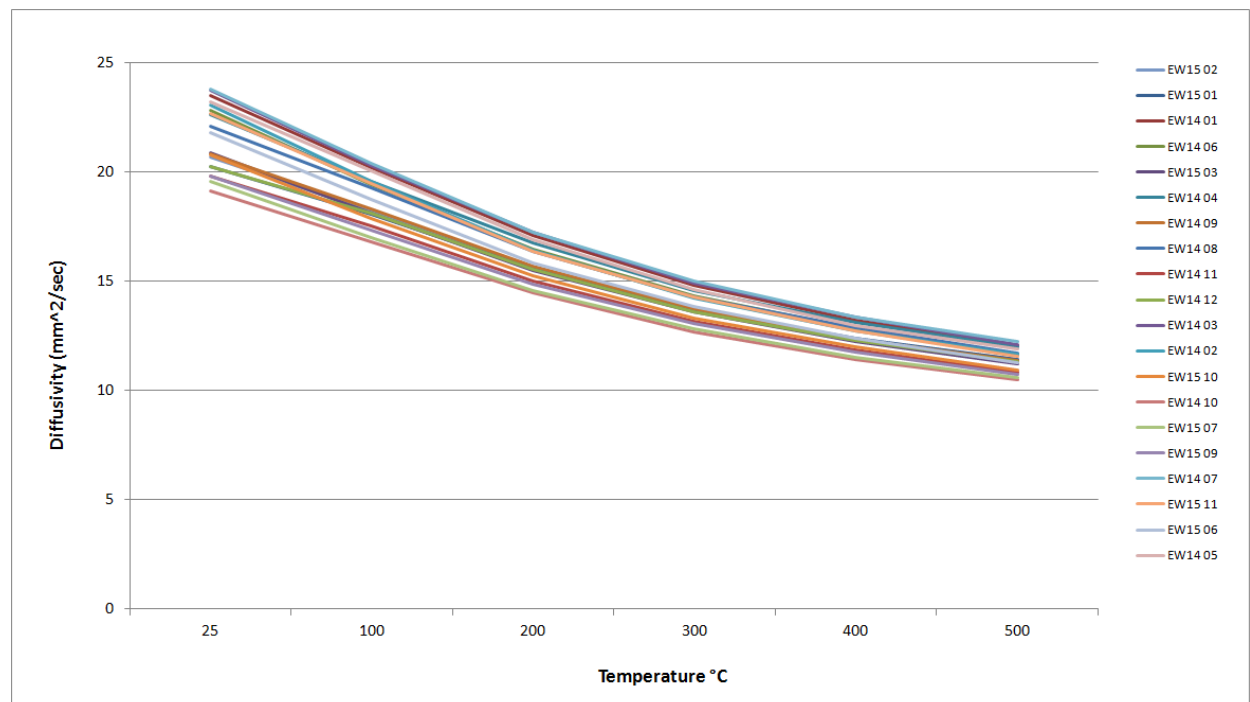


Figure A-153. IG-110 Piggyback Diffusivity.

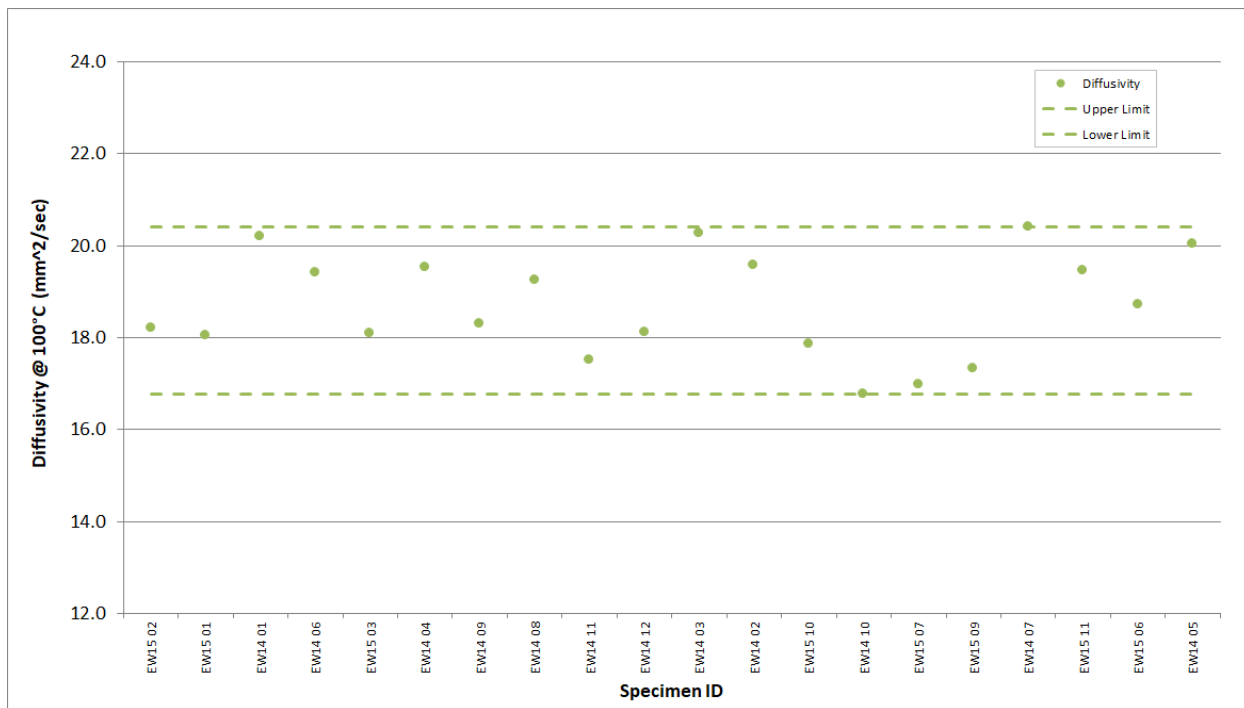


Figure A-154. IG-110 Piggyback Diffusivity @ 100°C.

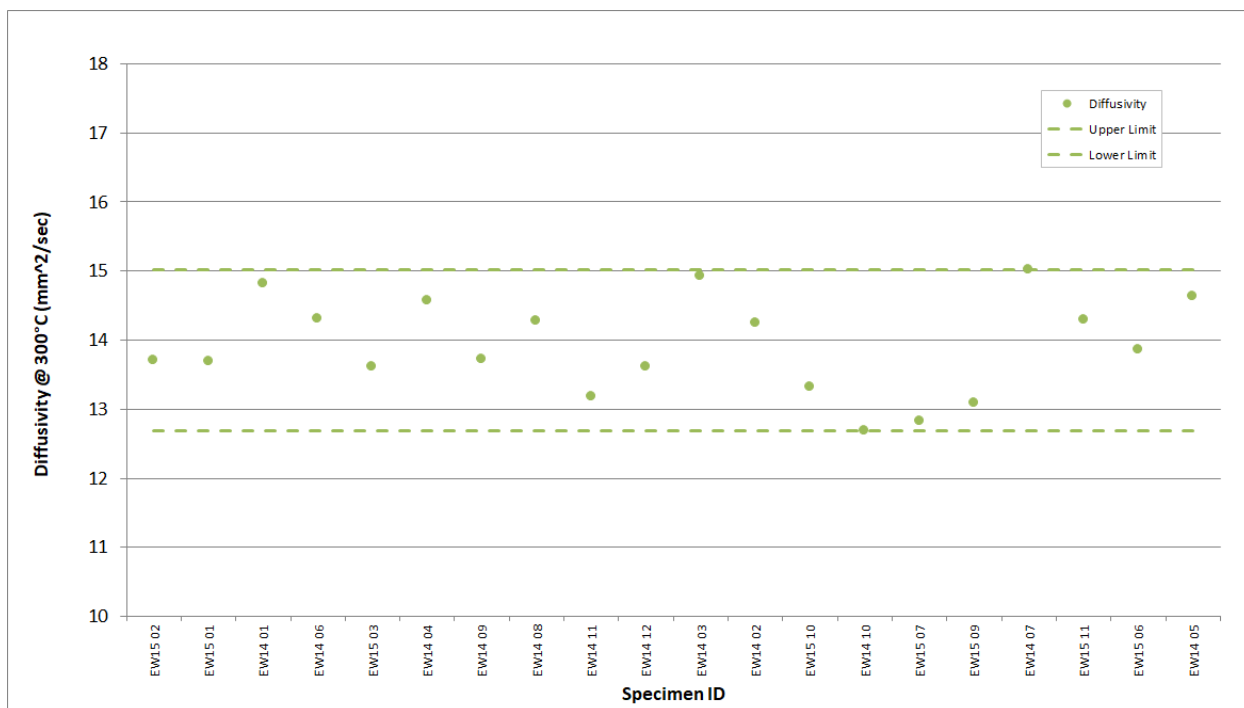


Figure A-155. IG-110 Piggyback Diffusivity @ 300°C.

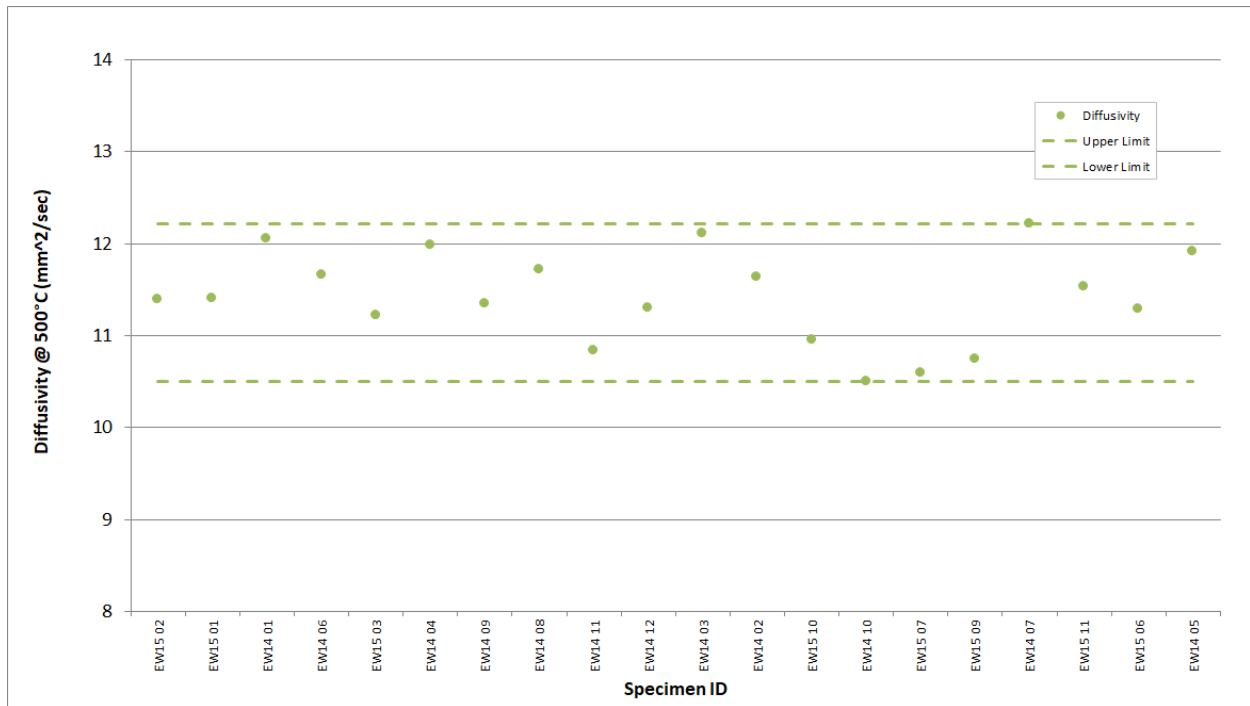


Figure A-156. IG-110 Piggyback Diffusivity @ 500°C.

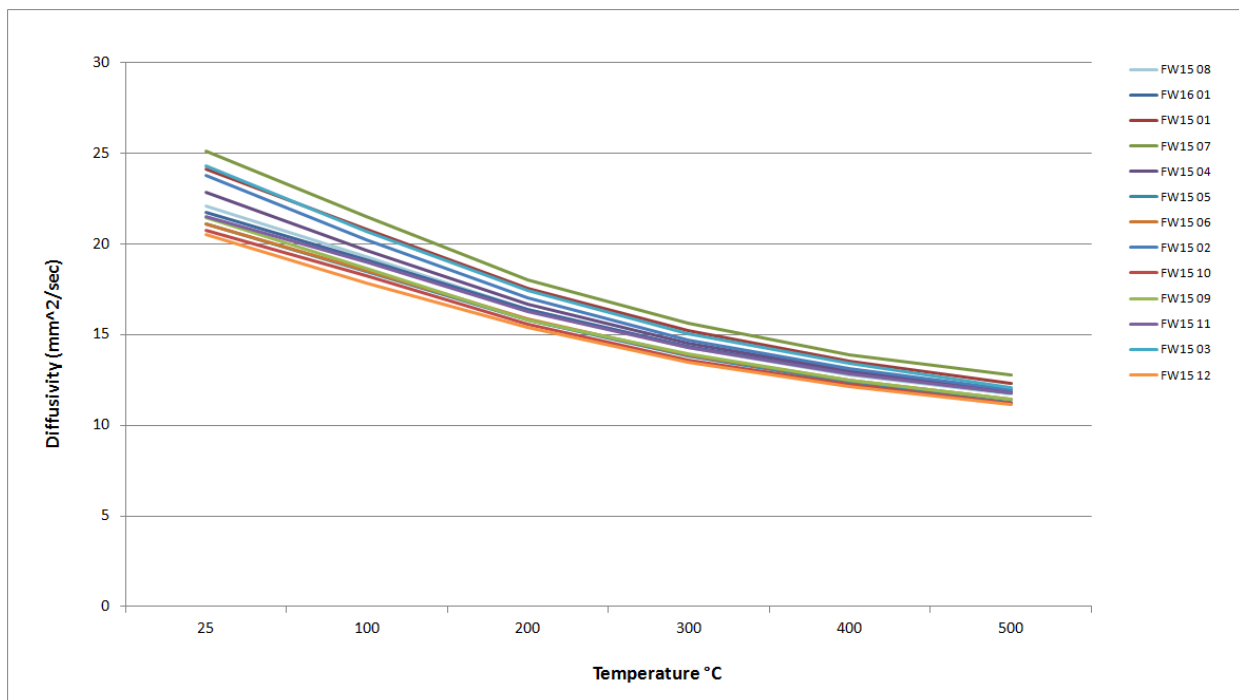


Figure A-157. IG-430 Piggyback Diffusivity.

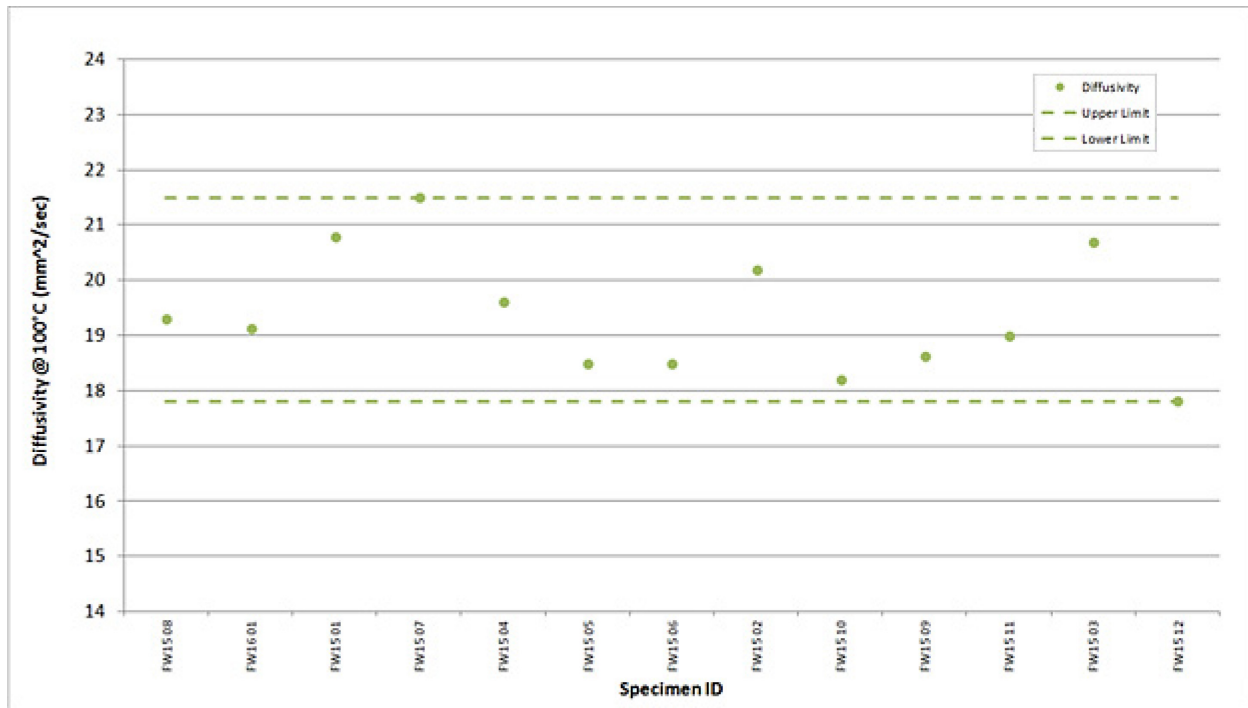


Figure A-158. IG-430 Piggyback Diffusivity @ 100°C.

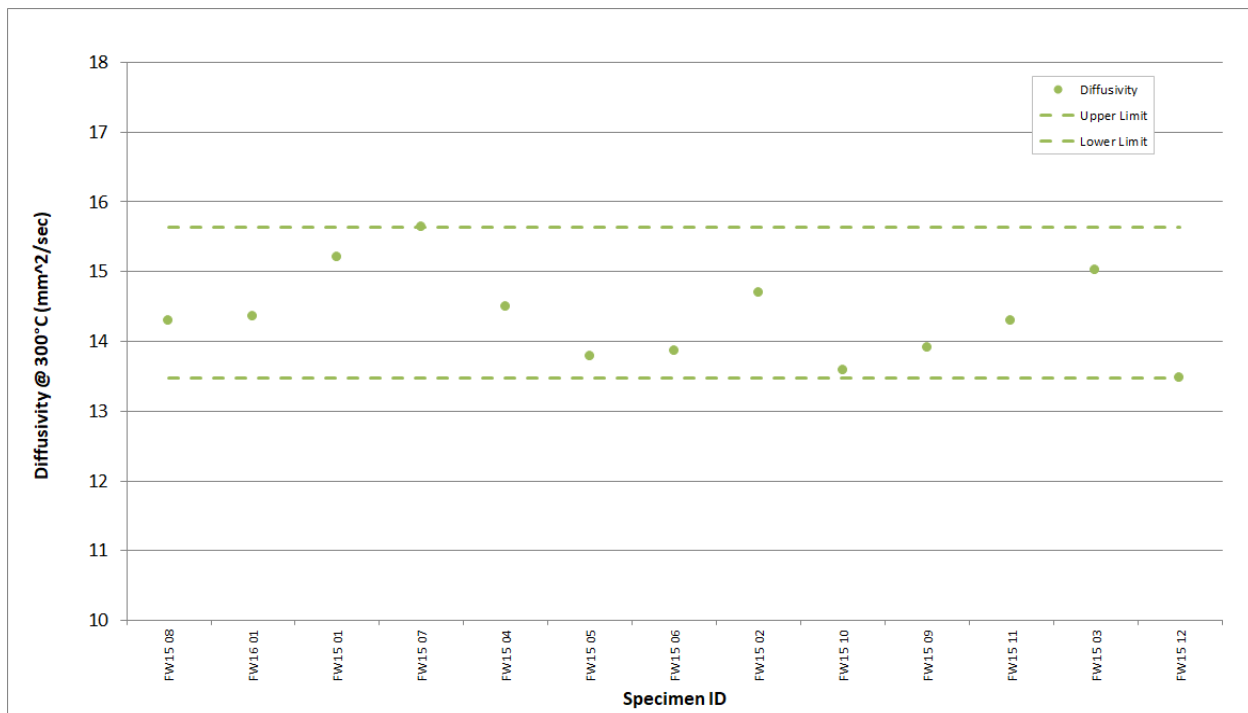


Figure A-159. IG-430 Piggyback Diffusivity @ 300°C.

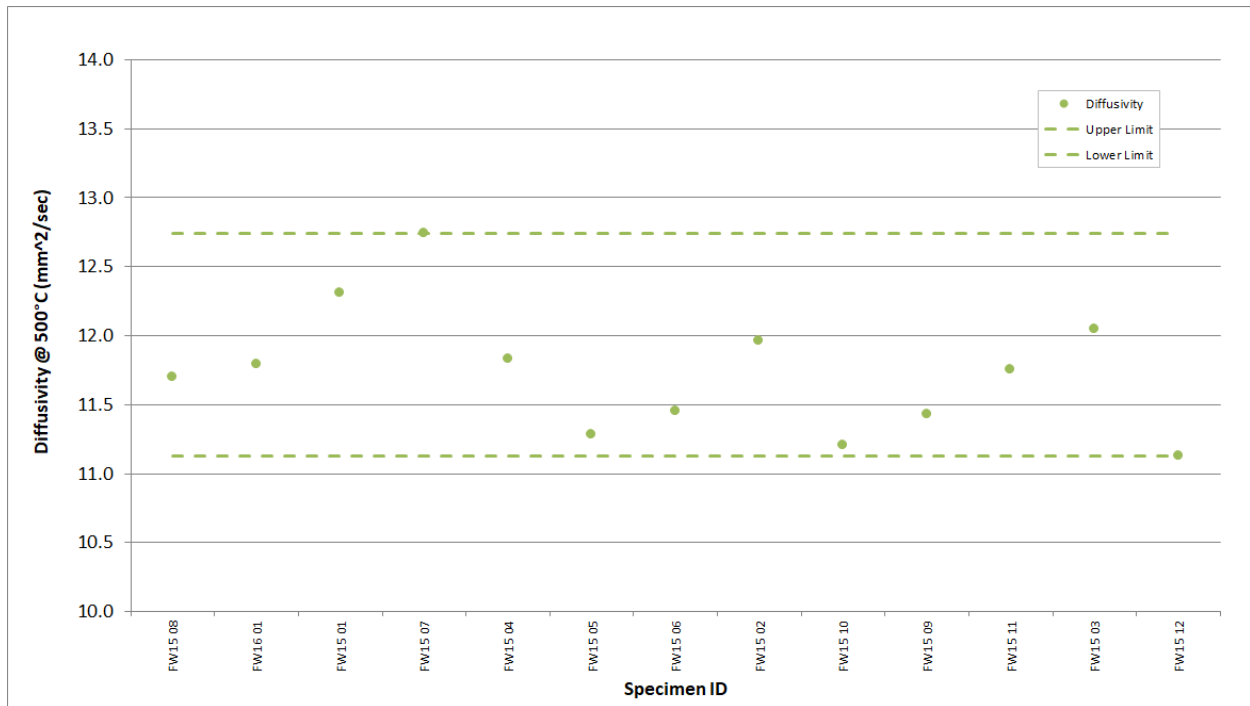


Figure A-160. IG-430 Piggyback Diffusivity @ 500°C.

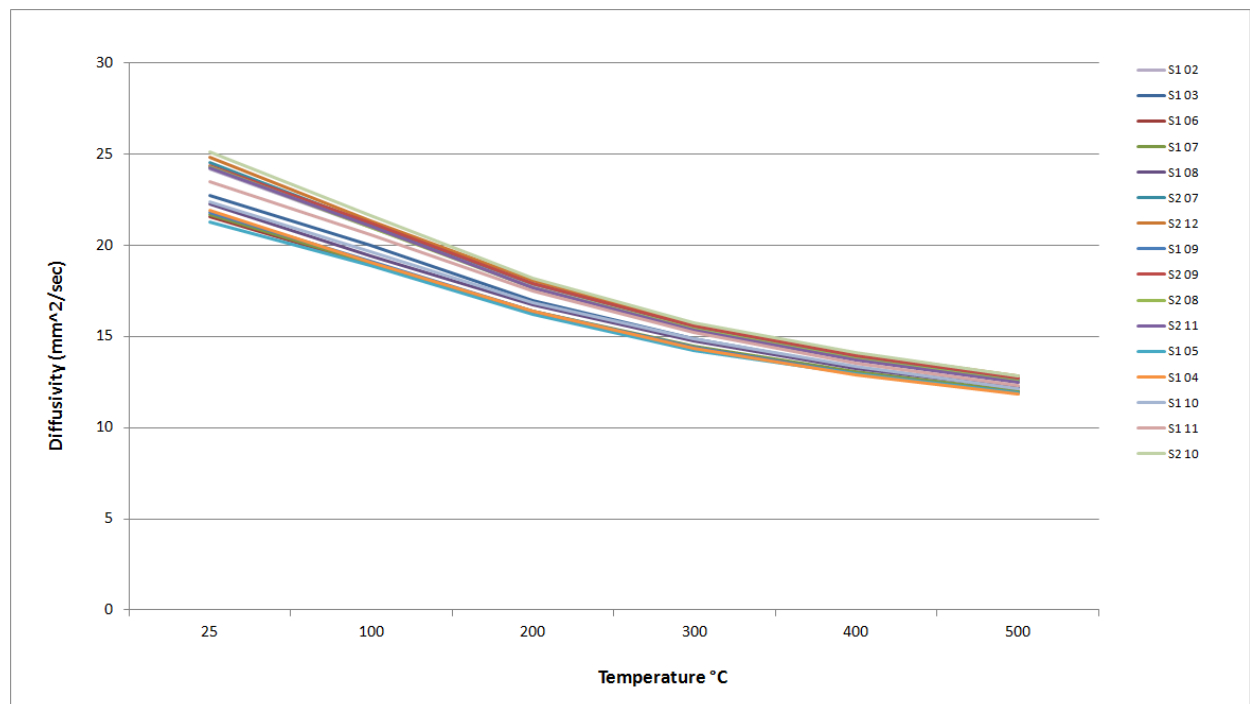


Figure A-161. NBG-10 Piggyback Diffusivity.

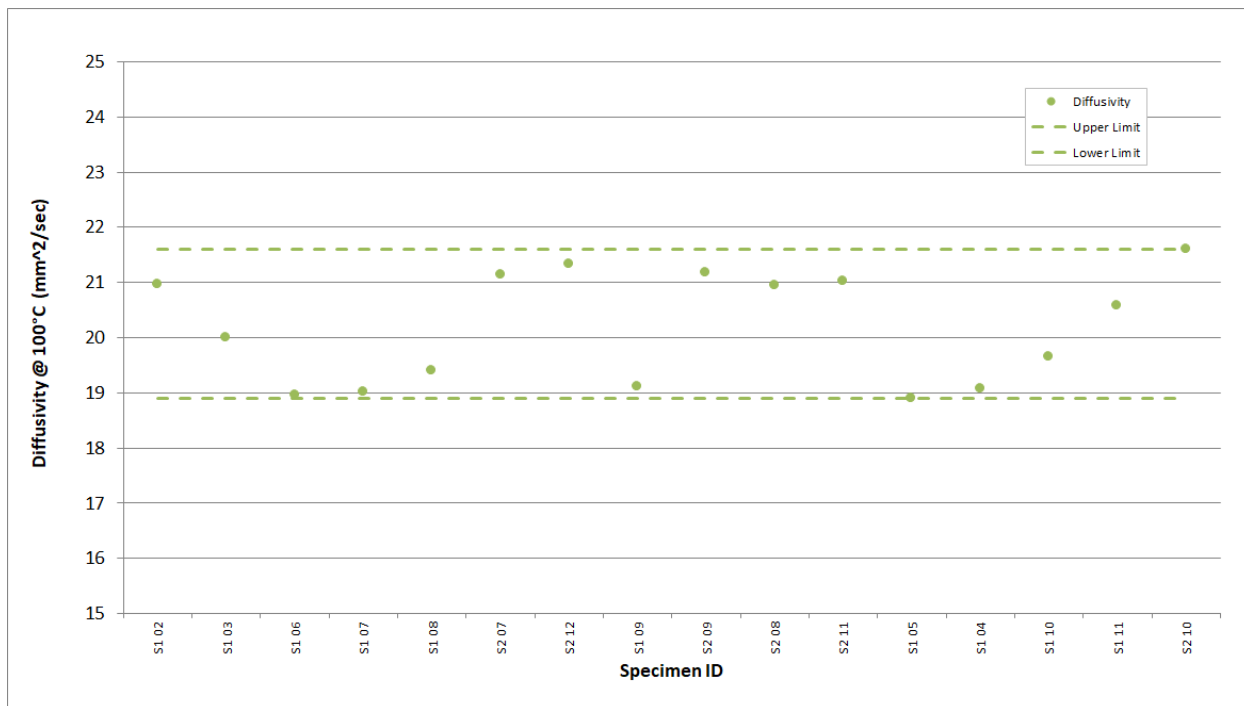


Figure A-162. NBG-10 Piggyback Diffusivity @ 100°C.

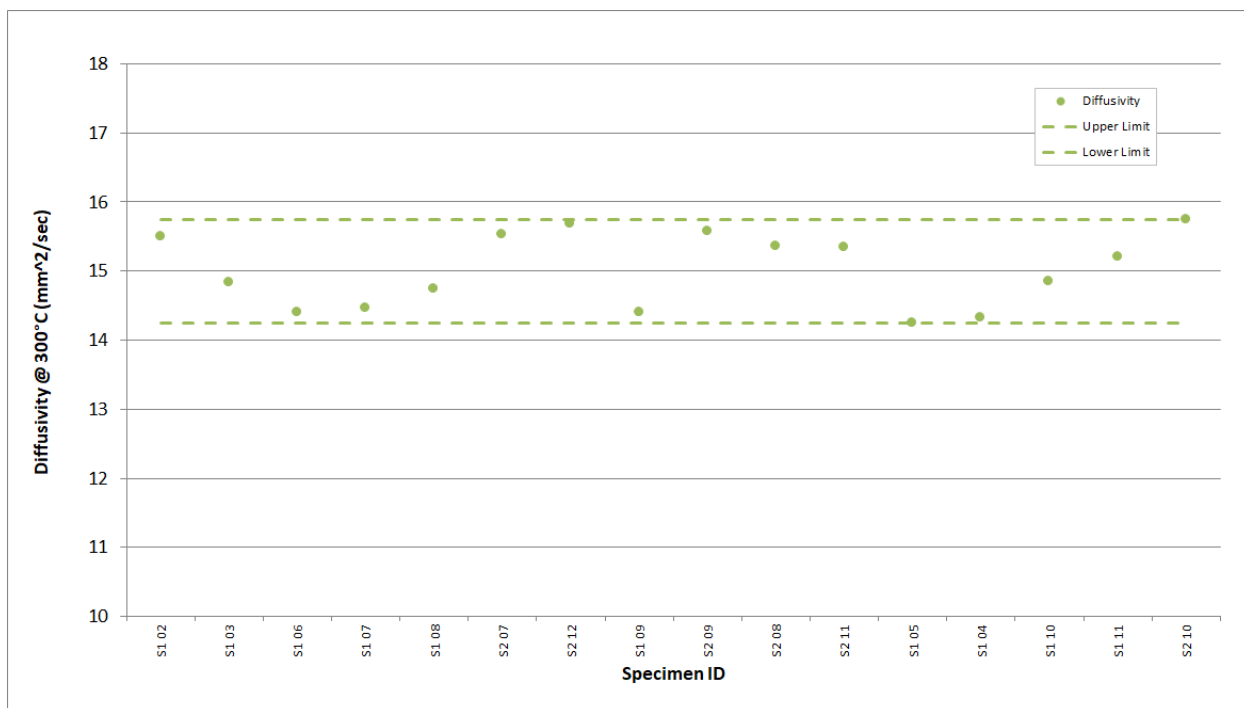


Figure A-163. NBG-10 Piggyback Diffusivity @ 300°C.

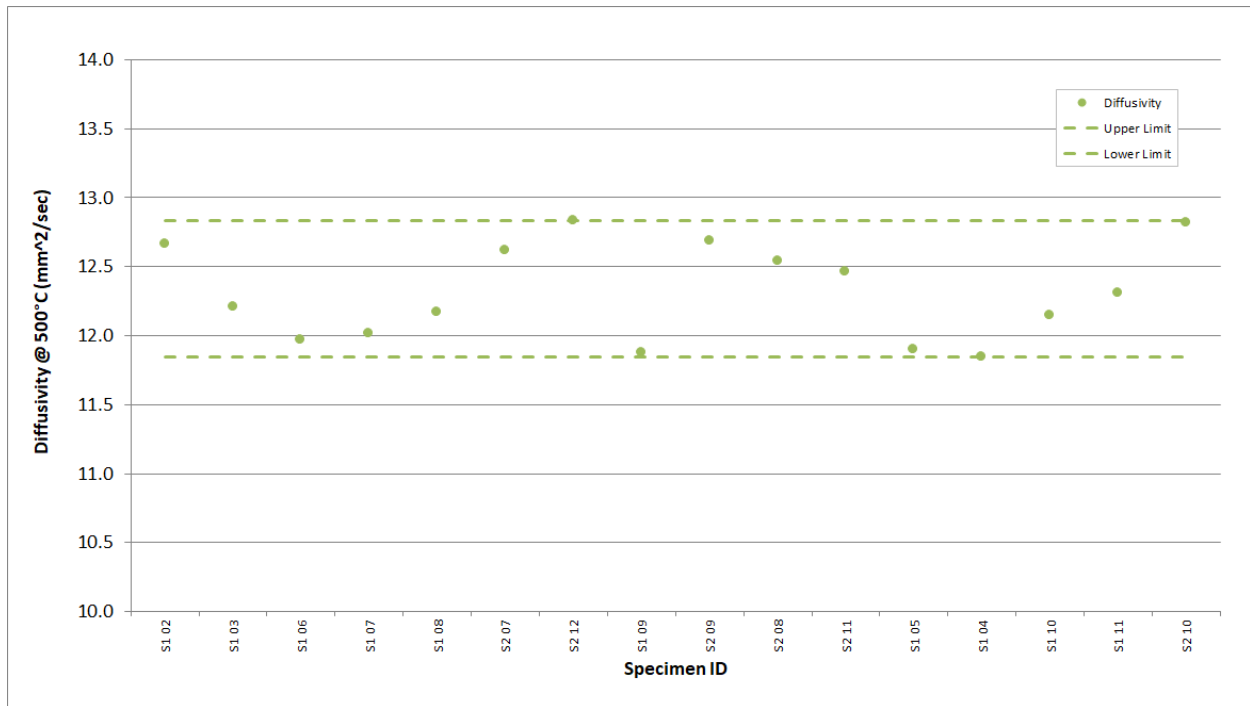


Figure A-164. NBG-10 Piggyback Diffusivity @ 500°C.

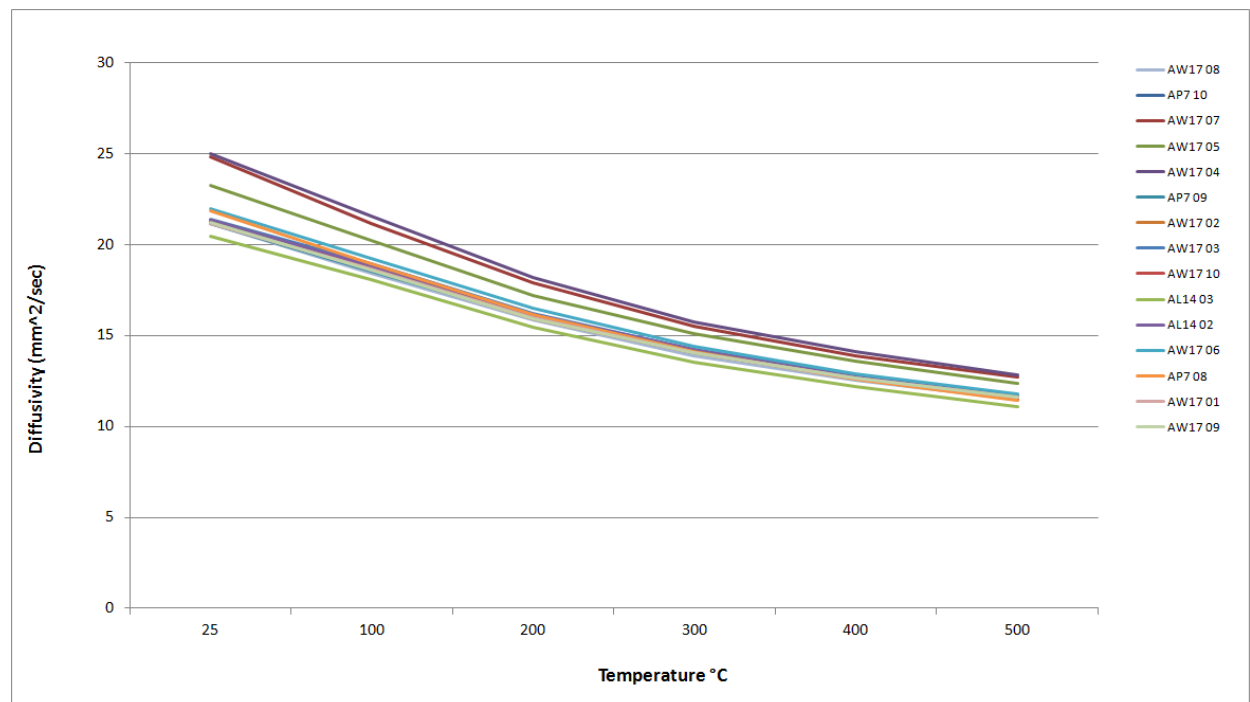


Figure A-165. NBG-17 Piggyback Diffusivity.

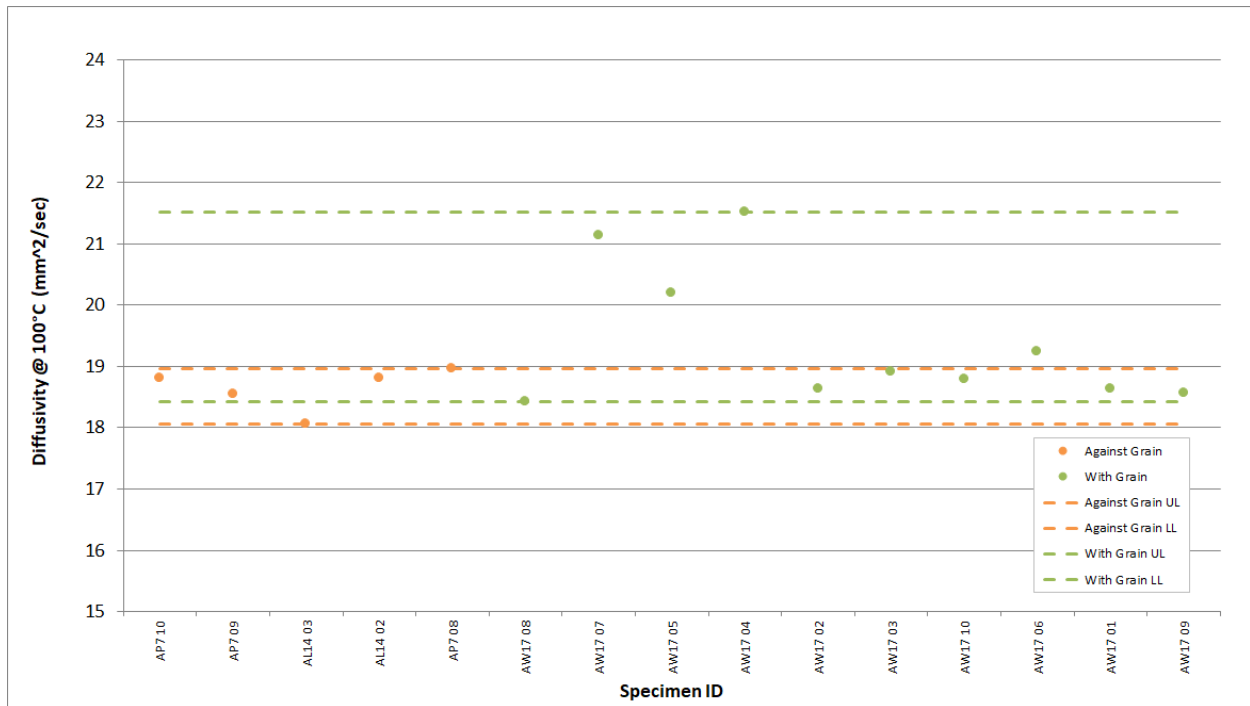


Figure A-166. NBG-17 Piggyback Diffusivity @ 100°C.

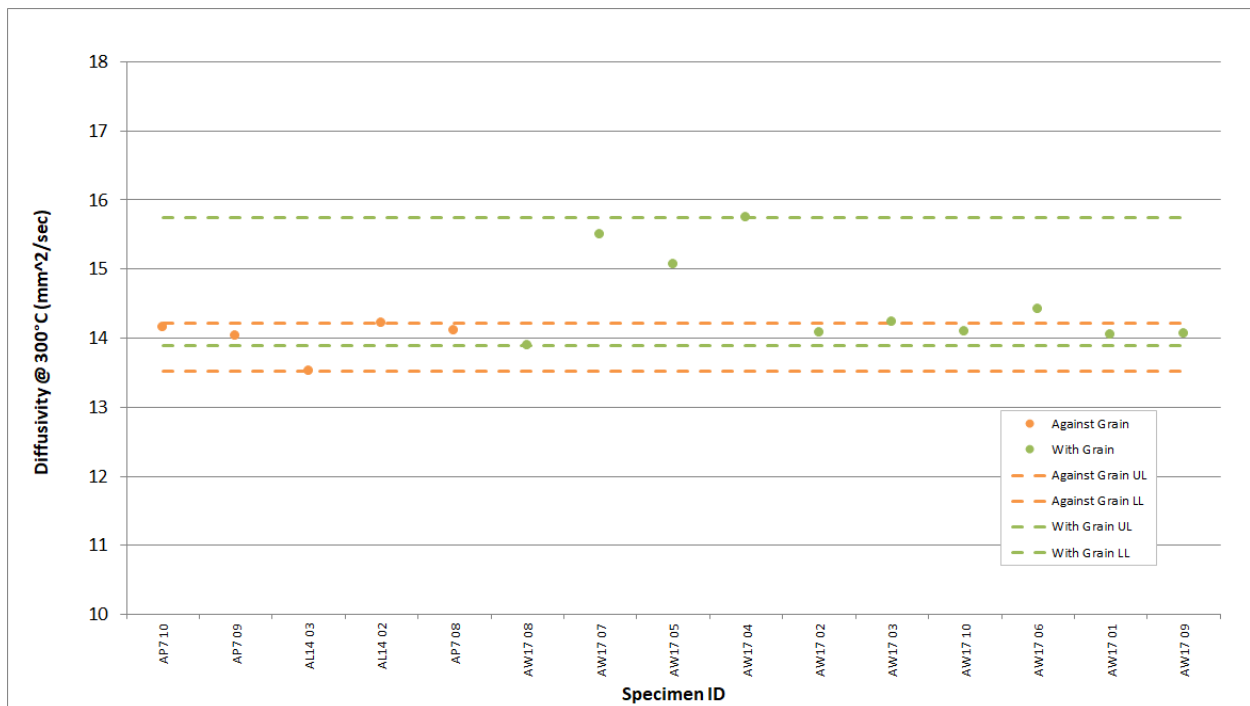


Figure A-167. NBG-17 Piggyback Diffusivity @ 300°C.

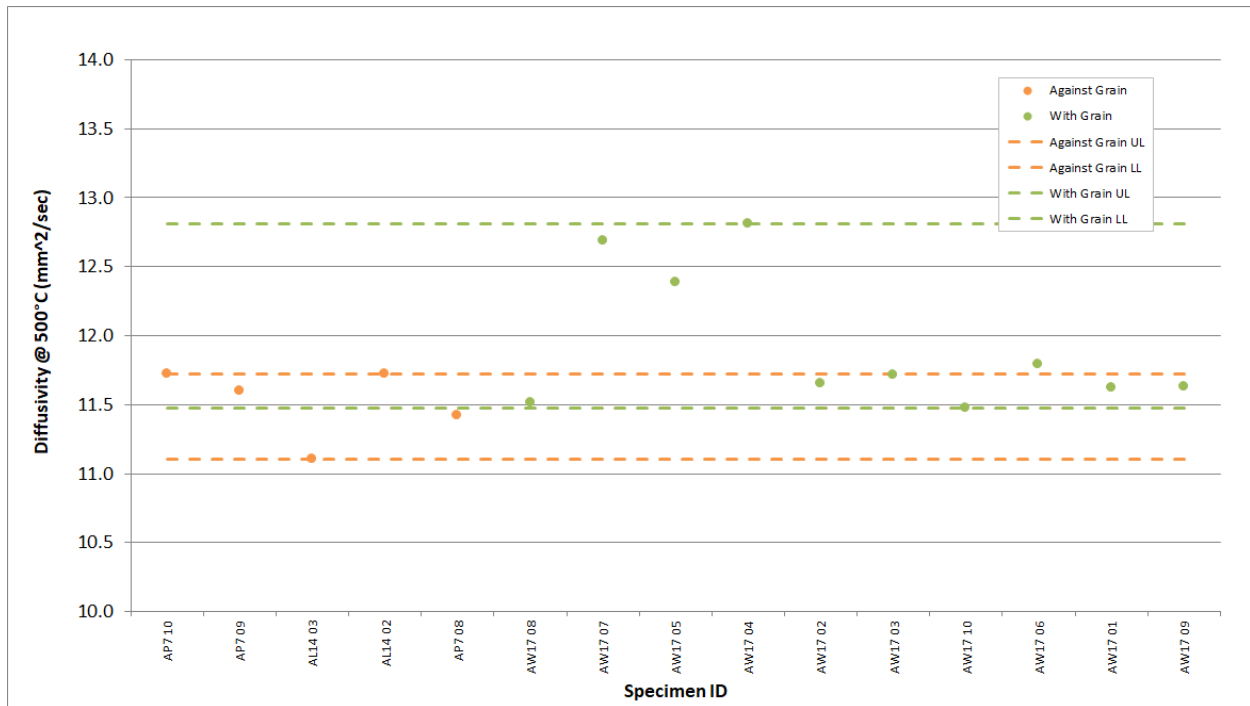


Figure A-168. NBG-17 Piggyback Diffusivity @ 500°C.

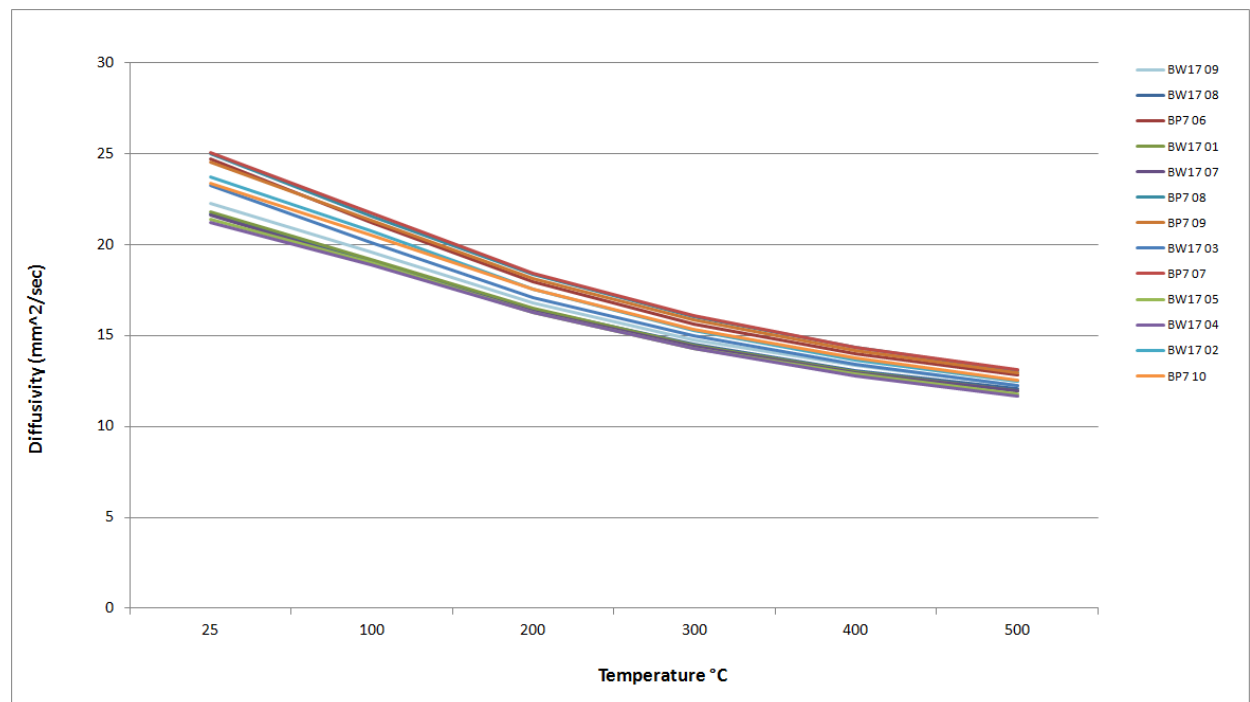


Figure A-169. NBG-18 Piggyback Diffusivity.

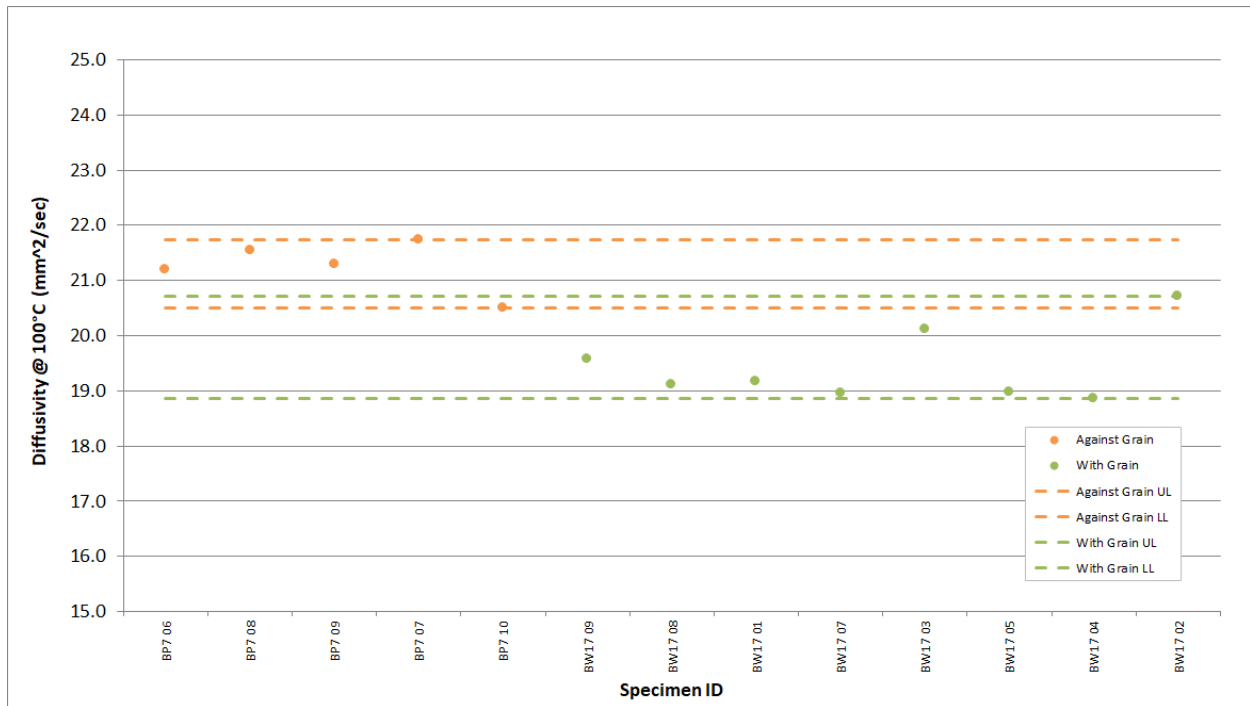


Figure A-170. NBG-18 Piggyback Diffusivity @ 100°C.

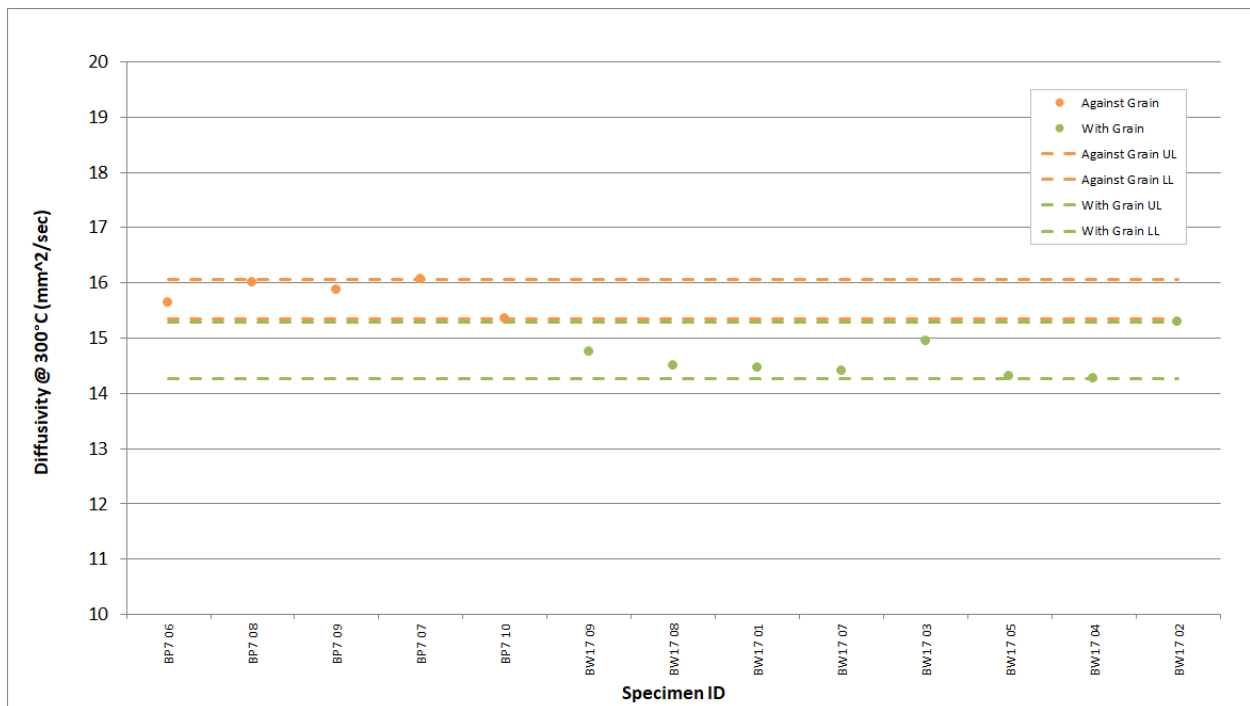


Figure A-171. NBG-18 Piggyback Diffusivity @ 300°C.

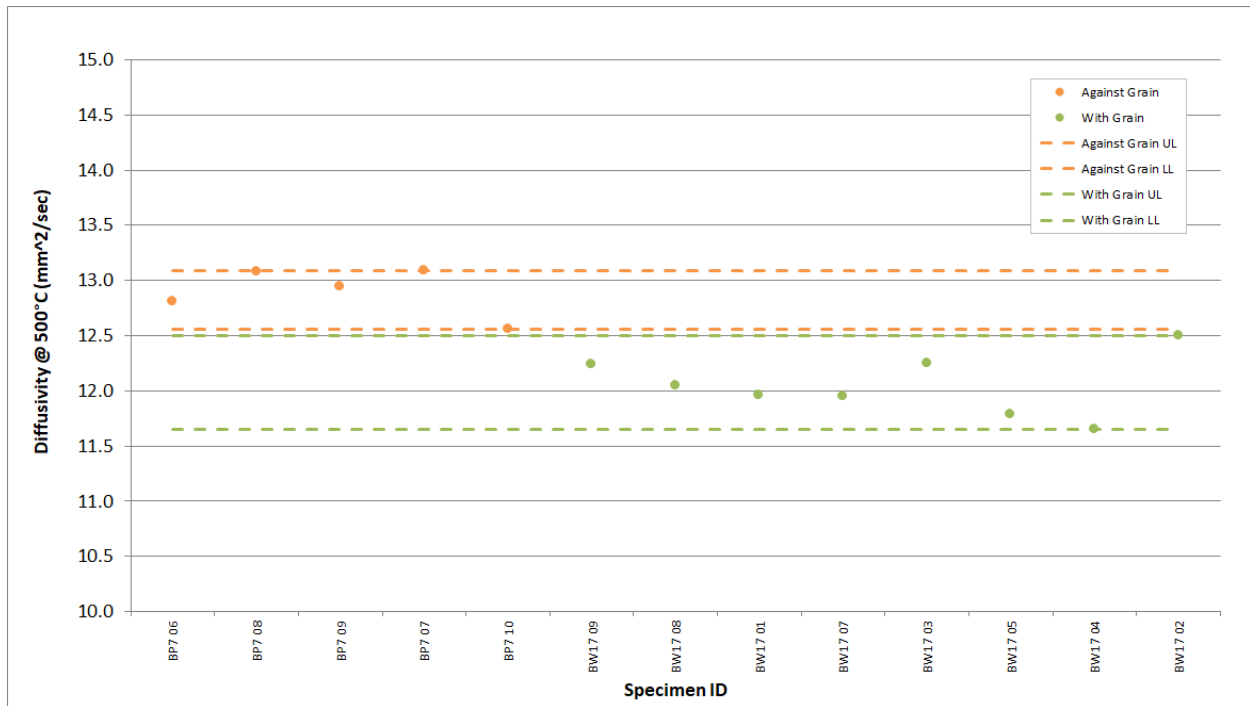


Figure A-172. NBG-18 Piggyback Diffusivity @ 500°C.

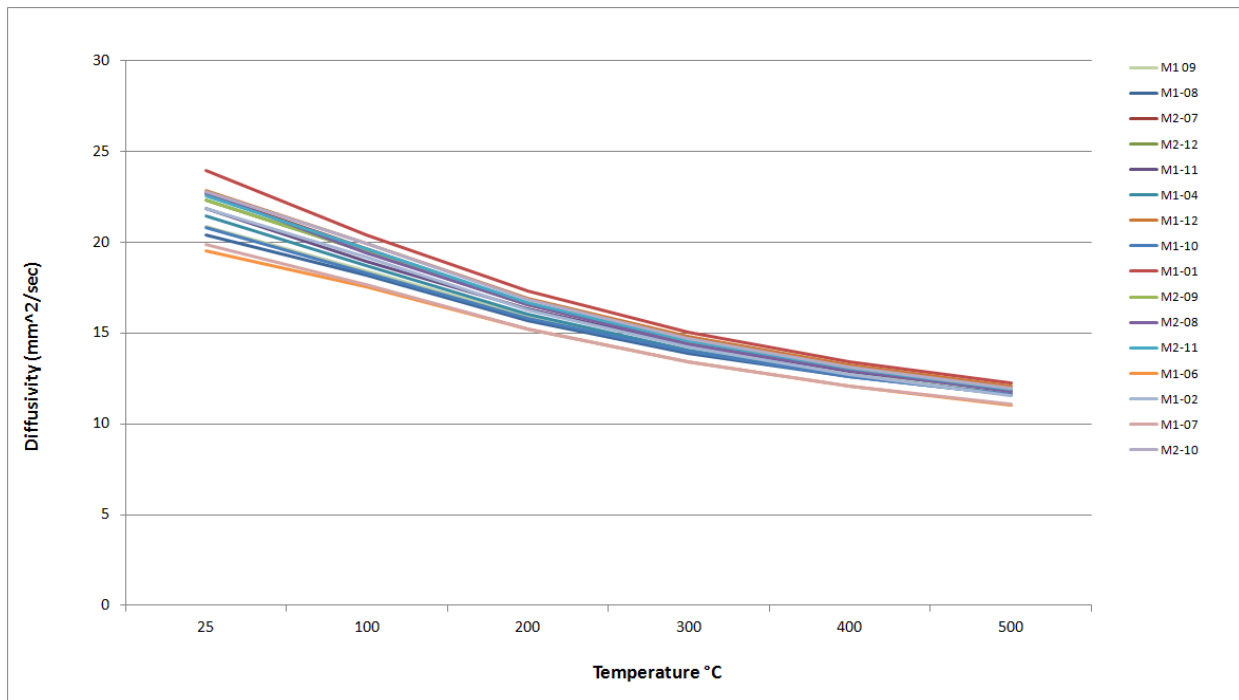


Figure A-173. NBG-25 Piggyback Diffusivity.

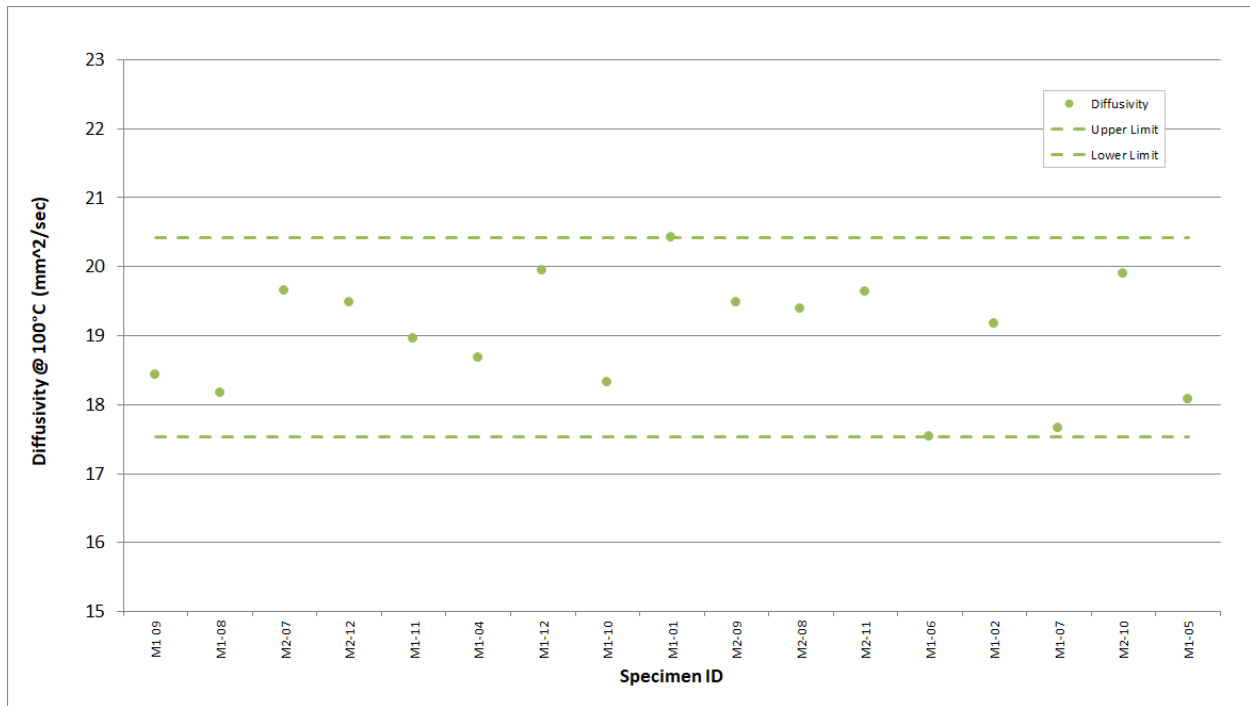


Figure A-174. NBG-25 Piggyback Diffusivity @ 100°C.

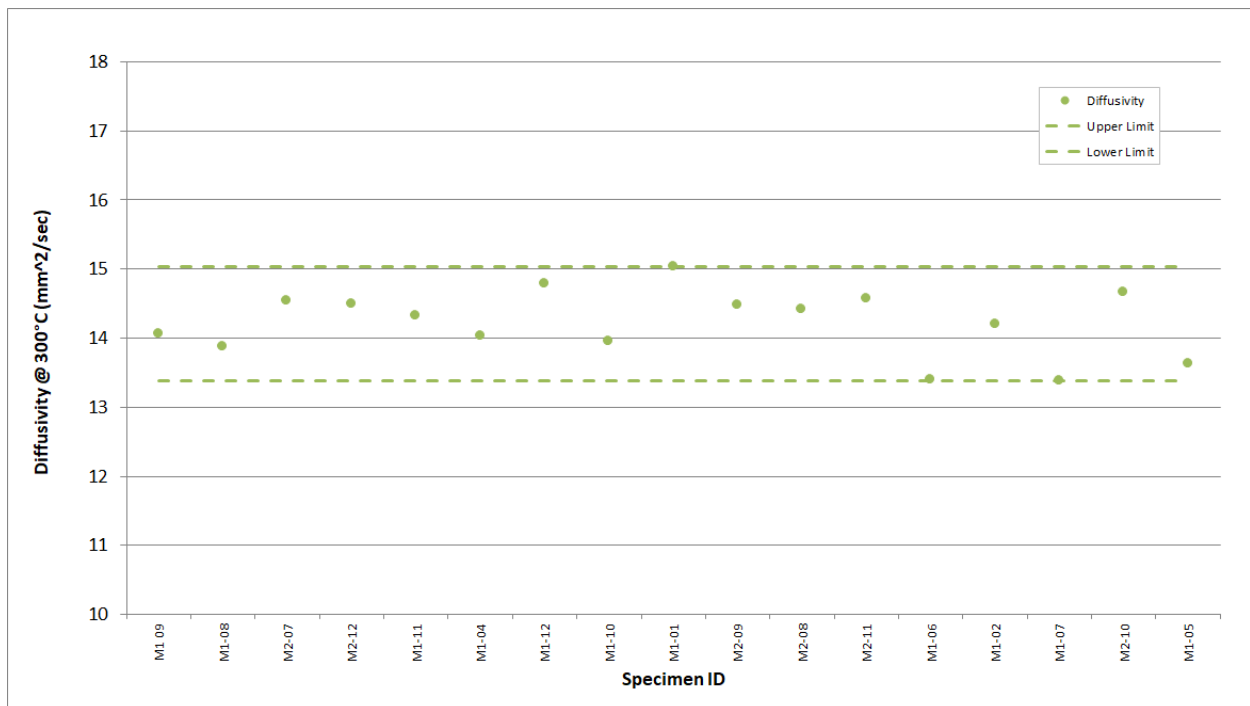


Figure A-175. NBG-25 Piggyback Diffusivity @ 300°C.

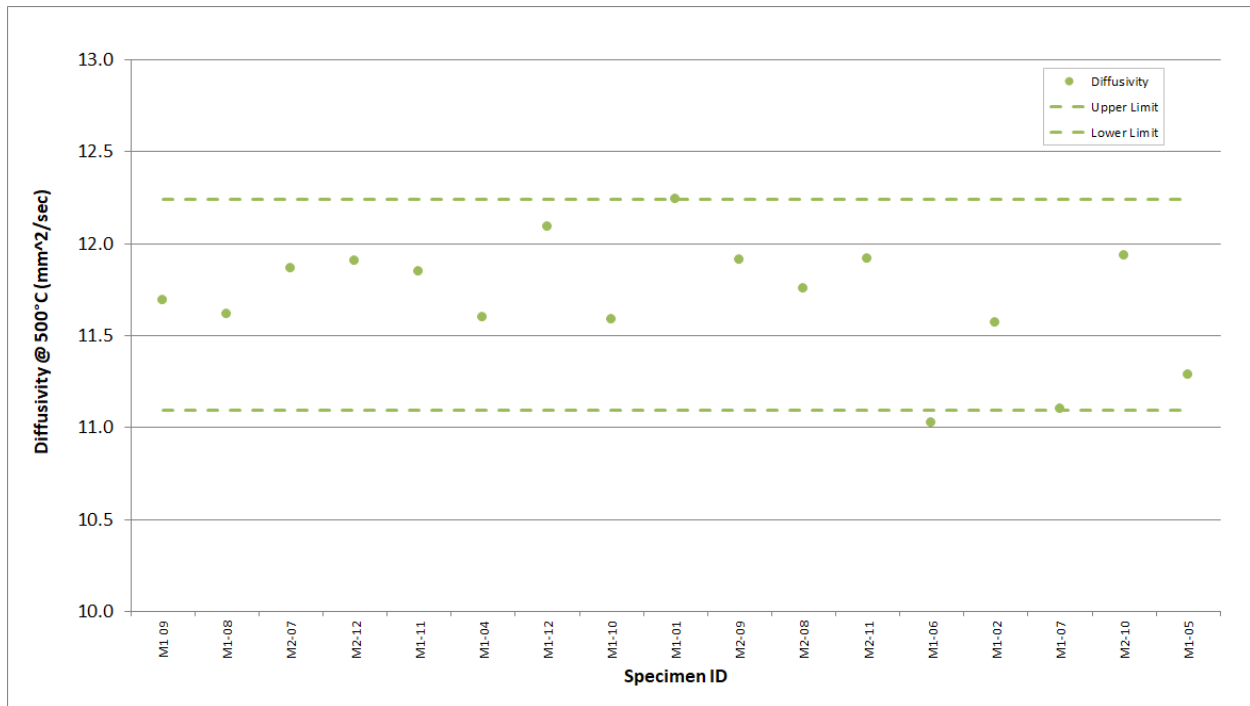


Figure A-176. NBG-25 Piggyback Diffusivity @ 500°C.

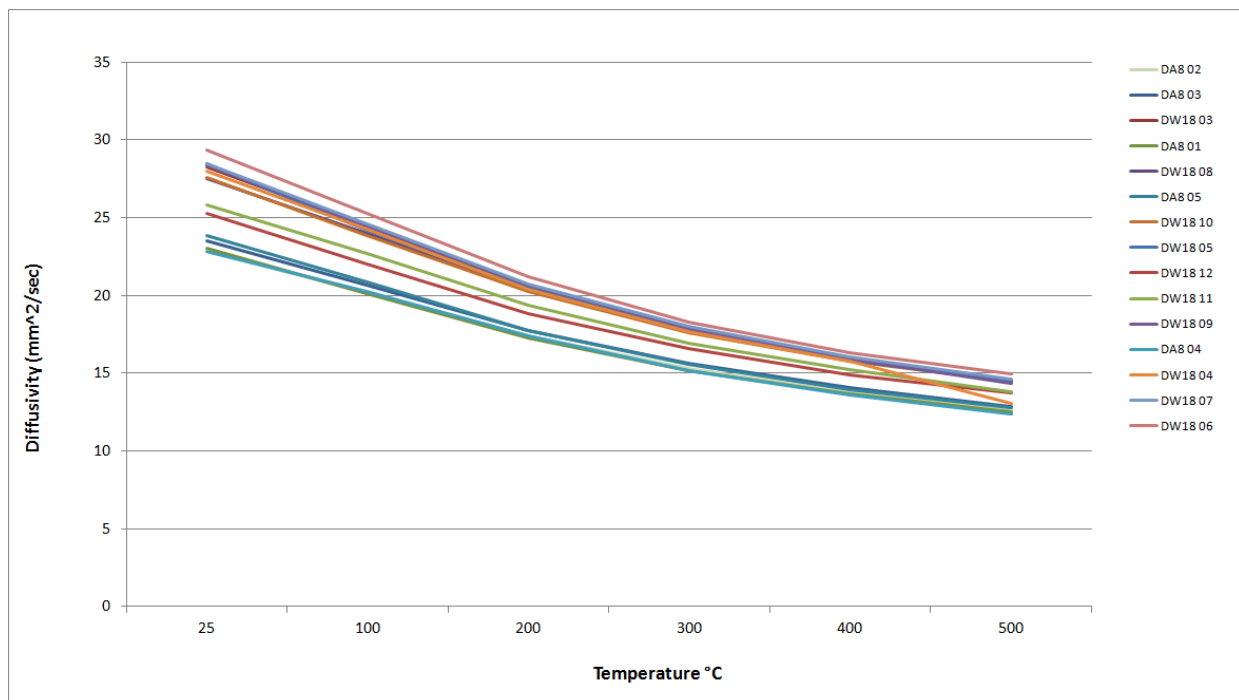


Figure A-177. PCEA Piggyback Diffusivity.

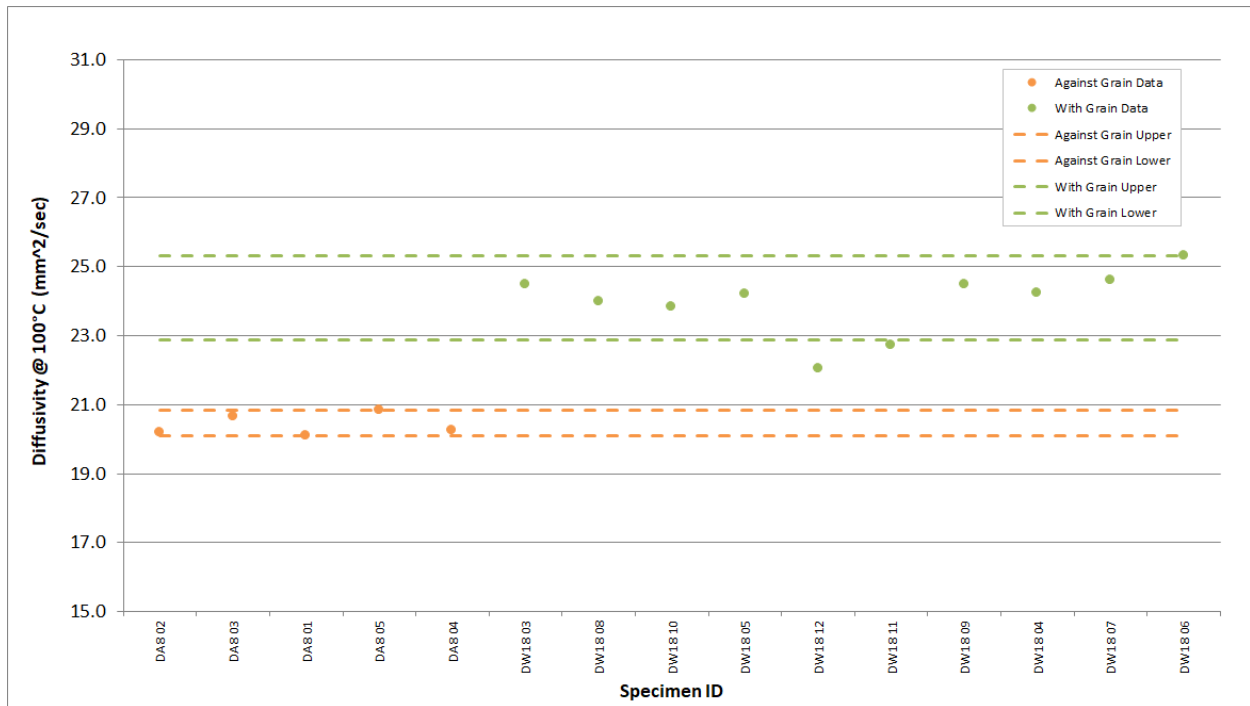


Figure A-178. PCEA Piggyback Diffusivity @ 100°C.

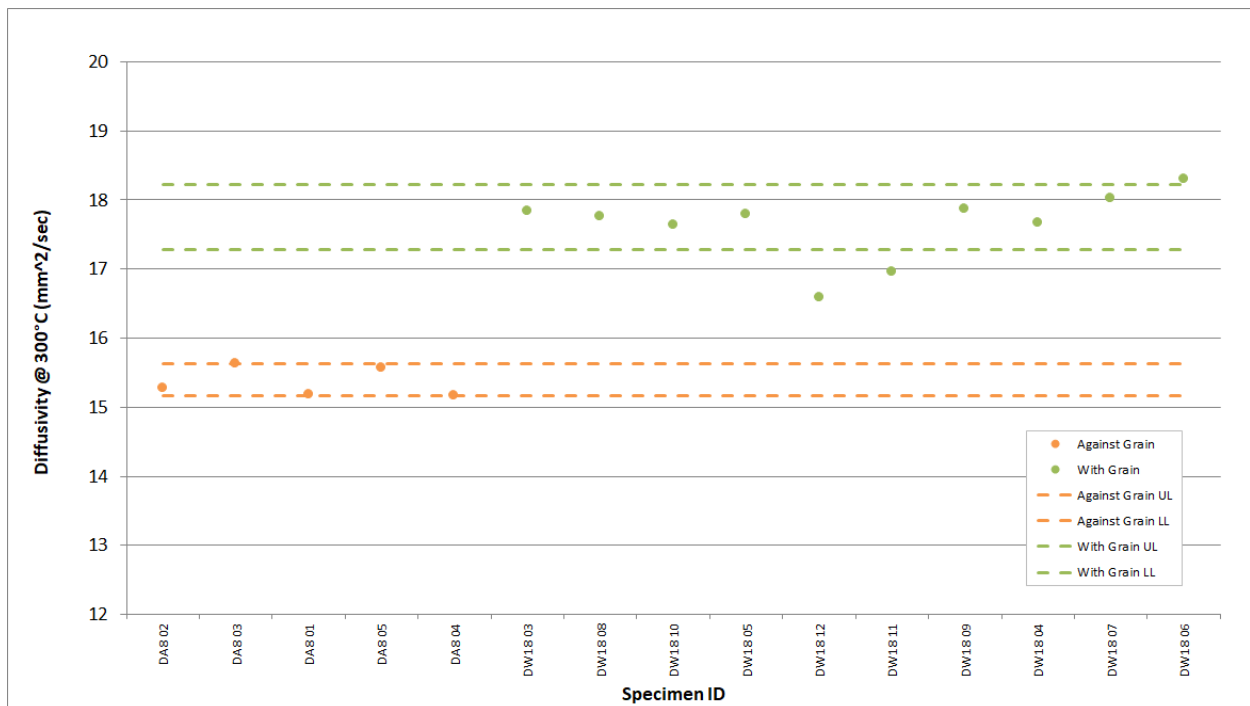


Figure A-179. PCEA Piggyback Diffusivity @ 300°C.

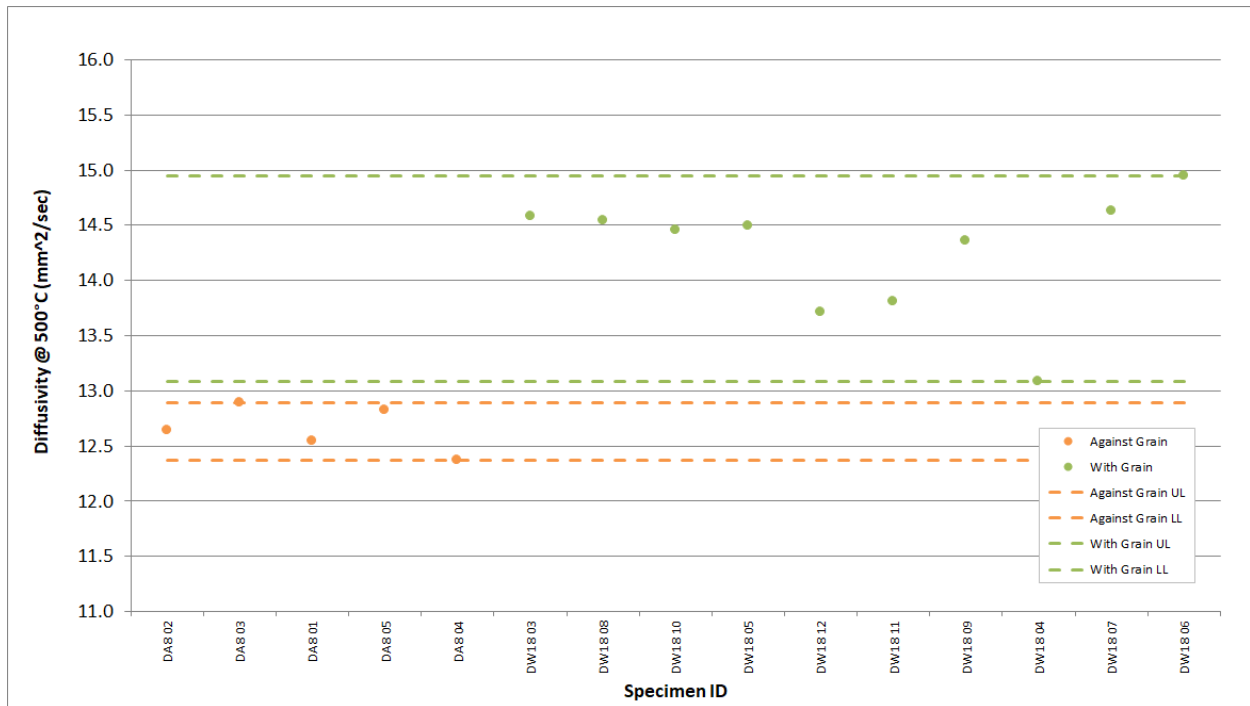


Figure A-180. PCEA Piggyback Diffusivity @ 500°C.

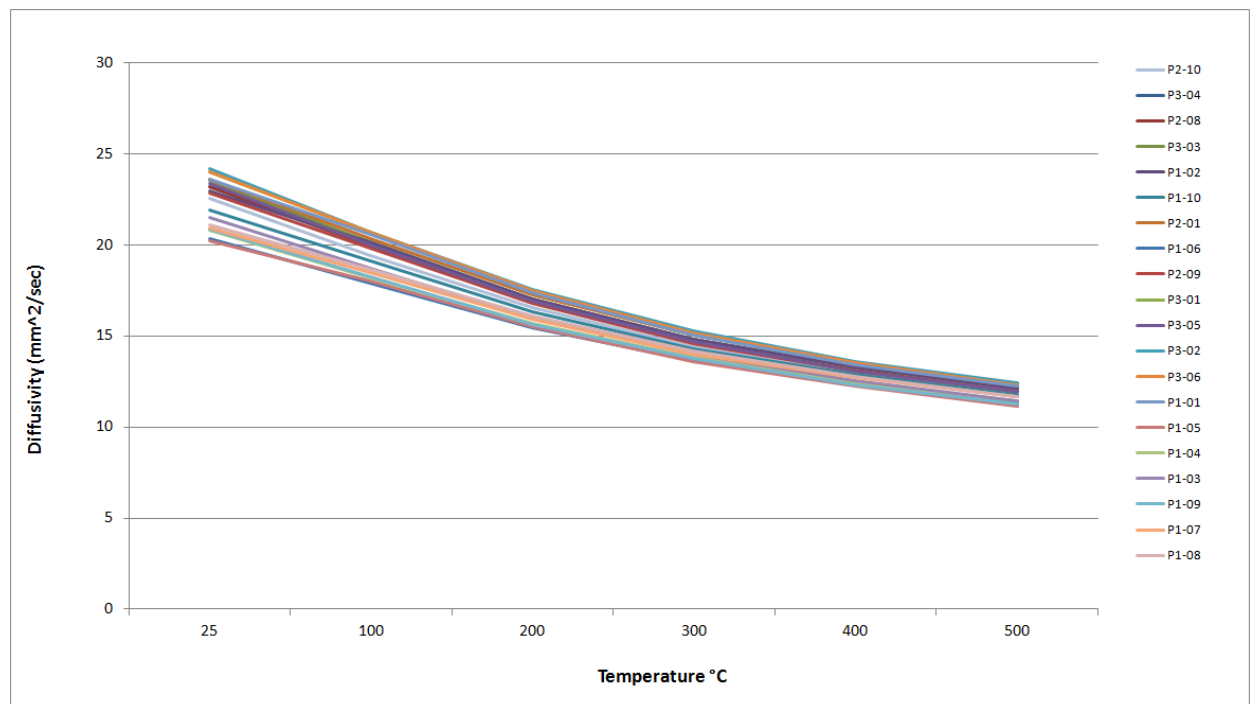


Figure A-181. PCIB Piggyback Diffusivity.

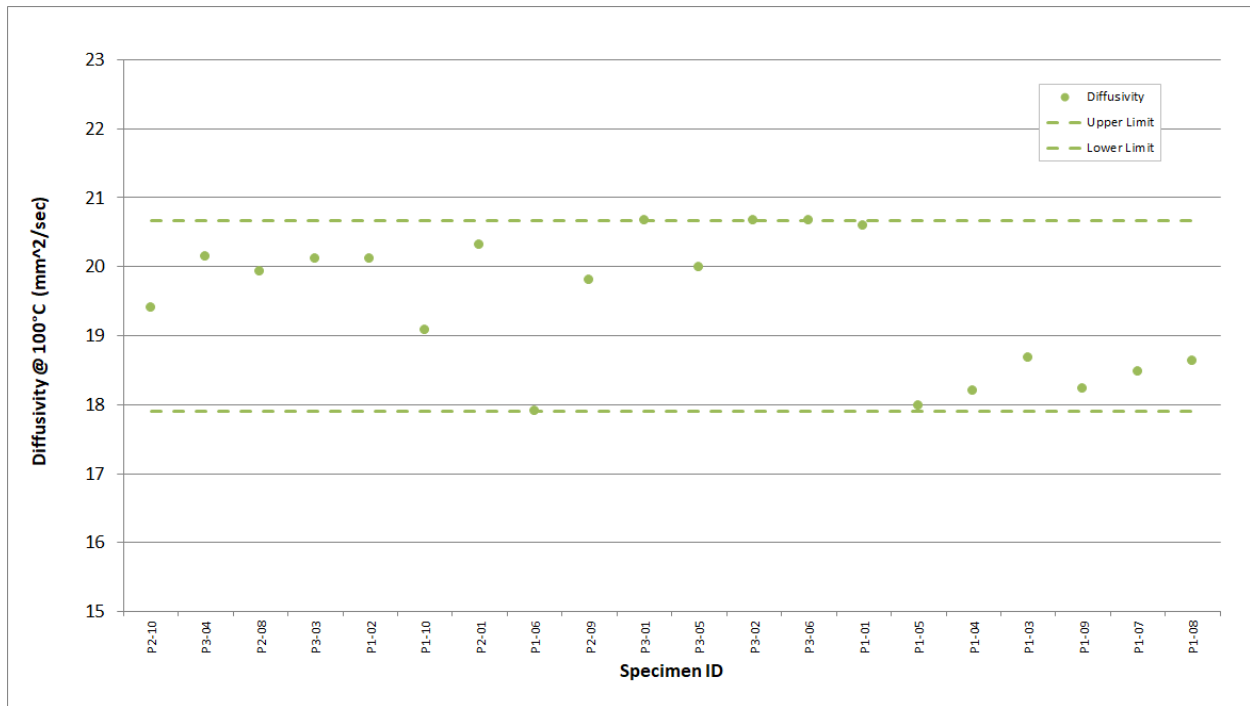


Figure A-182. PCIB Piggyback Diffusivity @ 100°C.

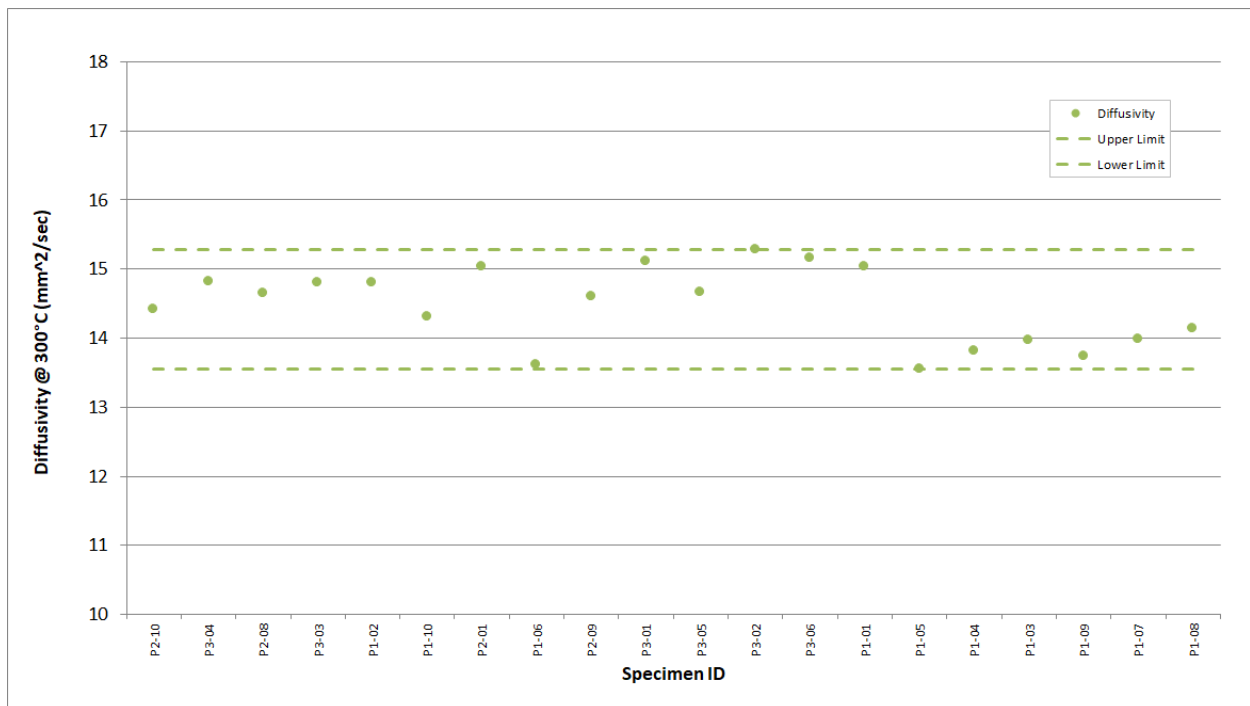


Figure A-183. PCIB Piggyback Diffusivity @ 300°C.

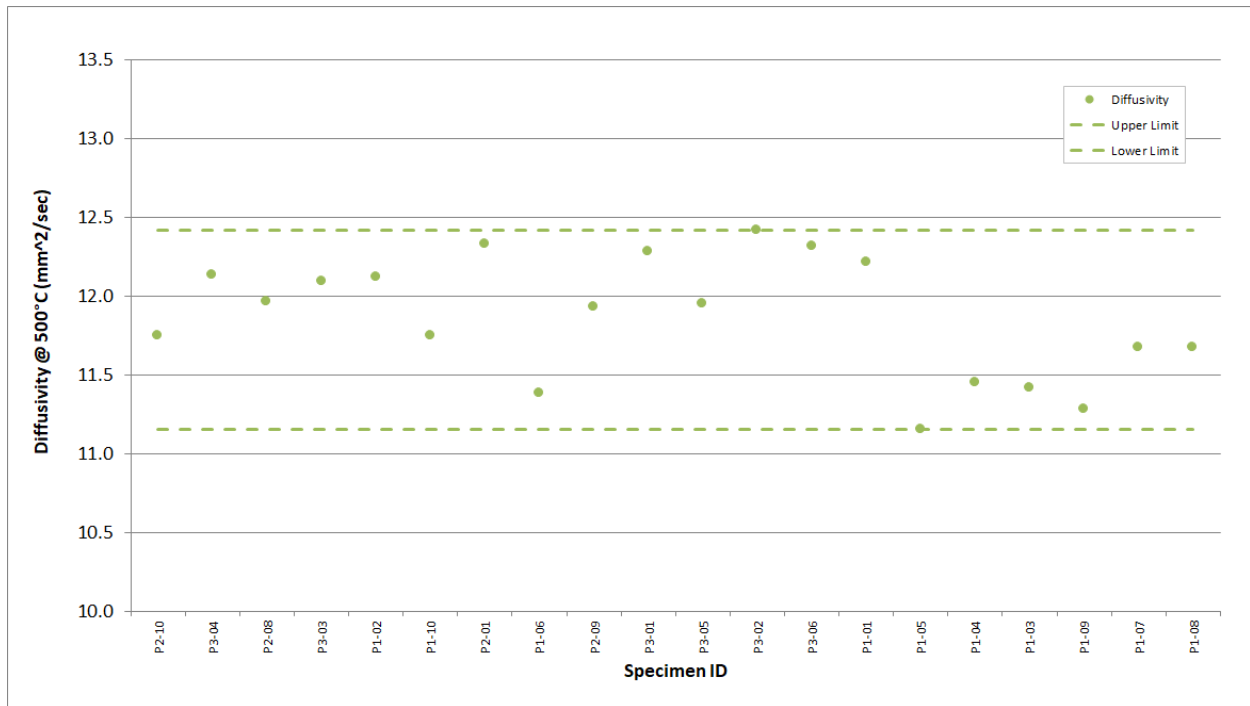


Figure A-184. PCIB Piggyback Diffusivity @ 500°C.

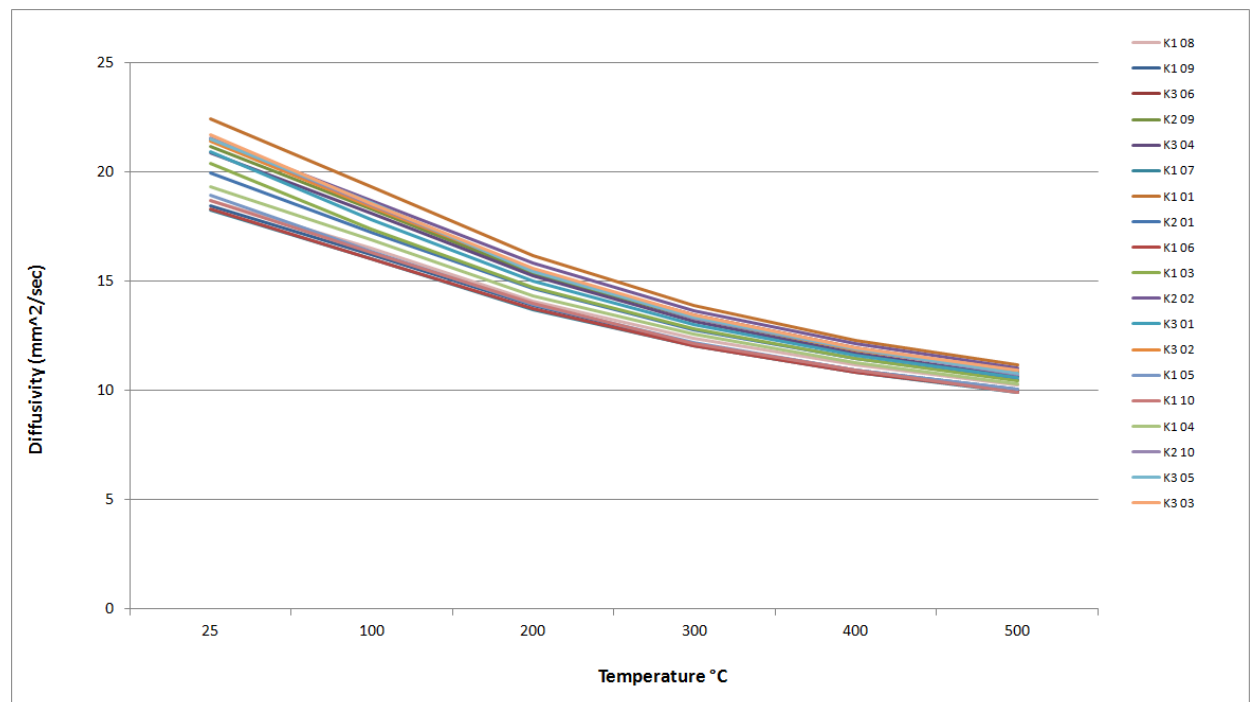


Figure A-185. PGX Piggyback Diffusivity.

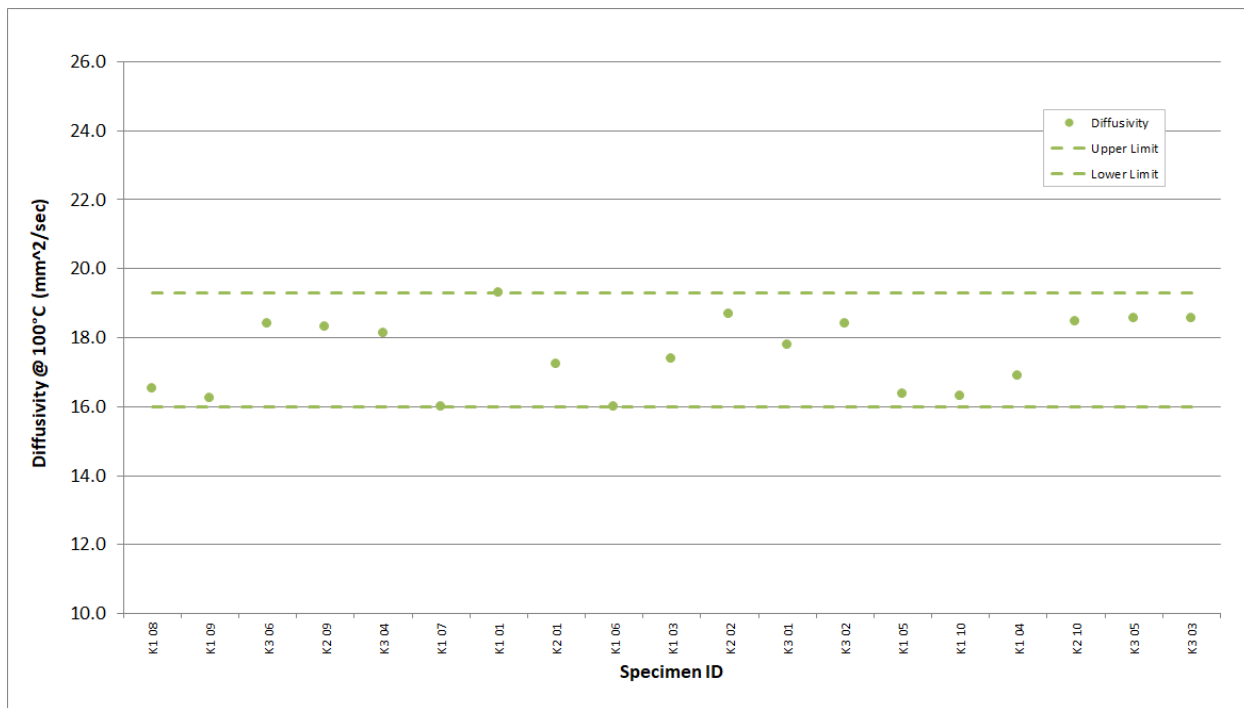


Figure A-186. PGX Piggyback Diffusivity @ 100°C.

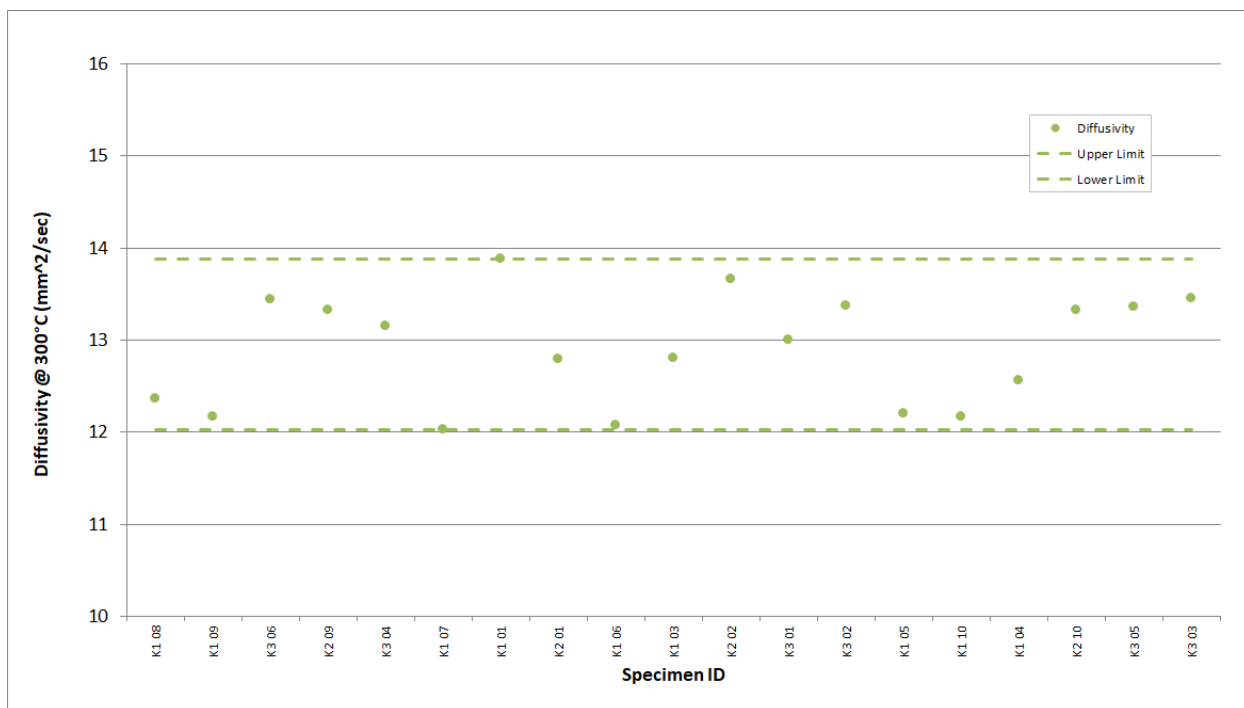


Figure A-187. PGX Piggyback Diffusivity @ 300°C.

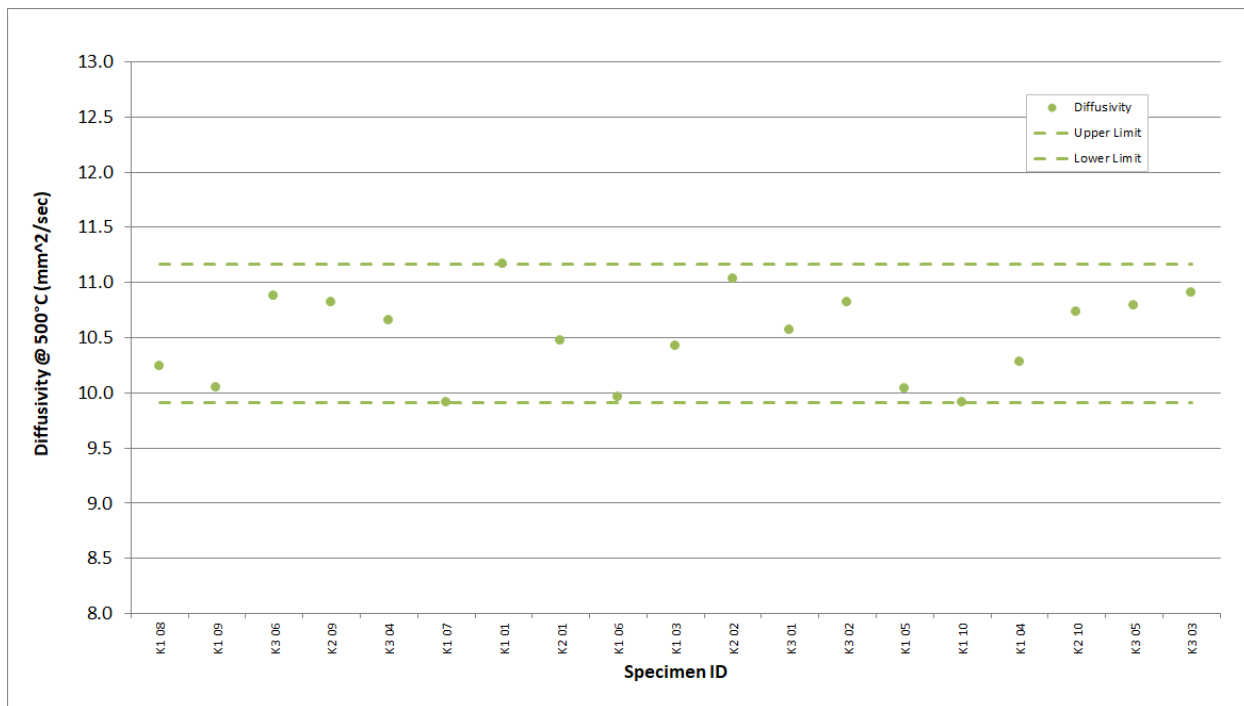


Figure A-188. PGX Piggyback Diffusivity @ 500°C.

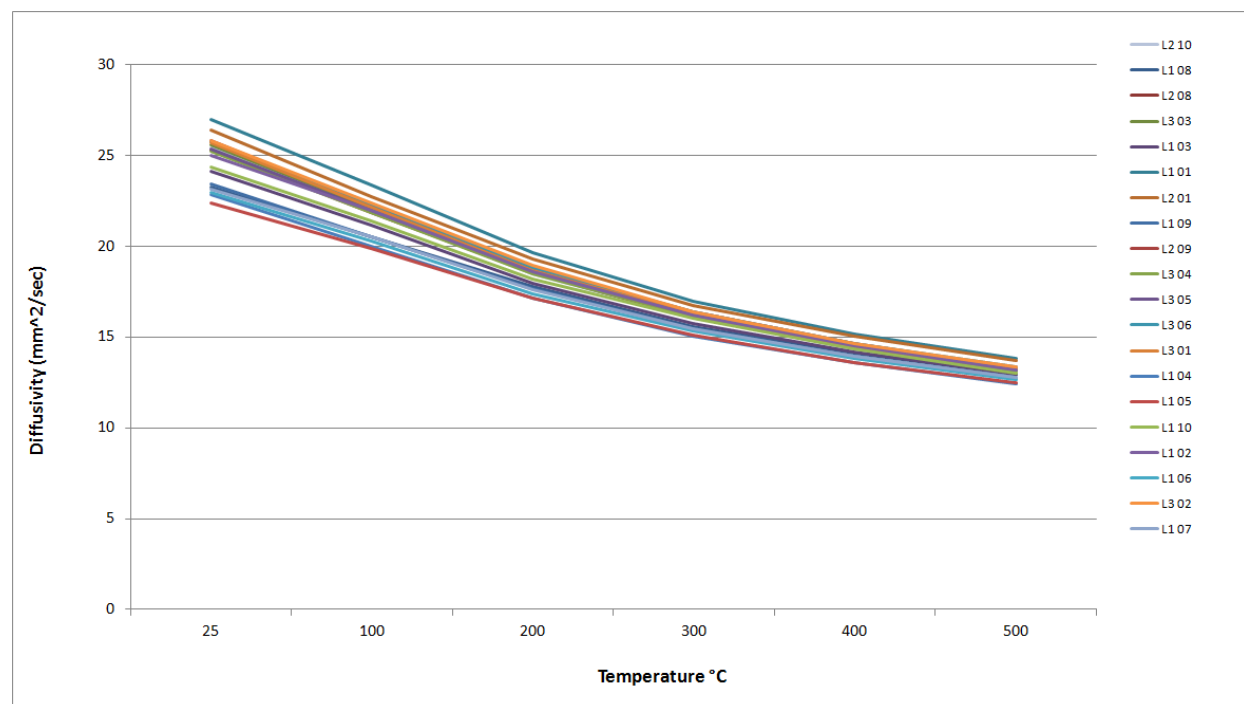


Figure A-189. PPEA Piggyback Diffusivity.

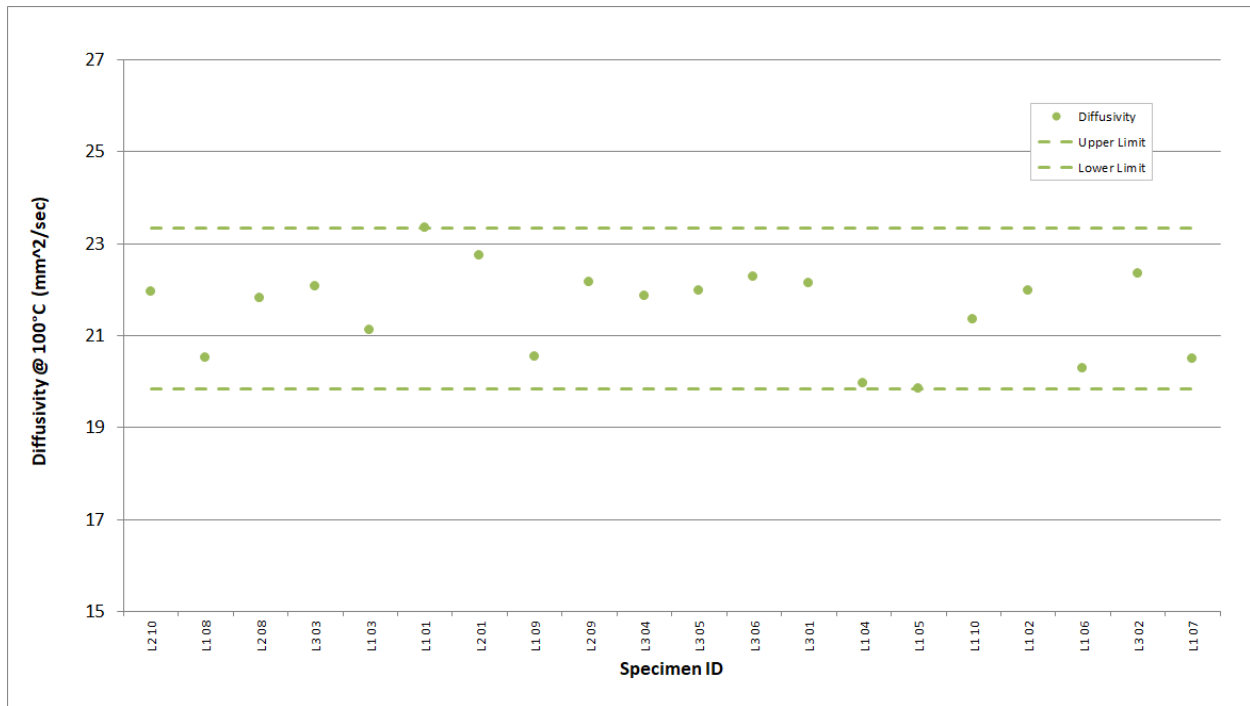


Figure A-190. PPEA Piggyback Diffusivity @ 100°C.

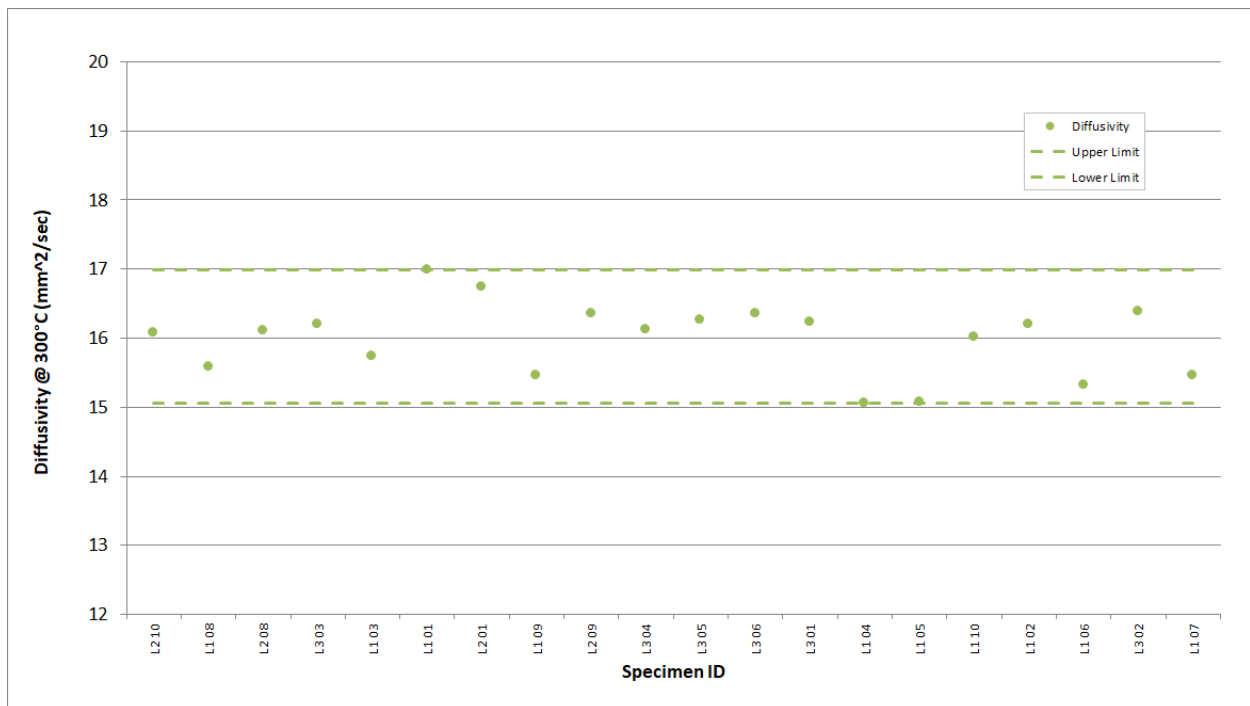


Figure A-191. PPEA Piggyback Diffusivity @ 300°C.

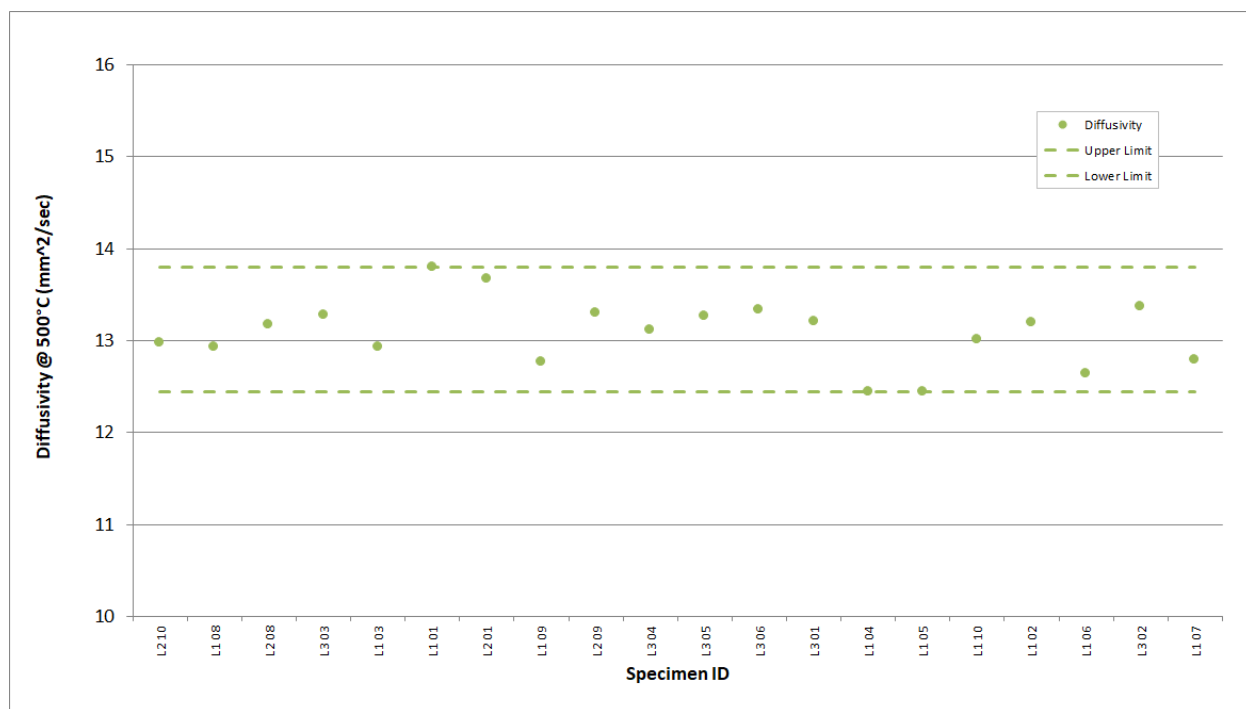


Figure A-192. PPEA Piggyback Diffusivity @ 500°C.

Page intentionally left blank

Appendix B

Summary of Statistical Parameters

Table B-1. Creep specimen Length (mm) Summary Statistics.

Combined Specimens	Mean	Std Dev	CoV (%)	Median	Upper Limit	Lower Limit
H-451	24.96	0.21	0.85	25.06	25.25	24.59
IG-110	25.02	0.19	0.76	25.12	25.25	24.61
IG-430	25.07	0.17	0.70	25.15	25.26	24.74
NBG-17	25.02	0.18	0.72	25.11	25.22	24.67
NBG-18	25.05	0.16	0.63	25.11	25.24	24.72
PCEA	24.97	0.22	0.89	25.07	25.24	24.48
Against Grain Specimens	Mean	Std Dev	CoV (%)	Median	Upper Limit	Lower Limit
H-451						
IG-110	24.67			24.67	24.67	24.67
IG-430						
NBG-17	25.01	0.21	0.82	25.05	25.21	24.73
NBG-18	25.05	0.16	0.64	25.11	25.23	24.74
PCEA	25.01	0.24	0.95	25.11	25.24	24.51
With Grain Specimens	Mean	Std Dev	CoV (%)	Median	Upper Limit	Lower Limit
H-451	24.96	0.21	0.85	25.06	25.25	24.59
IG-110	25.03	0.18	0.74	25.13	25.25	24.61
IG-430	25.07	0.17	0.70	25.15	25.26	24.74
NBG-17	25.02	0.18	0.71	25.11	25.22	24.67
NBG-18	25.05	0.16	0.64	25.12	25.24	24.72
PCEA	24.96	0.22	0.87	25.06	25.24	24.48

Table B-2. Creep specimen Diameter (mm) Summary Statistics.

Combined Specimens	Mean	Std Dev	CoV (%)	Median	Upper Limit	Lower Limit
H-451	12.67	0.04	0.28	12.68	12.73	12.62
IG-110	12.66	0.04	0.29	12.67	12.71	12.61
IG-430	12.66	0.04	0.28	12.66	12.71	12.60
NBG-17	12.66	0.03	0.25	12.67	12.71	12.61
NBG-18	12.66	0.03	0.26	12.67	12.72	12.61
PCEA	12.66	0.04	0.31	12.67	12.73	12.59
Against Grain Specimens	Mean	Std Dev	CoV (%)	Median	Upper Limit	Lower Limit
H-451						
IG-110	12.70			12.70	12.70	12.70
IG-430						
NBG-17	12.65	0.04	0.29	12.65	12.71	12.61
NBG-18	12.67	0.03	0.26	12.66	12.71	12.62
PCEA	12.67	0.04	0.32	12.67	12.73	12.60
With Grain Specimens	Mean	Std Dev	CoV (%)	Median	Upper Limit	Lower Limit
H-451	12.67	0.04	0.28	12.68	12.73	12.62
IG-110	12.66	0.04	0.29	12.67	12.71	12.61
IG-430	12.66	0.04	0.28	12.66	12.71	12.60
NBG-17	12.66	0.03	0.24	12.67	12.71	12.61
NBG-18	12.66	0.03	0.26	12.67	12.72	12.61
PCEA	12.66	0.04	0.31	12.66	12.72	12.59

Table B-3. Creep specimen Mass (g) Summary Statistics.

Combined Specimens	Mean	Std Dev	CoV (%)	Median	Upper Limit	Lower Limit
H-451	5.52	0.03	0.49	5.51	5.56	5.47
IG-110	5.65	0.02	0.37	5.66	5.68	5.61
IG-430	5.75	0.02	0.34	5.75	5.79	5.70
NBG-17	5.89	0.05	0.88	5.92	5.93	5.79
NBG-18	5.94	0.01	0.15	5.94	5.96	5.92
PCEA	5.66	0.03	0.46	5.65	5.69	5.61
Against Grain Specimens	Mean	Std Dev	CoV (%)	Median	Upper Limit	Lower Limit
H-451						
IG-110	5.67			5.67	5.67	5.67
IG-430						
NBG-17	5.92	0.00	0.04	5.92	5.92	5.91
NBG-18	5.93	0.01	0.15	5.93	5.95	5.92
PCEA	5.69	0.03	0.53	5.67	5.72	5.65
With Grain Specimens	Mean	Std Dev	CoV (%)	Median	Upper Limit	Lower Limit
H-451	5.52	0.03	0.49	5.51	5.56	5.47
IG-110	5.65	0.02	0.37	5.66	5.68	5.61
IG-430	5.75	0.02	0.34	5.75	5.79	5.70
NBG-17	5.88	0.06	0.96	5.91	5.93	5.79
NBG-18	5.95	0.01	0.10	5.95	5.96	5.94
PCEA	5.65	0.02	0.28	5.65	5.68	5.62

Table B-4. Creep specimen Density (g/cm³) Summary Statistics.

Combined Specimens	Mean	Std Dev	CoV (%)	Median	Upper Limit	Lower Limit
H-451	1.7801	0.0152	0.85	1.7807	1.8082	1.7527
IG-110	1.8226	0.0130	0.71	1.8216	1.8472	1.7921
IG-430	1.8543	0.0106	0.57	1.8555	1.8734	1.8282
NBG-17	1.9006	0.0130	0.68	1.9038	1.9195	1.8734
NBG-18	1.9141	0.0091	0.47	1.9154	1.9311	1.8987
PCEA	1.8276	0.0131	0.72	1.8281	1.8605	1.8039
Against Grain Specimens	Mean	Std Dev	CoV (%)	Median	Upper Limit	Lower Limit
H-451						
IG-110	1.8414			1.8414	1.8414	1.8414
IG-430						
NBG-17	1.9136	0.0050	0.26	1.9140	1.9195	1.9061
NBG-18	1.9102	0.0097	0.51	1.9094	1.9255	1.8987
PCEA	1.8313	0.0154	0.84	1.8280	1.8605	1.8077
With Grain Specimens	Mean	Std Dev	CoV (%)	Median	Upper Limit	Lower Limit
H-451	1.7801	0.0152	0.85	1.7807	1.8082	1.7527
IG-110	1.8221	0.0128	0.70	1.8215	1.8472	1.7938
IG-430	1.8543	0.0106	0.57	1.8555	1.8734	1.8282
NBG-17	1.8962	0.0118	0.62	1.8986	1.9136	1.8734
NBG-18	1.9154	0.0086	0.45	1.9164	1.9311	1.8999
PCEA	1.8263	0.0123	0.67	1.8281	1.8492	1.8039

Table B-5. Creep specimen Coefficient of Thermal Expansion (1/K) at 100°C Summary Statistics.

Combined Specimens	Mean	Std Dev	CoV (%)	Median	Upper Limit	Lower Limit
H-451	4.26E-06	5.61E-07	13.18	4.08E-06	5.13E-06	3.55E-06
IG-110	5.17E-06	5.91E-07	11.42	5.03E-06	6.15E-06	4.17E-06
IG-430	5.78E-06	6.91E-07	11.96	5.62E-06	6.90E-06	4.50E-06
NBG-17	5.52E-06	4.62E-07	8.37	5.46E-06	6.22E-06	4.99E-06
NBG-18	5.70E-06	4.32E-07	7.58	5.64E-06	6.37E-06	4.87E-06
PCEA	4.85E-06	5.25E-07	10.82	4.68E-06	6.05E-06	4.12E-06
Against Grain Specimens	Mean	Std Dev	CoV (%)	Median	Upper Limit	Lower Limit
H-451						
IG-110	6.09E-06	NaN	NaN	6.09E-06	6.09E-06	6.09E-06
IG-430						
NBG-17	5.67E-06	5.28E-07	9.31	5.74E-06	6.18E-06	5.04E-06
NBG-18	5.56E-06	4.42E-07	7.96	5.48E-06	6.33E-06	4.87E-06
PCEA	4.95E-06	5.77E-07	11.64	4.75E-06	6.05E-06	4.25E-06
With Grain Specimens	Mean	Std Dev	CoV (%)	Median	Upper Limit	Lower Limit
H-451	4.26E-06	5.61E-07	13.18	4.08E-06	5.13E-06	3.55E-06
IG-110	5.15E-06	5.77E-07	11.22	4.93E-06	6.15E-06	4.17E-06
IG-430	5.78E-06	6.91E-07	11.96	5.62E-06	6.90E-06	4.50E-06
NBG-17	5.47E-06	4.44E-07	8.10	5.37E-06	6.22E-06	4.99E-06
NBG-18	5.75E-06	4.24E-07	7.37	5.75E-06	6.37E-06	5.08E-06
PCEA	4.82E-06	5.11E-07	10.61	4.66E-06	5.65E-06	4.12E-06

Table B-6. Creep specimen Coefficient of Thermal Expansion (1/K) at 300 °C Summary Statistics.

Combined Specimens	Mean	Std Dev	CoV (%)	Median	Upper Limit	Lower Limit
H-451	4.37E-06	5.74E-07	13.13	4.09E-06	5.31E-06	3.68E-06
IG-110	5.32E-06	5.83E-07	10.97	5.17E-06	6.29E-06	4.42E-06
IG-430	5.92E-06	6.74E-07	11.38	5.66E-06	6.99E-06	4.81E-06
NBG-17	5.65E-06	4.64E-07	8.21	5.64E-06	6.35E-06	5.10E-06
NBG-18	5.83E-06	4.33E-07	7.43	5.81E-06	6.50E-06	5.00E-06
PCEA	4.99E-06	5.43E-07	10.88	4.80E-06	6.22E-06	4.26E-06
Against Grain Specimens	Mean	Std Dev	CoV (%)	Median	Upper Limit	Lower Limit
H-451						
IG-110	6.14E-06	NaN	NaN	6.14E-06	6.14E-06	6.14E-06
IG-430						
NBG-17	5.79E-06	5.31E-07	9.16	5.86E-06	6.33E-06	5.19E-06
NBG-18	5.67E-06	4.52E-07	7.98	5.61E-06	6.46E-06	5.00E-06
PCEA	5.11E-06	5.84E-07	11.42	4.91E-06	6.22E-06	4.39E-06
With Grain Specimens	Mean	Std Dev	CoV (%)	Median	Upper Limit	Lower Limit
H-451	4.37E-06	5.74E-07	13.13	4.09E-06	5.31E-06	3.68E-06
IG-110	5.29E-06	5.74E-07	10.85	5.03E-06	6.29E-06	4.42E-06
IG-430	5.92E-06	6.74E-07	11.38	5.66E-06	6.99E-06	4.81E-06
NBG-17	5.60E-06	4.46E-07	7.95	5.54E-06	6.35E-06	5.10E-06
NBG-18	5.88E-06	4.20E-07	7.14	5.94E-06	6.50E-06	5.20E-06
PCEA	4.95E-06	5.31E-07	10.73	4.79E-06	5.82E-06	4.26E-06

Table B-7. Creep specimen Coefficient of Thermal Expansion (1/K) at 500 °C Summary Statistics.

Combined Specimens	Mean	Std Dev	CoV (%)	Median	Upper Limit	Lower Limit
H-451	4.72E-06	5.61E-07	11.87	4.45E-06	5.57E-06	4.04E-06
IG-110	5.72E-06	5.65E-07	9.88	5.58E-06	6.70E-06	4.95E-06
IG-430	6.37E-06	6.47E-07	10.15	6.10E-06	7.39E-06	5.38E-06
NBG-17	5.99E-06	4.66E-07	7.78	5.99E-06	6.71E-06	5.41E-06
NBG-18	6.16E-06	4.35E-07	7.06	6.17E-06	6.82E-06	5.31E-06
PCEA	5.33E-06	5.43E-07	10.19	5.08E-06	6.61E-06	4.68E-06
Against Grain Specimens	Mean	Std Dev	CoV (%)	Median	Upper Limit	Lower Limit
H-451						
IG-110	6.41E-06	NaN	NaN	6.41E-06	6.41E-06	6.41E-06
IG-430						
NBG-17	6.14E-06	5.25E-07	8.55	6.22E-06	6.67E-06	5.55E-06
NBG-18	5.67E-06	4.52E-07	7.98	5.61E-06	6.46E-06	5.00E-06
PCEA	5.47E-06	5.90E-07	10.80	5.25E-06	6.61E-06	4.77E-06
With Grain Specimens	Mean	Std Dev	CoV (%)	Median	Upper Limit	Lower Limit
H-451	4.72E-06	5.61E-07	11.87	4.45E-06	5.57E-06	4.04E-06
IG-110	5.70E-06	5.60E-07	9.83	5.39E-06	6.70E-06	4.95E-06
IG-430	6.37E-06	6.47E-07	10.15	6.10E-06	7.39E-06	5.38E-06
NBG-17	5.94E-06	4.50E-07	7.57	5.87E-06	6.71E-06	5.41E-06
NBG-18	6.21E-06	4.19E-07	6.75	6.25E-06	6.82E-06	5.51E-06
PCEA	5.29E-06	5.28E-07	9.98	5.08E-06	6.20E-06	4.68E-06

Table B-8. Creep specimen Modulus (GPa) by Sonic Resonance Summary Statistics.

Combined Specimens	Mean	Std Dev	CoV (%)	Median	Upper Limit	Lower Limit
H-451	17.85	0.81	4.52	17.91	18.91	16.12
IG-110	18.14	0.86	4.76	18.07	19.94	16.43
IG-430	18.01	0.79	4.40	17.96	19.75	16.51
NBG-17	19.52	1.19	6.10	19.54	21.30	17.63
NBG-18	19.63	0.99	5.05	19.68	21.15	17.31
PCEA	17.03	1.33	7.78	17.06	19.33	13.69
Against Grain Specimens	Mean	Std Dev	CoV (%)	Median	Upper Limit	Lower Limit
H-451						
IG-110	18.75			18.75	18.75	18.75
IG-430						
NBG-17	19.53	0.70	3.59	19.53	20.44	18.50
NBG-18	19.63	1.05	5.36	19.70	21.15	17.22
PCEA	16.47	1.78	10.78	16.20	19.13	13.69
With Grain Specimens	Mean	Std Dev	CoV (%)	Median	Upper Limit	Lower Limit
H-451	17.85	0.81	4.52	17.91	18.91	16.12
IG-110	18.12	0.87	4.80	18.05	19.94	16.43
IG-430	18.01	0.79	4.40	17.96	19.75	16.51
NBG-17	19.51	1.33	6.82	19.54	21.30	17.63
NBG-18	19.62	0.98	5.02	19.67	21.03	17.40
PCEA	17.22	1.11	6.42	17.24	19.33	14.95

Table B-9. Creep specimen Resistivity (mW-m) Summary Statistics.

Combined Specimens	Mean	Std Dev	CoV (%)	Median	Upper Limit	Lower Limit
H-451	23.11	0.96	4.16	23.11	24.76	21.52
IG-110	25.12	1.21	4.80	24.95	27.77	22.93
IG-430	25.57	1.18	4.61	25.49	28.51	23.51
NBG-17	23.89	0.65	2.73	23.88	25.05	22.79
NBG-18	23.34	0.87	3.74	23.18	25.00	21.79
PCEA	22.23	1.07	4.81	21.90	25.40	20.68
Against Grain Specimens	Mean	Std Dev	CoV (%)	Median	Upper Limit	Lower Limit
H-451						
IG-110	23.29			23.29	23.29	23.29
IG-430						
NBG-17	23.92	0.62	2.59	23.89	24.02	23.74
NBG-18	22.68	0.85	3.76	22.25	24.22	21.79
PCEA	22.82	1.25	5.48	22.87	25.39	20.68
With Grain Specimens	Mean	Std Dev	CoV (%)	Median	Upper Limit	Lower Limit
H-451	23.11	0.96	4.16	23.11	24.76	21.52
IG-110	25.18	1.18	4.70	25.10	27.77	22.93
IG-430	25.57	1.18	4.61	25.49	28.51	23.51
NBG-17	23.89	0.68	2.85	23.84	25.05	22.66
NBG-18	23.55	0.78	3.29	23.42	25.00	22.44
PCEA	22.03	0.94	4.27	21.82	23.81	20.80

Table B-10. Creep specimen Young's Modulus (GPa) by Sonic Velocity.

Combined Specimens	Mean	Std Dev	CoV (%)	Median	Upper Limit	Lower Limit
H-451	21.43	1.12	5.23	21.23	23.62	19.72
IG-110	20.72	1.12	5.40	20.44	22.99	18.91
IG-430	20.61	0.92	4.49	20.43	22.85	19.39
NBG-17	23.89	1.84	7.70	24.40	26.14	20.39
NBG-18	24.63	1.27	5.15	24.92	26.93	21.23
PCEA	20.04	1.63	8.15	20.36	22.49	15.70
Against Grain Specimens	Mean	Std Dev	CoV (%)	Median	Upper Limit	Lower Limit
H-451						
IG-110	21.09			21.09	21.09	21.09
IG-430						
NBG-17	23.51	1.26	5.35	23.35	25.24	21.61
NBG-18	25.23	1.05	4.18	25.33	26.93	23.42
PCEA	19.15	1.93	10.08	19.11	22.10	15.70
With Grain Specimens	Mean	Std Dev	CoV (%)	Median	Upper Limit	Lower Limit
H-451	21.43	1.12	5.23	21.23	23.62	19.72
IG-110	20.71	1.13	5.48	20.40	22.99	18.91
IG-430	20.61	0.92	4.49	20.43	22.85	19.39
NBG-17	24.02	2.01	8.38	24.69	26.14	20.39
NBG-18	24.43	1.28	5.25	24.78	26.66	21.23
PCEA	20.33	1.43	7.04	20.82	22.49	17.36

Table B-11. Creep specimen Shear Modulus (GPa) by Sonic Velocity.

Combined Specimens	Mean	Std Dev	CoV (%)	Median	Upper Limit	Lower Limit
H-451	7.83	0.54	6.85	7.91	8.42	7.05
IG-110	7.91	0.42	5.26	7.88	8.74	6.83
IG-430	8.00	0.30	3.70	8.01	8.51	7.40
NBG-17	8.37	0.38	4.56	8.44	8.88	7.61
NBG-18	8.56	0.34	4.02	8.55	9.30	7.86
PCEA	7.54	0.43	5.69	7.55	8.33	6.47
Against Grain Specimens	Mean	Std Dev	CoV (%)	Median	Upper Limit	Lower Limit
H-451						
IG-110	6.77			6.77	6.77	6.77
IG-430						
NBG-17	8.37	0.16	1.86	8.41	8.56	8.12
NBG-18	8.66	0.27	3.17	8.55	9.25	8.33
PCEA	7.58	0.35	4.61	7.60	8.07	7.15
With Grain Specimens	Mean	Std Dev	CoV (%)	Median	Upper Limit	Lower Limit
H-451	7.83	0.54	6.85	7.91	8.42	7.05
IG-110	7.94	0.37	4.69	7.91	8.74	7.36
IG-430	8.00	0.30	3.70	8.01	8.51	7.40
NBG-17	8.37	0.44	5.20	8.45	8.88	7.61
NBG-18	8.53	0.36	4.25	8.55	9.08	7.84
PCEA	7.53	0.46	6.06	7.55	8.33	6.53

Table B-12a. Piggyback specimen Length (mm) Summary Statistics.

Combined Specimens	Mean	Std Dev	CoV (%)	Median	Upper Limit	Lower Limit
2114	6.282	0.034	0.54	6.295	6.313	6.256
A3 Matrix	6.291	0.047	0.75	6.272	6.375	6.248
BAN	6.297	0.013	0.20	6.300	6.316	6.277
H-451	6.293	0.017	0.27	6.292	6.319	6.271
HLM	6.275	0.020	0.32	6.278	6.302	6.244
IG-110	6.301	0.016	0.26	6.302	6.324	6.257
IG-430	6.301	0.010	0.15	6.300	6.321	6.288
NBG-10	6.292	0.017	0.26	6.292	6.318	6.268
NBG-17	6.264	0.035	0.55	6.268	6.303	6.205
NBG-18	6.284	0.008	0.12	6.283	6.297	6.272
NBG-25	6.293	0.010	0.16	6.297	6.305	6.275
PCEA	6.295	0.016	0.25	6.298	6.317	6.272
PCIB	6.302	0.009	0.15	6.303	6.316	6.289
PGX	6.285	0.017	0.26	6.284	6.312	6.260
PPEA	6.292	0.019	0.30	6.301	6.322	6.259

Table B-12b. Piggyback specimen Length (mm) Summary Statistics.

Against Grain Specimens	Mean	Std Dev	CoV (%)	Median	Upper Limit	Lower Limit
2114						
A3 Matrix						
BAN						
H-451	6.308	0.019	0.31	6.308	6.322	6.294
HLM						
IG-110						
IG-430						
NBG-10						
NBG-17	6.275	0.015	0.24	6.283	6.289	6.252
NBG-18	6.288	0.008	0.13	6.289	6.294	6.274
NBG-25						
PCEA	6.284	0.009	0.15	6.283	6.298	6.274
PCIB						
PGX						
PPEA						

Table B-12c. Piggyback specimen Length (mm) Summary Statistics.

With Grain Specimens	Mean	Std Dev	CoV (%)	Median	Upper Limit	Lower Limit
2114	6.282	0.034	0.54	6.295	6.313	6.256
A3 Matrix	6.291	0.047	0.75	6.272	6.375	6.248
BAN	6.297	0.013	0.20	6.300	6.316	6.277
H-451	6.285	0.011	0.18	6.286	6.297	6.271
HLM	6.275	0.020	0.32	6.278	6.302	6.244
IG-110	6.301	0.016	0.26	6.302	6.324	6.257
IG-430	6.301	0.010	0.15	6.300	6.321	6.288
NBG-10	6.292	0.017	0.26	6.292	6.318	6.268
NBG-17	6.258	0.041	0.65	6.265	6.303	6.199
NBG-18	6.282	0.007	0.11	6.282	6.291	6.272
NBG-25	6.293	0.010	0.16	6.297	6.305	6.275
PCEA	6.300	0.016	0.25	6.307	6.317	6.272
PCIB	6.302	0.009	0.15	6.303	6.316	6.289
PGX	6.285	0.017	0.26	6.284	6.312	6.260
PPEA	6.292	0.019	0.30	6.301	6.322	6.259

Table B-13a. Piggyback specimen Diameter (mm) Summary Statistics.

Combined Specimens	Mean	Std Dev	CoV (%)	Median	Upper Limit	Lower Limit
2114	12.679	0.026	0.21	12.674	12.734	12.638
A3 Matrix	12.514	0.092	0.73	12.491	12.633	12.388
BAN	12.673	0.019	0.15	12.673	12.707	12.649
H-451	12.667	0.019	0.15	12.666	12.689	12.646
HLM	12.637	0.037	0.29	12.640	12.701	12.587
IG-110	12.654	0.036	0.28	12.658	12.720	12.606
IG-430	12.657	0.028	0.22	12.647	12.708	12.623
NBG-10	12.657	0.032	0.25	12.656	12.697	12.612
NBG-17	12.656	0.030	0.23	12.645	12.710	12.621
NBG-18	12.653	0.024	0.19	12.653	12.688	12.626
NBG-25	12.650	0.027	0.22	12.653	12.687	12.609
PCEA	12.654	0.037	0.30	12.655	12.701	12.599
PCIB	12.684	0.014	0.11	12.687	12.708	12.659
PGX	12.640	0.039	0.31	12.658	12.688	12.578
PPEA	12.667	0.029	0.23	12.681	12.711	12.621

Table B-13b. Piggyback specimen Diameter (mm) Summary Statistics.

Against Grain Specimens	Mean	Std Dev	CoV (%)	Median	Upper Limit	Lower Limit
2114						
A3 Matrix						
BAN						
H-451	12.674	0.022	0.17	12.674	12.689	12.659
HLM						
IG-110						
IG-430						
NBG-10						
NBG-17	12.634	0.012	0.09	12.642	12.645	12.621
NBG-18	12.675	0.014	0.11	12.675	12.688	12.654
NBG-25						
PCEA	12.617	0.018	0.15	12.615	12.646	12.599
PCIB						
PGX						
PPEA						

Table B-13c. Piggyback specimen Diameter (mm) Summary Statistics.

With Grain Specimens	Mean	Std Dev	CoV (%)	Median	Upper Limit	Lower Limit
2114	12.679	0.026	0.21	12.674	12.734	12.638
A3 Matrix	12.514	0.092	0.73	12.491	12.633	12.388
BAN	12.673	0.019	0.15	12.673	12.707	12.649
H-451	12.663	0.020	0.16	12.660	12.687	12.646
HLM	12.637	0.037	0.29	12.640	12.701	12.587
IG-110	12.654	0.036	0.28	12.658	12.720	12.606
IG-430	12.657	0.028	0.22	12.647	12.708	12.623
NBG-10	12.657	0.032	0.25	12.656	12.697	12.612
NBG-17	12.667	0.030	0.24	12.666	12.710	12.628
NBG-18	12.639	0.016	0.13	12.633	12.669	12.626
NBG-25	12.650	0.027	0.22	12.653	12.687	12.609
PCEA	12.673	0.030	0.23	12.687	12.701	12.617
PCIB	12.684	0.014	0.11	12.687	12.708	12.659
PGX	12.640	0.039	0.31	12.658	12.688	12.578
PPEA	12.667	0.029	0.23	12.681	12.711	12.621

Table B-14a. Piggyback specimen Mass (g) Summary Statistics.

Combined Specimens	Mean	Std Dev	CoV (%)	Median	Upper Limit	Lower Limit
2114	1.4551	0.0056	0.39	1.4552	1.4612	1.4489
A3 Matrix	1.2361	0.1171	9.47	1.1729	1.4419	1.1288
BAN	1.4753	0.0093	0.63	1.4716	1.4894	1.4669
H-451	1.3985	0.0148	1.06	1.4072	1.4099	1.3790
HLM	1.4112	0.0025	0.18	1.4118	1.4144	1.4062
IG-110	1.4330	0.0047	0.33	1.4337	1.4404	1.4235
IG-430	1.4574	0.0032	0.22	1.4570	1.4628	1.4533
NBG-10	1.4361	0.0035	0.24	1.4356	1.4430	1.4307
NBG-17	1.4994	0.0077	0.52	1.5003	1.5046	1.4934
NBG-18	1.4993	0.0020	0.13	1.4998	1.5024	1.4962
NBG-25	1.4855	0.0018	0.12	1.4854	1.4887	1.4824
PCEA	1.4253	0.0026	0.18	1.4245	1.4296	1.4212
PCIB	1.4733	0.0030	0.21	1.4736	1.4783	1.4673
PGX	1.4217	0.0037	0.26	1.4216	1.4286	1.4135
PPEA	1.4760	0.0025	0.17	1.4760	1.4824	1.4720

Table B-14b. Piggyback specimen Mass (g) Summary Statistics.

Against Grain Specimens	Mean	Std Dev	CoV (%)	Median	Upper Limit	Lower Limit
2114						
A3 Matrix						
BAN						
H-451	1.3795	0.0007	0.05	1.3795	1.3800	1.3790
HLM						
IG-110						
IG-430						
NBG-10						
NBG-17	1.4997	0.0018	0.12	1.4997	1.5026	1.4974
NBG-18	1.5006	0.0011	0.07	1.5002	1.5024	1.4998
NBG-25						
PCEA	1.4248	0.0024	0.17	1.4245	1.4272	1.4212
PCIB						
PGX						
PPEA						

Table B-14c. Piggyback specimen Mass (g) Summary Statistics.

With Grain Specimens	Mean	Std Dev	CoV (%)	Median	Upper Limit	Lower Limit
2114	1.4551	0.0056	0.39	1.4552	1.4612	1.4489
A3 Matrix	1.2361	0.1171	9.47	1.1729	1.4419	1.1288
BAN	1.4753	0.0093	0.63	1.4716	1.4894	1.4669
H-451	1.4080	0.0014	0.10	1.4078	1.4099	1.4066
HLM	1.4112	0.0025	0.18	1.4118	1.4144	1.4062
IG-110	1.4330	0.0047	0.33	1.4337	1.4404	1.4235
IG-430	1.4574	0.0032	0.22	1.4570	1.4628	1.4533
NBG-10	1.4361	0.0035	0.24	1.4356	1.4430	1.4307
NBG-17	1.4992	0.0096	0.64	1.5020	1.5046	1.4945
NBG-18	1.4985	0.0020	0.13	1.4984	1.5020	1.4962
NBG-25	1.4855	0.0018	0.12	1.4854	1.4887	1.4824
PCEA	1.4255	0.0027	0.19	1.4248	1.4296	1.4216
PCIB	1.4733	0.0030	0.21	1.4736	1.4783	1.4673
PGX	1.4217	0.0037	0.26	1.4216	1.4286	1.4135
PPEA	1.4760	0.0025	0.17	1.4760	1.4824	1.4720

Table B-15a. Piggyback specimen Density (g/cm³) Summary Statistics.

Combined Specimens	Mean	Std Dev	CoV (%)	Median	Upper Limit	Lower Limit
2114	1.8347	0.0116	0.63	1.8330	1.8595	1.8136
A3 Matrix	1.5980	0.1549	9.70	1.5018	1.8441	1.4389
BAN	1.8571	0.0106	0.57	1.8574	1.8793	1.8359
H-451	1.7637	0.0249	1.41	1.7720	1.7876	1.7249
HLM	1.7932	0.0155	0.86	1.7876	1.8177	1.7701
IG-110	1.8083	0.0126	0.70	1.8083	1.8304	1.7855
IG-430	1.8382	0.0102	0.56	1.8406	1.8511	1.8200
NBG-10	1.8142	0.0126	0.69	1.8108	1.8386	1.7972
NBG-17	1.9028	0.0139	0.73	1.8998	1.9254	1.8783
NBG-18	1.8975	0.0088	0.46	1.9014	1.9108	1.8838
NBG-25	1.8783	0.0115	0.61	1.8793	1.8973	1.8633
PCEA	1.8004	0.0165	0.92	1.8007	1.8232	1.7767
PCIB	1.8503	0.0081	0.44	1.8501	1.8669	1.8370
PGX	1.8029	0.0171	0.95	1.7943	1.8312	1.7821
PPEA	1.8613	0.0149	0.80	1.8551	1.8856	1.8393

Table B-15b. Piggyback specimen Density (g/cm³) Summary Statistics.

Against Grain Specimens	Mean	Std Dev	CoV (%)	Median	Upper Limit	Lower Limit
2114						
A3 Matrix						
BAN						
H-451	1.7335	0.0121	0.70	1.7335	1.7421	1.7249
HLM						
IG-110						
IG-430						
NBG-10						
NBG-17	1.9063	0.0094	0.49	1.9011	1.9167	1.8977
NBG-18	1.8914	0.0065	0.34	1.8900	1.9014	1.8852
NBG-25						
PCEA	1.8134	0.0081	0.45	1.8171	1.8214	1.8007
PCIB						
PGX						
PPEA						

Table B-15c. Piggyback specimen Density (g/cm³) Summary Statistics.

With Grain Specimens	Mean	Std Dev	CoV (%)	Median	Upper Limit	Lower Limit
2114	1.8347	0.0116	0.63	1.8330	1.8595	1.8136
A3 Matrix	1.5980	0.1549	9.70	1.5018	1.8441	1.4389
BAN	1.8571	0.0106	0.57	1.8574	1.8793	1.8359
H-451	1.7789	0.0084	0.47	1.7795	1.7876	1.7689
HLM	1.7932	0.0155	0.86	1.7876	1.8177	1.7701
IG-110	1.8083	0.0126	0.70	1.8083	1.8304	1.7855
IG-430	1.8382	0.0102	0.56	1.8406	1.8511	1.8200
NBG-10	1.8142	0.0126	0.69	1.8108	1.8386	1.7972
NBG-17	1.9010	0.0159	0.83	1.8980	1.9254	1.8783
NBG-18	1.9013	0.0081	0.43	1.9038	1.9108	1.8914
NBG-25	1.8783	0.0115	0.61	1.8793	1.8973	1.8633
PCEA	1.7939	0.0159	0.89	1.7877	1.8232	1.7767
PCIB	1.8503	0.0081	0.44	1.8501	1.8669	1.8370
PGX	1.8029	0.0171	0.95	1.7943	1.8312	1.7821
PPEA	1.8613	0.0149	0.80	1.8551	1.8856	1.8393

Table B-16a. Piggyback specimen Diffusivity (mm²/sec) at 100 °C Summary Statistics.

Combined Specimens	Mean	Std Dev	CoV (%)	Median	Upper Limit	Lower Limit
2114	18.39	1.02	5.56	18.20	19.86	16.40
A3 Matrix	4.10	1.24	30.37	3.38	6.29	2.70
BAN	23.04	1.41	6.14	23.29	25.13	21.10
H-451	22.35	1.03	4.60	22.29	23.59	20.66
HLM	23.86	1.74	7.31	23.76	26.26	21.43
IG-110	18.70	1.13	6.06	18.51	20.40	16.78
IG-430	19.37	1.12	5.78	19.13	21.49	17.81
NBG-10	20.18	1.00	4.98	20.29	21.61	18.90
NBG-17	19.14	1.00	5.24	18.80	20.04	18.06
NBG-18	20.14	1.09	5.39	20.12	21.74	18.86
NBG-25	19.05	0.84	4.42	19.28	20.41	17.54
PCEA	22.80	1.92	8.41	23.85	25.31	20.10
PCIB	19.48	0.98	5.06	19.87	20.67	17.90
PGX	17.55	1.07	6.12	17.79	19.31	16.00
PPEA	21.54	0.97	4.50	21.90	23.35	19.85

Table B-16b. Piggyback specimen Diffusivity (mm²/sec) at 100 °C Summary Statistics.

Against Grain Specimens	Mean	Std Dev	CoV (%)	Median	Upper Limit	Lower Limit
2114						
A3 Matrix						
BAN						
H-451	21.51	1.19	5.55	21.51	22.35	20.66
HLM						
IG-110						
IG-430						
NBG-10						
NBG-17	18.63	0.35	1.89	18.80	18.95	18.06
NBG-18	21.26	0.48	2.24	21.29	21.74	20.50
NBG-25						
PCEA	20.41	0.32	1.57	20.26	20.84	20.10
PCIB						
PGX						
PPEA						

Table B-16c. Piggyback specimen Diffusivity (mm²/sec) at 100 °C Summary Statistics.

With Grain Specimens	Mean	Std Dev	CoV (%)	Median	Upper Limit	Lower Limit
2114	18.39	1.02	5.56	18.20	19.86	16.40
A3 Matrix	4.10	1.24	30.37	3.38	6.29	2.70
BAN	23.04	1.41	6.14	23.29	25.13	21.10
H-451	22.78	0.76	3.33	22.73	23.59	22.04
HLM	23.86	1.74	7.31	23.76	26.26	21.43
IG-110	18.70	1.13	6.06	18.51	20.40	16.78
IG-430	19.37	1.12	5.78	19.13	21.49	17.81
NBG-10	20.18	1.00	4.98	20.29	21.61	18.90
NBG-17	19.40	1.14	5.86	18.85	21.52	18.42
NBG-18	19.44	0.66	3.39	19.14	20.71	18.86
NBG-25	19.05	0.84	4.42	19.28	20.41	17.54
PCEA	23.99	0.95	3.96	24.22	25.31	22.88
PCIB	19.48	0.98	5.06	19.87	20.67	17.90
PGX	17.55	1.07	6.12	17.79	19.31	16.00
PPEA	21.54	0.97	4.50	21.90	23.35	19.85

Table B-17a. Piggyback specimen Diffusivity (mm²/sec) at 300 °C Summary Statistics.

Combined Specimens	Mean	Std Dev	CoV (%)	Median	Upper Limit	Lower Limit
2114	13.84	0.61	4.41	13.92	14.71	12.49
A3 Matrix	2.74	0.93	33.93	2.23	4.43	1.72
BAN	16.97	0.79	4.65	17.00	18.11	15.91
H-451	16.51	0.74	4.46	16.58	17.31	15.27
HLM	17.46	1.04	5.93	17.59	18.92	15.99
IG-110	13.92	0.69	4.98	13.79	15.02	12.69
IG-430	14.35	0.65	4.52	14.30	15.63	13.47
NBG-10	15.01	0.54	3.58	15.03	15.75	14.25
NBG-17	14.35	0.61	4.27	14.11	14.84	13.58
NBG-18	15.06	0.67	4.47	14.95	16.06	14.27
NBG-25	14.27	0.46	3.24	14.36	15.04	13.39
PCEA	16.88	1.19	7.05	17.64	18.30	15.16
PCIB	14.48	0.55	3.81	14.62	15.28	13.56
PGX	12.90	0.60	4.65	13.00	13.88	12.03
PPEA	15.99	0.52	3.28	16.11	16.98	15.06

Table B-17b. Piggyback specimen Diffusivity (mm²/sec) at 300 °C Summary Statistics.

Against Grain Specimens	Mean	Std Dev	CoV (%)	Median	Upper Limit	Lower Limit
2114						
A3 Matrix						
BAN						
H-451	15.72	0.63	4.01	15.72	16.16	15.27
HLM						
IG-110						
IG-430						
NBG-10						
NBG-17	14.01	0.28	1.98	14.11	14.21	13.53
NBG-18	15.78	0.29	1.84	15.86	16.06	15.35
NBG-25						
PCEA	15.36	0.22	1.44	15.28	15.62	15.16
PCIB						
PGX						
PPEA						

Table B-17c. Piggyback specimen Diffusivity (mm²/sec) at 300 °C Summary Statistics.

With Grain Specimens	Mean	Std Dev	CoV (%)	Median	Upper Limit	Lower Limit
2114	13.84	0.61	4.41	13.92	14.71	12.49
A3 Matrix	2.74	0.93	33.93	2.23	4.43	1.72
BAN	16.97	0.79	4.65	17.00	18.11	15.91
H-451	16.91	0.38	2.24	16.88	17.31	16.57
HLM	17.46	1.04	5.93	17.59	18.92	15.99
IG-110	13.92	0.69	4.98	13.79	15.02	12.69
IG-430	14.35	0.65	4.52	14.30	15.63	13.47
NBG-10	15.01	0.54	3.58	15.03	15.75	14.25
NBG-17	14.51	0.67	4.64	14.16	15.75	13.90
NBG-18	14.61	0.36	2.45	14.48	15.30	14.27
NBG-25	14.27	0.46	3.24	14.36	15.04	13.39
PCEA	17.64	0.51	2.87	17.78	18.23	17.28
PCIB	14.48	0.55	3.81	14.62	15.28	13.56
PGX	12.90	0.60	4.65	13.00	13.88	12.03
PPEA	15.99	0.52	3.28	16.11	16.98	15.06

Table B-18a. Piggyback specimen Diffusivity (mm²/sec) at 500 °C Summary Statistics.

Combined Specimens	Mean	Std Dev	CoV (%)	Median	Upper Limit	Lower Limit
2114	11.43	0.45	3.91	11.54	12.05	10.42
A3 Matrix	2.15	0.76	35.08	1.76	3.61	1.33
BAN	13.83	0.53	3.86	13.81	14.66	13.11
H-451	13.47	0.67	4.97	13.67	14.08	12.42
HLM	14.19	0.74	5.23	14.28	15.36	13.14
IG-110	11.42	0.51	4.46	11.40	12.22	10.50
IG-430	11.74	0.46	3.92	11.75	12.74	11.12
NBG-10	12.32	0.35	2.82	12.26	12.83	11.85
NBG-17	11.79	0.47	3.99	11.65	12.13	11.18
NBG-18	12.37	0.49	4.00	12.25	13.09	11.65
NBG-25	11.73	0.32	2.72	11.80	12.24	11.12
PCEA	13.73	0.91	6.62	13.81	14.94	12.37
PCIB	11.87	0.38	3.23	11.94	12.42	11.16
PGX	10.51	0.40	3.85	10.57	11.17	9.91
PPEA	13.08	0.36	2.73	13.14	13.80	12.45

Table B-18b. Piggyback specimen Diffusivity (mm²/sec) at 500 °C Summary Statistics.

Against Grain Specimens	Mean	Std Dev	CoV (%)	Median	Upper Limit	Lower Limit
2114						
A3 Matrix						
BAN						
H-451	12.66	0.34	2.68	12.66	12.90	12.42
HLM						
IG-110						
IG-430						
NBG-10						
NBG-17	11.51	0.26	2.26	11.60	11.73	11.10
NBG-18	12.90	0.22	1.72	12.94	13.09	12.56
NBG-25						
PCEA	12.65	0.21	1.66	12.64	12.89	12.37
PCIB						
PGX						
PPEA						

Table B-18c. Piggyback specimen Diffusivity (mm²/sec) at 500 °C Summary Statistics.

With Grain Specimens	Mean	Std Dev	CoV (%)	Median	Upper Limit	Lower Limit
2114	11.43	0.45	3.91	11.54	12.05	10.42
A3 Matrix	2.15	0.76	35.08	1.76	3.61	1.33
BAN	13.83	0.53	3.86	13.81	14.66	13.11
H-451	13.87	0.24	1.71	13.89	14.08	13.61
HLM	14.19	0.74	5.23	14.28	15.36	13.14
IG-110	11.42	0.51	4.46	11.40	12.22	10.50
IG-430	11.74	0.46	3.92	11.75	12.74	11.12
NBG-10	12.32	0.35	2.82	12.26	12.83	11.85
NBG-17	11.93	0.50	4.20	11.68	12.81	11.48
NBG-18	12.05	0.27	2.27	12.00	12.50	11.65
NBG-25	11.73	0.32	2.72	11.80	12.24	11.12
PCEA	14.26	0.56	3.90	14.48	14.94	13.08
PCIB	11.87	0.38	3.23	11.94	12.42	11.16
PGX	10.51	0.40	3.85	10.57	11.17	9.91
PPEA	13.08	0.36	2.73	13.14	13.80	12.45